UNIVERSITAT DE LES ILLES BALEARS
FACULTAT DE CIÈNCIES
DEPARTAMENT DE BIOLOGIA - IUNICS

Cellular and molecular pathogenic mechanisms involved in experimental Spinal Muscular Atrophy

Víctor CARABALLO MIRALLES

Tesi doctoral per a la obtenció del títol de Doctor en Neurociències

Programa Oficial de Postgrau en Neurociències per la
Universitat de les Illes Balears

El present treball ***'Cellular and molecular pathogenic mechanisms involved in experimental Spinal Muscular Atrophy'***, presentat per Víctor Caraballo Miralles per optar a l'obtenció del títol de Doctor, ha estat realitzat sota la meva direcció.

Revisat el text, estic conforme amb la seva presentació per a ser avaluat.

A Palma, 25 de juny de 2012

Els directors de la tesi,

Dra. Jerònia Lladó Vich

Dr. Gabriel Olmos Bonafé

L'autor de la tesi,

Víctor Caraballo Miralles

Aquesta tesi ha estat realitzada en el grup de Neurobiologia Cel·lular del departament de Biologia-IUNICS de la Universitat de les Illes Balears, gràcies a una beca predoctoral de formació de personal investigador (FPI-2008-43141877) de la Conselleria d'Educació, Cultura i Universitats del Govern de les Illes Balears i el Fons Social Europeu.

Als que sempre he estimat i estimaré

Acknowledgements

First, I wish to express my sincere gratitude to my PhD supervisors Dra Jerònia Lladó Vich and Dr Gabriel Olmos Bonafé. Without your advices and scientific knowledge any of this could had been possible.

A na Jerònia, moltes gràcies per la feina plegats a la poiata i al microscopi. Colze a colze, m'has ensenyat a fer bona ciència. No m'imaginava que una 'jefa' pogués fer de tot i alhora. Per fer tot això i més, sempre amb un somriure a la cara i amb total predisposició, gràcies! A Gabriel, gracias por la dedicación y la tenacidad con la que llevas a cabo los proyectos, eso te hace un excepcional investigador, ha sido un placer aprender de ti.

I wish to specially thank Dr Rafael Yáñez the warm welcome to your laboratory during my stay in the School of Biological Sciences in the Royal Holloway - University of London. You and your team make genetic engeeriering easy! I want to extend this aknowledgements to Dra Céline Rocca, Dr Martin Broadstock and Dr Sherif G Ahmed.

I want to thank Dra Rosa Soler and Dra Anna Garcerà for sharing with me your valuable lentivectors; Dra Lucía Tabares and all her group for all mouse samples; Dr Jordi Calderó and Dr Josep Esquerda for your valuable knowledge in neuroinflammation and gliosis; and Dr Priam Villalonga for introducing me to the RhoA/ROCK pathway.

També vull agrair especialment a la Dra Laia Tolosa i la Dra Margalida Mir per recolzar-me en els meus inicis, vosaltres obríreu el camí. Vull dedicar menció especial a n'Andrea per continuar el camí i fer-ho tan agradable, gràcies per les valuoses converses científiques i personals. Heu estat les millors companyes que hom podria desitjar.

Vull fer extensiu l'agraïment als companys de l'àrea de bioquímica i citologia, en especial: Gabriela, Dani, Jordi, Dra Gwendolyn Barceló, Maria Antònia, Dra Laura Martín i Amaia. També són al meu record totes les meves companyes de promoció, tot això va començar amb vosaltres.

Als meus amics, Miquel, Llucia, Pau, Javi, Toni i Júlia: *No camines delante mía, puede que no te siga. No camines detrás de mí, puede que no te guie. Camina a mi lado y sé mi amigo* (Albert Camus). Fa molts d'anys que caminam plegats, i per molts més, moltes gràcies!

A mi familia no le debo todo, solo mis triumfos, y no mis fracasos. A mu mare: *Tot el que sóc o esper ser li dec a l'angelical sol·licitud de la meva mare* (Abraham Lincoln). A mon pare: *Un buen padre vale por cien maestros* (Jean Jacques Rousseau). Sempre heu estat i sereu el pilar de la meva vida.

Sílvia, quiero agradacerte tu apoyo incondicional y ayudarme a relativizarlo todo. Eres la mejor hermana mayor que nadie puede imaginar, gracias! Al meu fillolet Martí, tot ha canviat des que tinc el gran plaer de coneixer-te! A Pedro, por ser el mejor cuñado mayor posible. *La felicitat és el que sentim quan esteim en companyia dels nostres èsser estimats* (anònim).

A tu, Lorena, perquè '*estimar és trobar a la felicitat de l'altre la felicitat pròpia*' (Gottfried Wilhelm Leibniz), i amb tu això s'ha convertit en la meva veritat, ara ja sempre pens en dos. Ets la persona amb la que compartir el camí vol dir fer un únic camí. Sense tu res d'això no hauria estat ni imaginable, MOLTES GRÀCIES!

This work was supported by a predoctoral fellowship from 'Govern Balear, Conselleria d'Educació, Cultura i Universitats' and 'Unió Europea, Fons Social Europeu' (FPI08-43141877H) and supported by the projects Gename and Fundame from 'Fundación Genoma-España'.

Govern de les Illes Balears
Conselleria d'Educació, Cultura i Universitats
Direcció General d'Universitats,
Recerca i Transferència del Coneixement

Unió Europea
Fons Social Europeu

Genoma España

FundAme

Resum

Cellular and molecular pathogenic mechanisms involved in experimental Spinal Muscular Atrophy

Mecanismes patogènics cel·lulars i moleculars implicats en l'Atròfia Muscular Espinal experimental

Víctor Caraballo Miralles

L'atròfia muscular espinal (SMA, de l'anglès *Spinal Muscular Atrophy*) és una malaltia neurodegenerativa que afecta a les motoneurones alfa de la medul·la espinal i és una de les principals causes genètiques de mort a la infància. La causa de la malaltia és la reducció de la proteïna per a la supervivència de la motoneurona, SMN (de l'anglès *Survival Motor Neuron protein*), provocada per una deleció homozigòtica o mutació específica al gen per a la supervivència de la motoneurona-1 (*SMN1*). Tot i que l'SMN s'expressa ubiquament, la seva mancança causa la pèrdua específica de motoneurones. Quatre funcions han estat assignades a l'SMN, tres d'elles són constitutives i necessàries per al manteniment de totes les cèl·lules, i l'altra és específica de les neurones i està relacionada amb el transport axonal de l'ARNm.

S'ha descrit que la reducció d'SMN provoca alteracions en la integritat del citoesquelet. El citoesquelet d'actina juga un paper important en la migració cel·lular. A més a més, la reducció en l'expressió de l'SMN provoca defectes en la neuritogènesi de l'hipocamp, associats a alteracions en els nivells d'expressió de les proteïnes requerides per als processos de creixement cel·lular i migració. Això suggereix que la patologia de l'SMA podria estar associada a alteracions en la capacitat de migració cel·lular. A la línia cel·lular d'astroglioma humà U87MG en la que s'ha disminuït l'expressió d'SMN amb shRNA, s'ha caracteritzat l'afectació de la seva migració com a conseqüència de la reducció d'SMN. La reducció d'SMN indueix defectes en la migració cel·lular, s'observa que la via RhoA/ROCK està activada i la profilina incrementa la seva expressió.

L'activació de la via RhoA/ROCK causa la fosforilació de la cadena lleugera de la miosina, proteïna que és coneguda per promoure la interacció de la miosina amb l'actina incrementant la velocitat del flux retrògrad als fil·lopodis i lamel·lipodis, procés que dificultaria la migració cel·lular.

A la medul·la espinal lumbar del model murí SMNΔ7 d'SMA s'han descrit canvis patològics a les motoneurones, com la reducció del soma i la fosforilació del neurofilament, ambdós previs a la pèrdua de motoneurones a l'estadi final. En aquest model s'ha observat un increment d'astròglia al voltant de les motoneurones en l'estadi presimptomàtic, i una astrogliosi generalitzada a la medul·la espinal lumbar en l'estadi simptomàtic. Per contra, la presència de micròglia només es veu incrementada en l'estadi simptomàtic. A les motoneurones de la medul·la espinal lumbar d'aquest model a l'estadi simptomàtic, s'ha descrit una reducció dels botons presinàptics, en els quals s'ha observat un increment a la fosforilació de la cadena lleugera de la miosina. Alhora, s'ha detectat una expressió incrementada de la isoforma neuronal de l'òxid nítric sintasa a motoneurones i interneurones, però la isoforma induïble només s'ha observat a interneurones, a l'estadi simptomàtic.

La via cel·lular de senyalització Notch i l'expressió incrementada dels seus lligands, Jagged i Delta, han estat àmpliament relacionades amb defectes a la neuritogènesi. A més a més, defectes a la neuritogènesi han estat directament vinculats amb la disminució d'SMN a models d'SMA. Malgrat això, la possible implicació de la via de senyalització cel·lular de Notch a la malaltia SMA no havia estat determinada. Després de la reducció d'SMN a la línia cel·lular d'astroglioma U87MG, s'han observat nivells incrementats dels lligands Jagged i Delta, del receptor Notch i del seu fragment actiu, NICD. Finalment, s'ha fet servir el model murí SMNΔ7 per a determinar si la glia o les motoneurones de la medul·la espinal lumbar presenten una activació incrementada de la via de senyalització de Notch. S'ha descrit una expressió incrementada dels lligands Jagged i Delta en astròcits en l'estadi simptomàtic. També s'han trobat nivells elevats del fragment actiu intracel·lular del receptor Notch, NICD, a motoneurones, astròglia i micròglia, associats a una expressió incrementada de Jagged i Delta a l'astròglia, en l'estadi simptomàtic. Per altra banda, s'ha observat que les motoneurones del ratolí SMNΔ7 que presenten nivells elevats del fragment actiu intracel·lular del receptor Notch, expressen menys Neurogenina, proteïna que està íntimament relacionada amb la neuritogènesi.

La reducció de la proteïna SMN en models *in vitro* i *in vivo* s'ha associat amb l'activació de les vies de senyalització cel·lular RhoA/ROCK i Notch, que resulta en alteracions del citoesquelet d'actina i en la reducció de l'expressió de Neurogenina, la qual cosa provoca defectes a la migració cel·lular, pèrdua de les

sinapsis a les motoneurones espinals i reducció de la mida del soma. A més a més, el procés d'astrogliosi en el ratolí SMNΔ7 podria contribuir a la creació d'un ambient perjudicial per a les motoneurones en els teixits d'SMA. Per tant, els nostres resultats suggereixen que la patogènia a l'SMA no és causada per un únic procés, sinó per la convergència de diversos processos patogènics a les motoneurones i a la glia que deriven en disfuncions de les motoneurones i posterior mort d'aquestes.

'It is well known that in order to use some kind of instrument, the first thing is to know its structure and operation (...) as in this magnificent organ that is the human brain'

'Es ben sabut que, per a fer ús d'un instrument qualsevol, en primer lloc s'ha de conèixer la seva estructura i funcionament (...) igual que en aquest òrgan magnífic que és el cervell humà'

Rita Levi Montalcini – The Tattered Ace Up the Sleeve

Contents

Abstract

Cellular and molecular pathogenic mechanisms involved in experimental Spinal Muscular Atrophy

Spinal muscular atrophy (SMA) is a neurodegenerative disease that affects alpha motoneurons in the spinal cord, being one of the leading genetic causes of death in childhood. The trigger of this disease is a reduction in the expression of the survival of motor neuron protein, SMN, owing to homozygous deletion or specific mutations in the survival motoneuron-1 (*SMN1*) gene. Although SMN is ubiquitously expressed, its lack specifically causes spinal motoneuron loss. Four functions have been assigned to SMN, three house-keeping functions, related to RNA splicing in all cells, and one neuron-specific, related to axonal transport of mRNA.

SMN depletion has been described to cause alterations in cytoskeletal integrity. The actin cytoskeleton plays an important role in cell migration. Also, reduced expression of SMN induces impaired hippocampal neurogenesis, associated to alterations in the expression levels of proteins required for cell growth and migration. This suggests that alterations in cellular migration could be related to SMA. In the U87MG human astroglioma cell line depleted of SMN via shRNA, we characterized the change in migration dynamics induced by SMN depletion. We determined that SMN reduction causes reduced cell migration, associated to RhoA/ROCK signalling pathway activation and profilin overexpression. The activation of RhoA/ROCK leads to myosin light chain phosphorylation, which is known to promote interaction of myosin light chain with actin, increasing the speed of retrograde flow in filopodia and lamellipodia, thus impairing cell migration.

In the lumbar spinal cord of the SMNΔ7 mouse model, we described pathological changes in motoneurons, such as soma reduction and neurofilament phosphorylation, previous to motoneuron loss at end-stage. In this model, we observed enhanced astrogliosis surrounding motoneurons at pre-symptomatic stage, and generalized astrogliosis in lumbar spinal cord at symptomatic stage. In contrast, microgliosis was only enhanced at symptomatic stage. In lumbar spinal cord motoneurons of this model, at symptomatic stage, we described a reduction in the number of pre-synaptic boutons, in which

increased phosphorylation of myosin light chain was found. In addition, we observed increased expression of the neuronal isoform of the nitric oxide synthase in motoneurons and in interneurons, but the inducible isoform of nitric oxide synthase only was found in interneurons of the lumbar spinal cord at symptomatic stage.

Notch signalling pathway and the overexpression of its ligands, Jagged and Delta, have been widely related to neuritogenesis. Moreover, neuritogenesis defects have been directly related to SMN reduction in models of SMA. However, the possible involvement of the Notch signalling pathway in the pathology of SMA has not been determined yet. After depletion of SMN in U87MG astroglioma cell line, we observed increased levels of Jagged and Delta ligands, Notch receptor and its active fragment, NICD. Thus, we used the SMNΔ7 mouse model to determine whether the glia or motoneurons in the lumbar spinal cord exhibited activation of the Notch signalling pathway. We found astroglial overexpression of Jagged and Delta ligands of Notch receptor at symptomatic stage. Increased levels of the active intracellular fragment of the Notch receptor, NICD, were also found in motoneurons, astroglia and microglia, associated to astroglial Jagged and Delta increased expression, at symptomatic stage. We observed that the motoneurons from SMNΔ7 mice at symptomatic stage, overexpressing the active fragment of Notch, expressed less Neurogenin, a protein known to be involved in neuritogenesis.

The depletion of SMN protein in *in vitro* and *in vivo* models is associated to an increased activation of the RhoA/ROCK and Notch signalling pathways resulting in actin cytoskeleton disturbance and decreased Neurogenin expression, thus causing cell migration impairment, loss of synapses onto spinal motoneurons and soma reduction. In addition, the observed gliosis found in the SMNΔ7 mice could contribute to create a detrimental environment in SMA tissue. Therefore, our results suggest that SMA pathogenesis is not only a single process, but a convergence of pathogenic processes in motoneurons and glia which lead to motoneuron specific impairment and later death.

List of Acronyms

AAV	adeno-associated viruses
ASOs	antisense oligonucleotides
BDNF	brain-derived neurotrophic factor
CNS	central nervous system
cDNA	complementary DNA by reverse transcription from mRNA
ESE	exonic splicing enhancer
ESS	exonic splicing silencer
FBS	foetal bovine serum
GFAP	glial fibrillary acidic protein
GFP	green fluorescent protein
HDAC	histone deacetylase proteins
HS	horse serum
IBA-1	ionized calcium binding adaptor molecule 1
ISE	intronic splicing enhancer
ISS	intronic splicing silencer
LV	lentiviral vectors or particles
MLC	myosin light chain II or myosin regulatory chain
MLCP	myosin light chain phosphatase
MLCK	myosin light chain kinase
NAIP	neuronal apoptosis inhibitory protein
NF	neurofilament
NF-κB	nuclear factor-kappaB
NF-H	neurofilament heavy chain
Ngn	neurogenin

NGS	normal goat serum
NHS	normal horse serum
NICD	Notch intracellular domain, also known as cleaved-Notch
NMJs	neuromuscular junctions
iNOS	inducible nitric oxide synthase
nNOS	neuronal nitric oxide synthase
NTF	neurotrophic factors
PNS	peripheral nervous system
RhoA	Ras-homologous guanosine triphosphatase A
RHA	RNA Helicase A
mRNA	messenger ribonucleic acid
RNAPII	RNA polymerase II
shRNA	short-hairpin ribonucleic acid
siRNA	small interfering ribonucleic acid
hnRNP	heterogeneous nuclear ribonucleoproteins
snRNP	small nuclear ribonucleoproteins
ROCK	Rho-associated kinase
SDS	sodium dodecyl sulfate
Sm	Smith antigen protein (a part of core proteins)
SMA	Spinal Muscular Atrophy
SMAs	group of diseases with symptomatology of SMA
SMI-31	antibody anti-phosphorylated NF-H from *Sternberger Monoclonal Inc.*
SMI-32	antibody anti-non-phosphorylated NF-H from *Sternberger Monoclonal Inc.*
SMN1 or SMN^T	Survival Motor Neuron human gene, telomeric copy
SMN2 or SMN^C	Survival Motor Neuron human gene, centromeric copy

Smn	Survival motor neuron non-human gene
SMN	Survival Motor Neuron human protein
SMNΔ7	Survival Motor Neuron protein with a deletion of exon 7
SMNΔ7	human transgene codifying 100% for SMNΔ7 protein
a-SMN	axonal Survival Motor Neuron protein
Syn	synaptophysin
UTR	3′ untranslated region in mRNA

I. INTRODUCTION

I. Introduction

1 Current view of neuroscience & neurodegenerative diseases

After Schleiden & Schwann and Virchow proposed the cell theory in the late 1830s, Gerlach and Deiters suggested that the nervous system was special in the sense that nerve cells are not independent units but instead form a continuous syncytium or reticular net. Camillo Golgi, after developing the silver chromate method, defined the Central Nervous System (CNS) as a continuous net. Nevertheless, the efforts did not end at this point, and the modern neuroscience was born with Santiago Ramón y Cajal (1852-1934), who applied the silver chromate method in brain tissue. He proposed that neurons interact by means of contact or contiguity rather than by continuity. This concept became known as the *neuron doctrine* and thus independent units were finally proven to exist when the electron microscope was used in the 1950s. The greater irony in the neuroscience is that Santiago Ramón y Cajal shared the Nobel Prize for Medicine in 1906 with Camillo Golgi, although they used the same technique to describe opposite views on nervous system organization. In 1931 Santiago Ramón y Cajal wrote *'What a cruel irony of fait to pair like Siamese twins united by*

the shoulders, scientific adversaries of such contrasting characters' demonstrating the great personal friction between them.

1.1 Central Nervous System

The Central Nervous System (CNS) is divided into brain and spinal cord and further divided in regions easily differentiated by dissection. All these structures are composed by neurons, but also by non-neuronal cells, called glia. Neurons in the CNS operate either within layered structures (cerebral cortex, cerebellum) or within clustered groups (nuclei in the CNS or ganglia in the Peripheral Nervous System).

1.1.1 Spinal Cord

The spinal cord is adjoined to the brainstem. Spinal cord (figure 1) is anatomically subdivided in four regions, from the upper to the lower region: cervical (C), thoracic (T), lumbar (L) and sacra (S). The transversal section of each region is anatomically and histologically different from the others.

The grey matter of the spinal cord is subdivided into anterior (AC), posterior (PC) and lateral horn or column (LC) that links with the contra-lateral horn via central grey commissure (CGC). Inside the central grey commissure it is located the central channel (CC).

In the white matter of the spinal cord there are ascendant and descendant fibers grouped in anterior (AF), lateral (LF) and posterior bundles (PF). The medial septum (MS) separates the posterior bundles and the anterior medial fissure (AMF) separates the anterior bundles.

The motoneurons are localized in the anterior horn of the ventromedial (NVm), *ventrolateral* (NVl) and *retrodorsolateral* nucleus (NRd). The sympathetic nuclei *intermediolateralis* (NIl) and *intermediomedialis* (NIm) are located in the lateral column, in the toracolumbar region from C_3 to $L_{2/3}$. The same nuclei from the parasympathetic are located in the sacra region from the S_2 to S_4.

The *dorsomarginal* nucleus (NDm) is composed by interneurons. Their axons are grouped forming the *fasciculi proprii* (FP), localized in the spongy zone (ZSp). The nucleus *proprius* (NP) formed by neurons are located in the Rolando's jelly substance (SGel). The anterior and posterior spinocerebellar tracts are formed by the dorsal nucleus (ND) neurons.

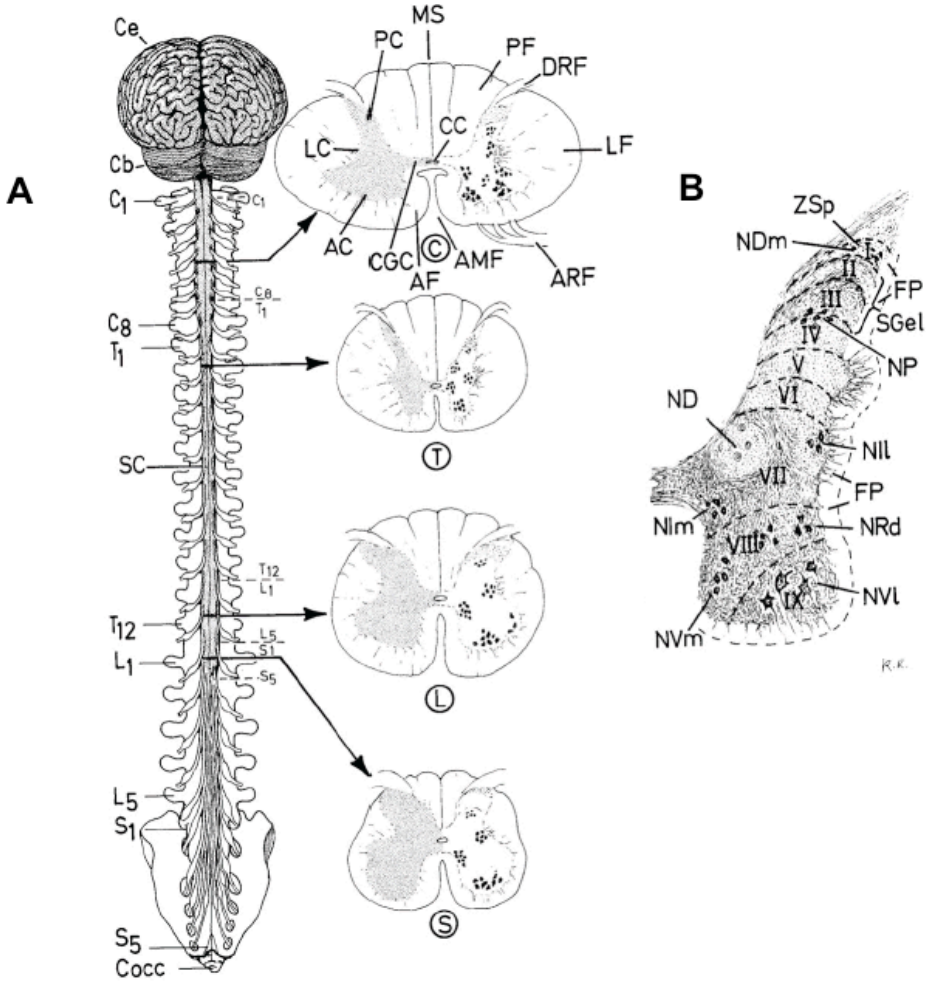

Figure 1: ***Scheme of the human spinal cord.*** (A) Macroscopic structure of the spinal cord. C, cervical; T, thoracic; L, lumbar; and S, sacra regions. The meaning of the abbreviations is explained in the text above. (B) Cell layers in the spinal cord (I to IX) and the distribution along the spinal cord of the neuron soma nuclei (Krsitc, 1997).

1.1.2 Motoneurons and motor unit

Motoneurons are the neurons that innervate the muscles and have been defined as *the final common path* to elicit muscular contaction (Sherrington, 1904). In 1925 Charles Sherrington also introduced the term motor unit to designate the basic unit of motor function, a motoneuron and the group of muscle fibers it innervates.

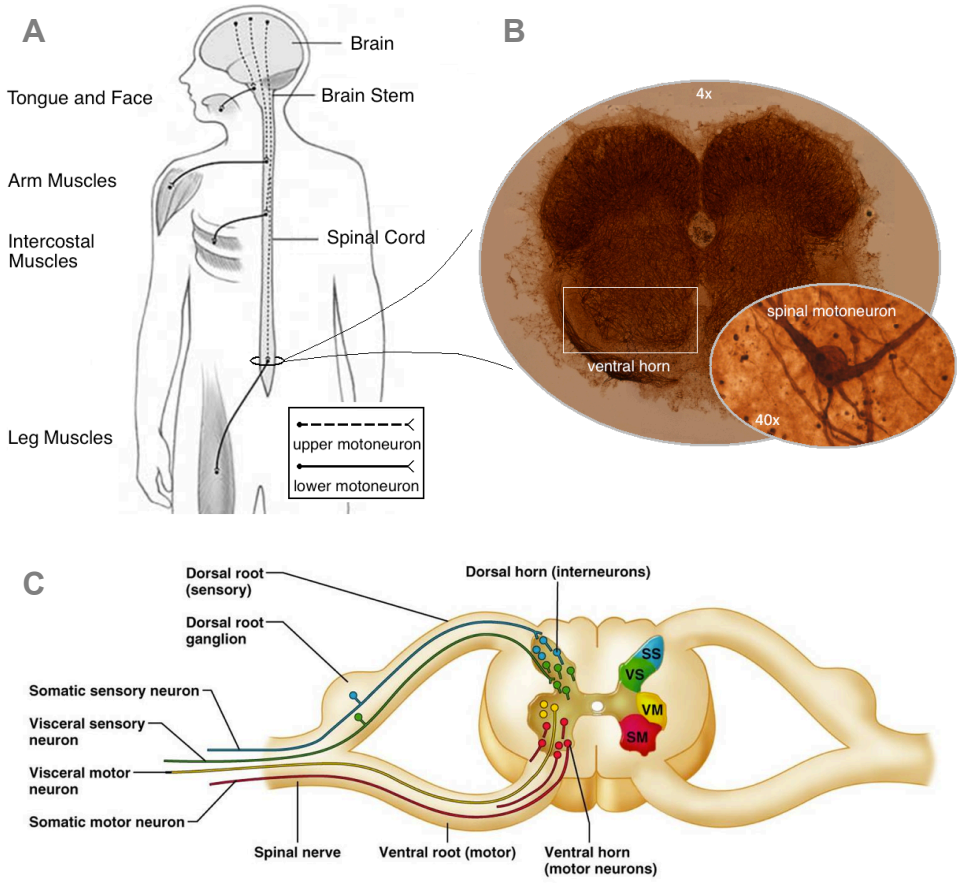

Figure 2: ***Location of motoneurons in the spinal cord.*** (A) Location of the upper and lower motoneurons along the CNS. (B) Spinal cord transversal slide and the location of the spinal motoneurons in the ventral horn. (C) Scheme of the nerons in a section of the spinal cord and the ventral roots formed by the axons of these motoneurons.

We can differentiate between upper motoneurons, or the first motoneuron, and lower motoneurons, or the second motoneuron. Being accurate, upper motoneurons (located in the brain cortex and some nuclei of the brain stem) are actually pre-motoneurons, because they synapse with lower motoneurons or spinal motoneurons (also located in the motor nuclei of the cranial nerves of the brain stem) but not with muscle fibers. Moreover, the spinal motoneurons are divided in three types –alpha (α), beta (β) and gamma (γ) motoneurons– according to the type of muscle fiber that each class innervates. Alpha motoneurons innervate extrafusal skeletal muscle and drive muscle contraction. Beta motoneurons are a non well-known population that innervates both intra and extrafusal skeletal fibers (reviewed by Kanning et al., 2010). Gamma

motoneurons innervate intrafusal muscle fibers of the muscle spindle, drive a slow axonal impulse and play complex roles in motor control. Alpha motoneurons are the most abundant ones, and they can in turn be classified into three subtypes according to the contractile properties of the motor units that they form with target muscle fibers: fast-twitch fatigable, fast-twitch fatigue-resistant and slow-twitch fatigue-resistant (Burke et al., 1973). Motoneurons integrate the signal from the upper motoneurons or local circuitry, such as dorsal root ganglia that control the motor reflex, and control skeletal muscles movement via their axons.

1.1.3 Interaccions neurons & glia

Interactions between neurons and glia is a very important field in modern neuroscience (Squire, 2003). Communication between neurons glia is essential for axonal conduction, synaptic transmission, and nutritional support and thus is required for normal functioning of the nervous system during development and throughout adult life (Fields and Stevens-Graham, 2002). Glia is divided into two groups, macroglia and microglia. Macroglia is the most abundant class of supportive cells and is also divided into astroglia and oligodendrocytes. Astrocytes are interposed between neurons and the vasculature and play a variety of metabolic support roles, such as furnishing energy intermediates and removing excessive extracellular neurotransmitter secretions.

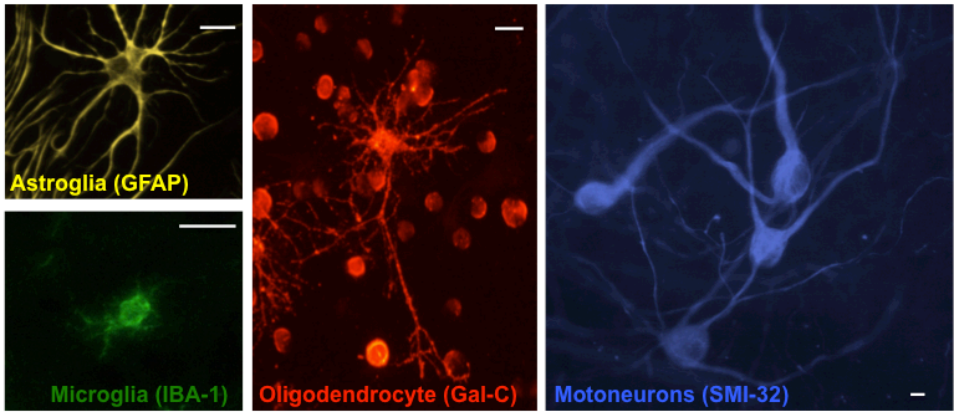

Figure 3: ***Representative images of glia and motoneurons marked by immunofluorescence.*** Astrocytes, yellow, in the upper corner, have been stained with anti-GFAP antibody; microglia, **green**, have been stained with anti-IBA-1 antibody; oligodendroglia, **red**, have been stained with anti-Gal-C antibody; and motoneurons, **blue**, have been stained with anti-SMI-32 antibody. Scale bars = 20 μm.

Oligodendrocytes are myelin-producing cells, and allow accelerated action potential conduction. Microglia is related to the macrophage/monocyte lineage, and during periods of intracerebral inflammation (infection, neurodegenerative diseases or traumatic injury) are recruited into the brain by endothelial signals to remove necrotic tissue and to try to defend against infection (Squire, 2003).

1.2 Neurodegenerative diseases

Neurodegenerative diseases are characterized by the selective loss of neurons in the Central Nervous System (CNS) - brain or spinal cord -. Although the neurodegenerative term implies that neuron loss causes the disease, in some cases neuronal death is merely the final stage of a preceding period of neuronal dysfunction. Temporally discrete insult leads to a localized loss of neurons at the site of injury and causes acute neurodegeneration. The loss of a particular neuronal subtype or generalized loss of neuronal populations is known as chronic neurodegeneration. Amyotrophic lateral sclerosis (ALS) and spinal muscular atrophy (SMA) involve the degeneration and loss of motoneurons in the brain-stem and spinal cord. In the brain, Parkinson disease involves the specific and localized loss of dopaminergic neurons in the *substantia nigra*, whereas Alzheimer disease and Huntington disease result in widespread loss of neurons (Lunn et al., 2011)

Neurodegenerative diseases are characterized clinically by their insidious onset and chronic progression. The onset can be sporadic, inhereited or both. These diseases are often categorized by whether they initially affect cognition (Alzheimer disease, Dementia with Lewi bodies, Prion disorders), movement (Parkinson disease, Huntington chorea), strength (SMA, ALS), coordination (Friedreich ataxia, Spinocerebellar atrophies) and sensation or autonomic control (Multiple sclerosis, Charcot Marie Tooth). However, patients frequently exhibit symptoms and signs referable to more than one system.

1.3 Motoneuron diseases: a type of neuromuscular disorder

It is considered that Edgar Adrian and Deltev Bronk started the study of the motor unit disorders in 1929 introducing the electromyography, a technique for recording the action potential from a single motor unit in human muscles. Nevertheless, physiological techniques are combined nowadays with molecular and cellular analysis to obtain more detailed understanding of the disease of the motor unit.

Most diseases of the motor unit cause weakness and wasting of skeletal muscles. The distinguishing features of these diseases vary depending on which of the four functional components of the motor unit is primarily affected: the cell body of the motoneuron, its axon, the neuromuscular junction, or the muscle fibers it innervates. The term neurogenic refers to the disorders affecting nerve cell bodies or peripheral nerves but only cause minor changes in muscle fibers. These diseases are subdivided into those that primarily affect the nerve cell bodies (motoneuron diseases) and those that primarily affect the peripheral axons (peripheral neuropathies). The term myopathy is used to describe diseases characterized by muscular degeneration but little changes in motoneurons or axons (Kandel et al., 2000).

Table 1: ***Neuromuscular disorders.*** The neuromuscular diseases listed below are classified upon the cause of the onset of the disease. The phenotype of these depends also on the kind of affectation that exhibits the motor unit.

Neuromuscular disorder	Diseases	Phenotype
Muscular dystrophies	Duchenne Muscular Dystrophy (DMD); Becker Muscular Dystrophy (BMD); Emery-Dreifuss Muscular Dystrophy (EDMD); Limb-Girdle Muscular Dystrophy (LGMD).	Defects in the genes that are responsible for normal muscle function.
Cerebral palsy	Cerebral palsy	Difficulty of the brain to control muscles.
Motoneuron diseases	Spinal muscle atrophy (SMA) type I, II, III; Spinal bulbar muscular atrophy (SBMA); Amyotrophic lateral sclerosis (ALS; Lou Gehrig's Disease).	Degeneration of motoneurons in the spinal cord and brain (lead to weakness and atrophy).
Disease of the NMJs	Lambert-Eaton Syndrome (LES); Myasthenia Gravis (MG); Congenital Myasthenic Syndrome (CMS).	Result from a malfunctioning of the NMJs.
Metabolic diseases of the muscle	Mitochondrial myopathy (MITO); Carnitine deficiency (CD); Lactate dehydrogenase deficiency (LDHA).	Inherited defects that interfere with the normal processing of chemical reactions at cellular level.
Diseases of the peripheral nerve	Charcot-Marie-Tooth Disease (CMT); Dejerine-Sottas Disease (DS); Friedreich's Ataxia (FA).	Damaged nerves in the PNS. Numbness and pain in the extremities.
Myopathies	Nemaline myopathy (NM); Periodic paralysis (PP); Central Core disease (CCD).	Usually cause gradual muscle weakness and atrophy closest to the centre of the body.

Disorders in upper motoneurons and their axons result in spasticity, overactive tendon reflexes and abnormal plantar extensor reflex (the Babinski sign). Disorders in lower motoneurons result in atrophy, fasciculations, decreased muscle tone and loss of tendon reflexes.

2 Spinal muscular atrophy

Spinal muscular atrophy was first described in the 1890s by Guido Werdnig of the University of Vienna and Johann Hoffman of Heidelberg University. The cardinal signs of SMA in all patients are muscle weakness and atrophy due to motoneuron loss (Werdnig, 1894; Hoffmann, 1900). With an incidence of 1:10,000, SMA is one of the most frequent autosomal recessive disorders in humans and the leading genetic cause of death in childhood (Pearn, 1978; Lorson et al., 2010).

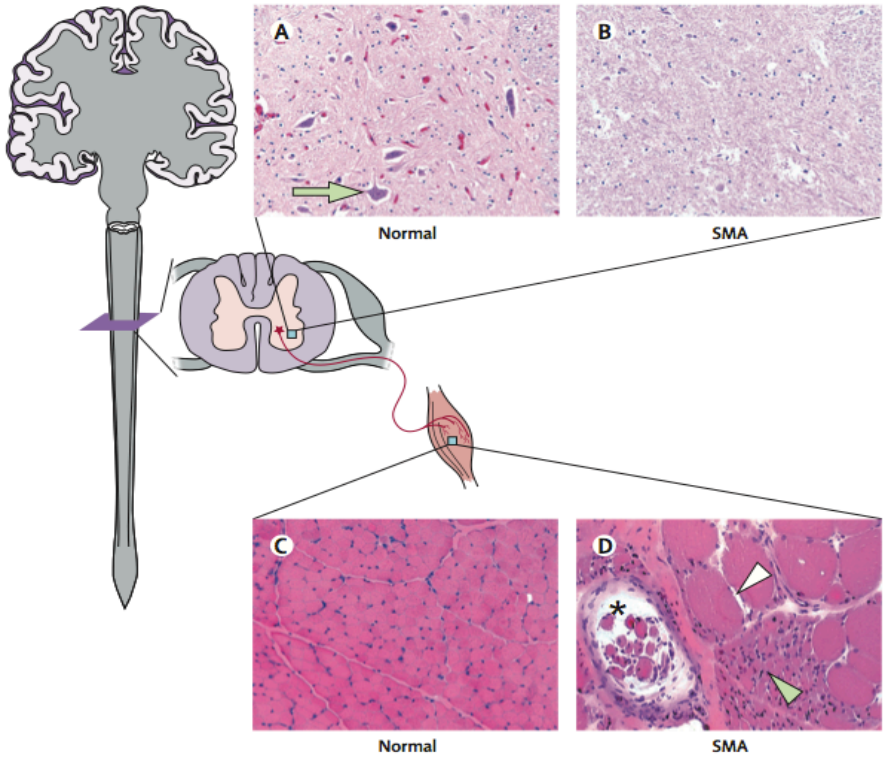

Figure 4: ***Affected spinal cord and muscles in SMA.*** The reduction of α-motoneurons (green arrow, A) in the spinal cord of SMA patients (B), and the presence of hypertrophic muscle fibers (white arrow) surrounded by atrophic fibers (green arrow) in D, are the distinctive histopathogenic features present in SMA patients (B and D) compared with healthy individuals (A and C) (Lunn and Wang, 2008).

2.1 Spinal muscular atrophies: features and classification

When used broadly, the term spinal muscular atrophy describes a collection of inherited and acquired diseases characterized by motoneuron loss in the spinal cord causing muscle weakness and atrophy. These disorders are distinguished by their different clinical presentations, inheritance patterns and causative gene abnormalities. Spinal muscular atrophy (SMA) is also the name given to the most common form of these disorders caused by mutation of the survival motor neuron (*SMN*) gene (Sumner, 2006).

2.1.1 SMAs: proximal SMA and non-5q SMAs

Proximal spinal muscular atrophy belongs to a group of genetically heterogeneous neurodegenerative diseases named Spinal muscular atrophies (SMAs). This group of diseases is characterized by a progressive spinal motoneuron loss, proximal and symmetric weakness and proximal weakness of muscular groups (Monani, 2005; Wirth et al., 2006a).

Table 2: ***SMAs disease group.*** The different forms of human spinal atrophies SMN-linked (proximal SMA) and not linked to SMN gene (non-5q SMA) (Monani, 2005; Wang et al., 2007).

Disease	Inheritance	Locus	Phenotype	Onset
Proximal SMA	Autosomal recessive	5q11.2-13.3	Proximal muscle weakness	Birth – adult
Distal SMA	Autosomal recessive	11q.13	Distal muscle weakness, diaphragmatic involvement	2 m - 20 y
SMARD	Autosomal recessive	IGHMBP2;11q13.2	Distal lower limb weakness, sensory, autonomic neurons also affected	1 – 6 m
X-linked infantile SMA	X-linked	Xp11.3-q11.2	Arthrogryposis, scoliosis, respiratory insufficiency, loss of anterior horn cells	at birth
SBMA (Kennedy's disease)	X-linked	Androgen receptor/ Xq11.2-12	Proximal muscle weakness, lower motoneuron loss, bulbar involvement	30 – 50 y
Distal SMA IV	Autosomal dominant	7p15	Distal muscles affected, bilateral weakness in hands, atrophy of peroneal muscle	12 – 36 y
Congenital SMA	Autosomal dominant	12q23-24	Arthrogryposis, nonprogressive weakness of distal muscles of lower limbs	at birth
Scapuloperoneal SMA	Autosomal dominant	12q24.1-q24.31	Congenital absence of muscles, progressive weakness of scapuloperoneal and laryngeal muscles	-
SMA with pontocerebellar hypoplasia	Autosomal recessive	-	Cerebellar and brainstem hypoplasia, neuronal loss in basal ganglia, cortical atrophy	0 – 6 m

The autosomal recessive proximal SMA is the most common disease of this group, being 95% of SMA cases proximal SMA, that is the reason why proximal SMA is known as SMA. But SMAs group also includes distal SMA or autosomal dominant, SMA linked to X chromosome, spinal bulbar muscular atrophy (SBMA), spinal muscular atrophy with respiratory distress and congenital SMA, all of them with a much lower incidence degree (Monani, 2005; Wirth et al., 2006a).

2.1.2 Proximal SMA

Proximal spinal muscular atrophy – hereafter referred as SMA– is a recessively inherited neuromuscular disease characterized by degeneration of spinal cord motoneurons, resulting in progressive muscular atrophy and weakness (Wang et al., 2007). The common feature of all SMA types is weakness that is usually symmetrical and more proximal than distal -in the limbs, the proximal muscles are more affected than distal ones-. However, the legs are more impaired than the arms, and the arms are more impaired than the face and diaphragm. Moreover, tendon reflexes are absent or diminished and sensation is preserved (Sumner, 2007). Nonetheless, there is a wide spectrum of phenotypic severity, while type I patients often dye before 2 years of age, some type IV patients experience only modest weakness and live a normal life span. Taking this into account, SMA has been divided into five types depending on the onset, that determines the severity of the disease, and the symptoms, as it was determined in Consensus Statement for Standard of Care in Spinal Muscular Atrophy by the International Standard of Care Committee for Spinal Muscular Atrophy (Wang et al., 2007).

Table 3: ***Proximal spinal muscular atrophy forms.*** Summary of the most important features in each type of SMA (Briese et al., 2005; Monani, 2005; Wirth et al., 2006a; Briese et al., 2006; Wang et al., 2007; Lunn and Wang, 2008).

Disease Name	Type		Age of Onset	Highest Function	Age of death
Embryonic form; prenatal form; congenital form	**0**		Embryonic	-	Neonatal
Werdnig-Hoffmann disease; Acute form; Severe form	**I**	**a** **b** **c**	Neonatal 0-6 m >6 m	Never sits	< 2 y
Intermediate form; Chronic form; Dubowitz disease	**II**		7-18 m	Never stands	> 2 y
Kugelberg-Welander disease; Juvenile form; Mild form	**III**	**a** **b**	18 m - 3 y > 3 y	Stands & walks	Adult
Adult form	**IV**		2nd or 3rd decade	Walks during adulthood	Adult

Although most patients with SMA manifest homozygous mutations involving the *SMN1* gene (95%), a phenotypic classification owing to severity is confused and there are patients that show intermediate phenotypes between forms due to modifying genes (Markowitz et al., 2012).

2.1.3 SMA type 0 – embryonic form – congenital form

SMA type 0 is diagnosed in infants that are born so weak that are able to survive only a few weeks. Decreased intrauterine movements suggest prenatal onset of the disease. Severe weakness and joint contractures are present at birth (MacLeod et al., 1999; Dubowitz, 1999). Weakness evolves within the first few months of life. There is general hypotonia, with axial and limb weakness. Whereas the diaphragm is spared, allowing adequate spontaneous respiratory activity, the intercostal muscles are always affected. With rare exception they die a few months after birth (Pearn, 1973; Dubowitz, 1999). Nevertheless, some researchers do not differentiate between type 0 and type I SMA.

2.1.4 SMA type I – Werdnig-Hoffmann disease – severe form – acute form

This type was originally described by Werdnig & Hoffmann in 1890s and is the most severe form with onset in childhood. It is called SMA type I or Werdnig-Hoffmann disease (Werdnig, 1894; Hoffmann, 1900). It is the most common type, affecting about 50% of patients diagnosed with SMA (Markowitz et al., 2004). The onset of the disease, in type I, is before 6 months of age and death within the first 2 years of life. The patients are distinguished by a profound hypotonia, in the limbs and trunk, symmetrical flaccid paralysis, and impaired head movement control, with a weak cry and cough. They are unable to sit and exhibit spared diaphragm, combined with weakened intercostal muscles, that results in characteristic paradoxical breathing and a bell-shaped trunk. The tongue may show atrophy and fasciculation due to bulbar denervation, with poor suck and swallow before 1 year of age (Pearn and Wilson, 1973; Wang et al., 2007; Lunn and Wang, 2008).

2.1.5 SMA type II – Dubowitz disease – chronic form

SMA type II disease, in some sources also known as Dubowitz disease, is characterized by onset between 7 and 18 months of age. The defining characteristic of these patients is an ability to sit unaided and a few are able to stand with leg braces, but none are able to walk independently. Fine tremors with extended fingers or handgrips are common. Poor bulbar function determine weak swallowing that leads to poor weight gain. Moreover, clearing of tracheal secretions and coughing become difficult. Respiratory insufficiency is a frequent cause of death during adolescence owing to weak intercostal muscles (Pearn, 1978; Zerres and Rudnik-Schöneborn, 1995).

2.1.6 SMA type III – Kugelberg-Welander disease – mild form

The SMA type III was defined by Kugelberg and Welander in 1952, but also studied by Wohlfart in 1955, that is why this syndrome is also known as Wohlfart-Kugelberg-Welander disease (Wohlfart et al., 1955; Kugelberg and Welander, 1956). They evidence profound symptom and age of onset is heterogeneous. This form is subclassified into 3a and 3b, depending on the onset before (3a) or after (3b) 3 year age. Patients typically reach independent walking, however some are only ambulatory after 40, whereas some might continue to walk and live productive adult lives with minor muscular weakness after 40. These patients frequently develop scoliosis, joint overuse symptoms and muscle aching, generally caused by weakness. Swallowing, cough and nocturnal hypoventilation are less common than in more severe forms (Garvie and Woolf, 1966; Wang et al., 2007; Lunn and Wang, 2008).

2.1.7 SMA type IV – adult form

Patients with SMA type IV usually exhibit onset of muscular weakness in the second or third decade of life. Motor impairment is mild without respiratory or gastrointestinal problems, and normal weight gain. Patients are able to walk in adult years and life expectancy is the same as healthy individuals (Wang et al., 2007; Lunn and Wang, 2008).

2.2 Genetic bases of SMA

Almost a century after the initial description of SMA, a new era of research of SMA was inaugurated when Conrad Gilliam and his group at Columbia University established genetic linkage for this motoneuron disorder to chromosome 5q (Brzustowicz et al., 1990). In a period of 10 years an extensive international effort had been made to identify the gene that determines SMA and it was documented in over 50 papers by 240 authors. One early spin-off of this search was the discovery that the genetic instability of SMA-critical region of chromosome 5q is likely responsible for the high incidence and worldwide distribution of SMA (Carpten et al., 1994; Theodosiou et al., 1994; Thompson et al., 1995; Crawford, 1996). In 1995, the search had narrowed sufficiently for two neighboring but dissimilar candidate genes for the disorder (Lefebvre et al., 1995; Roy et al., 1995a). The arguments strengthening the candidacy of each of these two genes contrasted strong biologic plausibility against high genetic probability. Neuronal apoptosis inhibitory protein gene (*NAIP*), the plausible candidate, has displayed anti-apoptotic function that matches perfectly with a standing hypothesis of SMA as developmental disorder. Survival motor neuron

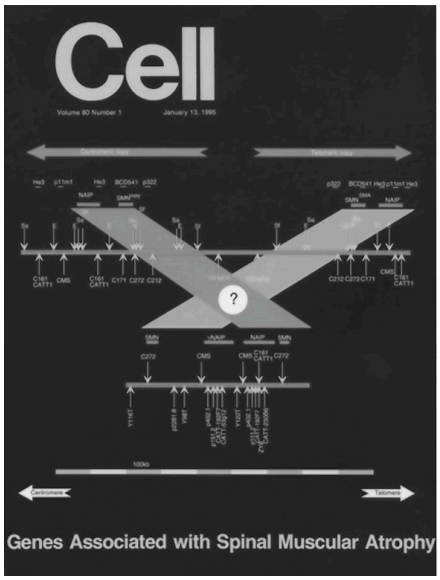

gene (*SMN*), the probable candidate, was shown to be deleted in over 95% of SMA patients (Crawford and Pardo, 1996; Wirth et al., 2006b).

Figure 5: SMN, *the SMA determining gene, in the cover of the Cell journal.* The *SMN* location in locus 5q was the cover of one of the most relevant journals for biomedical sciences (from the cover of Cell, volume 80, Number 1, January, 1995), because of the work published inside by Lefebvre et al. (Lefebvre et al., 1995).

2.2.1 Survival Motor Neuron genes (*SMN*)

In late 1995, the survival of motor neuron gene (*SMN*) was identified as the SMA disease-determining gene. It was mapped to chromosome 5, in the *locus* 5q13, that is a region where large-scale deletions had been reported (Lefebvre et al., 1995).

The group headed by Judith Melki described the inverted duplication of a 500 kb element in normal chromosomes and narrowed the critical region to 140 kb within the telomeric region. This interval contained a 20 kb length gene encoding a novel protein of 294 amino acids, the Survival Motor Neuron protein (SMN). A highly homologous gene was present in the centromeric element of controls (figure 6A). The telomeric copy (initially named SMN^T) was designed as *SMN1* gene, whereas the centromeric copy (SMN^C) was designed as *SMN2* gene (Lefebvre et al., 1995; Bürglen et al., 1996).

The *SMN* gene consists of nine exons interrupted by eight introns. The exon 2 is, in fact, composed of two exons separated by an additional intron (figure 6B). They referred to exons 2a and 2b to avoid modifications in the numbering of the following exons (especially exons 7 and 8), in which nucleotide substitutions allowed the *cBCD541* and *SMN* genes to be distinguished. All exon–intron boundaries display the consensus sequence found in other human genes (Bürglen et al., 1996).

The two *SMN* copies are almost identical except for 5 base pair exchanges (figure 6B) that are all localized within the 3' end of the genes. However, only the C-to-T transition at position +6 of exon 7 is localized within the coding region. Although it is a silent mutation and therefore not affecting the amino acid sequence of the encoded protein, it severely affects the correct splicing of exon 7 (Lorson et al., 1999; Monani et al., 1999a). This mutation is responsible for alternatively spliced transcripts that lack exon 7, that is specific from *SMN2* transcripts (Lorson et al., 1999).

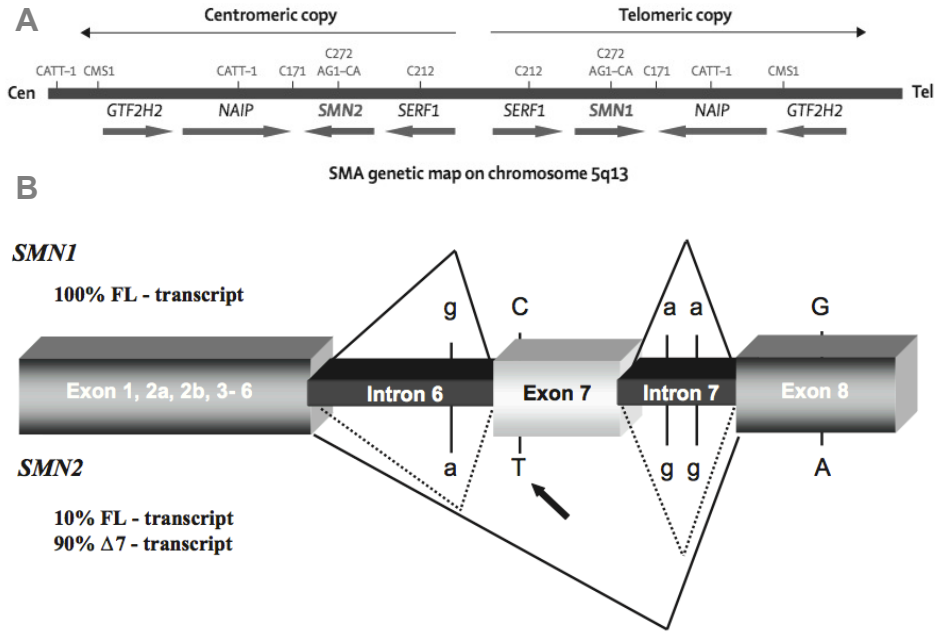

Figure 6: SMN, *the SMA determining gene.* (A) *SMN* location in locus 5q is surrounded by *NAIP* both in telomeric and centromeric copies. (B) Genomic structure, nucleotide, and splicing differences between *SMN1* and *SMN2*. *SMN1* differs from *SMN2* in 5 nucleotide exchanges. Only C-to-T in exon 7 is localized within the coding region, but it is a translationally silent mutation. Therefore, *SMN1* and *SMN2* might codify for identical proteins. However, in 90% of spliced *SMN2* mRNA, exon 7 is skipped. Adapted from (Wirth et al., 2006a; Lunn and Wang, 2008).

The *SMN1* transcripts are named *full length* SMN (fl-SMN) because in the splicing process there are no deletions, and the resultant protein is fully conserved. On the other hand, transcripts from *SMN2* have predominantly a deletion of exon 7, that is an isoform of SMN protein, named SMNΔ7, and is characterized by lacking the last C-terminal 16 residues (Lefebvre et al., 1995).

2.2.2 Molecular bases of SMA

The absence of *SMN1* copies is the cause of the SMA pathology. Whereas all the healthy individuals have at least one copy of the *SMN1* gene and 90 to 95% of them have different number of copies of the *SMN2* gene, all SMA patients have at least one copy of *SMN2*, but any copy of *SMN1* (Sumner, 2007). All the individuals with only one copy of the *SMN1* are carriers; the observed 1:35 carriers ratio was determined by direct molecular genetic testing (Feldkötter et al., 2002; Cusin et al., 2003). Mutations of *SMN1* and *SMN2* on both chromosomes have not been reported. Such a genotype would likely be responsible for either an extremely severe form of SMA or a non-viable foetus (Frugier et al., 2002). This hypothesis has been reinforced by the observation of early embryonic lethality resulting from *SMN* knock-out in other organisms in which *SMN* orthologue is not duplicated (Monani et al., 2000a).

In contrast to *SMN1* that almost exclusively produces correctly spliced full-length fl-SMN transcripts, *SMN2* produces only 10% fl-SMN transcripts but 90% of SMNΔ7. Healthy individuals, with at least one *SMN1* copy, can produce enough fl-SMN. On the other hand, SMA patients, without any copy of *SMN1*, have only 10% fl-SMN transcripts and 90% of SMNΔ7 transcripts from pre-mRNA *SMN2* splicing (Lefebvre et al., 1995). However, severity of disease might be dependent on the efficiency of *SMN2* splicing, and production of a full-length transcript of *SMN2* could range from 10% to 50% (Gavrilov et al., 1998). This low level of SMN protein allows embryonic development, but is not sufficient to sustain the survival of motoneurons in the spinal cord (Lunn and Wang, 2008).

A fundamental step in the molecular pathogenesis of spinal muscular atrophy is the altered splicing of SMN2-derived transcripts, compared with SMN1-derived transcripts. SMN exon 7 spans 54 bp and is characterized by a weak 3′ splice site (Lim and Hertel, 2001). Several groups have provided enough evidences that the C-to-T transition in *SMN2* dramatically increases exon 7 exclusion (Lorson et al., 1999; Monani et al., 1999a). In all cells, splicing is carried out by a complex macromolecular machine known as the spliceosome, which recognizes sequences at exon/intron junctions called the 5′ and 3′ splice sites. Additional auxiliary splicing elements are required to be recognized by the splicing machinery. Inclusion of exon 7 into SMN mRNA is regulated by a large number of positive-acting cis elements, so-called exonic splicing enhancers (ESEs) or intronic splicing enhancers (ISEs) and by negative-acting cis elements termed exonic splicing silencers (ESSs) or intronic splicing silencers (ISSs). These cis elements are recognized by trans-acting splicing proteins: serine-arginine–rich (SR) proteins or SR-like proteins and heterogeneous nuclear ribonucleoproteins

(hnRNPs) (Lorson and Androphy, 2000; Cartegni and Krainer, 2002; Kashima and Manley, 2003).

Full-length SMN transcript, encoded by 9 exons (1, 2a, 2b, 3-8), only includes exons 1-7 into translated SMN protein. Two models have been proposed to explain the inhibitory effect of the C-to-T transition in *SMN2* on exon 7 inclusion:

· The **enhancer model** proposes that *SMN1* exon 7 contains a heptamer sequence motif, localized at the 5′ end of SMN exon 7, that recruits the splicing factor SF2/ASF, which promotes exon 7 inclusion. However, when this ESE sequence is destroyed by the C-to-T transition (U in messenger RNA) in SMN2, such that SF2/ASF is not recruited anymore, the 3′ splice site is not recognized, and exon 7 is excluded (Cartegni and Krainer, 2002).

· According to the **silencer model**, in contrast, the C-to-T transition creates an exonic splicing silencer element (ESS) for hnRNP A1, a splicing factor that enhances the skipping of exon 7 (Kashima and Manley, 2003). Meanwhile, it was found that hnRNP A1 indeed has a strong inhibitory effect on exon 7 inclusion, but this observation is independent of the C-to-T transition and, therefore, an indirect event not specific to *SMN2* (Cartegni et al., 2006).

Both models are not necessarily mutually exclusive, and it may be that both mechanisms are simultaneous. Trying to combine both theories, one study showed that hnRNP A1 might antagonise the SF2/ASF exonic splice enhancer effect to promote exclusion of exon 7, especially in SMN2, where this exonic splice enhancer is inactivated. However, the exact mechanism surrounding exon 7 inclusion or exclusion (figure 7) during pre-mRNA splicing remains undetermined (Cartegni et al., 2006).

Furthermore it has also been shown that downstream of the heptamer motif, in the central part of exon 7, a strongly acting purin-rich (AG-rich) ESE region is recognized by the SR-like splicing factor Htra2-β1 (Hofmann et al., 2000). The function of Htra2-β1 is enhanced by interaction with a number of further splicing proteins (SRp30c, hnRNP G, and RBM), which all together facilitate the inclusion of exon 7 (Hofmann and Wirth, 2002). This interplay between this ESE, Htra2-β1, and the other splicing factors is most likely responsible for the 10% of correctly spliced fl-SMN2 transcripts. It has been demonstrated that overexpression of Htra2-β1 restored the fl-SMN2 transcript level to almost 80% (Hofmann et al., 2000; Hofmann and Wirth, 2002).

More ESS, ISE and ISS have been described so far. One ESS consisting of 7 nucleotides has been found further downstream near the 3′ end of exon 7 (Singh

et al., 2004). One among several ISEs and ISSs in introns 6 and 7, the intronic splicing silencer ISS-N1, is supposed to exert a strong effect on the activity of the other positive cis elements in exon 7 and intron 7, but its importance in exon 7 skipping is still unclear (Miyajima et al., 2002).

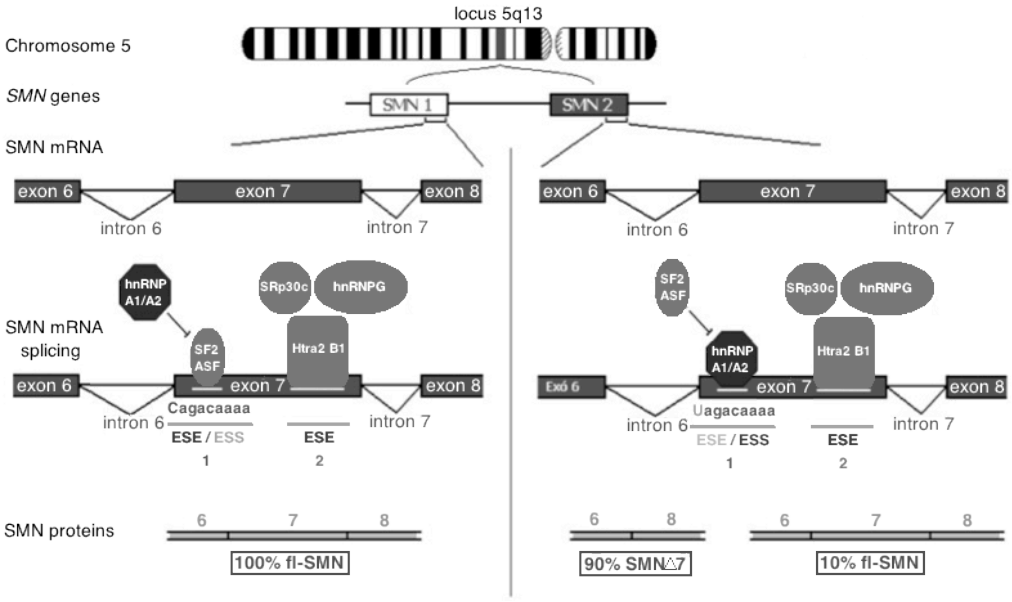

Figure 7: ***Molecular mechanisms of exon 7 inclusion or exclusion in SMN protein: splicing regulation of SMN exon 7.*** *SMN1* exon 7 contains ESE sequence at the 5′ end (ESE 1) that is recognized by the SR-protein SF2/ASF (left side). In *SMN2* (right side), the C-to-T transition disrupts the critical ESE sequence, and the splicing factor SF2/ASF cannot bind anymore to exon 7, which results in skipping of this exon. Furthermore, the C-to-T transition in *SMN2* exon 7 promotes an inhibitory effect of hnRNP A1 and thus facilitates the exclusion of exon 7. Both *SMN1* and *SMN2* contain an ESE in the central part of exon 7 (ESE 2) that is recognized by Htra2-β1 and its interacting partners hnRNP G and SRp30c. Altogether, they facilitate the inclusion of exon 7 in both SMN mature mRNA. ESE 2 domain must be intact for the production of fl-SMN transcripts. ESE: exonic silencer enhancer.

2.2.3 Influence of the number of *SMN2* copies on SMA phenotype

Since ≈ 95% of SMA patients were determined to be homozygously lacking exon 7 of the *SMN1* gene, regardless of clinical phenotype (Lefebvre et al., 1995), genotype-phenotype correlation for SMA has not been straightforward. However, additional research have shown that deletions of *SMN1* are more common in severely affected patients with type I SMA, whereas gene conversions between the *SMN1* and *SMN2* genes are associated with a milder disease phenotype (Burghes 1997; Campbell et al. 1997; DiDonato et al. 1997; McAndrew et al. 1997; Simard et al. 1997). The chromosomal region where SMA

is located is highly unstable, and gene conversion events of *SMN1* to *SMN2* mean that the *SMN2* gene copy number varies in the population (figure 8).

The *SMN2* copy number in SMA patients has a very important modifying effect on disease severity (Parsons et al., 1998). First evidence for a putative gene dosage effect was determined studing Spanish SMA patients (Velasco et al., 1996). Most patients with SMA type I have 1 or 2 *SMN2* copies; most patients with SMA type II carry 3 *SMN2* copies; type IIIa SMA patients, 3 *SMN2* copies; type IIIb SMA patients, 4 *SMN2* copies; and type IV, 4 to 6 *SMN2* copies (table 4) (Feldkötter et al., 2002). In spite of this, it has been reported one family where three unaffected family members of SMA patients, with confirmed *SMN1* deletion, were shown to have only five copies of *SMN2* (Prior et al., 2004). Moreover, there have been reported scattered families in whom notably different degrees of disease severity were present in siblings with the same *SMN2* copy number (Parano et al., 1996). It has been shown that eight *SMN2* copies fully protect from developing SMA (Brahe, 2000). These cases demonstrate that phenotype does not correlate uniquely with the gene dosage.

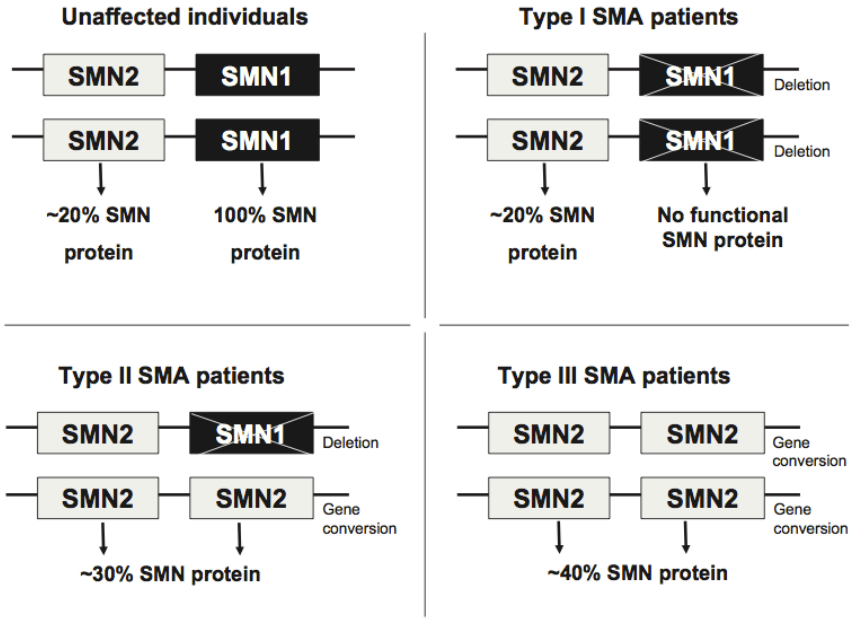

Figure 8: ***Relation between* SMN1 *to* SMN2 *gene conversion and SMA phenotype.*** Healthy individuals exhibit normal copy number of *SMN1* (top left). In type I patients, the *SMN1* deletions suppose no *SMN2* copies apparition (top right). In type II patients, at least one copy of *SMN1* is converted into *SMN2* gene. In type III patients, both copies are converted into *SMN2* gene (Wirth et al., 2006a).

Genotype-phenotype correlation for SMA also has been demonstrated at the protein level: the reduction of SMN protein in patients has been found to be directly correlated with the severity of the SMA phenotype (Coovert et al. 1997; Lefebvre et al. 1997). Because each *SMN2* copy produces about 10% of fl-SMN, more copies of *SMN2* gene improve pathogenic phenotype of SMA patients and thus influence the severity of SMA. Production of fl-SMN2 versus SMN2Δ7 transcripts in type I, II and III SMA patients (table 4) showed a ratio of 20:80 in type I, 30:70 in type II, and 40:60 in type III SMA patients. High differences of protein level are found when comparing type I-II SMA patients with type III patients and healthy individuals (Helmken et al., 2003). In cell lines isolated from patients, it has been demonstrated that augmented levels of full-length *SMN2* transcript and SMN protein correlate with augmented copy number of the *SMN2* genes and diminished disease severity (Lefebvre et al., 1997; Coovert et al., 1997).

Transgenic SMA mice carrying 2 to 8 copies of the human *SMN2* gene on a Smn-knock-out background exhibit different phenotypes; whereas animals with 2 copies only live for 5 days, 8 copies rescues this phenotype to normal lifespan in these mice (Hsieh-Li et al., 2000; Monani et al., 2000b). Moreover, overproduction of SMN2Δ7 transcripts in severe background SMA mice (*Smn-/-;SMN2+;SMN2Δ7)* revealed an increased lifespan compared with transgenic mice with only severe background (*Smn-/-;SMN2*+) (Le et al., 2005).

Table 4: ***SMA phenotype depending on* SMN2 *copies and fl-SMN transcripts.*** Phenotype is determined directly by the ratio of fl-SMN/SMNΔ7 transcripts, and indirectly by the number of *SMN2* copies.

Disease Name	Type		*SMN2* copies	fl-SMN/SMNΔ7 transcipts
Embriogenic form	**0**		Probably 0	-
Werdnig-Hoffmann disease; Acute form; Severe form	**I**	**a** **b** **c**	1 or 2	20 : 80
Intermediate form; Chronic form	**II**		3	30 : 70
Kugelberg-Welander disease; Juvenile form; Mild form	**III**	**a** **b**	3 4	40 : 60
Adult form	**IV**		4 to 6	-
Non-Affected individuals			< 7	-

3 SMN protein

The *SMN1* gene codifies for a 38 KDa protein of 294 amino acids, with a stop codon located in exon 7, and no significant homology to any other protein (Frugier et al., 2002). This protein, called Survival Motor Neuron protein (SMN) has been highly conserved through evolution, being also present in yeasts (*Schizosaccharomyces pombe*), indicating an essential role in evolution (Hannus et al., 2000). SMN is ubiquitously expressed and has been detected in human and mammal liver, muscle, lung, kidney, pancreas and central nervous system (Lefebvre et al., 1995; Novelli et al., 1997; Carvalho et al., 1999). Immunohystochemical studies have revealed a widespread, but not ubiquitous, expression of SMN in the CNS of humans and mammals (Francis et al., 1998), and it is most abundantly expressed in α-motoneurons (Coovert et al., 1997; Battaglia et al., 1997). In this spinal motoneuron, at cellular level, this protein is present in cytoplasm, nuclei and neurites – both axon and dendrites (Briese et al., 2006).

Expression of SMN is developmentally regulated (figure 9), and the highest levels are present during prenatal development as was shown in rat and chicken tissues (Zhang et al., 2003; Setola et al., 2007). It has been proposed that SMA diseases process could start when SMN levels fall below a critical threshold and the severity depends, in part, on when this decrease occurs during development (Sumner, 2007).

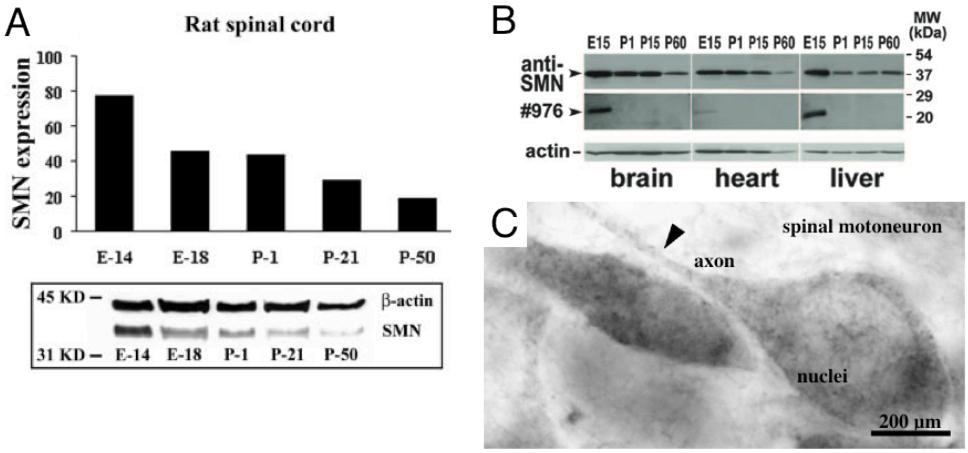

Figure 9: ***SMN protein is widely expressed along development and among tissues.*** (A) SMN decreases its expression during development. (B) SMN is expressed in brain, heart and liver, and it is also down-regulated during development. (C) SMN is distributed in motoneurons along axons and in nuclei (adapted from Zhang et al., 2003; Briese et al., 2006; Setola et al., 2007).

The concentration of the SMN protein (table 4) is crucial in the genotype-phenotype correlation for SMA. The lessening of SMN protein in patients directly correlates with the severity of the SMA phenotype (Coovert et al. 1997; Lefebvre et al. 1997).

SMN associates with several proteins to form a large multiprotein complex (figure 10). This complex is located both in cytoplasm and nucleus, where is concentrated in a structure called gems (for gemini of coiled bodies), most often associated with or identical to Cajal bodies, depending of cell type and tissue (Liu and Dreyfuss, 1996).

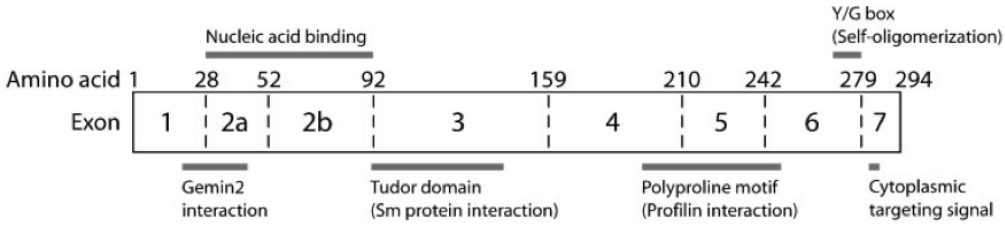

Figure 10: ***SMN protein primary structure scheme and binding sites.*** Schematic diagram of SMN showing amino acids, coding exons and the relative localization of selected domains with known functions (Briese, 2005).

3.1 fl-SMN functions

Since the functional SMN protein was determined to be critical for SMA development, it would be of great interest to know its exact cellular functions. Initially, it was speculated that this protein might have an exclusive neuronal function and that loss of its tissue-specific functions initiates the disease. However, SMN is a ubiquitously expressed protein, initially described as a housekeeping protein.

Nowadays, SMN protein has been demonstrated to have both common and cellular-specific functions. Three housekeeping functions and one neuronal-specific are accepted as SMN principal functions, but more roles have been proposed recently.

3.1.1 SMN housekeeping functions

Almost every protein-coding gene in humans includes non-coding sequences, known as introns. Splicing is the post-transcriptional process in which these introns are excised from precursor mRNA molecules (pre-mRNA) and the coding exons are ligated, forming the mature protein. Proteins that bind to regulatory elements within pre-mRNAs often affect the efficiency of this basic splicing reaction (Blencowe, 2000). The splicing reaction is promoted and controlled by a macromolecular entity named spliceosome. Its functional subunits are uridine-rich small nuclear ribonucleoproteins particles (U snRNPs), which are composed of one (U1, U2, U5) or two (U4/U6) uridine-rich RNAs together with other non-snRNP proteins (Will and Lührmann, 2001; Jurica and Moore, 2003). U snRNPs are key players in splicing because they recognize and activate intronic sites for splicing (Blencowe, 2000).

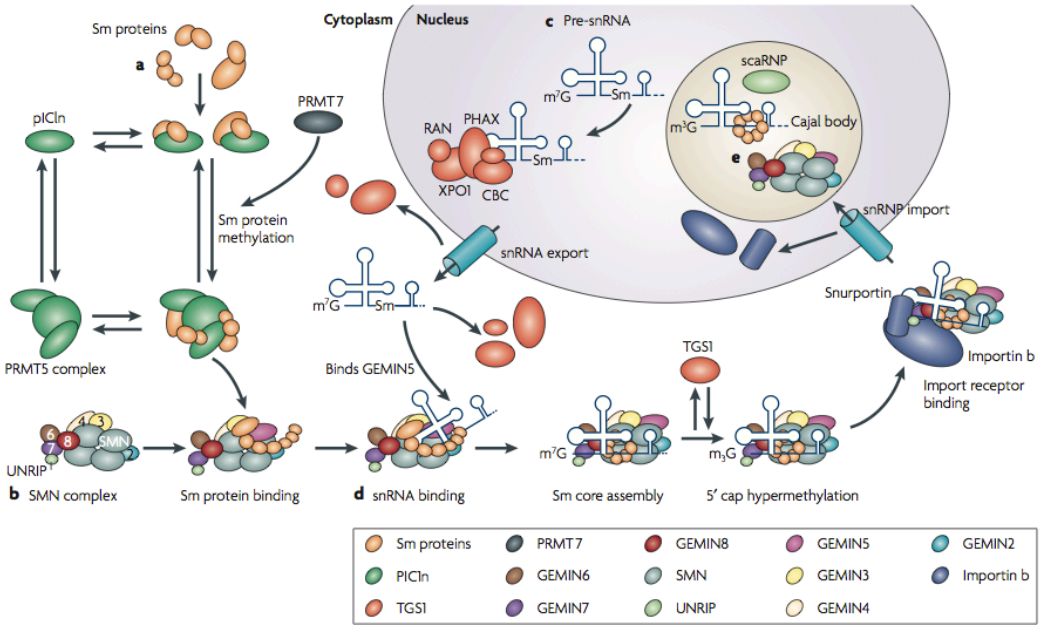

Figure 11: ***SMN protein complex function in snRNP assembly.*** (a) Seven Sm proteins form the Sm complex in cytoplasm, and bind with the SMN complex. (b) SMN complex is formed by Gemins 2-8 and SMN monomers. The exact number of SMN monomers is still unknown. (c) snRNA is transcribed in the nucleus and then binds the export proteins which transport it to the cytoplasm. (d) SMN complex with an assembled snRNP is transported into the nucleus. (e) In the nucleus, the SMN complex and snRNPs localize to the Cajal body and the snRNPs undergo further maturation (Burghes and Beattie, 2009).

Spliceosomes and their U snRNP subunits are formed in a highly ordered process (figure 11). Seven so-called Sm proteins, which are common to all spliceosomal U snRNPs, are assembled on the U snRNA to form the core structure of these particles (Kiss, 2004). These 'Sm core domains' of U snRNPs receive the SMN complex formed by SMN and a set of common 'core' proteins, termed Gemins from 2 to 8, and several transient sub-stoichiometric factors, which confer specific activities to each snRNP (Will and Lührmann, 2001). The reduction of SMN levels, as it occurs in SMA patients, impairs the assembly of U snRNPs (Feng et al., 2005; Wan et al., 2005), and inefficient supply of these splicing factors presumably compromises the outcome of splicing. Therefore, it is thought that the assembly of U snRNP core structures requires assistance by the SMN protein in vivo (Eggert et al., 2006).

Two other housekeeping functions have been described for SMN (figure 12). One function links SMN with the catalytic steps of pre-mRNA splicing, where SMN is proposed to be a recycling factor that regenerates U snRNPs after splicing catalysis (Pellizzoni et al., 1998).

Another SMN housekeeping function has been revealed to be an association of SMN with RNA helicase A (RHA) and RNA polymerase II (RNAPII), raising the possibility that SMN has a role on gene expression (Pellizzoni et al., 2001).

Despite improvement in the understanding of the function of SMN in assembly and regeneration of snRNPs, it is still unclear the cause for motoneuron-specificity in SMA. There is still no evidence that abnormalities of spliceosomal snRNP biogenesis and metabolism cause defects in motoneuronal mRNA splicing from mouse models or SMA patients (Rossoll et al., 2003).

3.1.2 SMN neuron-specific function

It was supposed to be at least one function of SMN unique to motoneurons which might explain specific motoneuron death in SMA. One specific role of SMN in neurons is the axonal transport of mRNA (Rossoll et al., 2003). This neuron-specific function of SMN was proposed after it was described that SMN interacts with hnRNP protein R and Q in motoneuron axons, proteins that bind to the 3′ untranslated region (UTR) of β-actin mRNA (Mourelatos et al., 2001; Rossoll et al., 2002). SMN is present in the axon and growth cones of motoneurons (Jablonka et al., 2001; Fan and Simard, 2002), but not colocalizing with Gemin2 – essential component of complexes that assemble snRNPs - (Jablonka et al., 2001). This finding suggests that SMN might have additional functions in axons of motoneurons other than snRNP assembly. Also one prerequisite for this hypothesis is the movement of SMN along axons (Zhang et al., 2003). Moreover, accumulation of neurofilament (NF) in cell body and at the

motor endplate in motoneurons had been demonstrated after SMN depletion in mouse models (Cifuentes-Diaz et al., 2002). Also, fluorescence imaging has confirmed the association of the SMN protein with axonal microtubules (Pagliardini et al., 2000).

It has been demonstrated that SMN plays a role in axon outgrowth, guidance and the formation of neuromuscular junctions (NMJs) in vertebrate and invertebrate models of SMA. In this sense, functional deficit and arrest of postnatal development of the NMJs have been described in SMA mouse models (Murray et al., 2008; Kariya et al., 2008; McGovern et al., 2008; Kong et al., 2009). Electrophysiological analysis shows that the number of synaptic vesicles that release neurotransmitter during an action potential is decreased (Kong et al., 2009). Moreover, a reduction in the number and in the section of axons in mouse models has been described (Kariya et al., 2008).

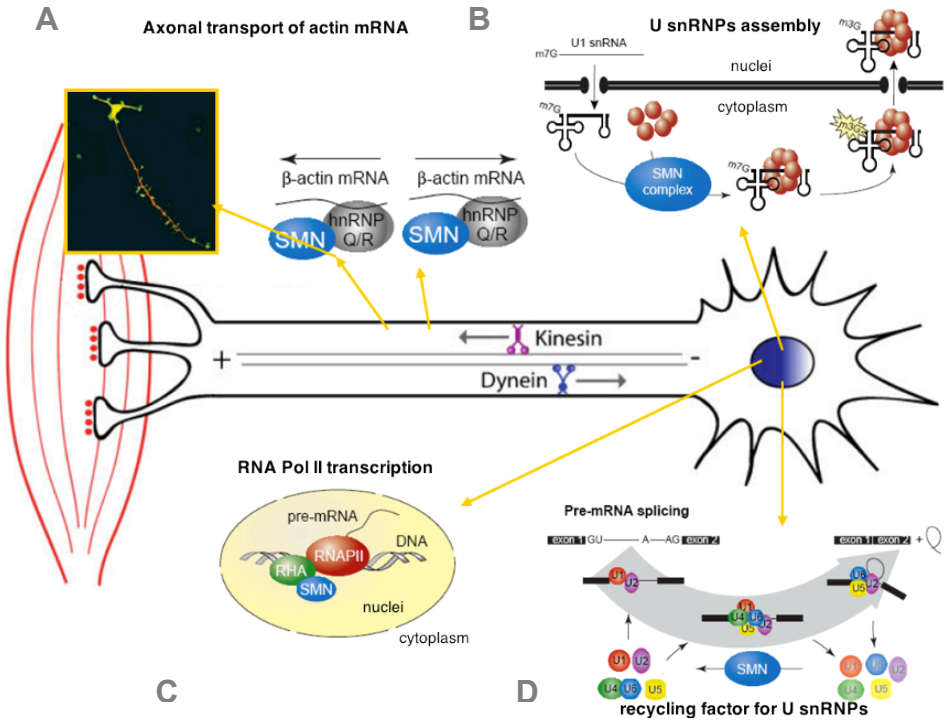

Figure 12: ***Main SMN protein functions.*** (A) Neuron-specific function. SMN has been described to lead actin mRNA all along the axon. (B to D) Housekeeping functions. (B) The most described function of SMN is its participation in the U snRNPs assembly process. (C) SMN is implied in the transcription mediated by RNAPII. (D) SMN participates in the recycling of U snRNPs (adapted from Eggert, 2006).

3.1.3 Other roles of SMN

Antiapoptotic function

Before the confirmation that SMN was the SMA-determining gene, it was thought that NAIP gene could be the causing gen of the disease. NAIP was a well-known anti-apoptotic protein, but SMN anti-apoptotic function was unclear. Although SMN itself has only a weak anti-apoptotic activity, Iwahashi and colleagues published a possible interaction of SMN with Bcl-2, another anti-apoptotic protein, and that co-expression of SMN with Bcl-2 might confer a synergistic preventive effect against Bax-induced or Fas-mediated apoptosis (Iwahashi et al., 1997). After that, motoneuron apoptosis has been tryed to relate to SMA pathology. Actually, it has been described apoptosis in motoneurons of postnatal Werdnig-Hoffmann disease (Simic et al., 2000), although this may reflect the end-stage of the disease. A significant increase in the number of TUNEL-positive cells in the anterior horn of SMA type I foetuses, suggests an apoptotic mechanism consistent with increased naturally occurring programmed cell death, thus showing apoptosis before end-stage of the disease (Soler-Botija et al., 2003).

Muscular function of SMN

Mutation or mislocalization of sarcomeric proteins is thought to be the cause of 20 different skeletal muscle diseases. In this regard, SMA patients have been shown to display variable degrees of myofibrillar/sarcomeric abnormalities. It has been described that SMN is a sarcomeric protein required for expression of muscle-specific actin. SMN provides then a plausible role for the protein in muscles and highlights the potential importance of muscular tissue in SMA pathophysiology (Rajendra et al., 2007).

3.2 SMNΔ7

The SMNΔ7 protein is a truncated isoform of the SMN protein that its unique difference in the primary structure with fl-SMN is the lack of the exon 7 in the C terminus. The transcripts encoded by *SMN2* gene are traduced into this truncated protein in 90% of the cases. The truncated protein is composed of only 282 amino acids, instead of 294 amino acids of fl-SMN. This isoform is rarely detectable in cells or tissues derived from human patients or from spinal muscular atrophy animal models, despite robust expression levels of SMNΔ7 mRNA, indicating that the SMNΔ7 protein is highly unstable. Due to this instability, SMNΔ7 is uncapable to rescue SMA phenotype (Cifuentes-Diaz et al.,

2001). The SMNΔ7 protein shows a reduced oligomerization capacity, which is essential for proper SMN function (Lorson et al., 1998; Lorson and Androphy, 2000). C terminal exon 7 contains a sequence that is essential for localization of SMN in the cytoplasm. The lack of the exon 7 in this protein drives to an abnormal accumulation of SMN in the nucleus and reduced neurite outgrowth. This demonstrates that exon 7 plays a necessary role in the active transport of SMN to cytoplasmic localization, which offers new insight into the biological basis of the neurodegeneration observed in SMA (Zhang et al., 2003).

3.3 Other SMN isoforms

3.3.1 a-SMN

Setola and colleagues described a novel isoform of the SMN protein that was selectively expressed in developing motoneurons and mainly localized in axons of the spinal cord. This isoform, called axonal SMN (a-SMN) is originated from the retention of SMN intron 3 and is preferentially transcribed from *SMN1* gene. They also demonstrated that a-SMN stimulates motoneuron axonogenesis in a time-dependent fashion, and that a-SMN induces axonal-like growth in non-neuronal cells such as HeLa. Exon 2b and 3 were described to be determinant for axonogenic effects. The specific localization and function of this SMN isoform suggest a concrete role in motoneurons. They propose that its loss may be determinant of SMA because human a-SMN is a specific product of the *SMN1* gene (Setola et al., 2007).

3.3.2 SMN missense mutations

A study published by Burghes & Beattie (2009) recapitulates all the SMA missense mutations found in patients. Activity of the resulting SMN 'isoforms' has been studied by genetic complementation assays. It has been demonstrated that SMN is able to oligomerize itself (Lorson et al., 1998), and when SMN is not able to oligomerize it is rapidly degraded, resulting in low levels of SMN protein (Burnett et al., 2009). SMNΔ7 mutation and certain missense mutations in exon 6 severely disrupt the ability of SMN to form oligomers (Lorson et al., 1998). All missense mutations that cause a major impairment in SMN's capability to oligomerize are classified as severe alleles because if they are present in patients with a low number of *SMN2* copies they result in a severe phenotype (Lorson et al., 1998; Sun et al., 2005). In this way, SMN levels from a type I patient with a mutation that disrupts oligomerization (Y272C) were similar to those of typical type I patients with complete loss of *SMN1* (Lefebvre et al., 1997). However, all mild mutations occurring in type II or type III patients produce proteins that

oligomerize with fl-SMN (Pellizzoni et al., 1999). The second group of severe SMA missense mutations, such as A2G or mutations in Tudor domain, impair the binding of SMN to the Sm proteins, however the mutant proteins can oligomerize (Bühler et al., 1999; Monani et al., 2003). Proteins containing severe mutations do not perform snRNP assembly in the presence of limiting amounts of fl-SMN, whereas those with mild missense mutations do (Shpargel and Matera, 2005; Workman et al., 2009). Therefore, mild missense mutations in SMN proteins do not impair the ability to oligomerize with wild-type SMN and bind Sm proteins. All in all, it has been demonstrated that SMN functions as an oligomer and that proteins with mild missense mutations are not functional alone (Burghes and Beattie, 2009).

3.4 The Threshold hypothesis vs the Neuron-specific function hypothesis

The question that arises in SMA pathology is why the most affected cells by a reduction of a protein that is widely expressed in and out of the CNS are motoneurons. Two hypothesis are red-hot now: according to one hypothesis, motoneurons require particularly high levels of the SMN protein for their development and/or normal function and, therefore, are especially vulnerable to the reduction of SMN levels. Furthermore, SMN might be required for splicing of pre-mRNAs required for motoneuron differentiation and survival. This hypothesis is also known as Threshold hypothesis (Béchade et al., 1999). The second hypothesis focuses on SMN motoneuron-specific functions more than on its housekeeping role in pre-mRNA splicing and other nuclear processes. Defects in specific functions either trigger or at least modulate the SMA disease phenotype (Fan and Simard, 2002).

3.4.1 The Threshold hypothesis

This hypothesis consideres only the absence of SMN housekeeping functions as the main cause of the SMA phenotype. It has been suggested that the lack of enough SMN prevents the formation of the splicing machinery, due to the inability to join the snRNPs. This fact could affect the splicing of important genes in the establishment of neuronal circuitry by motoneurons (Zhang et al., 2003; Eggert et al., 2006; Gabanella et al., 2007).

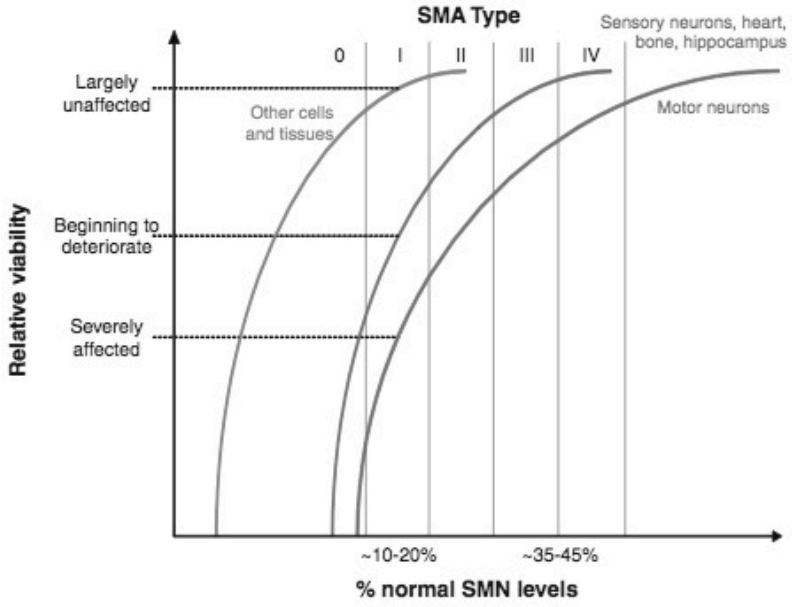

Figure 13: ***The threshold hypothesis in the SMA pathology.*** The level of SMN protein is relatively important in each cell type. Whereas motoneurons are really affected at 45% of SMN level and severely affected at 20%, other tissues as bone, brain and heart only begin to deteriorate at 10-20% of SMN level, and other cells are largely unaffected at lower levels of SMN protein (Sleigh et al., 2011a).

Another idea, more related to the threshold hypothesis, suggests that the quantity of necessary SMN for survival depends on the cell type. The motoneurons have a great demand of efficient assembly of the splicing machinery and correct processing of mRNA and an insufficient assembly could drive to an inappropriate splicing of essential mRNAs for the motoneuron survival (Wan et al., 2005). Therefore, the necessary level of SMN in motoneurons is higher than in any other cell type (figure 13) (Sleigh et al., 2011a).

3.4.2 The Neuron-specific function hypothesis

There is accumulating evidence that SMN plays a role in neuronal development, in particular in the outgrowth of neurites. The idea of a role for SMN in axons was strengthened by the finding that knock-down of *Smn* in zebrafish leads to specific motoneuron axonal defects, including truncated and/or branched axons (McWhorter et al., 2003). Sequences in *SMN* exon 7 are critical for motor axon outgrowth (Carrel et al., 2006). Using both human and synthetic mutations, it has been proven that SMN function in motor axons is independent of the properties needed for snRNP assembly such as oligomerization and Sm binding.

These data indicate that SMN has a critical function in motor axons and synapses that are independent of snRNP biogenesis (Fan and Simard, 2002; McWhorter et al., 2003; Rossoll et al., 2003; Carrel et al., 2006). All this studies support the idea of a possible neuron-specific function, the absence of which could lead to SMA phenotype. However, under this hypothesis, it is still unclear why only spinal motoneurons are affected if SMN is playing an important role in all the axons of all neurons in the CNS. Moreover, what is the exact function of SMN that is directly affected in SMA axons remains unknown (Burghes and Beattie, 2009).

3.4.3 A link between both hypotheses

It could be also possible that the two hypotheses were linked: reduced snRNP assembly could influence the splicing of a gene that is important for axons (Burghes and Beattie, 2009). Moreover, it could be a synergistic effect, incorrect oligomerization of splicing machinery and an inefficient transport of important mRNAs trough the axon could lead to lack of important mRNAs for the axon. There is evidence for both hypotheses, but there is still no clear indication of which is correct or whether both apply.

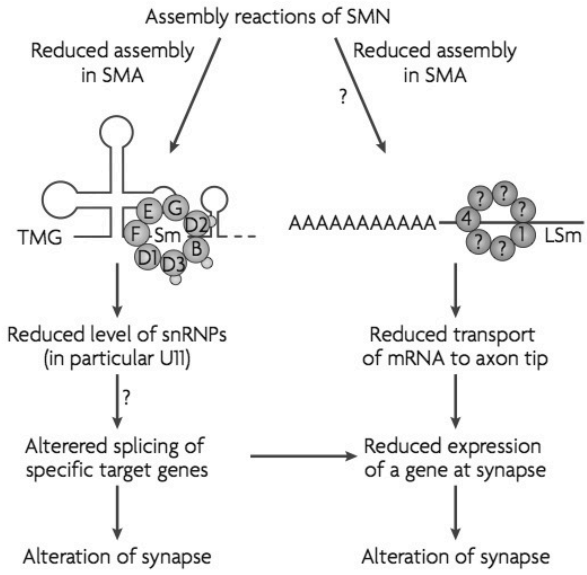

Figure 14: ***Two possible mechanisms to explain how reduced levels of SMN cause SMA pathology.*** The left side, according to threshold hypothesis, describes that reduced levels of snRNP are caused by an impairment in the assembly of splicing machinery that may affect target genes (?) altering synapses. A second hypothesis (right side), according to neuron-specific function, suggests that reduced SMN levels might affect the assembly of LSm proteins required for axonal transport of mRNA, leading to reduced expression of specific genes at the synapse. However, the first step (?) is still undemonstrated (Burghes and Beattie, 2009).

3.4.4 SMN binds to profilin: is this the lost function?

It has also been described the interaction of SMN with the actin-binding protein, profilin. This protein regulates actin dynamics through sequestration and release of actin monomers. SMN protein colocalizes with profilin IIa as distinct granules in neurite-like extensions and growth cones, but also inside the nuclei in coiled bodies. Immunoprecipitation analysis demonstrates the physical interaction between SMN and profilin. Mutant SMN protein fails to interact with profilin IIa in PC12 cells (Sharma et al., 2005). The affectation of the actin cytoskeleton, via SMN-profilin lack of interaction, could be the lost function of SMN that might explain the synaptic impairment and motoneurons dying-back.

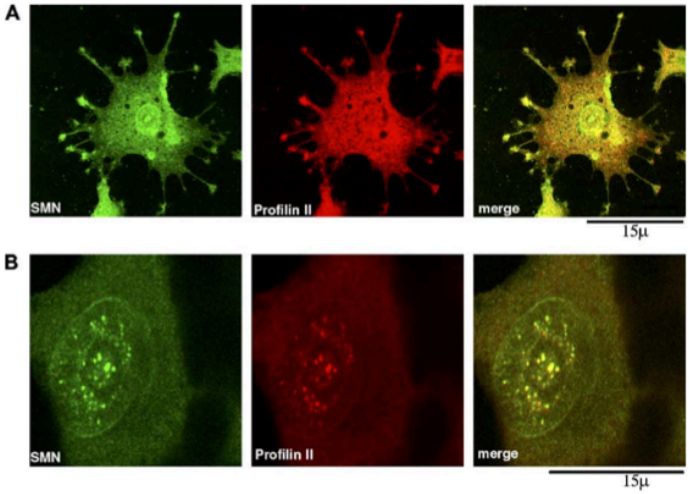

Figure 15: ***SMN and profilin colocalization.*** SMN and profilin are colocalizing in both nuclei and cytoplasm in PC12 cells. (A) Profilin and SMN colocalizes along all the cytoplasm, but both appear to be highly concentrated at the active cell edges. (B) Profilin is interacting with coiled bodies in the nuclei (Sharma, 2005).

4 Animal models of human Spinal muscular atrophy

Due to the high degree of evolutionary conservation of the *SMN* gene, the presence of SMN protein depletion can be modeled in several organisms. The lack of an equivalent *SMN* gene leads to lethality in all the organisms that have been used to model SMA. The animals used to model SMA are from yeast group (*Schizosaccharomyces pombe* (Owen et al., 2000; Hannus et al., 2000)) and both invertebrates (*Caenorhabditis elegans* (Briese et al., 2009) and *Drosophila melanogaster* (Chan et al., 2003; Chang et al., 2008)) and vertebrates groups (*Danio*

rerio: zebrafish (McWhorter et al., 2003; Boon et al., 2009), *Mus musculus* (Hsieh-Li et al., 2000; Monani et al., 2000b; Le et al., 2005)). However, given that the organization of neuromuscular function is evolutionary conserved between mice and humans, mouse models are probably best placed to answer fundamental questions about SMN role in the nervous system and the pathogenesis of SMA (Sleigh et al., 2011a).

4.1 Yeast model of SMA

The yeast *Schizosaccharomyces pombe* has been the organism modeled to analyze the effect of the lack of SMN in superior eukaryotes. Mutations in a highly conserved region of the orthologue of the *SMN1*, the *smn1*$^{+}$, have a dominant-negative effect on yeast growth. This dominant effect can be suppressed by overexpression of the murine *Smn* gene in those cells. Overexpression of the product of *smn1*$^{+}$, the Smn1p protein, results in an increased rate of growth (Owen et al., 2000). The absolute lack of the homologue SMN protein in this yeast by gene disruption leads to lethality (Hannus et al., 2000).

4.2 Invertebrate models of SMA

4.2.1 *Caenorhabditis elegans* SMA model

The nematode *Caenorhabditis elegans* has *smn-1*, an orthologue of the human SMN1 gene. The characterization of the *smn-1 (ok355)* deletion allele, which removes most of the *smn-1*, has been proved to reduce lifespan in those organisms. Moreover, this deletion leads to locomotion and pharyngeal pumping functions impairment (Briese et al., 2009). A novel characterization of the *smn-1 (cb131)* allele resembles a mild form of SMA (type IIIb). This new model is being used for drug testing of compounds with nerve/muscle activity profile (Sleigh et al., 2011b).

4.2.2 *Drosophila melanogaster* SMA model

The use of *Drosophila melanogaster* has been very relevant to study neuronal and muscular defects in SMA models, and implication of SMN protein at the neuromuscular junction (NMJs) and in the skeletal muscle (Chan et al., 2003; Rajendra et al., 2007). Interaction with the muscle and the long axons make motoneurons more sensible to a low SMN concentration, needing more protein for a proper function. Hence, a normal expression of SMN could make motoneurons survive by allowing normal axonal transport and maintaining the

integrity of NMJs (Chan et al., 2003; Rajendra et al., 2007). By inhibiting the expression of SMN directly in muscle and nerve of *D. melanogaster* via SMN RNAi, it has been demonstrated that the SMN function is required in both tissues, though it seems to be highly sensitive in muscle (Chang et al., 2008).

Moreover, after studies in *D. melanogaster* models, it was determined that the maternal SMN could replace the lack of SMN in the early stages of embryonic development. In this way, the removal of maternal SMN in the *D. melanogaster* SMA model leads to embryonic lethality (Chan et al., 2003).

4.3 Vertebrate model of SMA: Zebrafish

Danio rerio, known as zebrafish, is the less complex model within the vertebrate group. Using this model it has been shown, for the first time *in vivo*, that SMN has a function in motor axon development suggesting that early developmental defects may lead to subsequent motoneuron loss (McWhorter et al., 2003). The depletion of SMN in those animals does not lead to lethality due to the maternal SMN during larval stages. However, if the maternal contribution is ultimately depleted during larval stages, it results in defects at the presynaptic terminal and decreased survival. Interestingly, a transgenic animal expressing human SMN only in motoneurons could restore the presynaptic NMJ integrity. This data might explain the neuronal specificity in SMA (Boon et al., 2009).

4.4 Mouse models of SMA

Unlike the other models, mouse allows a biological view and assessment of gene and protein function in mammalian context. Moreover, the murine model is a very useful tool for preclinical testing. Nevertheless, a perfect mouse model should reproduce the levels of SMN protein seen in patients in order to preserve the relative selectivity for motoneuron degeneration. Models with very low level of SMN induce non-viable embryo or cell death in models with tissue-specific lack of SMN. This is caused by the disruption of the constitutive cellular function of the SMN. In that case, the model would not provide insights into motoneuron affectation. For this reason, the SMN levels should be quantified to ensure that the mouse lives enough to develop the SMA phenotype and can be used for therapeutic trials (Sleigh et al., 2011a).

Mice only possess one copy of *SMN* gene and the lack of this copy leads to non-viable embryo. This orthologue is called *Smn* and has 82% amino acid identity

with its human homolog and a similar expression pattern (Viollet et al., 1997; DiDonato et al., 1997; Bergin et al., 1997).

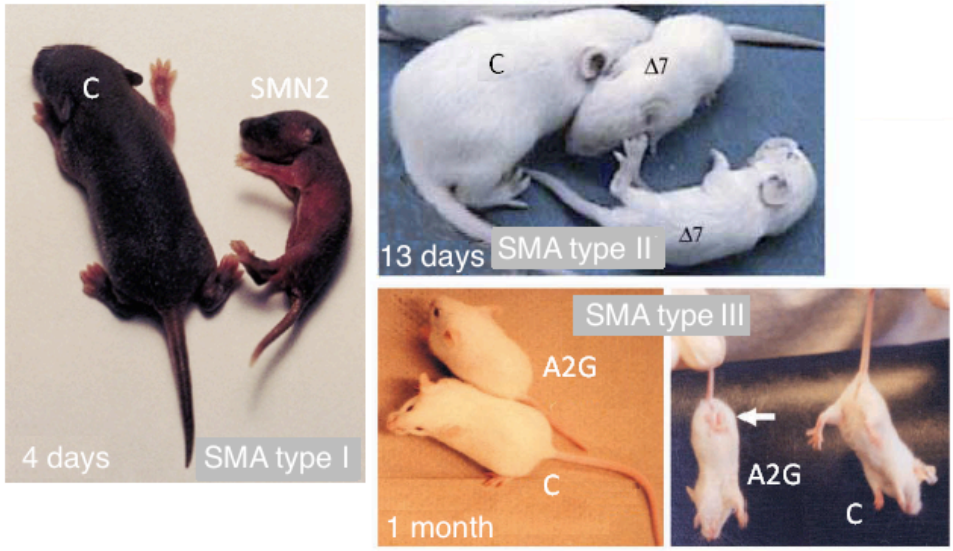

Figure 16: ***Three main mouse models of SMA pathology.*** The severe form, emulating SMA type I, the SMN2 mice, which lifespan is around 5 days (left). The SMNΔ7 (top right) is the mouse model of the human type II SMA, and its lifespan is around 15 days. The SMN A2G (bottom right) has a normal lifespan but a loss of weight and weakness, and shows a similar phenotype to SMA type III patients.

Several mouse models have been developed since *SMN* was described as SMA determining gene. Then, *Smn* became the target gene to produce SMA models.

4.4.1 *Smn*$^{-/-}$ transgenic mice: human SMA type 0 model

Schrank and colleagues proposed a novel murine model for SMA in 1997. They inactivated the *Smn* gene, creating an *Smn*$^{-/-}$ transgenic animal. This inactivation leads to a massive cell death in embryos prior to uterine implantation (Schrank et al., 1997).

4.4.2 *SMN2* transgenic mice: human SMA type I model

Using the *Smn*-null background proposed in the previous model, two groups tried to rescue lethality expressing human *SMN2* transgene in those mice (*Smn*$^{-/-}$; *SMN2*$^{+/+}$). At birth, the animals with one or two copies of human *SMN2* are indistinguishable from the controls, but die after one week. The phenotype difference between siblings appear at postnatal day 3, and is characterized by a severe muscular weakness and around 40% of motoneuron death, they are referred as the severe model, linking with type I or severe form of human SMA.

Nevertheless, animals carrying 4 or more copies of *SMN2* show a normal lifespan and a complete rescue from the SMA phenotype. This fact confirms that *SMN2* enhancement could be a therapeutic strategy (Hsieh-Li et al., 2000; Monani et al., 2000b).

4.4.3 *SMNΔ7* transgenic mice: human SMA type II model

After the previous model it was produced an analog to human SMA type II disease introducing a second transgene in that previous background. The human *SMNΔ7* cDNA extended the lifespan from 1 week to approximately 2 weeks (mean of 13 days). This model (*Smn*$^{-/-}$; *SMN2*$^{+/+}$; *SMNΔ7*$^{+/+}$) was initially created to assess SMNΔ7 protein potential toxicity (Kerr et al., 2000), but it has been suggested that the complexation between fl-SMN and SMNΔ7 proteins might stabilize SMN and could affect its turnover (Le et al., 2005).

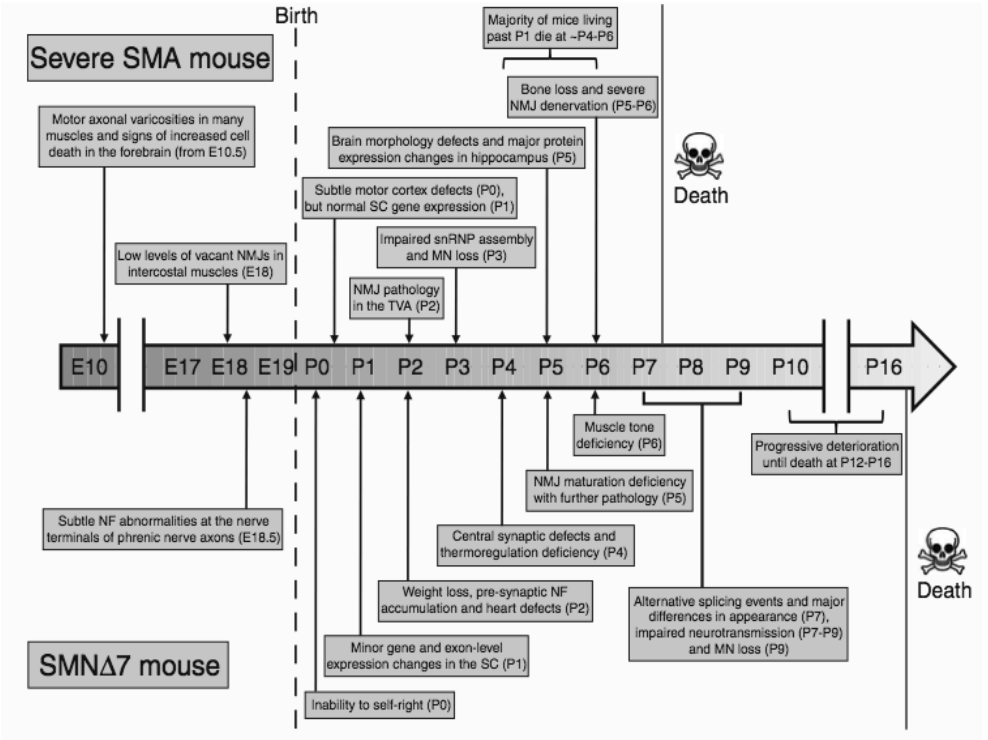

Figure 17: ***Comparative progress between SMN2 and SMNΔ7 mice.*** Timeline illustrating the major cellular and symptomatic events during the embryonic and postnatal development of severe and SMNΔ7 mouse models of SMA (Sleigh, 2011).

The phenotypic differences, appear at postnatal day 3, are characterized by neurogenic atrophy of the muscle and onset of motoneuron loss at postnatal day 9 (Le et al., 2005). The phenotypic differences between the severe model and the *SMNΔ7* model are exposed in figure 17.

4.4.4 *Smn*$^{2B/-}$ transgenic mice: human type II/III model

This is a model (*Smn*$^{2B/-}$) of the intermediate form of human SMA, between type II and type III, taking into account the phenotype of the mice. In this model a knock-in allele disturbs the *Smn* splicing site, reproducing what is happening in the human *SMN2*. This mutation results in a moderate severity, increasing lifespan to 1 month (Bowerman et al., 2009). The phenotypic defects in those mice, which appear after 10 days, are reduced body weight, motoneuron loss and motor defects. These animals show only a 15% of the normal SMN concentration (Bowerman et al., 2011).

4.4.5 *SMN A2G* transgenic mice: human SMA type III model

Other animals have been created adding transgenes carrying point mutations in human *SMN1* (*A2G, A111G*) in the severe model mouse. The *SMN A2G* model (*Smn*$^{-/-}$*; SMN2*$^{+/-}$*; SMN1(A2G)*$^{+/-}$) has increased notably its lifespan (reaching more than 200 days), exhibits muscle atrophy, motoneuron degeneration and loss, and abnormal electromyographs. The animals being homozygous for *SMN1(A2G)* are indistinguishable from controls. *SMN1(A2G)* missense mutation is unable to rescue Smn$^{-/-}$ embryonic lethality in the absence of the *SMN2* gene (Monani et al., 2003). This data indicates that at least some fl-SMN is necessary for the proper association of the SMN complex and normal cellular function (Monani et al., 2003). The other model, severe mice background carrying *SMN1(A111G)* missense mutated transgene, improves lifespan to 1 year with no obvious SMA-like phenotype (Workman et al., 2009).

4.4.6 *Smn*$^{+/-}$ transgenic mice: human SMA type III/IV model

This mouse model of human mild SMA is a heterozygous null mice, *Smn*$^{+/-}$, lacking a marked clinical phenotype. Nevertheless, some reports have demonstrated a loss of neuromuscular integrity (Schrank et al., 1997; Jablonka et al., 2000) and a progressive loss of motoneurons and denervation of motor endplates starting at 4 weeks of age. Moreover, it has been described spinal motoneuron loss between 1 and 12 months, reaching 40% of loss at end-stage in these mice. Although this motoneuron loss, the muscle strength is not reduced (Simon et al., 2010).

Table 5: ***Mainly used mouse models of human SMA.*** The mouse models of human SMA share common phenotype with human patients.

Mouse Model	Human SMA	Type	Lifespan
***Smn*$^{-/-}$**	Embryogenic form	0	non-viable embryos
***Smn*$^{-/-}$*; SMN2*$^{+/+}$**	Werdnig-Hoffmann disease; Acute form; Severe form	I	~ 5 days
***Smn*$^{-/-}$*; SMN2*$^{+/+}$*; SMNΔ7*$^{+/+}$**	Intermediate form; Chronic form	II	~ 14 days
***Smn*$^{2B/-}$**	Intermediate form	II/III	~ 28 days
***Smn*$^{-/-}$*; SMN2*$^{+/-}$*; SMN1(A2G)*$^{+/-}$**	Kugelberg-Welander disease; Juvenile form; Mild form	III	~ normal
***Smn*$^{+/-}$**	Adult form	III/IV	normal

4.4.7 Other mouse models of SMA

In order to reproduce the deletion that is occurring in *SMN2* exon 7, it has been performed a deletion of the *Smn* exon 7 from a conditional (floxed) allele *Smn*^{F7} using the Cre-loxP recombination system. This allele lacking exon 7 supposes the total absence of fl-Smn protein in the presence of Cre recombinase, culminating in death. But crossing this animal with tissue-specific Cre mouse supposes the total absence of Smn only in target tissues (Frugier et al., 2000; Cifuentes-Diaz et al., 2001; 2002). However, the total lack of Smn is not a real model of the disease, because this phenotype is lethal. A more recent study conditionally depleted the Smn in motoneuron progenitor cells, but importantly the Smn was not completely ablated owing to the background of the severe mouse model (Park et al., 2010). Unexpectedly, in that study normal levels of Smn in tissues other than motoneurons resulted in mild phenotype.

5 Therapeutic developments for SMA

The therapeutic view of the SMA disease changed completely after *SMN* genes were cloned in 1997. The old therapy based on symptomatic treatment was transformed on genetic engineering and techniques for mRNA manipulation.

5.1 Techniques targeting *SMN2* gene

The promoter regulating *SMN2* gene is nearly identical in sequence and activity to the *SMN1* promoter (Monani et al., 1999b). This promoter is associated with histone deacetylase (HDAC) proteins that may modulate the histone acetylation state and play a role in determining *SMN2* gene expression (Kernochan et al., 2005). HDAC inhibitors have been proposed as a possible therapy in SMA, such as valproic acid (Brichta et al., 2003; Sumner et al., 2003) and phenylbutyrate (Andreassi et al., 2004). Nevertheless, the use of HDACs are tricky, often nonspecific and known to affect expression around 2% of all known genes by opening up the chromatin structure of DNA and, thus, making it accessible to the transcriptional machinery of the cell. Moreover, the clinical studies using HDAC inhibitors have shown amelioration of SMA owing to activation of anti-apoptotic genes, but not to the pretended increase of SMN protein.

5.2 Gene therapy

One of the goals of SMA therapeutics research is to achieve *SMN1* replacement. Three different groups have transduced motoneurons in mouse models of SMA with adeno-associated viruses (AAV) over-expressing human SMN. The lifespan of those mice have been increased from 10 to 100 days (Foust et al., 2010; Passini et al., 2010; Valori et al., 2010). Other studies have rescued 100% of the normal phenotype in mice, such as weight and motor function, also using AAV but carrying a codon-optimized SMN1 gene (Dominguez et al., 2011). Moreover, it has been tested the use of nonintegrating lentiviral vectors, which have a greatly reduced risk of causing insertional mutagenesis and a lower risk of generating replication-competent recombinants (Yáñez-Muñoz et al., 2006; Wanisch and Yáñez-Muñoz, 2009).

5.3 *SMN2* transcripts manipulation

Techniques increasing SMN2 exon 7 are not necessary designed to correct the immediate consequences of the C-to-T change, but any area of the pre-mRNA that could be manipulated in order to promote the inclusion of exon 7.

5.3.1 Techniques increasing *SMN2* exon 7 inclusion

The use of antisense oligonucleotides (ASOs) increased the ratio of exon 7 inclusion in the *SMN2* transcripts, owing to a competition for the splicing machinery binding with the splicing site of SMN2 exon 7 (Hua et al., 2007).

5.3.2 Techniques targeting splicing silencers

Taking into account the theory of that C-to-T transition causes a change from ESEs to ESSs (the silencer model), there have been trials to interfere the hnRNPA1 by siRNA (Kashima et al., 2007a; 2007b) or silence their binding site (ESS and ISS) by ASOs. The use of ASOs has achieved an 80% of fl-Smn protein concentration and provided partial correction of motor deficits in mouse models (Williams et al., 2009). The use of siRNA knock-out of hnRNPA1 enhanced the ratio fl-SMN/ SMNΔ7 and influenced on that ratio more than the depletion of SF2/ASF – SR proteins that were thought to strongly regulate SMN2 exon 7 inclusion (Kashima et al., 2007a; 2007b).

5.3.3 Techniques targeting splicing enhancers

Taking into account the enhancer model where a crucial ESE is present in the central region of the exon 7, binding of SR like proteins hTra2-β1, SRp30c and ASF/SF2 might improve the exon 7 inclusion in *SMN2* transcripts (Hofmann et al., 2000; Young et al., 2002; Hofmann and Wirth, 2002).

5.4 Stabilizing SMN protein

Another approach in SMA therapy is stopping degradation of SMN protein, in one hand, achieving a more stable protein, or in the other hand, inhibiting its degradation. It has been speculated that aminoglycosides, by read-through of the initial stop codon in exon 8 of SMN2 transcripts, could elongate slightly C-terminus of those transcripts, promoting its stability (Wolstencroft et al., 2005). In the second case, the described system degrading SMN is the ubiquitin-proteasome complex. In that case, drugs inhibiting this pathway might increase SMN protein levels, as it has been demonstrated in patient-derived fibroblasts (Chang et al., 2004).

5.5 Neuroprotection

Another important goal in SMA therapeutics research is to identify ways to protect SMN-deficient motoneurons from degeneration. Some studies have revealed a neuroprotective effect of riluzole, a drug used in the treatment of ALS. Riluzole is known to limit glutamate release, inhibit excitotoxic mechanism, but also enhances BDNF expression, a neurotrophic factor which has been demonstrated to promote neuronal survival and guide axonal pathfinding (Haddad et al., 2003). Another molecule, cardiotrophine-1 (CT-1) has been shown to prolong lifespan and delay the motor defect in SMA mice lacking exon 7 in neurons (Lesbordes et al., 2003). Nevertheless, the effect of neurotrophic factors on SMA pathology has not been studied in depth.

5.6 Stem cells therapy

Stem cells therapy is an incipient field on neurodegenerative diseases therapy including SMA. There are two possible ways to replace the affected motoneurons. On one hand, embryonic stem (ES) cells are pluripotent cells that can be differentiated into motoneurons. In adult rat spinal cord, transplantation of motoneuron-committed ES cells resulted in the generation of motoneurons that exhibit features of native ones and display a log-term survival (Harper et al., 2004). On the other hand, novel induced pluripotent stem cells (iPS cells) generated from ALS patients have been successfully directed to differentiate into motoneurons, offer a new approach to replace damaged motoneurons in SMA too (Dimos et al., 2008).

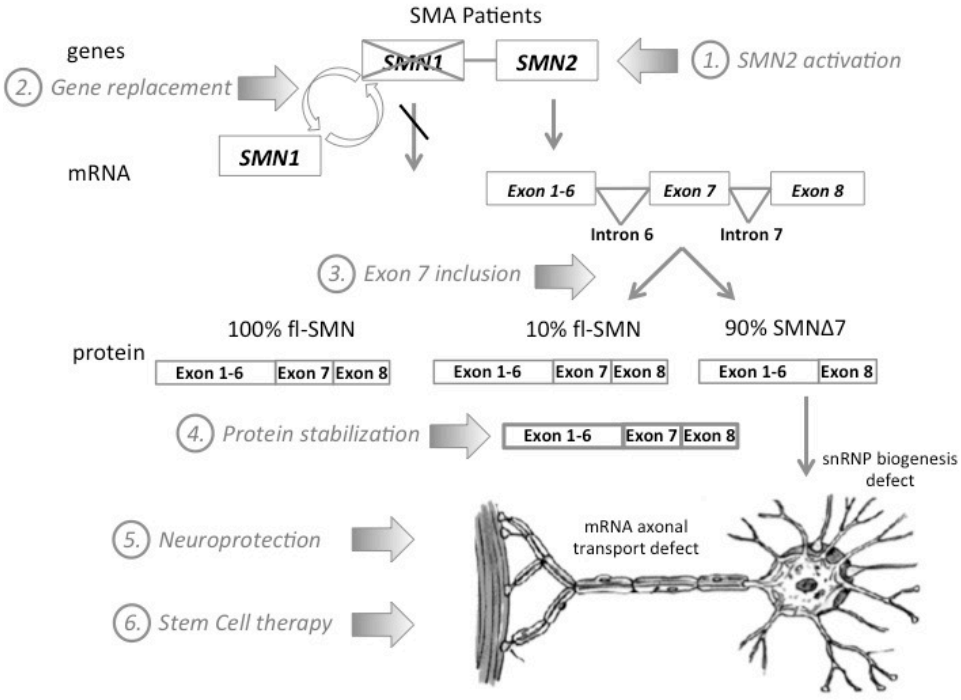

Figure 18: ***Scheme of SMA therapeutic strategies.*** The therapeutic approaches from 1 to 4 target the molecular level of the disease, whereas 5 and 6 target cellular level, trying to make motoneuron survive. (1) The increment of *SMN2* protein would increase the actual concentration of fl-SMN. (2) The impaired *SMN1* gene could be replaced, by genetic engeeniering, by a healthy *SMN1* gene. (3) The exon 7 inclusion would increase the ratio fl-SMN/SMNΔ7, allowing fl-SMN normal function. (4) The stabilization of SMN lets the protein act more time. (5) Some compounds could act as neuroprotective molecules, preventing motoneuron death. (6) The injured motoneurons could be replaced by healthy motoneurons via iPS cells.

6 Actin dynamics in SMA pathology

The actin cytoskeleton plays an important role in axon initiation, growth, guidance, branching, and retraction and also in synapse formation and stability (Dillon and Goda, 2005; Luo, 2002). The lack of SMN protein has been related to defects in neurite outgrowth, neuronal differentiation, axonal pathfinding and neuromuscular maturation (Murray et al., 2008; Kariya et al., 2008).

6.1 Cell migration and actin dynamics

Cell migration plays a key role in many physiological and pathological processes. Cell migration is critical at many stages of nervous system development (Bronner-Fraser, 1994). Neural crest cells are characterized by striking cell migration capacity to colonize target tissues during vertebrate embryogenesis (Locascio and Nieto, 2001). And also, cell migration is required for morphogenetic processes during embryonic development (Keller, 2005). Moreover, the immune response is accompanied by the movement of several cell types (Luster et al., 2005).

Cell migration is a highly coordinated multistep process. For a migration process, a cell acquires a polarized morphology in response to extracellular signals. The closer edge to the stimulus becomes the front of the cell. Therefore, actin assembly drives the extension of flat membrane protrusions called lamellipodia and finger-like protrusions called filopodia. At the leading edge of the lamellipodium, the cell creates adhesions that bind the extracellular matrix to the actin cytoskeleton to anchor the protrusion and tract the cell body. After those processes, the cell shrinks its trailing edge by combining actomyosin contractility and disassembly of adhesions at the rear (Le Clainche and Carlier, 2008).

Migration varies from one cell type to another. Nevertheless, generally speaking, role and regulation of actin dynamics associated with membrane protrusion and cell-matrix adhesion are accepted as common features of cell migration. Therefore, actin dynamics is the result of a concerted regulation of parameters that govern the assembly, stability, and organization of actin filaments by a specific set of proteins (Le Clainche and Carlier, 2008).

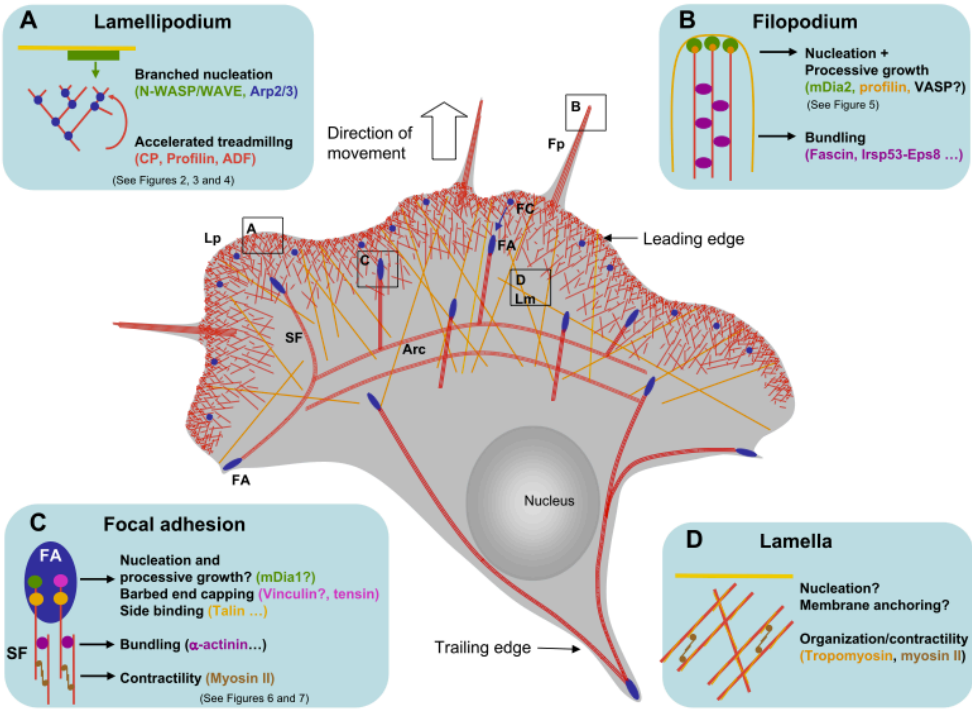

Figure 19: ***Schematic illustration of the actin cytoskeleton in a migrating cell.*** Schematic cell containing the major structures in migrating cells. (A) Lamellipodia (Lp), branched actin filaments are generated at the plasma membrane and maintained in fast treadmilling by a set of regulatory proteins, such as ADF, capping proteins and profilin. (B) Filopodia (Fp) extend beyond the leading edge of protruding lamellipodia to sense the environment. At the tip of filopodia, formins catalyze the processive assembly of profilin-actin. (C) Slow moving cells form focal adhesions in response to RhoA signaling. Focal adhesions connect the extracellular matrix to contractile bundles made of actin filaments, myosin II, and bundling proteins. (D) Lamella (Lm) are characterized by a slow actin turnover and contain the proteins tropomyosin and myosin II. The mechanisms by which actin filaments are nucleated and anchored to the plasma membrane are unknown. SF, stress fiber; FA, focal adhesion; FC, focal complex (Le Clainche and Carlier, 2008).

6.2 Actin-profilin interaction and actin turnover

The actin-binding protein profilin is also a key regulator of actin polymerization in cells and actin-based motility processes (Goldschmidt-Clermont et al., 1992). Profilin only binds to ATP-G-actin (globular or monomeric actin) and does not bind to F-actin (filamentous actin) (Didry et al., 1998). Profilin-ATP-G-actin complex exclusively enlarges actin filaments assembling to barbed ends (Pantaloni and Carlier, 1993). When all barbed ends are blocked by capping proteins, profilin only sequesters G-actin (Didry et al., 1998). The function of profilin in actin filament regulation is shown in figure 20.

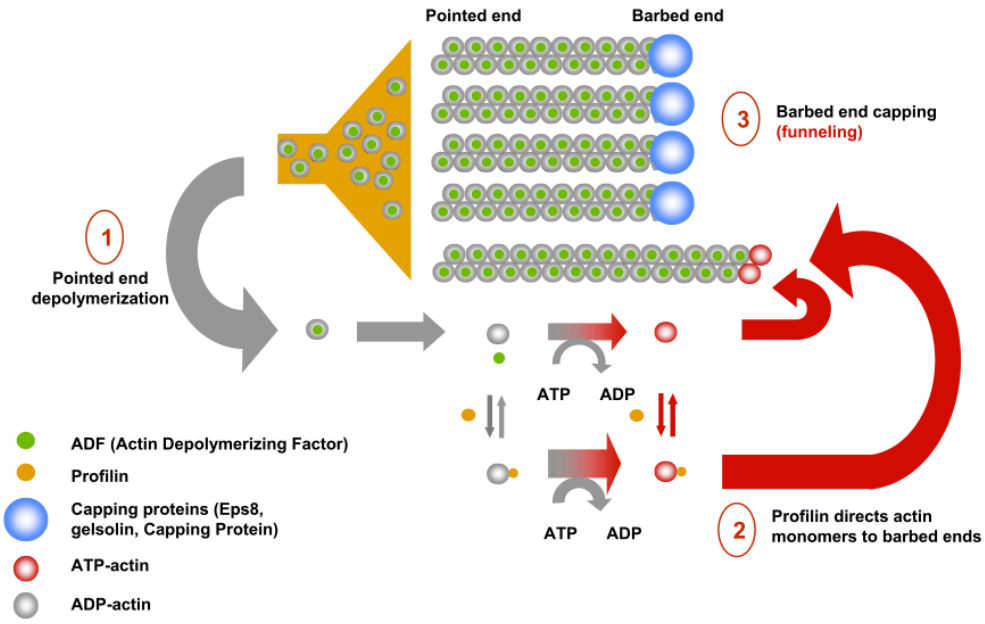

Figure 20: ***Regulation of actin treadmilling.*** (1) ADF binds to the side of ADP-actin filaments and induces pointed-end depolymerization to increase the concentration of monomeric actin at steady state. (2) Profilin enhances the exchange of ADP for ATP to recycle actin monomers. The profilin-actin complex assembles exclusively at the barbed end. (3) By blocking the majority of actin filament barbed ends, capping proteins increase the concentration of monomeric actin at steady state and funnel the flux of actin monomers to the noncapped filaments, which individually grow faster (Le Clainche and Carlier, 2008).

7 The RhoA/ROCK pathway in the control of actin dynamics

Ras-homologous guanosine triphosphatases (Rho family GTPases) are molecules that control the dynamics of the cytoskeleton and mediate the effects of multiple signals, such as Rac, Cdc42 and RhoA. In the nervous system, Rho GTPases and their intracellular effectors are essential regulators of neuritic growth and regeneration, thus participating in neuronal differentiation and survival (Negishi and Katoh, 2002; Benarroch, 2007; Linseman and Loucks, 2008). In addition to their prominent effects on the actin cytoskeleton, Rho family GTPases also modulate other important cell functions as cell migration, adhesion and survival (Keely et al., 1997; Linseman and Loucks, 2008). GDP-Rho is the inactive form that is converted into GTP-Rho, the active form, upon stimulation. Activated Rho interacts with effector molecules such as ROCK

(Rho-associated kinase). ROCK is able to regulate the phosphorylation of myosin light chain (MLC) by direct phosphorylation of MLC and by inactivation of myosin phosphatase (MLCP) (Amano et al., 2000; Luo, 2002; Newey et al., 2005).

7.1 RhoA/ROCK pathway controls cell migration via actin dynamics regulation

It is well-known that the actin cytoskeleton and members of the Ras superfamily of GTPases, and specifically the Rho proteins, play a prominent role in cell migration (Ridley, 2001; Etienne-Manneville and Hall, 2002). The actin dynamics is regulated via RhoA/ROCK pathway through profilin and through MLC (figure 21). On one hand, the phosphorilation of myosin II leads to actin-myosin contraction process, essential for cell migration. One important function of myosin is to act as the motor of retrograde flow of filopodia and lamellipodia, necessary to change direction and continue with the migration process. On the other hand, profilin, a key player in actin dynamics, and therefore in cell migration, is regulated via RhoA/ROCK pathway (Da Silva et al., 2003).

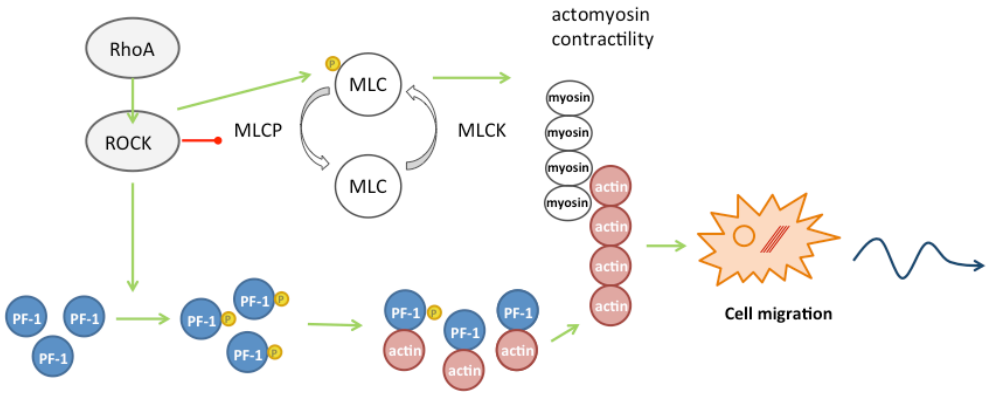

Figure 21: ***Regulation of cell migration via RhoA/ROCK pathway.*** Cell migration is regulated by RhoA/ROCK pathway. ROCK controls profilin phosphorylation and enhances MLC phosphorylation, potentiating actomyosin contractility, necessary for migration process.

7.2 Role of RhoA/ROCK in neuritogenesis

Rac, Cdc42 and RhoA play major roles in modulation of growth cone morphology in neurons. Ras and Cdc42 promote growth cone advance and neurite outgrowth, while RhoA causes growth cone collapse and neurite retraction (Linseman and Loucks, 2008). In addition, Rho family is a dominant regulator of the dendritic spine morphology. Whereas Rac promotes spine formation, RhoA diminishes it. Moreover, RhoA affects synaptogenesis, inhibiting synaptic pasticity (Elia et al., 2006; Linseman and Loucks, 2008). RhoA inhibits dendritic and axonal growth through different effectors that promote actin polymerization and its interaction with myosin (Fournier et al., 2003; Da Silva et al., 2003; Newey et al., 2005).

7.3 Implication of RhoA/ROCK pathway, via actin dynamics regulation, in SMA

SMN protein is involved in mRNA actin transport within the motoneuron, and regulates its anterograde transport. Some studies have demonstrated the direct interaction between SMN and profilin, a crucial factor for actin polymerization (Giesemann et al., 1999). Recent studies have related the profilin-SMN interaction to cellular migration (Bowerman et al., 2007). A role for SMN in neurite outgrowth, neuronal differentiation, axonal pathfinding and neuromuscular maturation has been described (Fan and Simard, 2002; Kariya et al., 2008; Kong et al., 2009; McWhorter et al., 2003; Murray et al., 2008; Rossoll et al., 2003). In this sense, it has been detected a significant increase in synapses lacking motor axon inputs in embryonic SMA mice (McGovern et al., 2008).

SMN depletion in PC12 cells induces defects in neuritogenesis caused by alterations in cytoskeletal integrity (Bowerman et al., 2007). In a mouse model of SMA, the activity of RhoA, a major regulator of actin dynamics, increases prior to disease suggesting that RhoA activity in the spinal cord is altered when SMN is depleted (Bowerman et al., 2010). Additionally, pharmacological inhibition of Rho-kinase (ROCK), a direct downstream effector of active RhoA, dramatically increases the survival and maturation of neuromuscular junctions in a SMA mouse model (Bowerman et al., 2010). SMN physically interacts and co-localizes in the cytoplasm with profilin, reducing its actin-sequestering activity (Giesemann et al., 1999; Sharma et al., 2005). Together, these findings suggest that actin-cytoskeleton dynamics may be linked to SMA pathogenesis.

It has been proposed that SMA pathogenesis in lower motoneurons is related to abnormal motoneuron differentiation and migration (Simic, 2008). Also, reduced expression of SMN induces impaired hippocampal neurogenesis, related to alterations in the expression levels of proteins required for cell growth and migration (Wishart et al., 2010). This suggests that alterations in cellular migration could be related to SMA. However, the possible role of SMN in cell migration has not been studied yet.

8 Neuroinflammation and motoneuron pathology

In the last years, it has been considered that neuroinflammation plays an active role in the pathology of different neurodegenerative diseases such as Alzheimer's disease, Parkinson's disease or amyotrophic lateral sclerosis (ALS) (Araki et al., 2003; Frank-Cannon et al., 2009). In a motoneuron disease, such as ALS, numerous pathological processes appear to contribute to motoneuron injury (Beers et al., 2011). Neuroinflammatory response is a prominent feature in this inexorable disease, highlighted by the presence of activated microglia and infiltrating lymphocytes at sites of motoneuron injury, that also contributes to this pathogenic process (McGeer and McGeer, 2002; Boillée et al., 2006). Chronic inflammation might be maintained by cellular distress signals emanating from neurons that survive for prolonged periods despite significant injury to their presynaptic terminals or dendritic processes. Synaptic degeneration is indeed a prominent feature of neurodegenerative diseases. In experimental models of nerve injury, degenerating synapses trigger the rapid activation of astrocytes and microglia and the release of inflammatory mediators (Aldskogius et al., 1999). Degenerating cells can trigger inflammation until they are cleared by phagocytes. Whether the death of neurons and other CNS cells gives rise to inflammatory reactions may depend, at least in large part, on how they die (Wyss-Coray and Mucke, 2002).

Gliosis is a consistent feature of neuroinflammation in motoneuron diseases. The term gliosis, also sometime called reactive astrocytosis, refers to scarring produced by astrocytes, evidenced by increased GFAP stainability of the tissue, increased numbers of astrocytes, increased size of astrocytes, or a combination of all of the above. It is also possible to comment on the status of other glial cells such as oligodendrocytes and microglia (Papadimitriou et al., 2010). Astrocytes, in conjunction with microglia, respond profoundly to neuronal injury and undergo a series of metabolic and morphological changes, also observed in a variety of conditions, including cerebral ischemia, Alzheimer's disease, Parkinson's disease, Hungtinton's disease and ALS (Pekny and Nilsson, 2005).

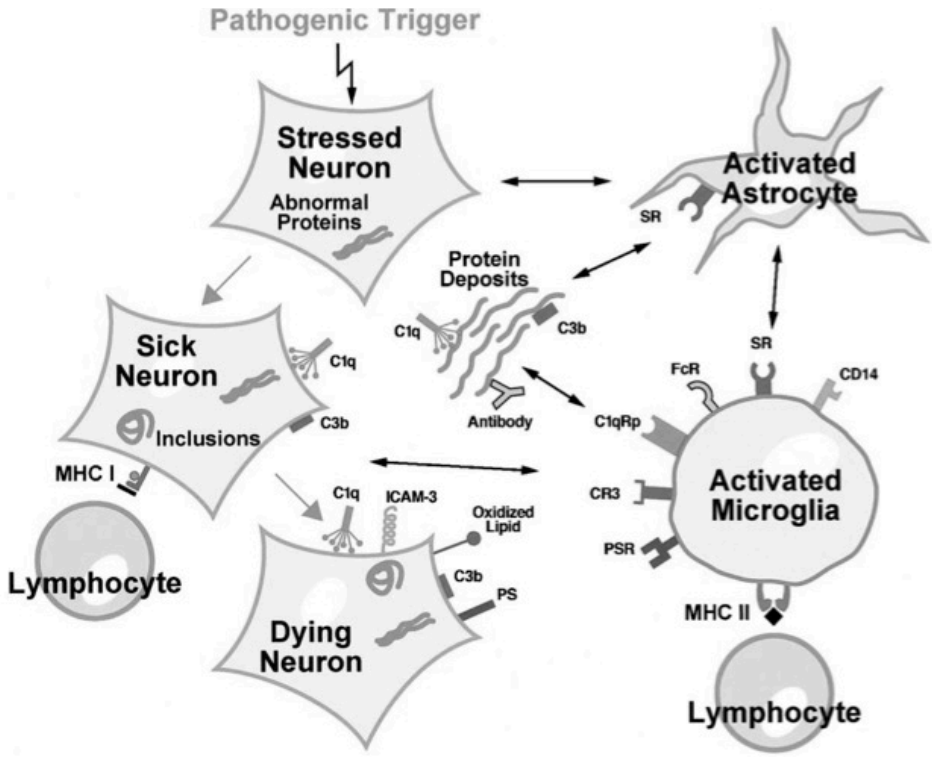

Figure 22: ***Components of the inflammatory response to CNS degeneration.*** Pathogenic triggers, such as accumulation of abnormal proteins in cells or extracellular spaces, elicit cellular stress responses and can result in the progressive dysfunction and degeneration of neurons. Cytokines and other mediators of the innate immune response are released by astrocytes and microglia to orchestrate defense mechanisms and initiate the removal or sequestration of the pathogenic triggers. Abnormal proteins and degenerating neurons are tagged by complement proteins such as C3b or C1q or by antibodies for recognition and phagocytosis by glial cells. Degenerating neurons may be phagocytosed if they display intercellular adhesion molecule-3 (ICAM-3), phosphatidyl serine (PS), or oxidized lipids on their cell surface. Receptors on glial cells recognize these tags and initiate inflammatory responses. MHC molecules might display abnormal proteins with novel antigenic epitopes to lymphocytes, resulting in acquired immune responses. C1qRp, C1q receptor for phagocytosis; CR3, complement receptor 3; FcR, Fc receptor; PSR, phosphatidyl serine receptor; SR, scavenger receptor (Wyss-Coray and Mucke, 2002).

8.1 Neuroinflammatory process in SMA

Although SMA is characterized by a selective loss of motoneurons within the anterior horn, glial bundle formation is another pathological hallmark of SMA in the areas of neurodegeneration (Araki et al., 2003). Gliosis has been reported to be associated with areas of motoneuron degeneration in the spinal cord and brainstem in all three types of human SMA (Araki et al., 2003; García-Cabezas et

al., 2004; Kuru et al., 2009). Glial cells may propagate injury and it is now believed that, under certain circumstances, astrocytes and microglia may initiate neurodegeneration (Papadimitriou et al., 2010). In addition, in SMA, a singular pathological feature, called glial bundles, can be observed at the level of spinal roots (Chou and Fakadej, 1971; Kumagai and Hashizume, 1982; Ghatak, 1983; Kuru et al., 2009); these glial bundles are thought to correspond to a protrusion of reactive astrocytes into the neurilemmal tubes containing degenerating myelinated axons (Ghatak, 1983). However, the relevance of activated microglia/astrocytes has not been studied in depth in the SMA mouse models.

The nitric oxide synthases (NOSs) are a family of enzimes that produce NO from L-arginine and oxygen, and uses NADPH as electron donator and FAD and FMN as cofactors. There exist at least three isoforms: neuronal-NOS (nNOS), inducible-NOS (iNOS), both solubles, and endothelial-NOS (eNOS), bound to membrane. The NO produced by this enzimes is able to interact with O_2^-, producing preoxinitrite ($ONOO^-$) that also lead to protein nitration and oxidation (Aktan, 2004).

Upregulation of nNOS is a common hallmark, occurring in motoneurons and reactive astrocytes in ALS (Sasaki et al., 2001; Catania et al., 2001; Anneser et al., 2001), in neurons and/or glial cells in Parkinson's disease and Alzheimer's disease (Eve et al., 1998; Lüth et al., 2000; Simic et al., 2000; Fernández-Vizarra et al., 2004), and in the striatum of Huntington's disease models at early stages (Deckel et al., 2002; Pérez-Severiano et al., 2002). Additionally, NO participates in synapse loss suffered by motoneurons after motor nerve injury (Sunico et al., 2005; Moreno-López and González-Forero, 2006). The expression of nNOS is "sufficient" to induce synaptic withdrawal in adult motoneurons, which normally lack this enzyme (Sunico et al., 2010).

The level of iNOS in healthy CNS is undetectable (Wang et al., 2011) and the induction of iNOS has been characterized in numerous cells types as a consequence of the inflammatory processes that follow disease (Heneka and Feinstein, 2001). In line with the hypothesis that iNOS may participate in the neuroinflammatory pathological mechanisms involved in some neurodegenerative diseases, it has been found iNOS expression in neurons and in glial cells in Alzheimer's, Parkinson's and Huntington's diseases (Eve et al., 1998; Lüth et al., 2000; Simic et al., 2000; Fernández-Vizarra et al., 2004), ALS (Sasaki et al., 2000), as well as in Multiple Sclerosis (Lee et al., 2003).

8.2 Motoneuron pathology in SMA

Both in SMA patients (Byers and Banker, 1961) and mice models (Frugier et al., 2000; Monani et al., 2000a), the morphological changes in motoneurons represent the early events of neuronal degeneration which lead to a late loss. It has been reported that only a modest loss on motoneurons is evident at the end-stage (Monani et al., 2000b; Le et al., 2005; Kariya et al., 2008), indicating that motoneuron loss may be a late event in SMA disease pathogenesis (Kong et al., 2009). Common pathological changes in motoneurons have been described in SMA patients and disease models which consist of ballooned motoneurons (Chou and Fakadej, 1971), phosphorylated neurofilament (Kato and Hirano, 1990), and irregular nuclei and apparition of indentations of the nuclei (Frugier et al., 2000).

In mouse models of SMA, it has been described an important denervation of some muscles together with immaturity of neuromuscular junctions (NMJs), showing clusters of unoccupied acetylcholine receptors (McGovern et al., 2008). A diminished density of synaptic vesicles and evoked postsynaptic potentials has also been described (Kong et al., 2009; Ruiz et al., 2010) as well as severe structural and functional alterations in the organization of the organelles and the cytoskeleton of motor nerve terminals (Torres-Benito et al., 2011; Dachs et al., 2011). Moreover, synaptic stripping from the motoneuron surface occurs in the progression of several motoneuron pathologies, such as amyotrophic lateral sclerosis (ALS), progressive muscular atrophy, and traumatically damaged adult motor axons (Sasaki and Maruyama, 1994; Sunico et al., 2005).

9 Notch pathway in the CNS

Notch-1, a key player in neurodevelopment, is highly expressed in embryonic mouse and human brain (Higuchi et al., 1995; Berezovska et al., 1997), but continues being expressed at low level at adult stage (Berezovska et al., 1999). Notch's role in neurodevelopment has been extensively examined (Ma et al., 1997) and its role in postmitotic neurons has been *a posteriori* determined (Berezovska et al., 1999). The presence or absence of Notch in SMA patients or in SMA animal models has not been studied, and any relation between SMA pathology and Notch pathway has been described.

9.1 Notch pathway

Notch signaling is a cell-cell communication system which plays an important role in developing and adult mouse and human brain (Higuchi et al., 1995; Berezovska et al., 1997; 1999). Its family includes four integral membrane receptors (Notch 1 to 4) that bind to several different ligands, such as Delta and Jagged, from adjacent cells (Lai, 2004). Upon ligand binding, Notch is cleaved within the transmembrane domain presenilin-1, the enzymatic component of the c-secretase complex, resulting in the release of its active intracellular domain (NICD). This active fragment is translocated into the cell nucleus where it binds to DNA-cofactors and activates the transcription of target genes (Venkatesh et al., 2011; Schwanbeck et al., 2011).

Canonical Notch signalling involves the binding of Notch intracellular domain to DNA-binding cofactors and the subsequent activation of the transcription of target genes, such as hairy and enhancer of split (Hes), that act as transcriptional repressors (Iso et al., 2003).

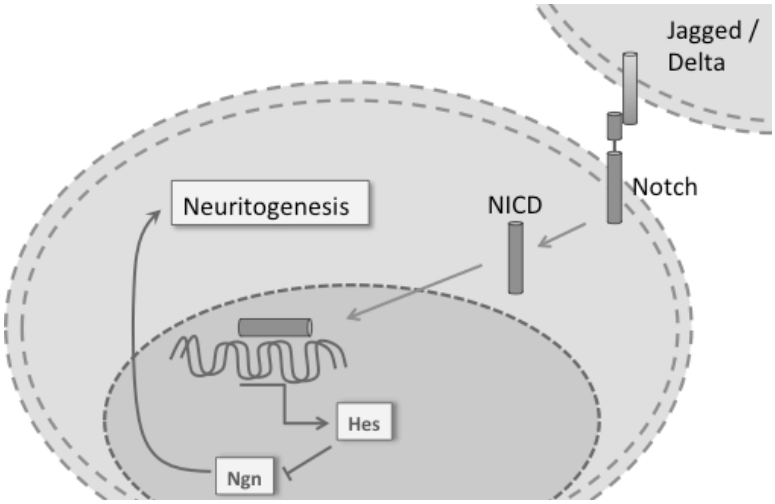

Figure 23: ***Notch pathway.*** The present scheme shows the activation of Notch transmembrane receptor immediately after binding with Jagged or Delta ligand from a neighbour cell. NICD is translocated into the nucleus and there inhibits Neurogenin (Ngn) via Hes transcriptional repressor (Arevalo et al., 2011).

9.2 Notch functions

Notch signaling plays context-dependent roles in differentiation, proliferation, and apoptosis, and has been implicated in cancer progression both as an oncogene and a tumor suppressor (Osipo et al., 2007).

9.2.1 Notch role in neuritogenesis

Notch signalling plays an important role in the regulation of neuritic growth (Redmond et al., 2000). In postmitotic neurons, there is an inverse correlation between Notch1 expression and total neurite length and branching, and overexpression of constitutively active Notch leads to a reduction in total neurite length (Berezovska et al., 1999; Sestan et al., 1999; Redmond and Ghosh, 2001). Also in N2A neuroblastoma cells and in PC12 cell line, differentiated with NGF, Notch activation inhibited neurite outgrowth (Franklin et al., 1999; Levy et al., 2002). Moreover, in *Drosophila* neurons, Notch has been suggested to play a role in axonal guidance (Giniger, 1998). These effects of Notch are associated with an increase in the expression of the transcription factor Hes1 (Salama-Cohen et al., 2005). In turn, Hes1 negatively controls the expression of a series of proneural genes, such as Neurogenin 3 (Ngn-3) (Salama-Cohen et al., 2006). Notch signalling inhibits Ngn-3, an essential protein in dendritogenic and axogenic processes in hippocampal neurons (Salama-Cohen et al., 2005; 2006; Simon-Areces et al., 2010).

Furthermore, it has been recently demonstrated that in human primary endothelial cells Notch signalling activates the RhoA/ROCK pathway and this is associated to a disruption of the F-actin network (Venkatesh et al., 2011). These findings suggest that in the central nervous system (CNS) Notch could inhibit neuritic growth through the activation of RhoA and thus, impaired neuritogenesis in SMA could be related to an abnormal activation of Notch/RhoA/ROCK signalling pathway.

9.2.2 Notch role in glia

The chronic deployment of the inflammatory system can lead to a loss of astrocytic protective and reparative function and its emergence as a destructive force in pathogenic processes such as multiple sclerosis and Alzheimer's disease (Morga et al., 2009). The role of Notch signaling in astrocytes has been described as the initiator of inflammation and inducer of expression of characteristic elements for gliosis. On activated astrocytes, the inhibition of Jagged1 has antiinflammatory effects and results in a decrease of proinflammatory cytokines, characteristic elements of gliosis, as well as the iNOS expression (Morga et al., 2009).

Microglial cells exhibit Notch signaling expression. Moreover, microglia expresses enhanced Notch pathway upon activation (Cao et al., 2008). It has also been described that enhanced Notch expression in activated microglia modulates production of proinflammatory cytokines and nitric oxide (NO), leading to a neuroinflammatory process (Cao et al., 2008). It has been shown that activated murine BV-2 microglial cells and amoeboid microglia primary culture of postnatal rats overexpress Notch (Cao et al., 2010). Since microglial cells are tightly integrated into a dense tissue, numerous cellular contacts with neighboring cells are established (Davalos et al., 2005). It thus seems likely that cell-contact mediated signaling will also play an important role during the activation process of microglial cells (Grandbarbe et al., 2007).

9.2.3 Notch role in CNS cell fate

Moreover, Notch is playing an essential role in multipotent CNS progenitors differentiation. Notch field has been dominated by studies of cell-fate specification, where the general view is that Notch maintains the neural progenitor state and inhibits differentiation. Disruption of positive regulators of the pathway has been grossly consistent with this view. However, more detailed analyses have also revealed that Notch is likely to regulate progenitor pool diversification and neuronal maturation. In addition, emerging data suggests that Notch signaling has a role in neuronal function in the adult brain (Yoon and Gaiano, 2005).

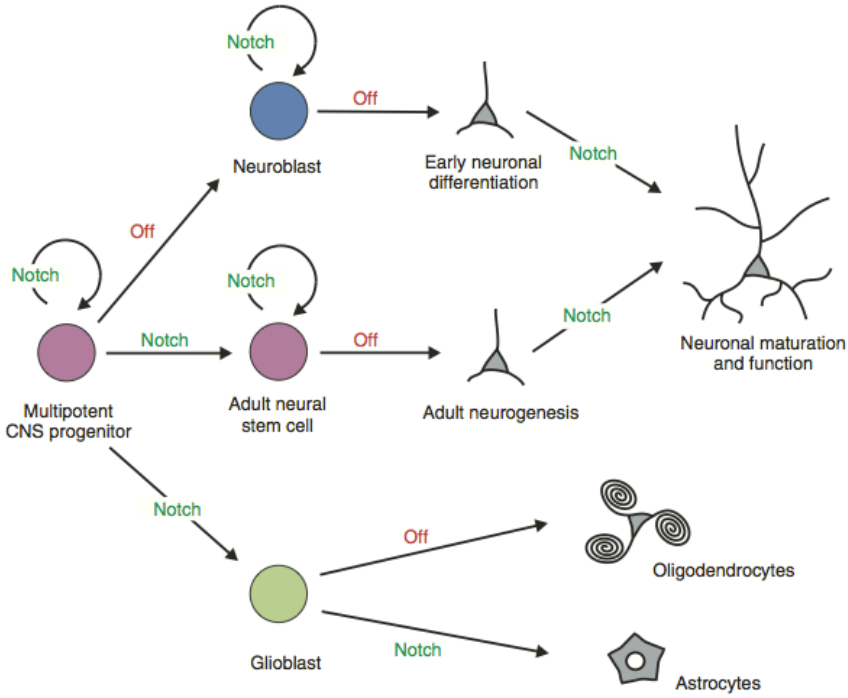

Figure 24: ***Notch signaling in the developing CNS.*** Processes that are likely to involve pathway signaling are labeled 'Notch', and those that are likely to require downregulation of Notch signaling are labeled 'Off'(Arevalo et al., 2011) (Arevalo et al., 2011) (Arevalo et al., 2011). Notch signalling is at first step inducing multipotent CNS progenitors differentiation in glioblast or adult neural stem cell. Absence of Notch in this firs step leads to neuroblast differentiation. Neuroblast and adult neural stem cell needs Notch pathway inactivation and posterior reactivation to become mature neurons. Glioblast become oligodendrocyte if Notch pathway is inactive, but become astrocyte if the pathway is still active (Yoon and Gaiano, 2005).

9.3 Interaction between NF-κB and Notch pathways

Notch signaling could crosstalk with important pathways of inflammation like NF-κB pathway, AP-1, or JAK-STAT signaling. The manner in which other pathways crosstalk with Notch signaling appears to be extraordinarily complex and, not surprisingly, context-dependent (Morga et al., 2009).

On one way, it has been identified Jagged1 as a novel Rel/NF-κB-responsive gene. Jagged1 gene expression can be induced specifically by transcriptionally competent NF-κB subunits. The finding that NF-κB-mediated induction of Jagged1 can initiate signaling downstream of Notch correlates with the expression of Jagged1 in peripheral lymphoid tissues. These results suggest a

direct interplay of the Notch and NF-κB signaling pathways in the immune system, both of which have been implicated in lymphoid cell proliferation and function (Bash et al., 1999). On the other way, a number of reports have shown that Notch signaling leads to NF-κB activation in T cells and hematopoietic progenitor cells and blocking of the Notch pathway results in a reduction of the NF-κB activation (Cheng et al., 2001). The interaction between NF-κB and Notch pathway has been demonstrated in activated microglia where it was concluded that Notch-1 signaling can trans-activate NF-κB/p65 by amplifying NF-κB/p65-dependent proinflammatory functions (Cao et al., 2010). During inflammatory and gliotic events of the CNS, Jagged1/Notch signaling sustains the inflammation mainly through NF-κB pathway (Morga et al., 2009).

II. AIMS

II. Aims

Proximal spinal muscular atrophy is one of the leading genetic causes of death in early childhood and so far a cure is not available. However, since *SMN* was identified as the SMA determining gene in 1995, comprehensive knowledge regarding the pathological disease mechanisms and the underlying molecular principles has been gained. The trigger of the disease is the lack of SMN protein, which is involved in several critical intracellular functions. The growing knowledge about the molecular basis of SMA has enabled the design of SMA models, such as transgenic mice and depletion of SMN in cell cultures, and may lead to the rational development of therapies.

SMN has been shown to be involved in neuromuscular junction maturation, axonal pathfinding and actin dynamics regulation. These data suggest that alterations in cellular migration could be related to SMA. Thus, an aim of this work was to study whether depletion of SMN could alter the motility of a well-characterized cell line for migration studies, the U87MG astroglioma cell line.

Moreover, in patients and models of the disease there have been described glial bundles and motoneuron pathological markers and posterior loss at end-stage. In this sense, we have studied the neuroinflammatory response in the SMNΔ7

mouse model of SMA and the possible implication of gliosis in the development of the disease.

The Notch signalling pathway has been described to control the neuritogenesis and glial activation in some neurodegenerative diseases. However, the potential implication of this pathway in SMA pathogenesis has not been studied yet. In this regard, we have studied the possible implication of Notch pathway in SMA pathogenesis in two models: SMN-depleted U87MG astroglioma cells and the SMNΔ7 mouse model of the SMA.

Therefore, the aim of this work was the characterization of cellular and molecular mechanisms involved in the pathology of SMA. Our hypothesis is that the interaction between glia and motoneurons could affect the development of SMA disease. According to this hypothesis, the main objectives of this thesis have been:

First objective

To study the possible alterations in cytoskeleton structure and cellular migration caused by SMN deficiency and the potential involvement of the RhoA/ROCK signalling pathway

This objective involves the following points:

- Analysis of the neurofilament alterations in motoneurons of rat spinal cord embryonic explants after Smn-depletion.
- Effects of SMN depletion in U87MG astroglioma cell line migration.
- Determination of the implication of the RhoA/ROCK signalling pathway in the migration disturbance in SMN-depleted U87MG cells.
- Analysis of the implication of profilin in the cell migration impairment of SMN-depleted U87MG cells.
- Changes in the ratio of F-/G-actin in SMN-depleted U87MG astroglioma cell line.

Second objective

To study the neuroinflammatory response in the spinal cord of the SMNΔ7 mouse model of SMA

This objective involves the following points:

· Analysis of pathological hallmarks in lumbar spinal cord motoneurons.

· Characterization of glial involvement in the pathogenesis of SMA.

· Study of the possible loss of central synapses on spinal cord motoneuron soma.

· Determination of the implication of nitric oxide synthase isoforms in the pathogenesis of this model.

Third objective

To study the activation of Notch signalling pathway in SMN-depleted models

This objective involves the following points:

· Determination of Notch pathway activation in U87MG SMN-depleted cells.

· Characterization of Notch pathway activation in glia of the spinal cord in SMNΔ7 mouse model.

· Activation of Notch pathway in lumbar spinal cord motoneurons of the SMNΔ7 mouse model.

· Evaluation of Neurogenin expression in lumbar spinal cord motoneurons of the SMNΔ7 mouse model.

III. MATERIALS AND METHODS

III. Materials and Methods

1 Solutions

Table 6: ***Solutions: preparation and composition.*** Common solutions used in this study are listed in this table.

	Buffers	Composition and Preparation
	U87MG Culture	
1	**Dulbecco's Modified Eagle's Medium (DMEM)**	Supplemented with 2 mM L-glutamine, 5% Foetal Bovine Serum (Gibco, Invitrogen) heat inactivated and penicillin 50 U/ml and Streptomycin 50 µg/ml (Sigma).
	Organotypic Culture	
2	**L15 Medium**	Supplemented with 0.6% D-glucose and 15 µg/ml Gentamicin (Sigma-Aldrich).
3	**L15 Medium – L-laminin**	L15 medium supplemented with 3 µg/ml of L-laminin (Sigma-Aldrich).

4	**Borate Buffer pH: 8.3 – poli-D-L-ornithine**	1.5 µg/mL poly-DL-ornithine in borate buffer 150 mM, pH: 8.3.
	Western Blot	
5	**Lysis Buffer (for U87MG cell line)**	50 mM Tris HCl pH: 6.8, 2 mM EDTA, 0.5% Triton x-100, in distilled water.
6	**Lysis Buffer (for E15 organotypic culture)**	50 mM Tris HCl pH: 6.8, 150 mM NaCl, 1 mM EDTA, 1% Triton x-100, in distilled water.
7	**Loading Buffer**	500 mM Tris HCl pH: 6.8, 30% glycerol, 8% β-mercaptoethanol, 8% SDS and 0.5% bromophenol blue, in distilled water.
8	**PBS 1x (Phosphate buffered saline)**	137 mM de NaCl, 2.7 mM de KCl, 12 mM de Na_2HPO_4, 1.38 mM de KH_2PO_4, pH: 7.4.
9	**Stacking Gel**	4% acrylamide–bisacrylamide, 166 mM Tris HCl, pH: 6.8, 0.1% SDS, 0.2% ammonium persulfate (APS) and 0.08% N,N,n',N'-tetramethylethylenediamine (TEMED).
10	**Running Gel**	7-12 % acrylamide-bisacrylamide, 0.75 M de Tris HCl pH: 8.8, 0.1% SDS, 0.05% APS i 0.05% TEMED.
11	**Running Buffer**	0.3% Tris base, 1.44% glycine and 0.1% SDS, pH ~ 8,5-8,6.
12	**Transfer Buffer**	48 mM Tris, 39 mM glycine, 0.04% SDS and 5-20% methanol (20% for proteins < 100KDa; 5% for proteins > 100KDa).
13	**Blocking Solution**	5% skim milk, 0.5% bovine serum albumin and 0.2% Tween-20, in PBS 1x.
	Immunochemistry	
14	**TBS 1x (Tris-buffered saline)**	137 mM NaCl, 2.7mM KCl, 20 mM Tris, in distilled water, pH: 7.6.
15	**0.1 PB (Phosphate buffer)**	0.1 M H_2NaO_4P, 0.1M HNa_2PO_4 in distilled water.
16	**Paraformaldehyde 4%**	4 g PFA (Sigma) in 100 ml of 0.1 PB.
17	**Quenching solution**	3% H_2O_2, 0.1% Triton x-100 in TBS 1x.
18	**Blocking solution**	5% normal goat serum and 0.1% Triton x-100 in TBS 1x

2 Antibodies

Table 7: ***Antibodies.*** List of all the antibodies used in this work, molecular weight (MW), commercial firm, hostage, usual dilution for Western Blott (WB) and Immunochemistry (IC).

Antibodies	MW (kDa)	Commercial firm	Hostage	IC dilution	WB dilution
Actin	43	Cytoskeleton	rabbit	-	1:500
Delta	75	Sta. Cruz	rabbit	1:200	-
GFAP	50	Dako Cytomation	rabbit	1:1000	-
IBA-1	17	Wako	rabbit	1:200	-
iNOS	130	BD Transduction Laboratories	mouse	1:200	-
nNOS	165	Millipore	rabbit	1:400	-
Jagged	150	Sta. Cruz	rabbit	1:200	-
MAP-2	75, 82, 280	Millipore	rabbit	1:200	-
MLC	18	Cell Signaling	rabbit	-	1:500
P-MLC	18	Cell Signaling	rabbit	-	1:500
Neurogenin	27	Millipore	rabbit	1:200	-
NICD	120	Sta. Cruz	goat	1:50	-
Notch-1	300, 120	Cell Signaling	rabbit	1:200	-
Profilin I	15	Cell Signaling	rabbit	1:100	1:1000
RhoA	22	Cytoskeleton	mouse	-	1:500
SMI-31	160, 200	Sternberger Monoclonals Inc.	mouse	1:1000	-
SMI-32	200	Sternberger Monoclonals Inc.	mouse	1:1000	-
SMN	39	Sta. Cruz	rabbit	1:200	-
SMN	40	BD Transduction Laboratories	mouse	1:100	1:5000
Synaptophysin	38	Millipore	mouse	1:200	-
α-Tubulin	50	Sigma-Aldrich	mouse	-	1:5000

3 Cell culture

The *in vitro* models used in this work were U87MG astroglioma cell line and rat spinal cord embryonic explants, previously developed in our laboratory.

3.1 Astroglioma cell line U87MG culture

U87MG human astroglioma cells were kindly provided by Dr. Priam Villalonga (IUNICS, Universitat de les Illes Balears) and Dr. Joan Seoane (Institut de Recerca Hospital Universitari Vall d'Hebron, Barcelona), and were selected since they are frequently used in motility studies (De Hauwer et al., 1997; Valster et al., 2005). U87MG cells were subconfluently grown and passaged, routinely tested for mycoplasma contamination and subjected to frequent morphological tests and growth curve analysis as quality-control assessments. U87MG cells were plated at a density of 25,000 cells/ml in 6-well plates and were grown in Dulbecco's Modified Eagle's Medium (DMEM) supplemented with 2 mM L-glutamine and 5% heat-inactivated fetal calf serum (FCS) in a humidified incubator at 37 °C with 5% CO_2.

For the migration assay, U87MG cell line was plated at 25,000 cells/ml, and 3 hours later cells were transduced with lentiviruses carrying shRNA EV, shSMNa or shSMNb. Figure 26 represents the common steps in all experiments analysing pathogenic phenotype of SMN-depleted U87MG astroglioma cells.

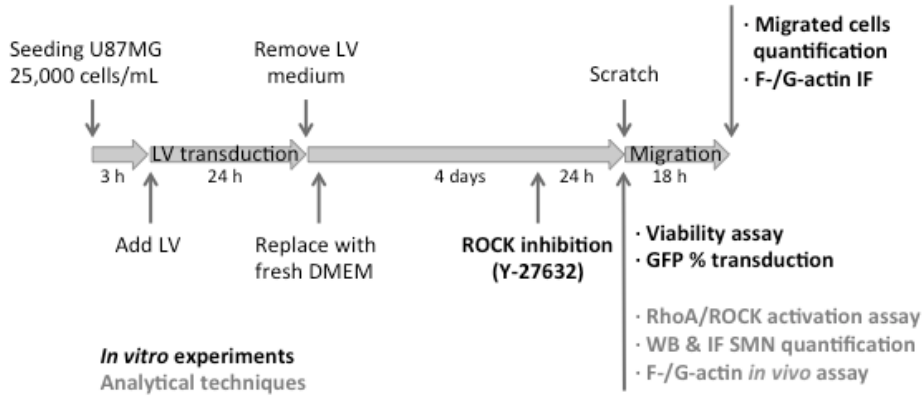

Figure 25: ***Astroglioma cell line U87MG experiments: timing,* in vitro *experiments and analytical techniques.*** In black bold letters are pointed out *in vitro* experiments and in grey bold letters, analytical techniques.

3.1.1 U87MG cell viability

Controlling viability of cells is a prerequisite for starting any analysis. Cells were collected and dyed with trypan blue. Live cells do not absorb toluidine-derived compounds because they are very selective in compounds that cross trough the membrane. The viability of U87MG cells was determined with an Automated 430 Cell Counter from Invitrogen using an exclusion method. This method quantifies the percentage of viable cells excluding dead cells, which show blue cytoplasm, because they do not select compounds traversing the membrane.

3.1.2 ROCK inhibition

RhoA has been described to play an important role in actin dynamics. In order to determine its role in U87MG migration, its activity has been inhibited through Y-27632, the ROCK inhibitor. For this purpouse, 24 hours before starting wound-healing assay, cells were incubated with Y-27632 (10 μM) (Calbiochem; Darmstadt, Germany).

3.2 Rat spinal cord embryonic explants

Rat spinal cord embryonic explants were performed according to the protocol described by Mir et al. (Mir et al., 2009). Embryos at gestational age of 15–16 days (E15-16) were removed by cesarean section from pregnant Sprague–Dawley rats (Charles River, Barcelona, Spain). Lumbar spinal cords were dissected from each embryo with forceps, transferred to ice cold Leibowitz's 15 medium (L15) and the meninges and ganglia carefully removed. Cords were transversely sectioned into 350 μm slices with a MacIlwain tissue chopper (Gomshall, Surrey, UK). Sections were carefully placed at a density of 20 sections per well on 35 mm-wells precoated with poly-DL-ornithine (30 μg/ml) and L-laminin (2 μg/ml) and containing 2 ml of Eagle's minimal essential medium (MEM) supplemented with 5% heat-inactivated horse serum, 5% fetal bovine serum, 2 mM glutamine, 0.6% glucose and 15 μg/ml gentamicin. Explants were maintained at 37 °C under a humidified 5% CO_2 atmosphere. To avoid the detachment of explants the wells were not manipulated during the first 4 days after platting; then, medium was changed and thereby every 3 days. After 5 days *in vitro*, some cells of the spinal cord, including motoneurons, started the migration outside the explant (figure 26). All treatments started 10 days after the explant procedure.

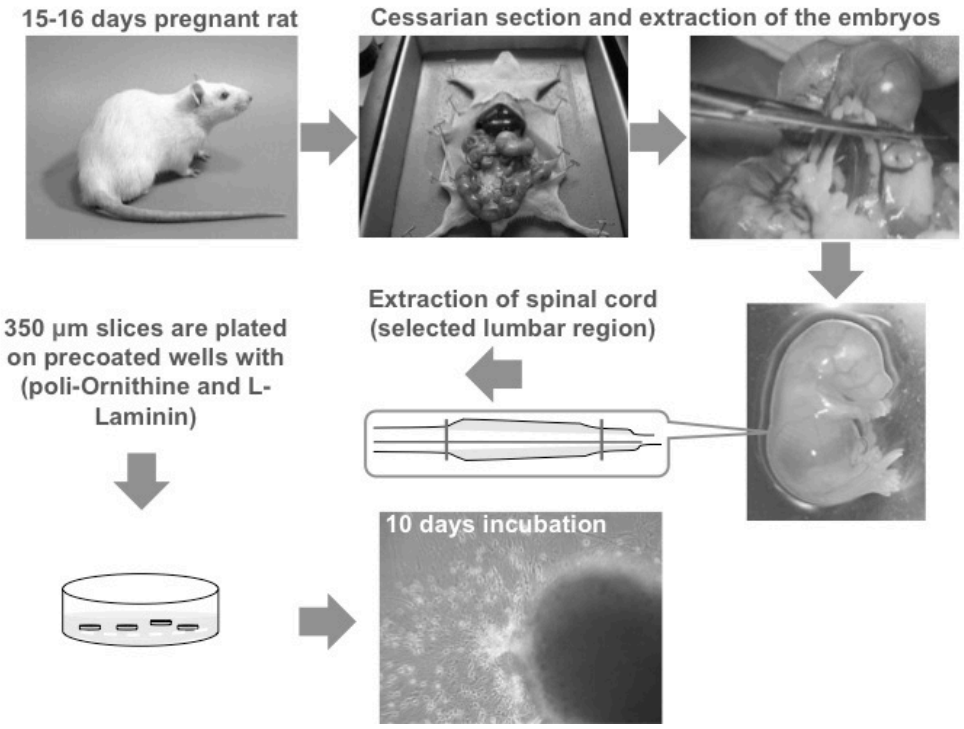

Figure 26: ***Rat spinal cord embryonic explants.*** From pregnant Sprague-Dawley rats, 15-16 days embryos are removed by caesarean. The spinal cord was dissected and the lumbar spinal cord was selected. After selection, the lumbar spinal cord was chopped in 350 µm slices, which were plated in poli-D,L-Ornithine/ L-laminin precoated wells. The explants were cultured for 10 days before the onset of transduction protocol.

4 Lentiviral transduction

To reduce SMN expression, RNA interference experiments were employed. The lentiviral vectors were kindly provided by Dr. Rosa Soler's group (IRBLLEIDA, Universitat de Lleida). Constructs were generated in pSUPER.retro.puro (Oligo-Engine; Seattle, WA, USA) using two specific oligonucleotides targeting SMN sequence (table 8), indicated by capital letters: shSMNa, forward: gatccccTGACAAGTGTTCTGCTGTTttcaagagaAACAGCAGAACACTTGTCAttt tt and reverse: agctaaaaa TGACAAGTGTTCTGCTGTTtctcttgaaAACAGCAGAA CACTTGTCAggg; shSMNb, forward: gatccccCGACCTGTGAAGTAGCTAAttca agagaTTAGCTACTTCACAGGTCGttttt and reverse: agctaaaaaCGACCTGTGA AGTAGCTAAtctcttgaaTTAGCTACTTCACAGGTCggg. Oligonucleotides were obtained from Invitrogen (Carlsbad; CA, USA). Adaptors to clone the

oligonucleotides into the BglII/HindIII sites of pSUPER.retro.puro were added as required. Lentiviral constructs were generated by digesting pSUPER-sh with EcoRI and ClaI to replace the H1 promoter with the H1-short hairpin RNA (shRNA) cassette in pLVTHM (table 8). pLVTHM vector contains the green fluorescent protein (GFP) under the control of an EF-1 alpha promoter for monitoring transduction efficiency. Lentiviruses were propagated in human embryonic kidney 293T (HEK293T) cells using the polyethylenimine (Sigma-Aldrich; St Louis, MO, USA) cell transfection method. Twenty micrograms of pLVTHM-SMNa, pLVTHM-SMNb, or pLVTHM-EV (empty vector), 13 µg of pSPAX2, and 7 µg of pMD2G were transfected to HEK293T cultures. pLVTHM, pSPAX2, and pMD2G were kindly provided by Dr. Trono (Université de Genève, Geneva, Switzerland). Cells were allowed to produce lentiviruses for 4 days. Then the medium was centrifuged at 1200 g for 5 min and the supernatant was filtered using a 22 µm filter. The medium containing the lentiviruses was stored at 4 °C. Biological titers of the viral preparations, expressed as the number of transducing units per ml (TU/ml), were determined by transducing HEK293T cells in limiting dilutions. After 48 h the percentage of GFP-positive cells was measured and viruses at $4x10^5$ – $1x10^6$ TU/ml were used for the experiments.

Table 8: ***Oligonucleotides targeting SMN sequence.*** In dark grey bold letters the forward sequence and in mild grey the reverse sequence of each construct.

siRNA	Location	Designed Primers: SMN RNAi	
shSMNa	421-430	gatcccc**AGTAAAGCACACAGCAAGT**ttca agaga**ACTTGCTGTGTGCTTTACT**tttt agctaaaaa**AGTAAAGCACACAGCAAGT**tc tcttgaa**ACTTGCTGTGTGCTTTACT**ggg	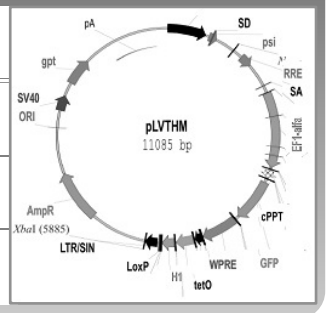
shSMNb	529-538	gatcccc**CGACCTGTGAAGTAGCTAA**ttca agaga**TTAGCTACTTCACAGGTCG**tttt agctaaaaa**CGACCTGTGAAGTAGCTAA**tc tcttgaa**TTAGCTACTTCACAGGTCG**ggg	

4.1 U87MG cell transduction

Before determining SMN-depletion, it is necessary to quantify the efficiency of transduction. Hence, cells were plated at a density of 25,000 cells/ml and 3 hours later medium was replaced with medium containing lentiviruses (2

TU/cell) carrying shRNA empty vector (EV), shSMNa or shSMNb. The constructs carried by lentiviral vectors in this study codify also for GFP protein. The medium was replaced with fresh medium 24 h later and infection efficiency was monitored in each experiment. Phase contrast and green fluorescence images of U87MG 90% confluent cultures were taken. Using ImageJ (http://rsbweb.nih.gov/ij/) software, the whole cells were selected with the cell-counter plug-in in phase-contrast images. The transduced cells were selected in the same way in fluorescent images.

Cells were grown for 4 additional days before starting the migration assay or sample collection for western blot, RhoA activation and cell viability assays (figure 26). The frequency of transduction rose 99% (see results section).

4.2 Rat spinal cord embryonic explant transduction

After 10 days in culture, embryonic explants medium containing lentiviruses ($4x10^5$ – $1x10^6$ TU/ml) carrying shRNA empty vector (EV), shSMNa or shSMNb was added to the cultured explants. The medium was replaced with fresh medium 24 h later and infection efficiency was monitored in each experiment by direct counting of GFP-positive motoneurons, using an epifluorescence microscope. Explants were left in the same conditions for 11 days before starting determination of SMN motoneuron depletion, soma reduction and axon affectation.

5 SMNΔ7 mouse model

Mouse lines were kindly provided by Dr. Lucía Tabares (Department of Medical Physiology and Biophysics, University of Seville). Experimental mice were obtained by breeding pairs of SMA carrier mice (*Smn*$^{+/-}$;*SMN2*$^{+/+}$;*SMNΔ7*$^{+/+}$) on a FVB/N background. Identification of wild-type and mutant mice (*Smn*$^{-/-}$;*SMN2*;*SMNΔ7*) was done by PCR genotyping of tail DNA as previously described (Le et al., 2005). All wild-type mice used were age-matched littermates of mutants. All experiments were performed according to the guidelines of the European Council Directive for the Care of Laboratory Animals.

Mice were anesthetized with tribromoethanol (2%, 0.15 ml/10 g body weight, i.p.) and intracardiacally perfused with saline solution followed by 4% paraformaldehyde in 0.1 M phosphate buffer, pH 7.4.

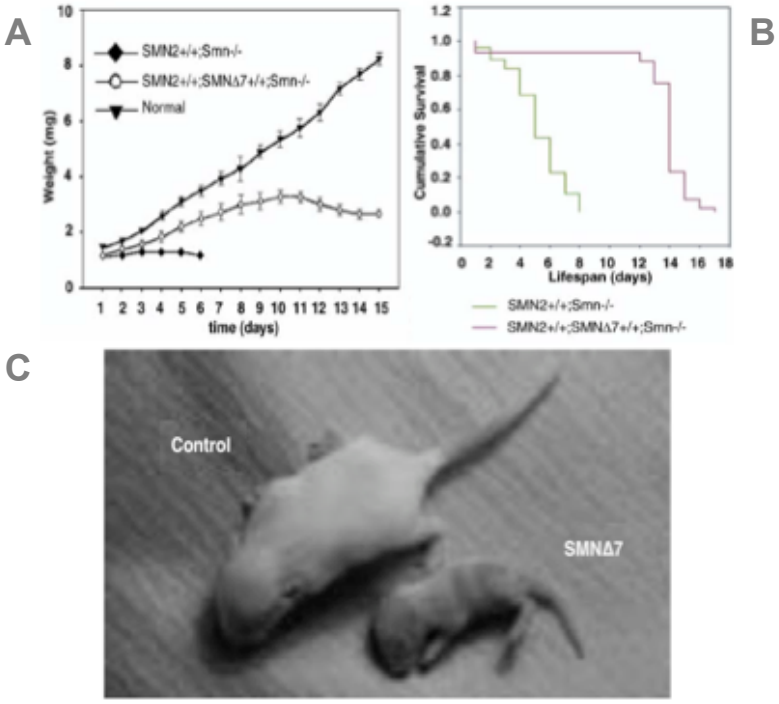

Figure 27: ***SMNΔ7 mouse model.*** Phenotypically the main differences between controls and SMNΔ7 mice are a reduction of 60% of weight at P13, evident muscular weakness, discrete motoneuron death at end point and a lifespan of only two weeks. (A) Weight curve evolution comparing control, SMNΔ7 and SMN2 models. (B) Lifespan curve compared between control, SMNΔ7 and SMN2 models. C. Images of control and SMNΔ7 mice (Le et al., 2005; Torres-Benito et al., 2012).

6 Monolayer wound-healing assay

The monolayer wound-healing assay is a proven method to study astrocyte cell migration (Környei et al., 2000; Höltje et al., 2005). U87MG cells were plated at 25,000 cells/ml in 6-well plates and exposed to shRNA EV, shSMNa or shSMNb for 24 h. Cells were grown for 4 additional days before starting the migration assay. At confluence, two parallel scratch wounds of approximately 400 μm width and an additional one, perpendicular to the first two were made with a P200 pipette tip. The cells were washed twice with PBS 1x before re-incubation with culture medium. This procedure makes possible to image the entire width of the wound using a 10x objective. The wounds were observed using phase contrast microscopy on an inverted microscope. Images were taken in four areas flanking the intersections of the horizontal wounds with the vertical wound at the time the wound was performed (t=0), and at selected times between 3 and

27 h after. The cells that repopulated the four areas were counted and the percentage of migrated cells in each experimental condition was calculated referred to empty vector exposed cells.

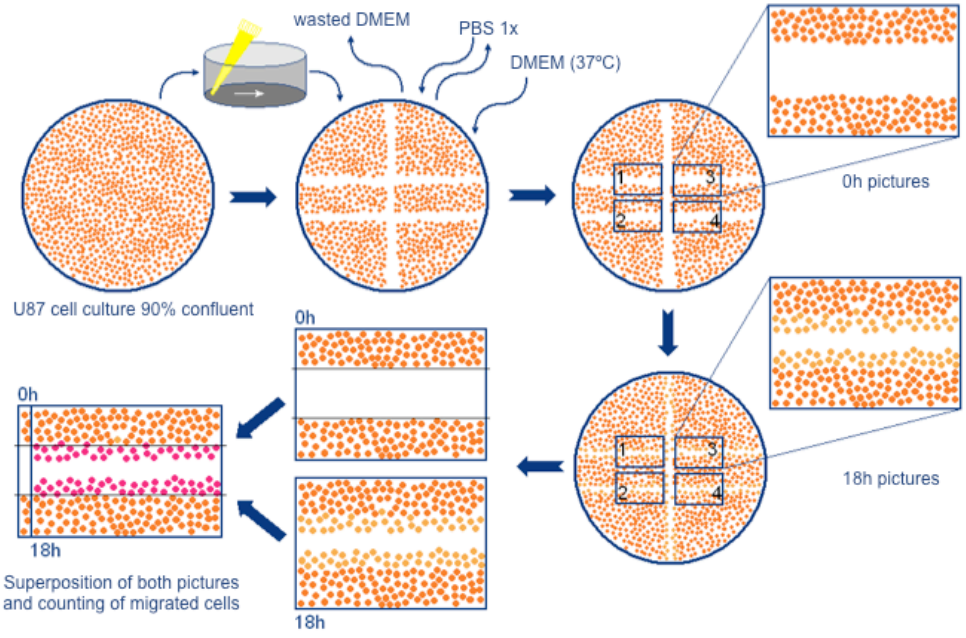

Figure 28: ***Monolayer wound healing assay.*** Starting with 90% confluence U87MG cell line, three scratches were done (400 µm width). Pictures were taken at time 0 h. The cells grew for 27 h, and pictures were taken periodically every 3 hours, from 3 to 27 hours. The migrated cells were counted in every time point.

7 Western Blotting

Western blotting analysis is a semi-quantitative molecular technique widely used for protein quantification, always referring the results to a housekeeping protein, which is supposed not to be altered by the experimental conditions. It is considered an immunological technique owing to the use of antibodies to detect the protein in the gel. The proteins are isolated in a SDS-PAGE (SDS-polyacrylamide gel electrophoresis), where the SDS makes all the proteins become negatively charged. Therefore, the proteins only differ in the molecular weight, and the lower molecular weight, the more they run through the gel.

7.1 U87MG Western Blotting

Cells were rinsed in ice-cold PBS and lysed with 50 mM Tris HCl, pH 6.8, 150 mM NaCl, 1 mM EDTA, 1% Triton X-100 containing a cocktail of protease inhibitors (Complete Mini; Roche Pharmaceutical, Basel, Switzerland). Lysates were sonicated and proteins quantified by means of the DC Protein Assay from Bio-Rad Laboratories (Hercules; CA, USA). Protein equivalents from each sample were resolved in SDS-polyacrilamide gel electrophoresis and electrotransferred to 0.45 μm nitrocellulose membranes (Amersham; Buckinghamshire, UK) using a Bio-Rad semidry trans-blot, according to the manufacturer's instructions. Membranes were blocked at 21±1 °C for 1 h with PBS containing non-fat dry milk, 0.5% bovine serum albumin (BSA) and 0.2% Tween 20. Membranes were probed overnight at 4 °C using antibodies directed to SMN, myosin light chain-2, also known as myosin regulatory light chain, phospho-MLC, profilin I, Jagged, Delta, NICD, Notch and α-tubulin, (Sigma-Aldrich). Finally, membranes were incubated with secondary antibody, bound to a horseradish peroxidase reporter enzyme, directed against rabbit, mouse or goat (1:2000).

8 Immunohistochemistry

A common technique to localize a protein directly in the cell or tissue where it is expressed is the immunocytochemistry or immunohistochemistry. This technique also allows to determine if two or more proteins are co-localized in the cell. Moreover, the localization within the cell –nucleus, cytoplasm or organelles– can be discerned. Like western blotting, immunohistochemistry is considered an immunological technique. The cells or tissue are permeabilized, blocked and incubated with an antibody recognizing the epitope of interest in the studied protein.

8.1 SMNΔ7 spinal cord sections immunofluorescence

The mouse spinal cords were dissected and fixed with 4% paraformaldehyde in 0,1 PB for 1 hour. Sections (10 μm) were obtained with a Leica criostat (LeicaCM3050) and mounted in microscope slides. Sections were quenched with H_2O_2 3% in TBS 1x or PBS 1x and permeabilized with methanol 100% for 5 minutes. After that, there were blocked with 5% NGS and 0.2% Triton X-100 in TBS 1x or PBS 1x for 1 h. Sections were incubated overnight at 4ºC with the

primary antibody diluted in 5% NGS and 0.2% Triton X-100 in TBS 1x or PBS 1x. Different primary antibodies were used: anti-neurofilament heavy chain (NF-H) (SMI-32), anti-phosphorylated neurofilament (SMI-31), anti-IBA-1, anti-GFAP, anti-iNOS, anti-nNOS, anti-MAP-2, anti-P-MLC, anti-Neurogenin, anti-Synaptophysisn, anti-Delta, anti-Jagged, anti-NICD and anti-Notch-1. Sections were incubated for 1 h with the appropriate secondary antibody, Alexa Fluor 555 goat anti-mouse IgG (1:200) or Alexa Fluor 488 goat anti-rabbit IgG (1:200) (Invitrogen; Paisley, UK). In the experiments were Nissl NeuroTracer (1:200) (Invitrogene; Paisley, UK) was used, it was added together with the secondary antibody incubation. Sections were then washed and mounted using Fluorescent Mounting Medium (Dako Cytomation; Glostrup, Denmark). Immunohistochemical controls, performed by omitting the primary antibody, resulted in the abolition of the immunostainig.

8.2 U87MG Immunofluorescence

Cells were fixed with paraformaldehyde 4% in 0,1 PB for 30 minutes, and permeabilized in 100% methanol for 5 minutes. Before blocking with 5% NGS and 0.2% Triton X-100 in TBS 1x or PBS 1x for 1 h, cells were washed twice with TBS 1x or PBS 1x. To assess the localization pattern of SMN in U87MG cells, incubation with anti-SMN primary antibody from BD Transduction Laboratories (Becton, Dickinson & Co.; Franklin Lakes, NJ) was performed overnight, at 4ºC. In some experiments profilin expression was studied with anti-profilin I. After three washes in TBS 1x or PBS 1x, cells were incubated with an appropriate Alexa Fluor secondary antibody conjugated with 488 or 555 fluorescent dyes (Invitrogene; Paisley, UK), against rabbit or mouse, for 1 hour. Images were obtained using an epifluorescence microscope and a confocal laser-scanning microscope. Immunofluorescence was quantified using ImageJ (http://rsbweb.nih.gov/ij/) software. In order to determine SMN nuclear localization, U87MG cells were stained with Hoechst 33258 (10 µg/ml, 20 min) in PBS 1x, after immunofluorescence with SMN antibody, as described previously. After Hoechst 33258 binding, cells were washed with PBS 1x and fixed. The cells were mounted with fluorescent mounting media (Dako Cytomation; Glostrup, Denmark).

8.3 E15 motoneurons immunofluorescence

Motoneurons from embryonic explants were fixed with paraformaldehyde 4% in 0,1 PB for 30 minutes, and permeabilized in 100% methanol for 5 minutes. Before blocking with 5% NGS and 0.2% Triton X-100 in TBS 1x or PBS 1x for 1 h, explants were washed twice with TBS 1x or PBS 1x. To assess the depletion of SMN in motoneurons, incubation with anti-SMN primary antibody was performed overnight, at 4ºC. Moreover, motoneurons were stained with anti-neurofilament phosphorylated heavy chain (SMI-31). After three washes in TBS 1x or PBS 1x, explants were incubated with an appropriate Alexa Fluor secondary antibody conjugated with 488 or 555 fluorescent dyes (Invitrogene; Paisley, UK), against rabbit or mouse, for 1 hour.

9 Pull-down assays for the measurement of RhoA activation

The Rho activation assay kit (Cytoskeleton; Denver, USA) was used for RhoA activity measurements after SMN depletion. This kit is based on the capacity of Rho-GTP to bind to GST-Rhotekin (Ren and Schwartz, 2000), and was used according to the manufacturer's instructions. Briefly, cells (5–10e06) were lysed, cleared (10,000 g) and incubated for 1 h at 4 °C with glutathione sepharose- 4B beads coupled with GST-Rhotekin. An aliquot of the lysates was stored for the determination of the amount of total RhoA per sample. Beads were washed 4 times in lysis buffer. Bound proteins were solubilized by the addition of 35 µl of Laemmli loading buffer and separated on 12.5% SDS-polyacrilamide gels. The amounts of total RhoA in the input lysate and of active RhoA in the bound fraction were detected by western blotting.

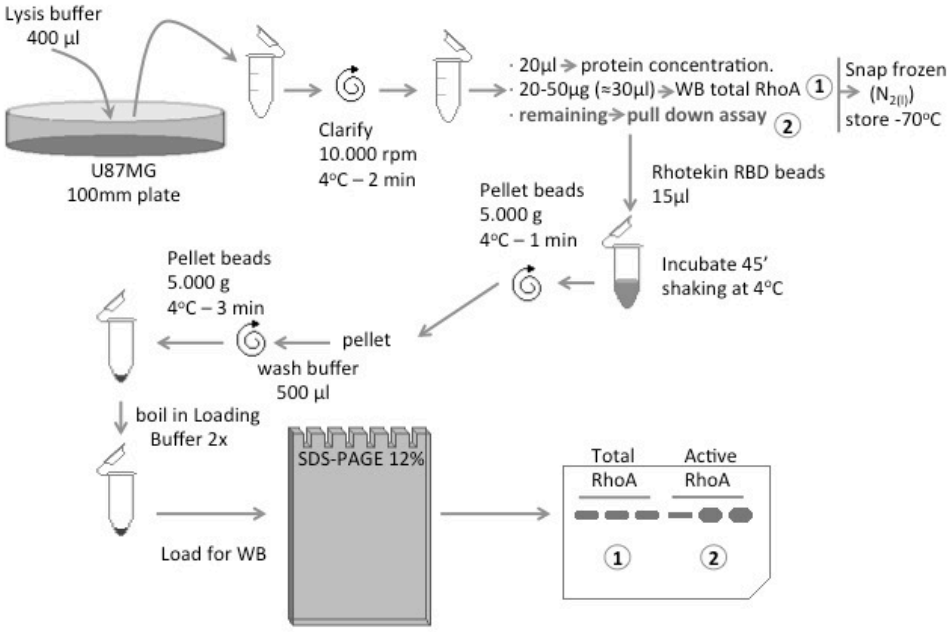

Figure 29: ***Schemeatic protocol of the pull-down assay for RhoA activation measurement.*** Cells were lysed and collected. An aliquot (1) of this collected sample was used for total RhoA determination. After centrifugation for clarifying the samples, incubate samples with the Rhotekin RBD beads. After a set of centrifugations, the active RhoA is isolated. Finally, the ratio active RhoA/ total RhoA was determined by means of Western Blot.

10 F- and G-actin determination

Determination of the percentage of F- and G-actin in the cell culture was performed via two different methods: *in vivo* assay and fluorescent determination.

10.1 *In vivo* F- and G-actin assay

The ratios of F- and G-actin were determined in U87MG cells using an F-/G-actin in vivo assay kit (Cytoskeleton; Denver, USA), following the manufacturer's protocol, as described by (van Bergeijk et al., 2007).

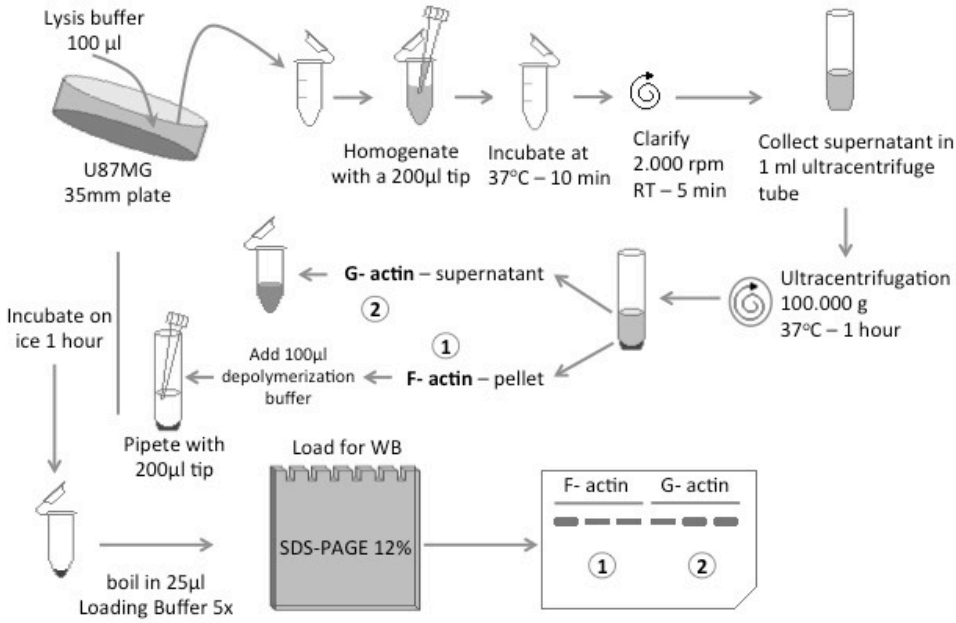

Figure 30: ***Scheme of the protocol of F- and G- actin assay.*** Cells were lysed and collected and ultracentrifugated at 100.000 g at 37ºC for 1h. The supernatant was collected for G-actin determination and the pellet was used for F-actin determination. F-actin fraction was depolymerizated. After boiling the samples, the ratio F-/G-actin was determined by means of Western Blot.

Briefly, cells were lysed, homogenized, incubated for 10 min at 37 °C and clarified by centrifugation at 2000 rpm for 5 min at 21±1 °C (figure 30). The supernatant was then centrifuged at 100,000 g at 37 °C for 1 h. After ultracentrifugation, supernatants containing the G-actin fraction were transferred to another tube and placed on ice. The pellet containing the F-actin was resuspended in F-actin depolymerization buffer and incubated for 1 h. Aliquots of both the supernatant and the pellet fractions were analyzed by western blot and probed with the anti-actin antibody (1:500) supplied with the kit.

10.2 F- and G-actin fluorescence determination

To study the actin cytoskeleton in U87MG cells after depletion of SMN, cells were fixed with paraformaldehyde 4% in 0,1 PB for 20 minutes, avoiding the use of 100% methanol as it disrupts actin filaments. Cells were permeabilized with 0.1% Triton X-100 in PBS 1x for 6 min and blocked with 1% BSA and 0.1% Triton X-100 in PBS 1x for 30 min. After blocking, filamentous (F)- and monomeric (G)-actin in cells were labeled with Alexa Fluor 350 phalloidin (1:40) and deoxyribonuclease I (DNAseI) Alexa Fluor 594 conjugate (1:500) (Molecular Probes; Carlsbad, CA, USA), respectively, diluted in 1% BSA and 0.1% Triton X-100 in TBS 1x for 30 min, as described in the protocol by (Da Silva et al., 2003).

11 Motoneuron morphological analysis

Motoneurons in SMNΔ7 mouse model and rat embryonic explants were studied via immunohistochemistry. In that sense, motoneuron count, presence of phosphorylated NF, motoneuron soma area score and synaptophysin-immunoreactive puncta per motoneuron were determined.

11.1 Motoneuron count

Motoneurons from lumbar spinal cord of P14 mice were identified by SMI-32 immunostaining and on the basis of their morphology and size (>25 μm), and their localization in the ventral horn. All motoneurons meeting these criteria were blindly counted in each spinal cord section. At least 100 motoneurons were counted per animal, in controls and SMNΔ7 mice, in at least 20 sections per aninal. Three animals per condition were used. Finally, the results were expressed as percentage of motoneuron per section, referring the counts in SMNΔ7 mice to each control.

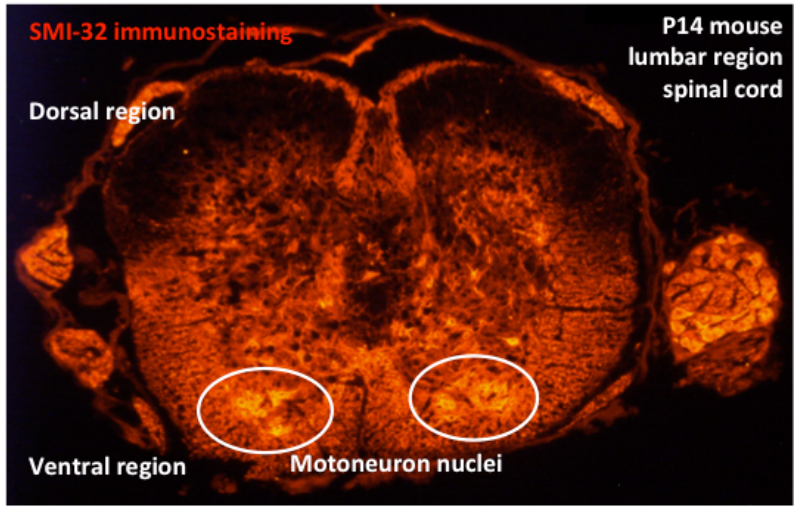

Figure 31: ***Motoneuron nuclei in P14 mouse spinal cord.*** Motoneurons were identified by SMI-32 immunostaining and on the basis of their morphology and size (>25 μm), and their localization in the ventral horn. In the image, SMI-32 overexposed slice is represented in order to identify the whole spinal cord slice and the anatomic localization of motoneurons within the slide.

11.2 Phosphorylated NF in motoneurons

SMI-31 is an antibody against phosphorylated NF heavy-chain, which is a marker of pathologic motoneurons (Kato and Hirano, 1990). Motoneurons from lumbar spinal cord of P14 mice were labelled with SMI-31, as described in immunochemistry section. In P14 mice, at least 100 motoneurons were counted per animal, in control and SMNΔ7 mice, in three animals per condition. Finally, the results were expressed as the percentage of SMI-31 positive motoneuron, referred to the total number of motoneurons.

11.3 Area of motoneuron soma

In the SMNΔ7 mice and controls, after SMI-32 immunostaining in spinal cord sections, we identified all motoneuron on the basis of their morphology and size (>25 μm), and their localization in the ventral horn. Using ImageJ software, the soma area was selected with the measure tool. NIH ImageJ software scored the selected area of at least 80 motoneurons in three diferent animals per group. The area mean in the SMNΔ7 mice was compared with the area mean in controls.

In the embryonic explants, the motoneurons migrate out of the spinal cord slice and they are isolated from the high amount of cells in organotypic culture. These motoneurons are easily transduced with lentiviruses. All fields containing motoneurons were scored and the area of motoneurons was determined using NIH ImageJ software after immunofluorescence with the SMI-31 antibody. There were counted at least 80 motoneurons per group. The area mean, expressed in μm^2, in the SMN-depleted motoneurons was compared with the area mean in shRNA EV transduced motoneurons and non-transduced motoneurons (controls).

11.4 Quantification of synapses on motoneurons

Synaptophysin is a synaptic vesicle protein, component of the synaptic vesicle fusion pore and involved in the biogenesis and stability of synaptic vesicles (Fykse et al., 1993). After immunofluorescence against synaptophysin and SMI-32, synaptic boutons were quantified with ImageJ software, using the counter plug-in.

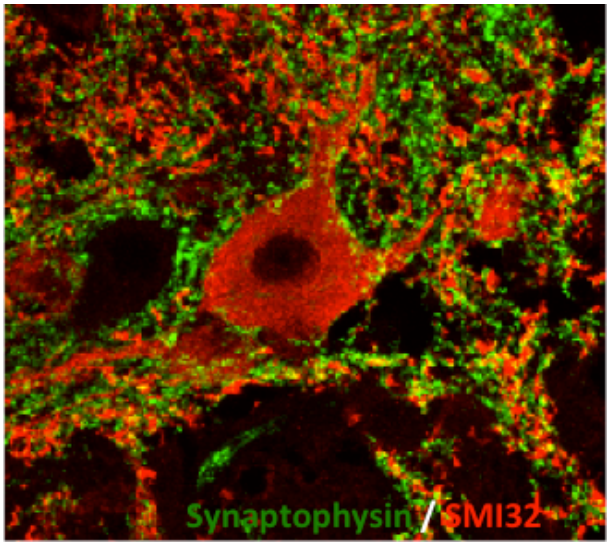

Figure 32: ***Synaptophysin and SMI-32 in P14 mouse motoneurons.*** Motoneuron (in **red**) surrounded by synaptic boutons, positive for synaptophysin (in **green**).

11.5 Determination of axonal disruptions in embryonic explant motoneurons

The number of axonal disruptions was assessed by counting the number of points where a discontinuity in the phosphorylated neurofilament could be observed. All fields in which motoneurons could be observed were scored. The results were expressed as a number of disruptions per mm^2 in control, shRNA EV tranduced and SMN-depleted motoneurons.

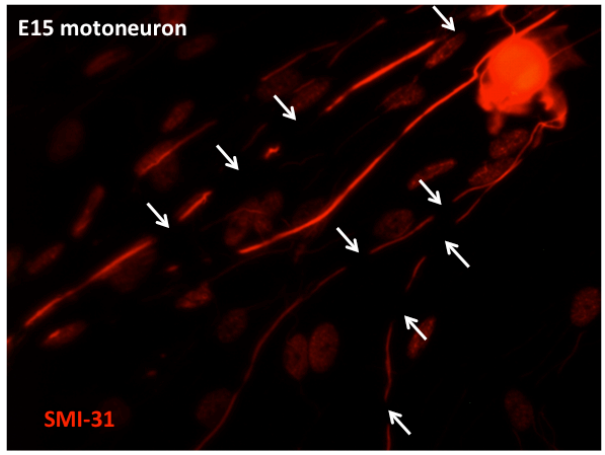

Figure 33: ***Axonal disruptions in E15 motoneurons.*** Arrows indicate points were axonal disruptions were clear and counted. Motoneurons and axons were stained with SMI-31 antibody.

11.6 Imaging

Images were obtained using a Leica DMR epifluorescence microscope (Leica Microsystems; Wetzlar, Germany), equipped with a Leica DC 300 camera and software and a Leica TCS SP2 confocal laser-scanning microscope. Immunofluorescence was quantified using ImageJ (http://rsbweb.nih.gov/ij/) software.

12 Statistical analysis

Data have been analysed with GraphPad Prism 5.0c software. All results have been expressed as a mean ± SEM of at least 3 independent experiments. The statistical analysis used has been one-way ANOVA, followed by a Bonferroni post-test. In the experiments where only two conditions have been compared, it was used the t-Student test. The values with a $p<0.05$ have been accepted as statistically significant.

IV. RESULTS

IV. Results

This section has been subdivided into three parts, according to objectives described in Aims section.

First Objective

1 SMN deficiency causes alterations in cytoskeleton structure and cellular migration

1.1 Pathological hallmarks affecting motoneuron neurofilament after SMN depletion by use of shRNA

Interference of RNA represents a powerful method to inhibit gene expression at posttranscriptional level, and is an appropriate tool to generate an in vitro model of Smn loss-of-function (Dykxhoorn et al., 2003). To investigate the pathology of motoneurons associated to SMA, we carried out a lentiviral-based knock-down of Smn in cultured motoneurons from rat embryonic explants, at gestational age of 15-16 days (E15-16) (Mir et al., 2009).

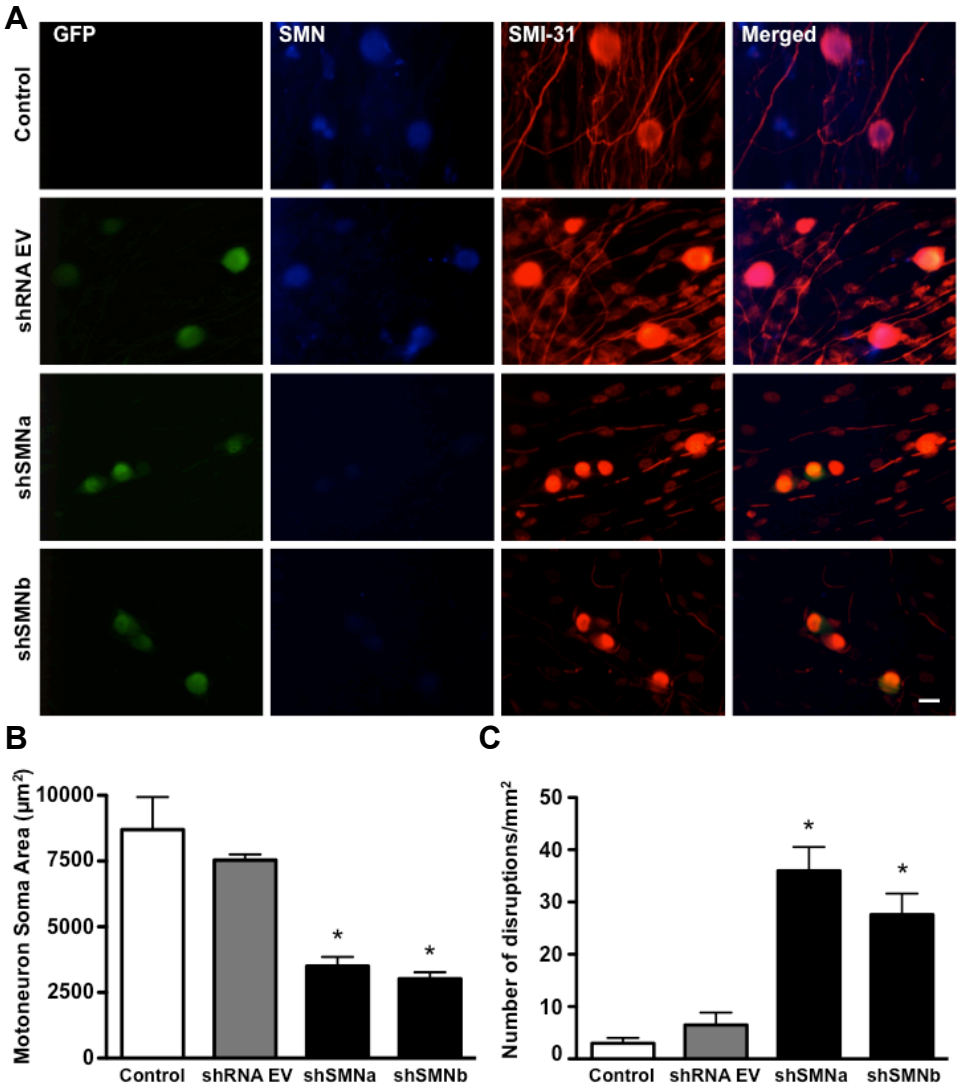

Figure 34: ***Effect of Smn reduction in rat spinal cord motoneurons.*** (A) Representative microscopy images from rat spinal cord embryonic explants 11 days after lentiviral transduction: immunofluorescence with anti-SMN antibody (blue) or anti-SMI-31 antibody (red) and GFP (green). C, indicates control U87MG cells; EV, indicates lentiviral transduced cultures carrying an empty vector; and shSMNa or shSMNb, indicate cultures transduced with lentivirus carrying the constructs targeting SMN sequence. Scale of bar is 50 µm. (B and C) Rat explants were transduced by lentiviral constructs carrying EV or shSMNa or shSMNb, or not transduced (controls). Ten days after transduction the area of cell somas (B) and the neurite disruptions (C) were measured. Values are the mean of two independent experiments for each condition ± SEM (error bars). Asterisks indicate significant differences when comparing the data from shSMN cultures with EV cultures using one-way ANOVA test (* at least $p<0.05$).

To this end, two different shRNA sequences targeting specific sites of mouse and rat Smn sequence (shSMNa and shSMNb) were used to knock-down the expression of this protein in motoneurons. Five days after lentiviral transduction, cells were monitored by fluorescence microscopy, and nearly 99% motoneurons were efficiently transduced, as they were GFP positive.

In figure 34, images show that Smn protein level (in blue) was clearly reduced after 10 days of shSMN transduction in motoneurons (identified by morphological features and by immunostaining for phosphorylated neurofilament with the SMI-31 antibody).

We observed that neuronal cell bodies were smaller than EV controls and untreated controls, and neurites also showed a disrupted morphology. Measuring the size of motoneurons soma and the number of neurite disruptions (see materials and methods section), we concluded that both parameters were altered when Smn protein level was decreased. Motoneurons from shSMN transduced explants showed a higher number of neurite disruptions ($p<0.01$) and significantly smaller soma size ($p<0.001$) (figure 34C). Taken together, these *in vitro* results suggested that Smn protein knock-down causes motoneuron degeneration.

1.2 SMN deficiency attenuates migration of U87MG astroglioma cells through the activation of RhoA

1.2.1 SMN knock-down in U87MG cells by use of short hairpin (sh) RNA interference

After describing cytoskeleton alterations in a model of the SMA disease, where the SMN expression was decreased, it is logical to evaluate the affectation of migration mechanism after SMN depletion. To investigate the role of SMN in cell migration, U87MG astroglioma cells, a well-established cell line for migration studies, was employed (De Hauwer et al., 1997).

As it is described above, two different shRNA sequences targeting SMN (shSMNa and shSMNb) were used to knock-down the expression of this protein in U87MG astroglioma cell line. Four days after lentiviral transduction, a cell viability assay showed that the reduction of SMN induced by shSMNa and shSMNb did not impair cell survival (figure 35A). Cells were monitored by

fluorescence microscopy, and nearly 99% cells were efficiently transduced, as they were GFP positive (figure 35B).

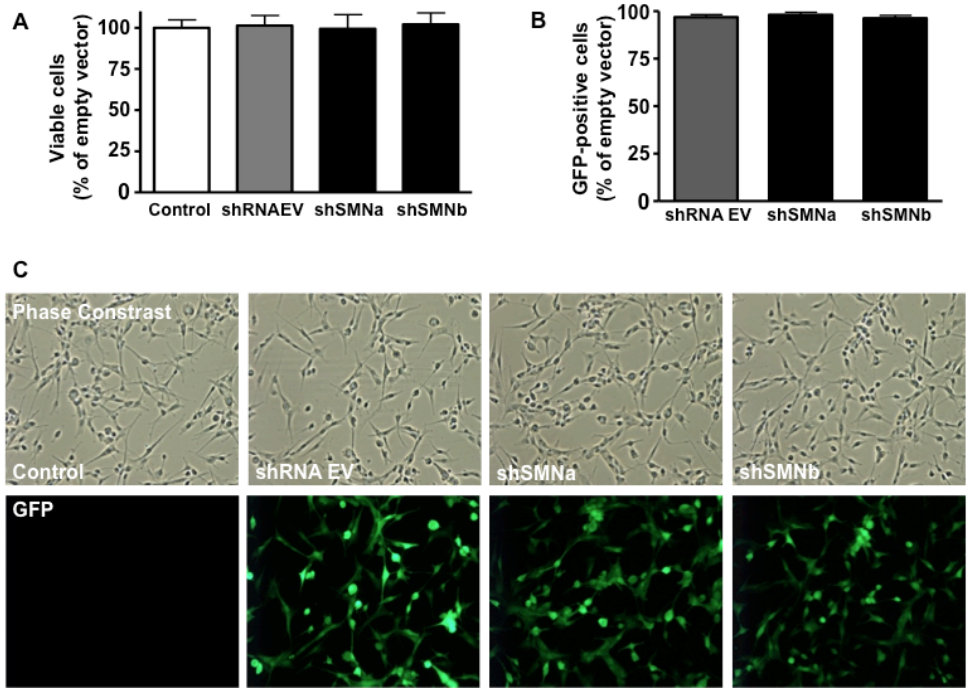

Figure 35: ***shSMN lentiviral transduction of U87MG cells.*** (A) Column bars indicate the percentage of U87MG viable cells determined by trypan blue exclusion method (using an Automated 430 Cell Counter from Invitrogen) with respect to shRNA EV cells, and are the mean ± SEM of three independent experiments. *p<0.01 as compared to shRNA EV (ANOVA followed by Bonferroni's test). (B) Column bars indicate the percentage of U87MG GFP-positive cells determined by fluorescence microscopy and ImageJ cell counter (using an Automated 430 Cell Counter from Invitrogen) with respect to shRNA EV cells, and are the mean ± SEM of three independent experiments. *p<0.01 as compared to shRNA EV (ANOVA followed by Bonferroni's test). (C) Representative microscopy images of control (non-transduced) U87MG cells or after transduction with lentiviruses containing the empty vector (shRNA EV), shSMNa or shSMNb constructs, as indicated. GFP indicates green fluorescent protein expressing cells present in the same microscopic field of that shown by phase contrast. Scale bar = 100 μm.

Immunofluorescence studies indicated that SMN was located both in the cytoplasm and nucleus of U87MG cells (figure 36). In the nucleus, SMN immunofluorescence displayed a punctate pattern consistent with its previously described co-localization with Cajal bodies (Liu and Dreyfuss, 1996).

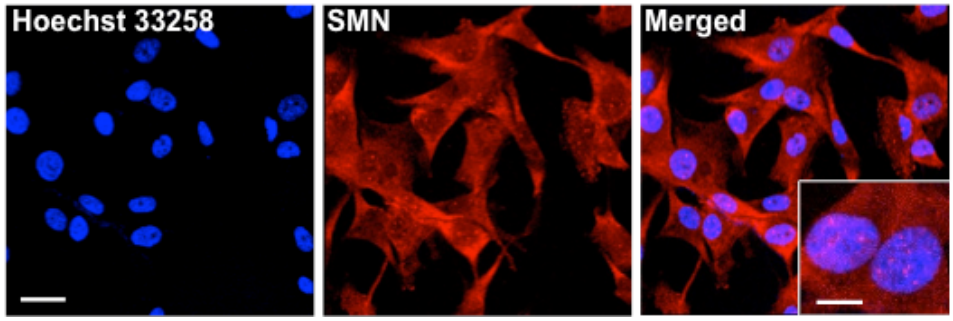

Figure 36: ***SMN protein distribution in human U87MG astroglioma cell line.*** Representative images of U87MG cells exposed to Hoechst 33258 (10 µg/ml, 20 min) to label cell nuclei and immunostained with anti-SMN (Alexa Fluor 555) to show the subcellular distribution of SMN. Scale bar = 25 µm, scale bar in insert = 12.5 µm.

When cells were transduced with lentiviruses carrying the shSMNa or shSMNb constructs, a decrease in SMN-immunofluorescence was found (figure 37A). To assess efficiency of shRNA, cell lysates were analyzed by western blotting several days after transduction. After 4 days, the time-point of maximum inhibition, both shSMNa and shSMNb sequences induced nearly a 60% reduction in SMN expression levels as compared to that transduced with shRNA EV (empty vector) (figure 37B).

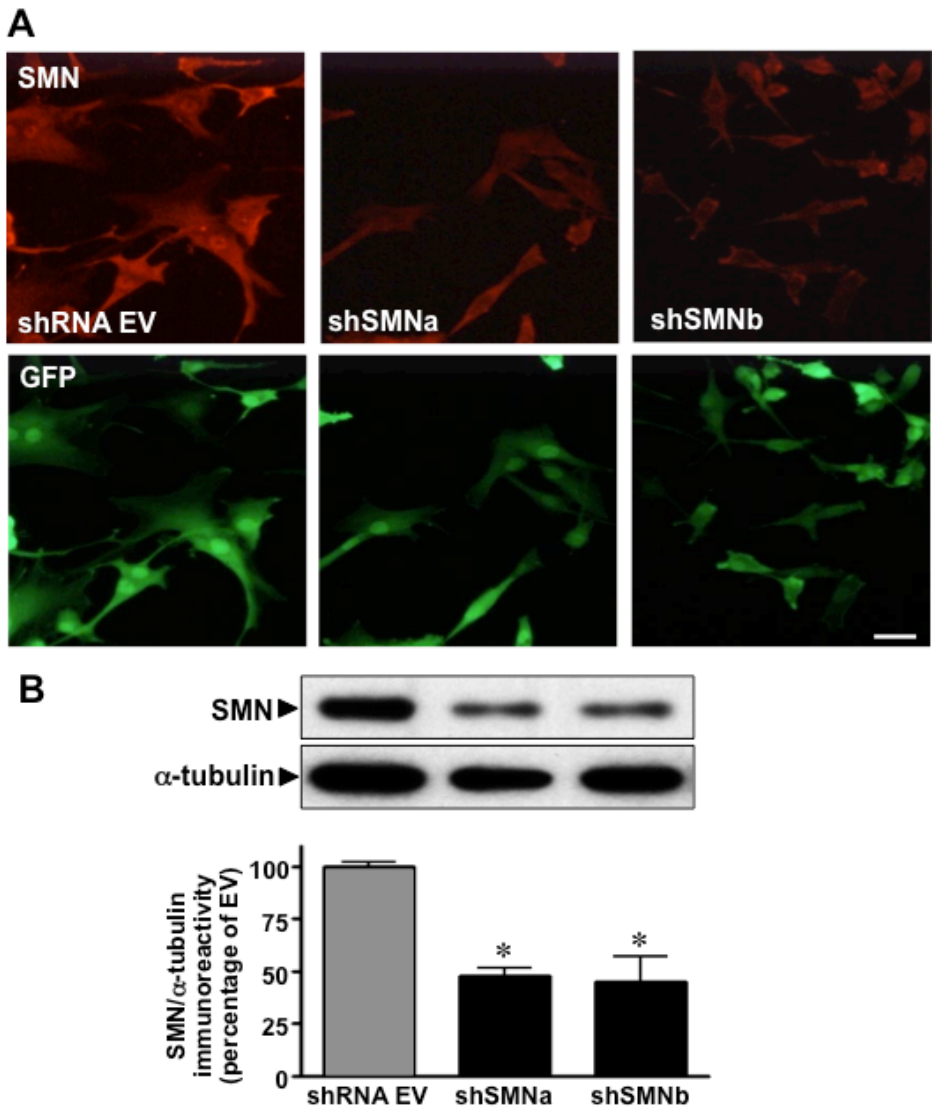

Figure 37: ***Effect of shSMN lentiviral transduction of U87MG cells on endogenous SMN protein levels.*** (A) Representative images of U87MG cells transduced with shRNA EV, shSMNa or shSMNb constructs as indicated. The cells are double-labeled with anti-SMN (Alexa Fluor 555) to show the expression of the protein SMN, and with green fluorescent protein (GFP). Scale bar = 50 μm. (B) Top. Representative western blot showing the expression of SMN in U87MG cells after transduction with shRNA EV, shSMNa or shSMNb constructs, as indicated. α-tubulin immunoreactivity is shown as a control of total protein (10 μg) loaded per lane. Bottom. Column bars indicate the percentage of immunoreactivity of SMN determined by densitometric analysis (integrated optical density of SMN vs. α-tubulin bands) with respect to shRNA EV cells, and are the mean ± SEM of three independent experiments. *$p<0.01$ as compared to shRNA EV (ANOVA followed by Bonferroni's test).

1.2.2 Affectation of U87MG migration via RhoA/ROCK signaling pathway after SMN knock-down

To investigate the role of SMN protein in cell migration, U87MG cells were grown in monolayer and exposed to shRNA EV, shSMNa or shSMNb and then wounded as described in materials and methods section. Images from the same field were taken at the indicated time-points between 0 and 27 h after the wound, then the number of cells that re-colonized the cell-free area was counted, as a measure of the cell migration rate (figure 38A). Significant differences between shRNA EV and shSMNa or shSMNb exposed cells were found from 9 to 27 h after the wound. The maximum difference (50% reduction) in cell-migration was observed at 18h (figure 38B), and then decreased at higher time-points. Thus, in SMN-depleted cells a delay in migration rather than a permanent inability to migrate was found (figure 38A and B), and different cell morphology were observed in the migrating edge between SMN-depleted cells and shRNA EV cells (figure 39), suggesting that cells near the edge of the wound were in active process of migration.

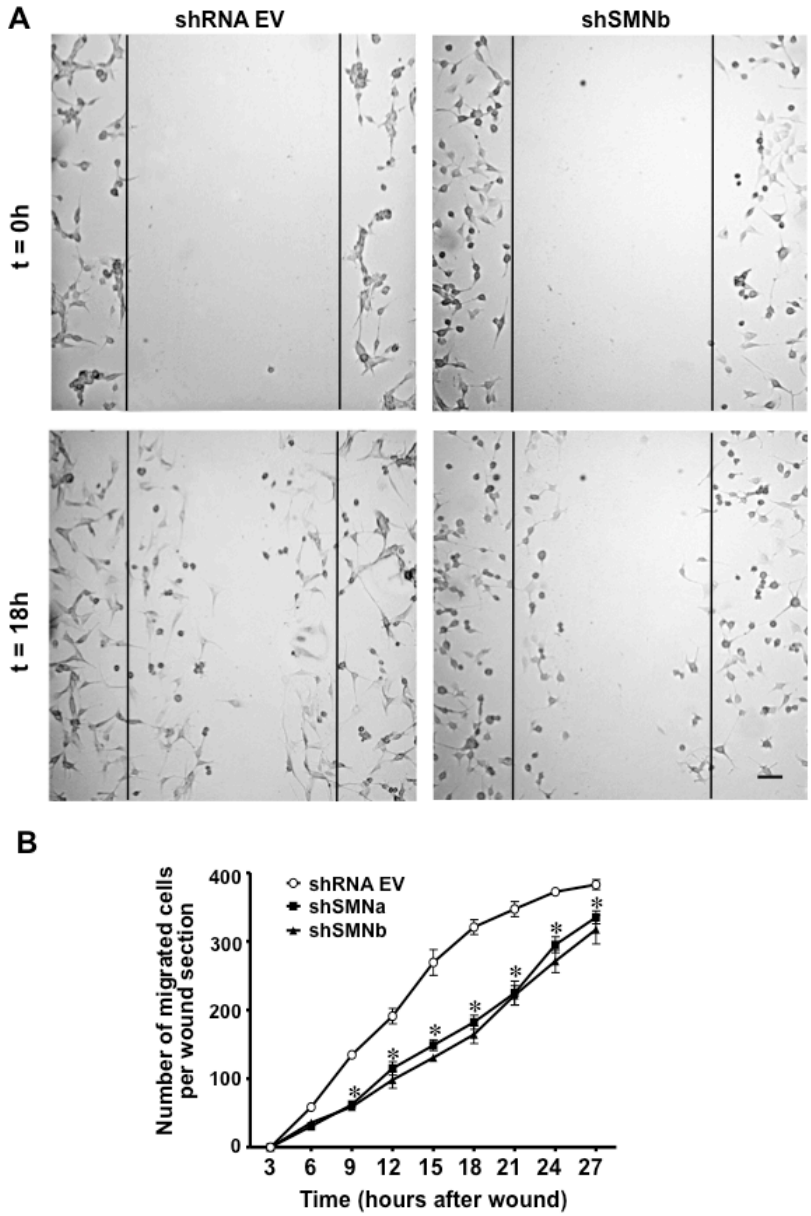

Figure 38: ***Reduced cell migration of U87MG cells depleted of SMN.*** Confluent monolayers of U87MG cells transduced with lentiviruses containing the empty vector (shRNA EV), shSMNa or shSMNb constructs were scratched with a pipette tip to generate a cell-free wound area. Migrated cells were quantified as described in materials and methods section. (A) Plots represent the number of cells exposed to shRNA EV, shSMNa or shSMNb that migrated into the cell-free area at the indicated time-points. Data are the mean ± SEM of three independent experiments. *At least $p<0.01$ for shSMNa and shSMNb compared to shRNA EV (ANOVA followed by Bonferroni's test). (B) Representative images showing cells exposed to shRNA EV and shSMNb, at 0 and 18 h after the wound. Scale bar = 50 μm.

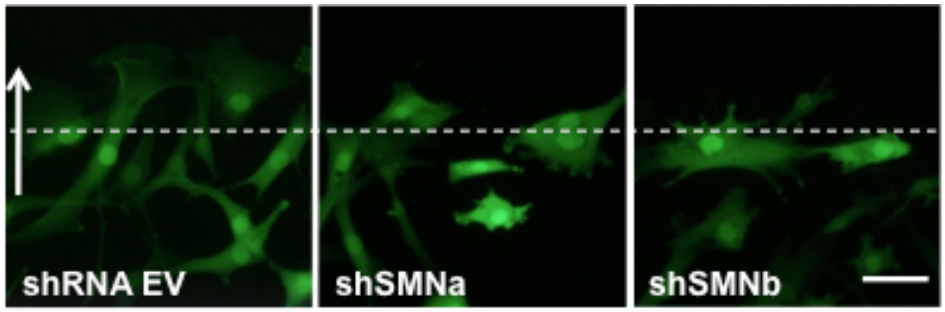

Figure 39: ***Differences in cell migration edge of U87MG cells depleted of SMN.*** Confluent monolayers of U87MG cells transduced with lentiviruses containing the empty vector (shRNA EV), shSMNa or shSMNb constructs were scratched with a pipette tip to generate a cell-free wound area. U87MG SMN-depleted cells in the migrating edge showed different morphology when compared to shRNA EV cells. Scale bar = 25 μm.

Since Rho GTPases are key regulators of cell motility (Takaishi et al., 1993; Ridley, 2001; Govek et al., 2011), and increased RhoA activation has been observed in SMN-depleted models (Bowerman et al., 2007; 2010), we investigated the possible role of RhoA/ROCK in the reduction of U87MG cell migration upon SMN knock-down. Interestingly, SMN depletion with shSMNa or shSMNb induced the activation of RhoA in U87MG cells (percent increase: 170% in shSMNa and 266% in shSMNb; $p<0.0001$) (figure 40).

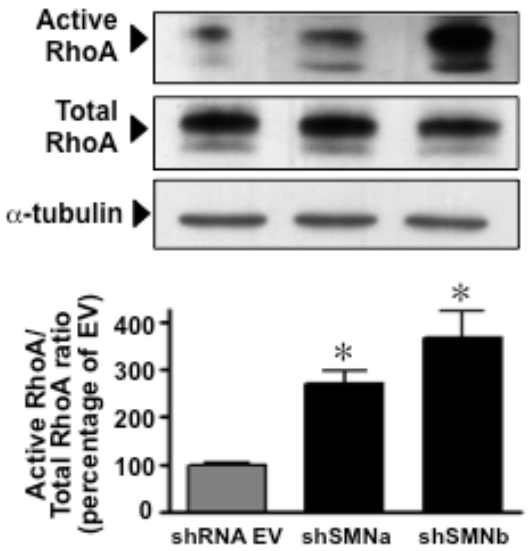

Figure 40: ***The RhoA/ROCK pathway is activated in SMN-depleted U87MG cells.*** Top. Representative western blot of active and total RhoA in U87MG cells after transduction with lentiviruses containing the empty vector (shRNA EV), shSMNa or shSMNb constructs, as indicated. Total RhoA and α-tubulin immunoreactivities are shown as a control of total protein (30 μg) loaded per lane. Bottom. Column bars indicate the immunoreactivity ratio of active RhoA versus total RhoA, determined by densitometric analysis (integrated optical density of active RhoA band vs. total RhoA band), with respect to cells exposed to shRNA EV, and are the mean ± SEM of three independent experiments. *$p<0.01$ as compared to shRNA EV (ANOVA followed by Bonferroni's test).

Activation of the RhoA/ROCK pathway was also confirmed as increased levels of phosphorylated myosin light chain (P-MLC), a substrate of ROCK, were detected both in shSMNa and shSMNb cells (figure 41). In addition, the peptide Y- 27632, a synthetic compound that inhibits ROCK by competing with its ATP binding site (Ishizaki et al., 2000), completely reverted MLC phosphorylation (figure 41).

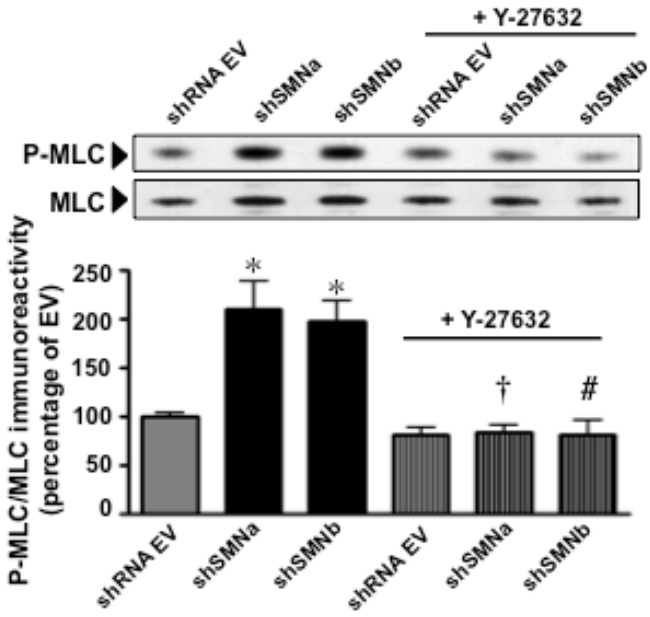

Figure 41: ***The SMN-depleted U87MG cells had increased levels of phosphorylated MLC protein.*** Top. Representative western blot of phosphorylated myosin regulatory light chain (P-MLC), a substrate of ROCK, in U87MG cells after transduction with lentiviruses containing the empty vector (shRNA EV), shSMNa or shSMNb constructs, as indicated. The selective ROCK inhibitor Y-27632 (10 μM) was added, where indicated, 24 h prior to harvesting cells. MLC immunoreactivity is shown as a control of total protein (5 μg) loaded per lane. Bottom. Column bars indicate the percentage of immunoreactivity of P-MLC determined by densitometric analysis (integrated optical density of P-MLC vs. total MLC), with respect to cells exposed to shRNA EV and are the mean ± SEM of three independent experiments. *$p<0.01$ as compared to shRNA EV, †$p<0.001$ as compared to shSMNa, and #$p<0.001$ as compared to shSMNb (ANOVA followed by Bonferroni's test).

Finally, when SMN knock-down cells were assayed for motility in the presence of Y-27632, the rate of cell migration was restored to levels of control cells (shRNA EV) (figures 42A and B).

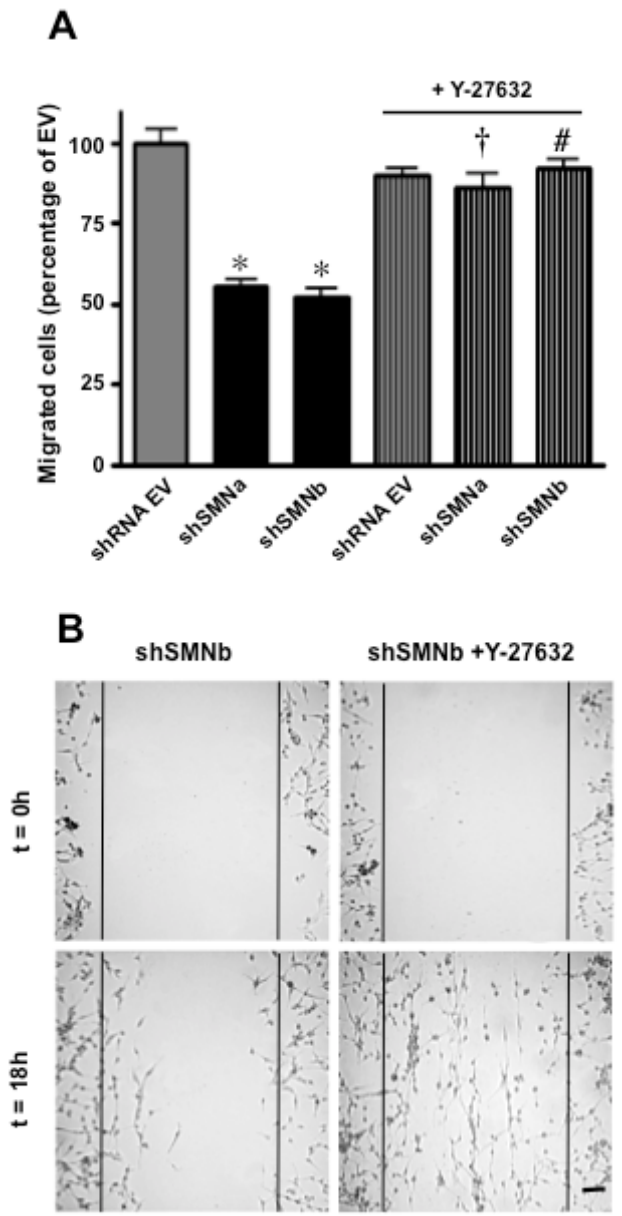

Figure 42: ***The RhoA/ROCK pathway is involved in the migration defects of SMN-depleted U87MG cells.*** (A) Confluent monolayers of U87MG cells were transduced with lentiviruses containing the empty vector (shRNA EV), shSMNa or shSMNb constructs and exposed to Y-27632 (10 μM) 24 h prior to the wound-healing assay where indicated. Column bars represent the percentage of cells that repopulated the cell free area 18 h after the wound with respect to cultures exposed to shRNA EV and are the mean ± SEM of three independent experiments. *$p<0.001$ as compared to shRNA EV, †$p<0.001$ as compared to shSMNa, and #$p<0.001$ as compared to shSMNb (ANOVA followed by Bonferroni's test). (B) Representative images showing cells exposed to shSMNb and shSMNb plus Y-27632, at 0 and 18 h after the wound. Scale bar = 50 μm.

1.2.3 SMN knock-down affects actin cytoskeleton and increases profilin I expression

Cell migration, changes in cell morphology and adhesive properties are regulated by continuous remodeling of the actin cytoskeleton; since SMN has been involved in actin dynamics (Bowerman et al., 2007; van Bergeijk et al., 2007; Bowerman et al., 2009; 2010), we next studied actin distribution in SMN shRNA cells. Confocal microscopy indicated that knocking-down SMN resulted in the disappearance of stress fibers (figure 43A). Quantification of the immunofluorescence for filamentous (F)- and globular (G)-actin indicated a significant reduction in the ratio of F-/G-actin (figure 43B). Then, the amounts of filamentous and globular actin were measured by an in vivo assay using differential precipitation of F-actin (pellet fraction) and G-actin (supernatant) after centrifugation of cell lysates. Western blots indicated a shift from filamentous to monomeric (globular) actin in cells exposed to shSMNa or shSMNb, thus confirming the immunofluorescence results (figure 44).

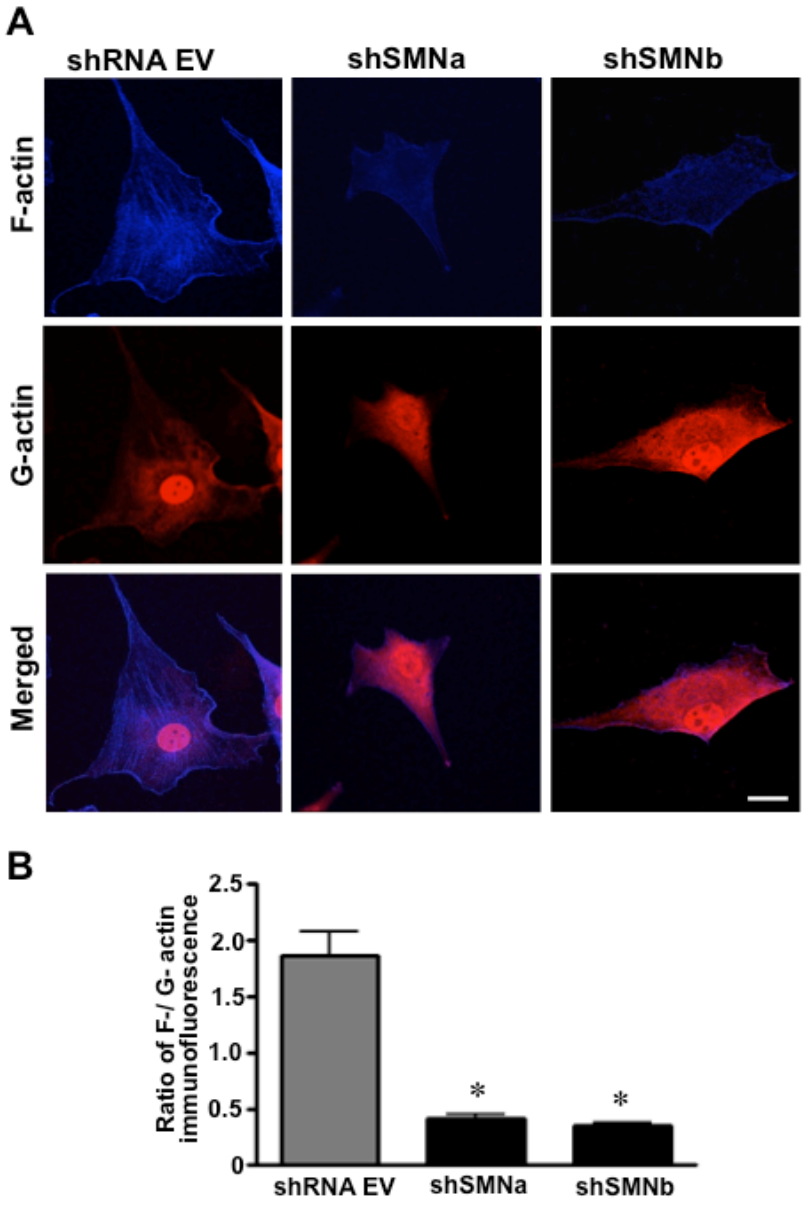

Figure 43: ***Decreased F-/G-actin immunofluorescence ratio in U87MG cells depleted of SMN.*** (A) Representative images of double immunofluorescence for filamentous (F)-actin (Alexa Fluor 350 phalloidin) and globular (G)-actin (Alexa Fluor 594 DNAseI) in U87MG-migrating cells after transduction with lentiviruses containing the empty vector (shRNA EV), shSMNa or shSMNb constructs, as indicated. Scale bar = 25 μm. (B) Column bars represent the F-/G-actin immunofluorescence ratio in U87MG cells transduced with shRNA EV, shSMNa or shSMNb and are the mean ± SEM of three independent experiments. *$p<0.001$ as compared to shRNA EV (ANOVA followed by Bonferroni's test).

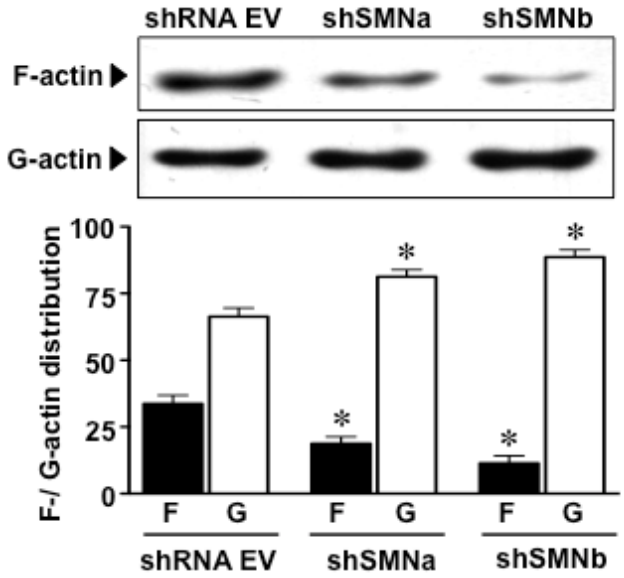

Figure 44: ***Decreased F-/G-actin ratio in U87MG cells depleted of SMN.*** Top. Representative western blot showing the expression of F- and G-actin in U87MG cells after transduction with lentiviruses containing the empty vector (shRNA EV), shSMNa or shSMNb constructs, as indicated, and after the in vivo assay described in materials and methods section. Bottom. Column bars indicate the relative proportions of F- and G-actin determined by densitometric analysis of their respective immunoreactivities and are the mean ± SEM of three independent experiments. *At least $p<0.01$ as compared to the corresponding F- or G-actin in shRNA EV (ANOVA followed by Bonferroni's test).

Increased levels of profilin, a protein that sequesters monomeric actin and prevents its polymerization (Cao et al., 1992) have been found in SMN-depleted models (Bowerman et al., 2007; 2009; 2010). An increase in the immunofluorescence of profilin I was also detected in SMN-depleted U87MG cells (figures 45A and B). This result was corroborated by western blot experiments showing also an increased expression of profilin I after SMN depletion (figure 46). To determine if this increased expression of profilin I could be related to the increased RhoA/ROCK activity found in SMN-depleted cells, U87MG cells were exposed to the ROCK inhibitor Y-27632. Interestingly, profilin I levels were not modified in the presence of this inhibitor (figure 46).

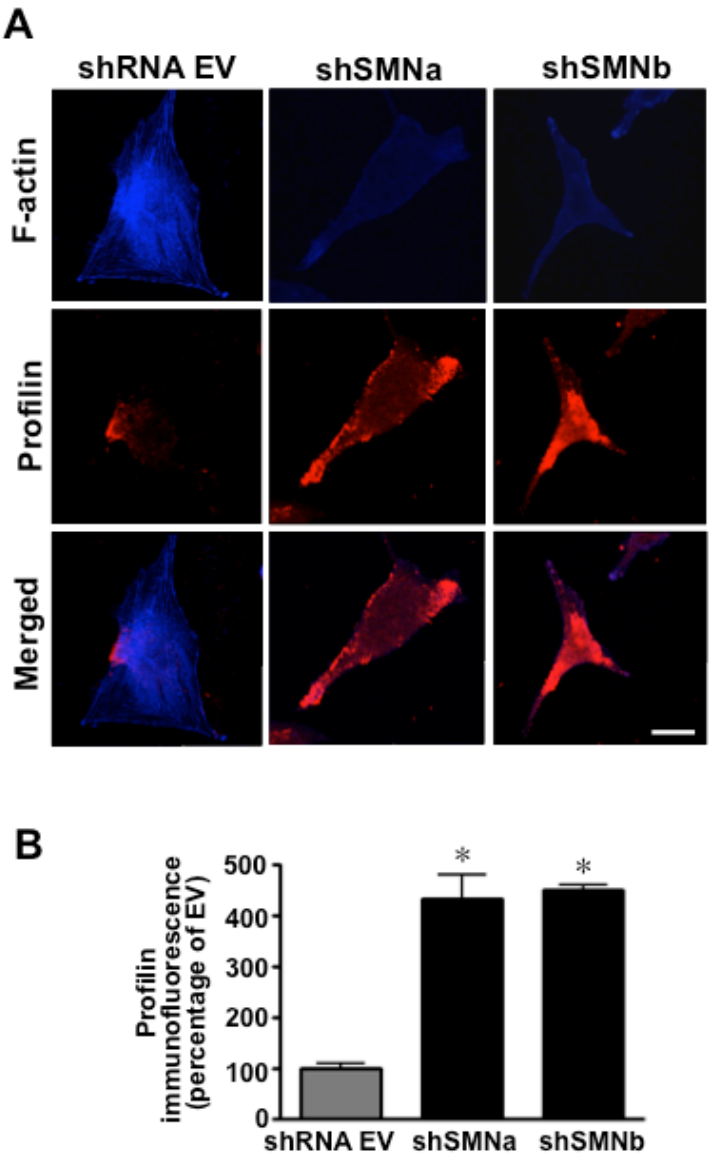

Figure 45: ***Increased profilin I immunoreactivity in U87MG cells depleted of SMN.*** (A) Representative images of double immunofluorescence for fibrilar (F)-actin (Alexa Fluor 350 phalloidin) and profilin I (Alexa Fluor 555) in U87MG-migrating cells after transduction with lentiviruses containing the empty vector (shRNA EV), shSMNa or shSMNb constructs. Scale bar = 25 μm. (B) Column bars represent the percentage of profilin I immunofluorescence in U87MG cells transduced with shSMNa or shSMNb with respect to cells exposed to shRNA EV and are the mean ± SEM of three independent experiments. *$p<0.001$ as compared to shRNA EV (ANOVA followed by Bonferroni's test).

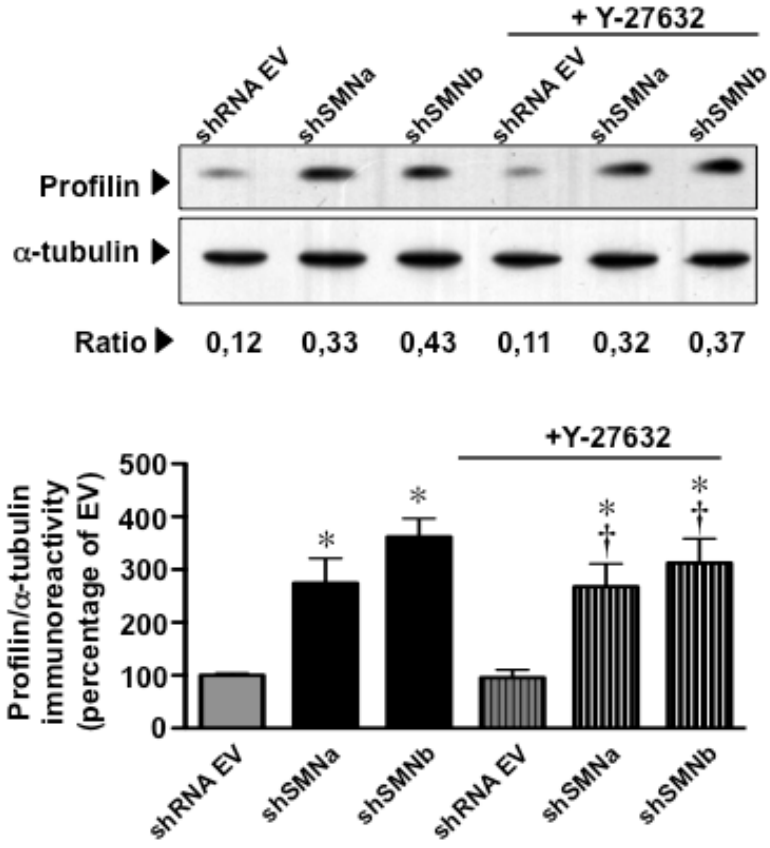

Figure 46: ***Increased profilin I expression in U87MG cells depleted of SMN.*** Top. Representative western blot showing profilin I immunoreactivity in U87MG cells after transduction with lentiviruses containing the empty vector (shRNA EV), shSMNa or shSMNb constructs, as indicated. The selective ROCK inhibitor Y-27632 (10 μM) was added, when indicated, 4 days prior to harvesting the cells. α-tubulin immunoreactivity is shown as a control of the total protein (10 μg) loaded per lane. The profilin I/α-tubulin ratio shown below represents the mean of three independent experiments. Bottom. Column bars indicate the percentage of immunoreactivity of profilin I determined by densitometric analysis (integrated optical density of profilin I vs. α-tubulin), with respect to cells exposed to shRNA EV, and are the mean ± SEM of three independent experiments. *$p<0.001$ as compared to shRNA EV, †$p<0.001$ as compared to shRNA EV plus Y-27632 (ANOVA followed by Bonferroni's test).

Second objective

2 Neuroinflammatory response in the spinal cord of the SMNΔ7 mouse model of SMA

2.1 Motoneuron loss and pathological changes in SMNΔ7 mice

We studied the loss of motoneurons in the lumbar spinal cord in the SMNΔ7 mouse model of the SMA disease, and we observed a moderate but significant loss of them. The reduction in the number of motoneuron was significative at P14-15, with a reduction of 24.2% (figure 47A). These results suggest that at terminal stages of the disease there is still loss of motoneurons. Besides the decrease in the number of surviving motoneurons at P14-15, another evidence of pathological alterations affecting the surviving motoneurons, especially at terminal stages, is the reduction in the area of motoneuron soma: there are less motoneurons and the surviving motoneurons have a smaller area (controls = 3780 ± 145 μm^2; SMNΔ7 = 2390 ± 116 μm^2) (figure 47B). Another pathological hallmark of motoneuron pathology is the presence of abnormally phosphorylated neurofilament (Ackerley et al., 2004); in this regard, a significant increase in the number of ventral horn motoneurons positive for SMI-31 antibody against phosphorylated neurofilament (figure 47C) from about 12% in controls to almost 70 % in SMNΔ7 animals at P14 was observed.

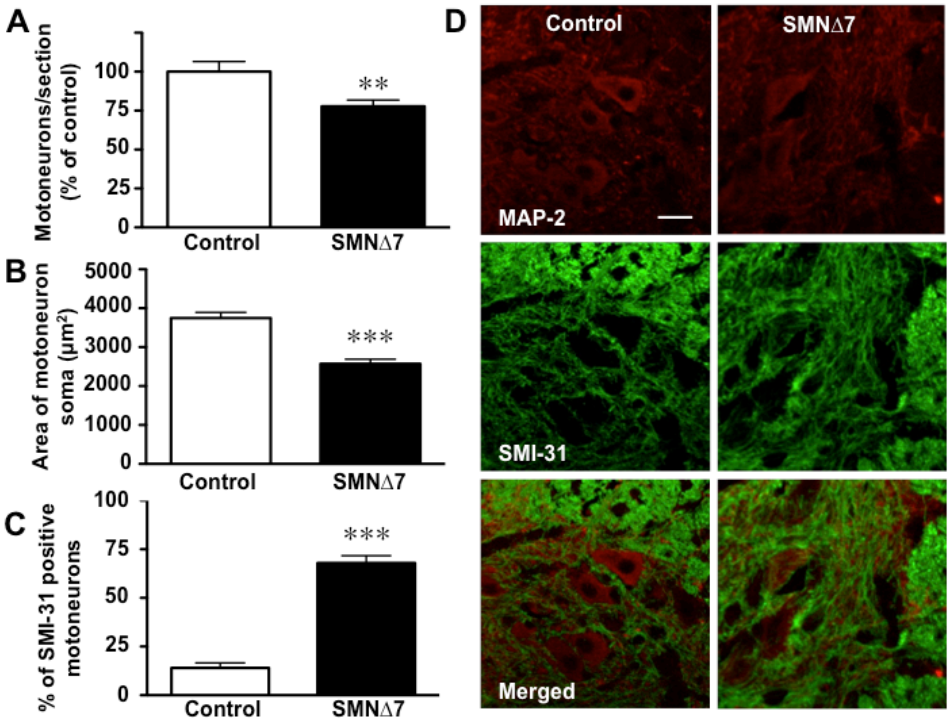

Figure 47: ***Reduction in the number of spinal cord motoneurons and pathological alterations in SMNΔ7 mice.*** Immunofluorescence performed in lumbar spinal cord of P14 SMNΔ7 mice with MAP-2, SMI-32 and SMI-31 antibodies showing an increase in motoneuron pathological markers and a reduction in the number of motoneurons. (A) Column bars represent the percentage of increase in SMI-31 (phosphorylated heavy-chain neurofilament) positive motoneurons in SMNΔ7 mice as compared to age-matched controls, and are the mean ± SEM (error bars) in 50 motoneurons of at least 4 mice per group. ***p<0.0001 as compared to age-matched control animals (t-Student test). (B) Column bars represent the motoneuron area in μm² after immunofluorescence for SMI-32 and are the mean ± SEM (error bars) of 40 motoneurons of at least 4 mice per group. ***p<0.0001 as compared to control animals from each age (t-Student test). (C) Column bars represent the reduction in the number of motoneurons per section after immunofluorescence for SMI-32, and represent the average ± SEM (error bars) in 40 motoneurons of at least 4 mice per group. **p<0.001 as compared to control animals (t-Student test). (D) Representative images of SMI-31 immunofluorecence in motoneurons from the lumbar spinal cord section of SMNΔ7 mice at P14 and age-matched controls.

2.2 Selective astroglial activation in the ventral area of the lumbar spinal cord of SMNΔ7 mice before motoneuron death

To detect other pathological changes in the spinal cord of SMNΔ7 mice, immunofluorescence studies with GFAP were performed in sections of lumbar spinal cord from different time-points ranging from early stage (P5) to pre-symptomatic (P8), symptomatic (P11) and end-stages (P14), and showed an increased number of GFAP-positive astrocytes compared to their age-matched controls, starting at P5 (figure 48A). Interestingly, motoneurons were observed surrounded by an increased number of GFAP-positive astrocytes as compared to their age-matched controls (figure 49).

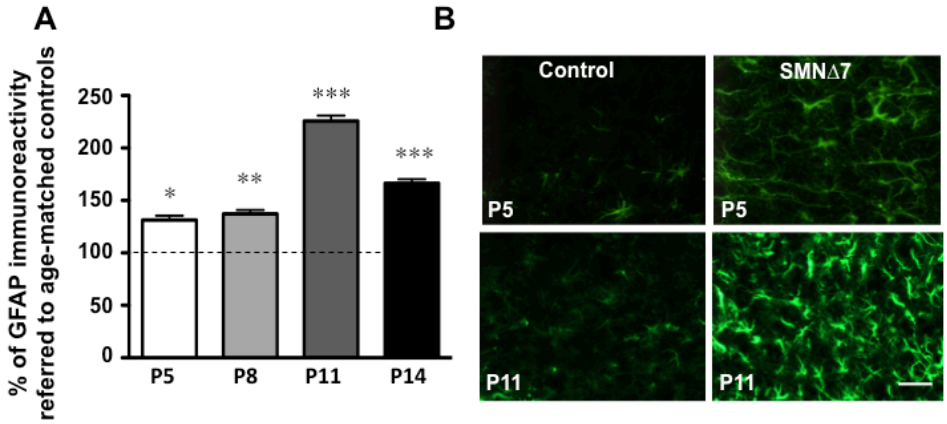

Figure 48: ***Astroglial activation in SMNΔ7 mice.*** Immunofluorescence with anti-GFAP performed in lumbar sections of SMNΔ7 mice revealed an increase in the astroglial activation starting at P5, showing a maximum at P11. (A) Column bars represent the increase in GFAP positive astrocytes in mice at the indicated ages between P5 and P14 as compared to age-matched controls, and are the average ± SEM (error bars) in 8 sections per animal and 4 fields per section of at least 4 mice per group. *p<0.01, **p<0.001 and ***p<0.0001 as compared to age-matched control animals (ANOVA followed by Bonferroni's test). (B) Immunofluorescence images show that the astrogliosis process in SMNΔ7 mice is more intense in P11 than in P5 mice. Scale bar = 50 μm.

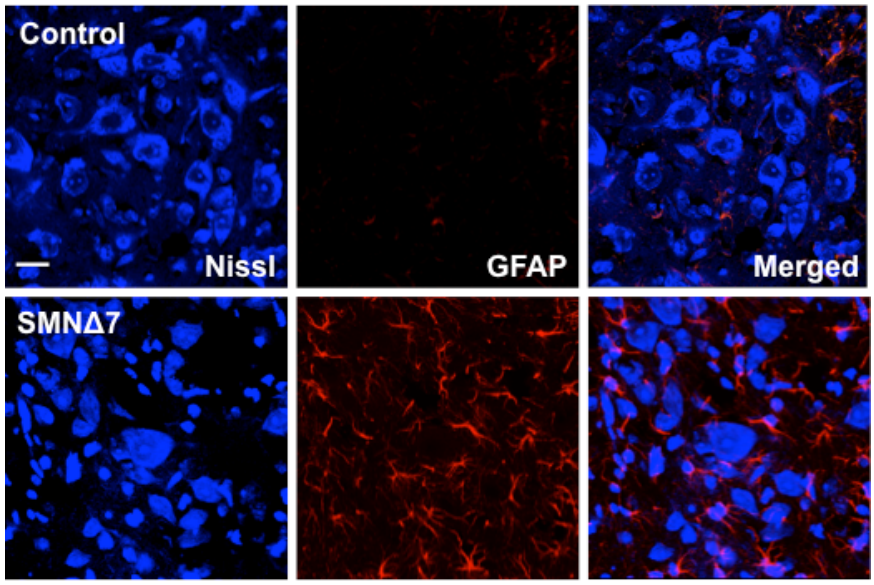

Figure 49: ***Astroglia surrounding motoneurons in SMNΔ7 mice.*** Immunofluorescence with anti-GFAP performed in lumbar spinal cord sections of SMNΔ7 mice revealed the increased presence of astrocytes surrounding motoneurons in the ventral horn at P11 in the SMNΔ7 model. Scale bar = 25 μm.

In order to study the pattern of glial activation and thus possible differences in astroglial activation between dorsal and ventral areas (surrounding motoneurons), immunofluorescence studies with GFAP was performed independently in dorsal and ventral areas of the lumbar spinal cord from P5 and P11 SMNΔ7 mice. In SMNΔ7 at P5, astroglial activation was only observed in the ventral horn, and dorsal horns were negative for GFAP. By contrast, at P11, glial activation was observed also in the dorsal horn of the SMNΔ7 mice (figures 50A and B).

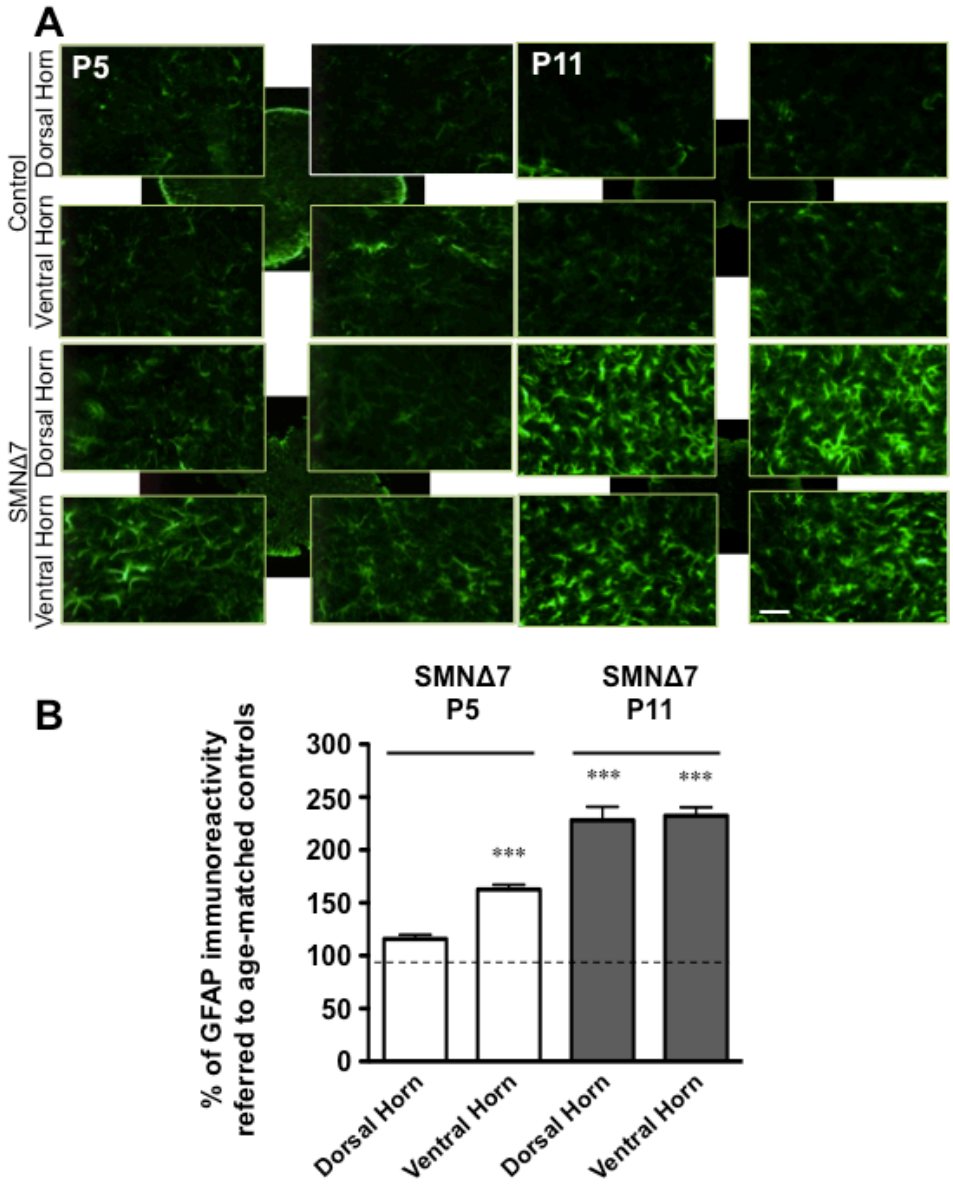

Figure 50: ***Differences in astroglial activation between ventral and dorsal horn of lumbar spinal cord in SMNΔ7 mice.*** Immunofluorescence performed with GFAP antibody in lumbar spinal cord sections of P5 and P11 SMNΔ7 mice, revealed a differential activation in the ventral horn compared to dorsal horn at P5, but no differences in glial activation between dorsal and ventral at P11, which is much more extense. (A) Representative images show the increase in astroglial activation between dorsal and ventral horn at P5, but no differences between dorsal and ventral horn at P11. Scale bar = 50 μm. (B) Column bars represent the increase in GFAP positive astrocytes in P5 and P11 SMNΔ7 mice as compared to age-matched controls, and are the average ± SEM (error bars) in 8 sections per animal and 4 fields per section of at least 4 mice from each group studied. ***p<0.0001 as compared to control animals from each age (ANOVA followed by Bonferroni's test).

2.3 Microglial activation in the spinal cord of SMNΔ7 mice accompanies motoneuron death

Immunofluorescence with the anti-IBA-1 antibody against microglia performed in sections of the lumbar spinal cord of SMNΔ7 mice (P5 to P14) showed increased density of microglial cells at P11 (140%) as compared to age-matched controls (figure 51A). Interestingly, many IBA-1-positive profiles were observed in the ventral horn surrounding the motoneurons (figure 51C) but no differences were observed in terms of number of microglial cells between dorsal and ventral horns (figure 51B).

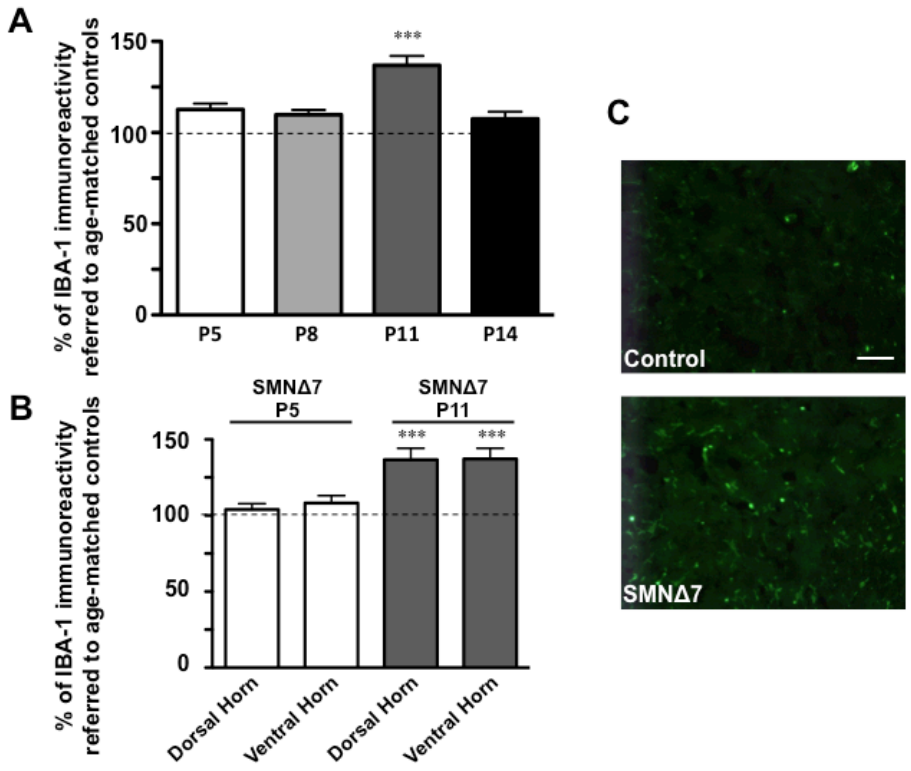

Figure 51: ***Increase in microglial cells in P11 SMNΔ7 mice.*** Immunofluorescence with IBA-1 antibody was performed in lumbar sections of SMNΔ7 mice reflected an increase in microglial cells at P11. (A) Column bars represent the immunoreactivity for IBA-1 and are the average of immunoreactivity ± SEM (error bars) in 8 sections per animal and 4 fields per section of at least 4 mice from each group studied. ***p<0.0001 as compared to aged-matched control animals (ANOVA followed by Bonferroni's test). (B) Column bars represent the immunoreactivity for IBA-1 both in ventral and dorsal horn of lumbar spinal cord in P5 and P11 mice and are the average ± SEM (error bars) in 8 sections per animal and 4 fields per section of at least 4 mice from each group studied. ***p<0.0001 as compared to age-matched controls (ANOVA followed by Bonferroni's test). (C) Immunofluorescence images show the increased number of IBA-1 immunoreactive cells in lumbar spinal cord from 11-day-old animals, compared to their age-matched controls. Scale bar = 50 μm.

2.4 Decreased synaptophysin-ir puncta around motoneurons of SMNΔ7 mice

Increasing evidence suggests a neuromuscular junction dysfunction preceding axonal degeneration and loss of spinal cord motoneurons in a severe mouse model (Kong et al., 2009). To explore the possible loss of synapses on spinal cord motoneurons in the SMNΔ7 mice at different time-points, immunofluoresce against the major synaptic vesicle protein synaptophysin (syn) were performed together with SMI-32 staining for motoneurons to show the total synaptic puncta surrounding motoneurons (Sunico et al., 2010). A significant decrease on the synaptic boutons was observed in SMNΔ7 mice at end-stage (P14). The syn-ir positive puncta around motoneurons showed a decrease in SMNΔ7 mice: whereas controls had 45.3 ± 3.8 μm of positive synaptophisin puncta around motoneurons per 100 μm, SMNΔ7 mice had only 19.1 ± 01.8 μm (figure 52).

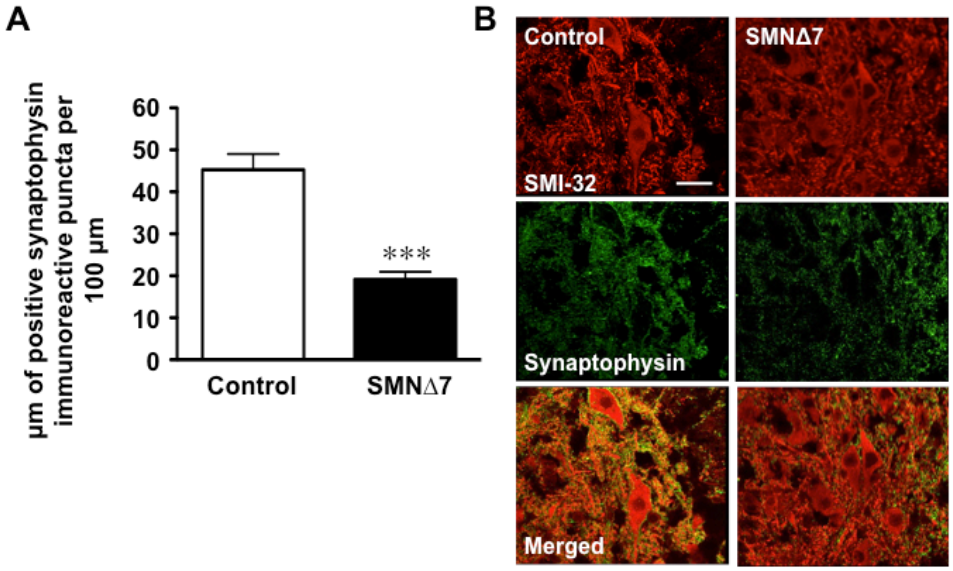

Figure 52: ***Decrease of positive synaptophysin immunoreactive puncta around P14 SMNΔ7 motoneuron somata.*** Immunofluorescence with synaptophysin antibody was performed in lumbar spinal cord sections of SMNΔ7 mice and showed a decrease of synaptophysin immunoreactive puncta (syn-ir puncta) at P14 in SMNΔ7 mice. (A) Column bars represent the positive perimeter for synaptophysin and are the average of positive perimeter ± SEM (error bars) in 30 motoneurons per animal of at least 4 mice from each group studied. ***$p<0.0001$ as compared to aged-matched control animals (t-Student test). (B) Immunofluorescence images show the reduction in the perimeter immunoreactive for synaptophysin in lumbar spinal cord motoneurons from 14-day-old animals, compared to their age-matched controls. Scale bar = 25μm.

2.5 nNOS and iNOS are upregulated in interneurons, and only nNOS in motoneurons in the lumbar spinal cord of SMNΔ7 mice

NO has been involved in synaptic remodelling in adult motoneurons (Sunico et al., 2005), mediating synaptic loss from pathological neurons (Moreno-López et al., 2011). Thus, we investigated the possible induction of nNOS in motoneurons, as a possible cause of the synaptic loss that we observed in the SMNA7 mice.

The expression of the proinflammatory enzymes nNOS and iNOS was assessed in spinal cord slices of control and SMNΔ7 mice from different ages. Immunofluorescence studies were performed in sections of lumbar spinal cord from different time-points ranging from early stage (P5) to pre-symptomatic (P8), symptomatic (P11) and end-stages (P14).

The nNOS enzyme was found increased both in motoneurons (positive for SMI-32, present in the ventral horn) (figure 53) and in interneurons (identified with MAP-2) (figure 54) in the SMNΔ7 mice as compared to age-matched control animals. In motoneurons, nNOS is overexpressed from P5 until end-stage, P14. At P8, nNOS is increased to 180 ± 9 % referred to age-matched controls, and the maximum expression nNOS in SMNΔ7 is present at P14 with a 213 ± 6 % referred to age-matched controls (figure 53).

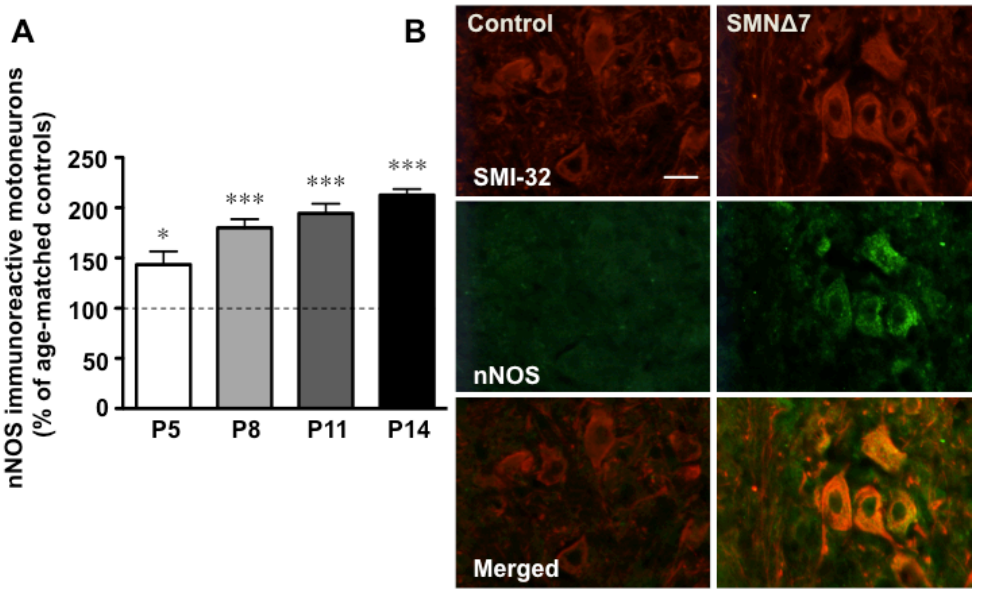

Figure 53: ***Motoneurons nNOS positive in the lumbar spinal cord of SMNΔ7 mice.*** Immunofluorescence performed in lumbar sections of the SMNΔ7 with SMI-32 and nNOS antibody. (A) Column bars represent the percentage of increase of nNOS immunoreactive motoneurons ± SEM (error bars) in 50 motoneurons per animal of 4 mice from each group studied in SMNΔ7 as compared to control animals. **p<0.001 and ***p<0.0001 as compared to control animals from each age (ANOVA followed by Bonferroni's test). (B) Representative images from P11 SMNΔ7 and wild-type mice. The number of nNOS immunoreactive motoneurons is increased in SMNΔ7 animals. Scale bar = 20 μm.

In interneurons, the overexpression of nNOS is already present at P5 animals. At P8 the value is 154 ± 5 % (referred to age-matched controls) and still overexpressed at P11 (185 ± 12 % referred to age-matched controls) and P14 (183 ± 7 % referred to age-matched controls) (figure 54).

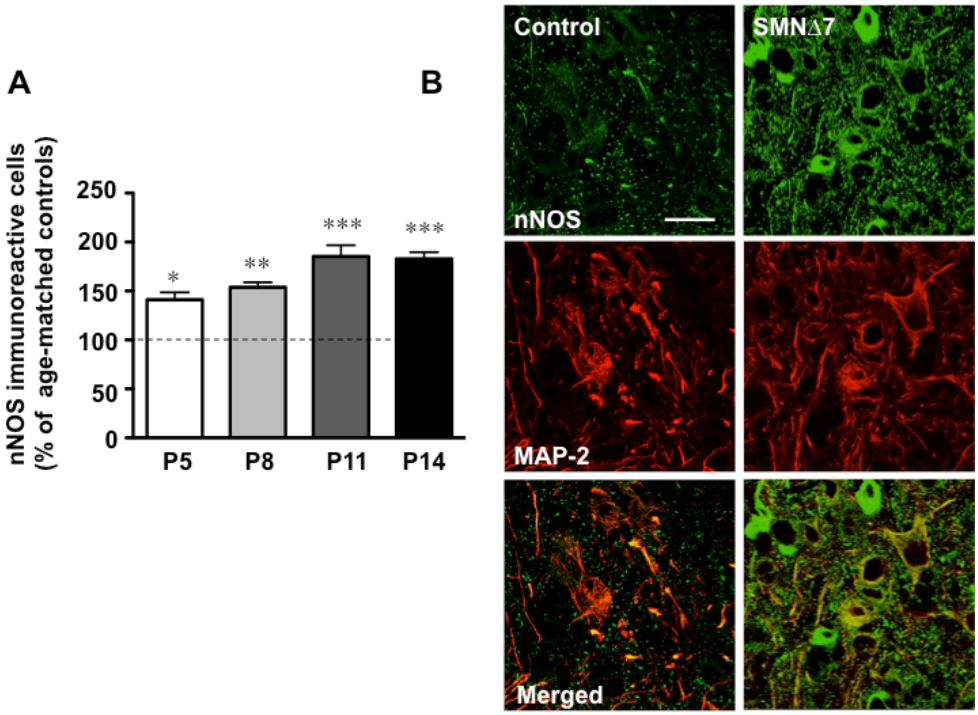

Figure 54: ***Presence of interneurons positive for nNOS in the intermediate grey matter of the lumbar spinal cord of SMNΔ7 mice.*** Immunofluorescence performed in lumbar spinal cord sections of the SMNΔ7 mice with MAP-2 and nNOS antibody. (A) Column bars represent the average of nNOS immunoreactive interneurons ± SEM (error bars) in 8 sections per animal and 4 fields per section of at least 4 mice from each group studied. **p<0.001 and ***p<0.0001 as compared to control animals from each age (ANOVA followed by Bonferroni's test). (B) Immunofluorescence images showing co-localization of MAP-2 and nNOS thus showing that the nNOS immunoreactive cells are interneurons in intermediate gray matter of lumbar spinal cord of P11 SMNΔ7 and control mice showing that the number of nNOS immunoreactive interneurons is increased in SMNΔ7 mice. Scale bar = 20 μm. (C) Representative images of lumbar spinal cord from P11 SMNΔ7 and control mice showing an increase in the nNOS positive interneurons. Scale bar = 25 μm.

SMNΔ7 mice showed an increased iNOS expression as compared to control mice. Immunohistochemistry studies were performed to assess which cell type in the spinal cord was responsible for the increased iNOS expression. Double immunofluorescence with iNOS and MAP-2 showed an increased amount of iNOS-positive neurons in the intermediate gray matter in the SMNΔ7 mice as compared to age-matched controls (figure 55). An increase in the number of positive iNOS interneurons already started at P8 (202 ± 13 % referred to age-matched controls) and a maximum of overexpression at P11 (390 ± 51 % referred to age-matched controls). Double immunolabelling with SMI-32 and iNOS did

not show co-localization between these markers and thus, the possibility of induction of iNOS in motoneurons was ruled out.

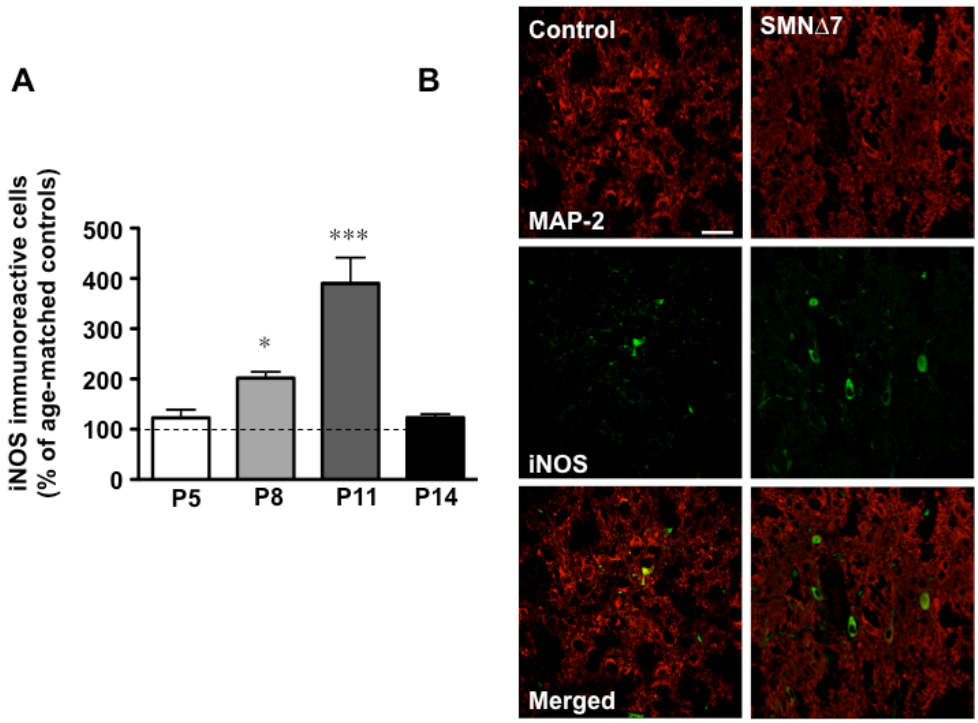

Figure 55: ***Presence of interneurons positive for iNOS in the intermediate grey matter of the lumbar spinal cord of SMNΔ7 mice.*** Immunofluorescence performed in lumbar spinal cord sections of the SMNΔ7 mice with MAP-2 and iNOS antibody. (A) Column bars represent the average of iNOS immunoreactive interneurons ± SEM (error bars) in 8 sections per animal and 4 fields per section of at least 4 mice from each group studied. *p<0.01 and ***p<0.0001 as compared to age-matched controls (ANOVA followed by Bonferroni's test). (B) Representative images of lumbar spinal cord from P11 SMNΔ7 and control mice showing an increase in the number of iNOS positive interneurons. Scale bar = 40 μm.

2.6 Synaptophysin immunoreactive puncta around motoneurons express more P-MLC in SMNΔ7 mice

Synaptophysin is a synaptic vesicle membrane protein that is ubiquitously expressed throughout the CNS. Motoneurons are surrounded by synaptic contacts, containing synaptic vesicles, which allow an interaction between motoneurons and presynaptic neurons. Motoneuron high concentration of nNOS produces more NO, which through paracrine/retrograde action activates RhoA/ROCK pathway in the presynaptic neuron. Enhanced ROCK

phosphorylates MLC into P-MLC, which in turn increase the synaptic bouton retraction (Sunico et al., 2010). Figure 56 shows increased syn-ir colocalizing with P-MLC-ir puncta surrounding motoneurons in SMNΔ7 mice at P11, compared to control.

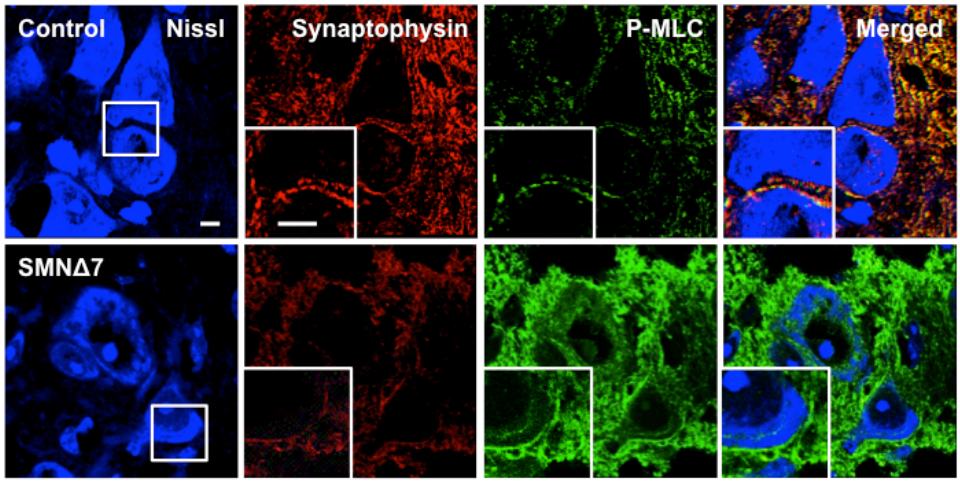

Figure 56: ***Increased colocalization of synaptophysin-ir puncta and P-MLC-ir around motoneurons in P11 SMNΔ7 mice.*** Representative images of P-MLC (green) and synaptophysin (red) presence in motoneurons (Nissl, blue) from lumbar spinal cord of P11 SMNΔ7 and wild-type mice. Scale bar both in images and inserts = 12.5 μm.

Third Objective

3 Activation of Notch pathway in SMN-depleted models

In the context of SMA, it has been described a relationship between reduced levels of SMN and impaired neuritogenesis in PC12 cells. In these cells, SMN knock-down reduced the length of neurites after differentiation and increased the incidence of beading and swelling along their length, which is usually indicative of cytoskeletal perturbation and impairment of axonal transport (Bowerman et al., 2007). In this sense, it has been widely described the paper of Notch inhibiting neuritogenesis in diferent models (Franklin et al., 1999; Ruiz-Palmero et al., 2011).

Gliosis has been described also in SMA (Ling et al., 2010). Moreover, Notch has been related to glial activation, both in astroglia and microglia (Grandbarbe et al., 2007; Cao et al., 2008; Morga et al., 2009). However, the role of Notch pathway has not been studied yet in the context of the SMA.

3.1 Activation of Notch pathway in U87MG astroglioma cells depleted of SMN

Firstly, as in objective 1, two different shRNA sequences targeting SMN (shSMNa and shSMNb) were used to knock-down the expression of this protein in U87MG astroglioma cell line. The transduction process was the same as described in objective 1. After transduction, we studied the expression of the ligands and receptors of the Notch pathway in U87MG astroglioma cells where the SMN had been depleted, by means of western blott.

Western blott experiments revealed that U87MG cells depleted of SMN overexpressed Jagged and Delta, ligands of the Notch pathway, as well as the receptors of the Notch pathway. In figure 57 we show that, after SMN depletion, the ligands Jagged and Delta increased their expression around 2-3 fold compared to shRNA empty vector. Moreover, the receptor Notch increased its expression around 2 fold, whereas its activated form of Notch (NICD) was found increased, around 4 fold, all compared to shRNA EV transduced U87MG cells. In the graphic of figure 57, it is represented the ratio of each protein referred to α-tubulin immunoreactivity from each sample.

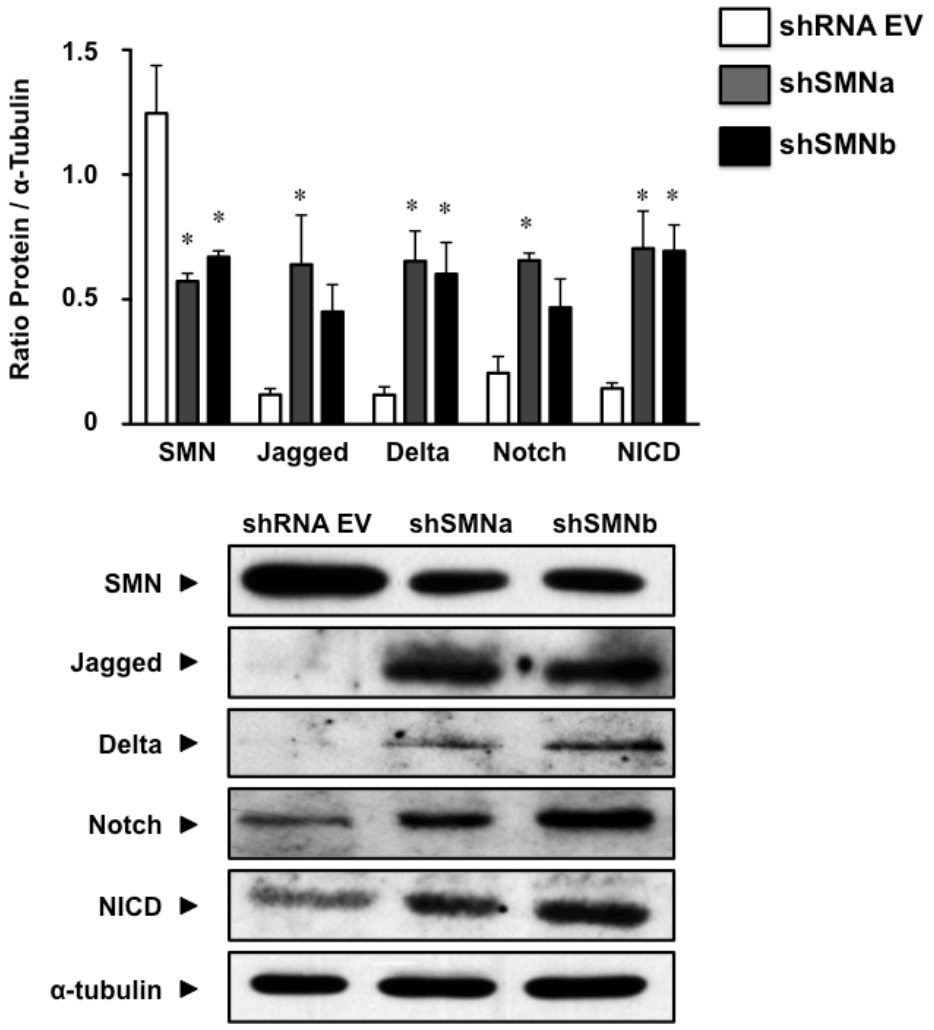

Figure 57: ***Notch pathway is active in U87MG astroglioma cell line after SMN depletion.*** Top. Column bars indicate the ratio of immunoreactivity of each protein (SMN, Jagged, Delta, fl-Notch and NICD) vs. α-tubulin, determined by densitometric analysis (integrated optical density of each protein and α-tubulin), and are the mean ± SEM of three independent experiments. At least *$p<0.01$ as compared to each protein shRNA EV (ANOVA followed by Bonferroni's test). Bottom. Representative western blot showing SMN, Jagged, Delta, fl-Notch and NICD immunoreactivity in U87MG cells after transduction with lentiviruses containing the empty vector (shRNA EV), shSMNa or shSMNb constructs, as indicated.

3.2 Astroglia overexpress Jagged, Delta, Notch, and Notch activated fragment (NICD) in the SMNΔ7 mouse model

The role of Notch signaling in astrocytes has been described as initiator of inflammation and inducer of expression of characteristic elements for gliosis (Grandbarbe et al., 2007; Cao et al., 2008; Morga et al., 2009). In activated astrocytes, the inhibition of Jagged1 has antiinflammatory effects and results in a decrease of proinflammatory cytokines as well as iNOS expression (Morga et al., 2009).

As we observed Notch pathway activation after SMN depletion in U87MG cells, we have studied the possible activation of Notch pathway in spinal cord of SMNΔ7 mouse model. P11 animals were dissected and lumbar spinal cord sections were analysed by means of immunohistochemistry, in order to identify expression of Notch family components in glia and motoneurons.

In figure 58, we observed that Notch ligands were found overexpressed in astrocytes: Jagged expression was 281 ± 25 %, and Delta expression was 249 ± 49 %, compared to P11 age-matched controls. Astrocytes surrounding motoneurons in the ventral horn of the lumbar spinal cord were studied. In figure 58 (insert) we showed that the astrocytes that overexpressed Jagged and Delta where in intimate contact with motoneurons.

Figure 58: ***Jagged and Delta ligands are overexpressed in spinal cord astroglia of SMNΔ7 mice.*** (A) Representative images of Jagged in astroglia in the lumbar spinal cord of P11 SMNΔ7 and wild-type mice. Jagged immunoreactivity was increased in P11 SMNΔ7 animals. Scale bar = 20 μm and 10 μm in the insert, also in B. (B) Representative images of Delta in astroglia from lumbar spinal cord of P11 SMNΔ7 and wild-type mice. Delta immunoreactivity was increased in P11 SMNΔ7 animals. (C) Quantification of Jagged immunoreactivity in astroglia from lumbar spinal cord. Column bars represent the percentage of increase of Jagged immunoreactivity in astroglia ± SEM (error bars) in 8 sections per animal and 4 fields per section of at least 4 mice from each group studied. ***$p<0.0001$ as compared to age-matched controls (ANOVA followed by Bonferroni's test). (D) Quantification of Delta immunoreactivity in astroglia from lumbar spinal cord. Column bars represent the percentage of increase of Delta immunoreactivity in astroglia ± SEM (error bars) in 8 sections per animal and 4 fields per section of at least 4 mice from each group studied. *$p<0.01$ as compared to age-matched controls (ANOVA followed by Bonferroni's test). Next page.

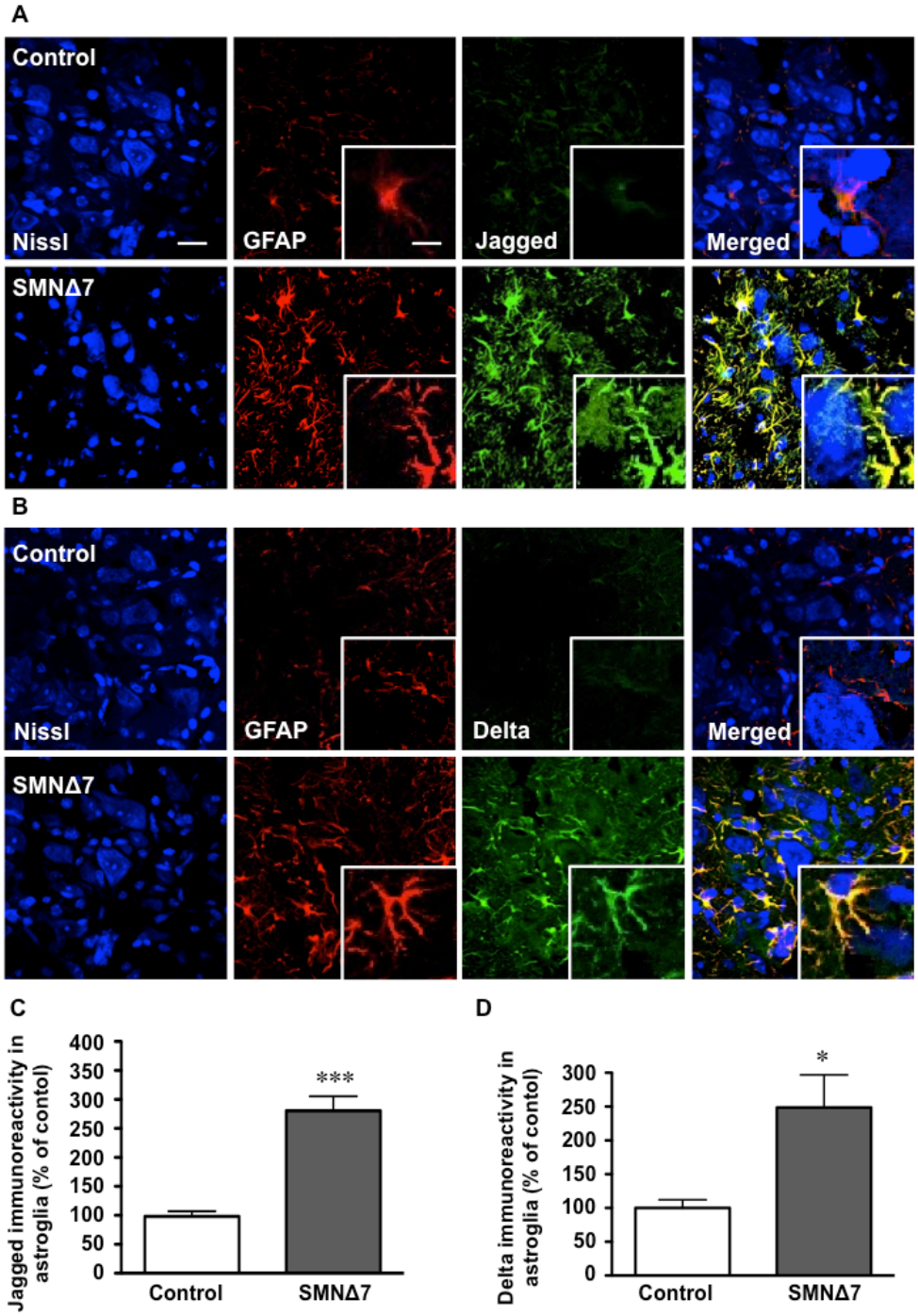
A
Control
Nissl
GFAP
Jagged
Merged
SMNΔ7
B
Control
Nissl
GFAP
Delta
Merged
SMNΔ7
C
Jagged immunoreactivity in astroglia (% of contol)
400
350
300
250
200
150
100
50
0
***
Control
SMNΔ7
D
Delta immunoreactivity in astroglia (% of contol)
300
250
200
150
100
50
0
*
Control
SMNΔ7

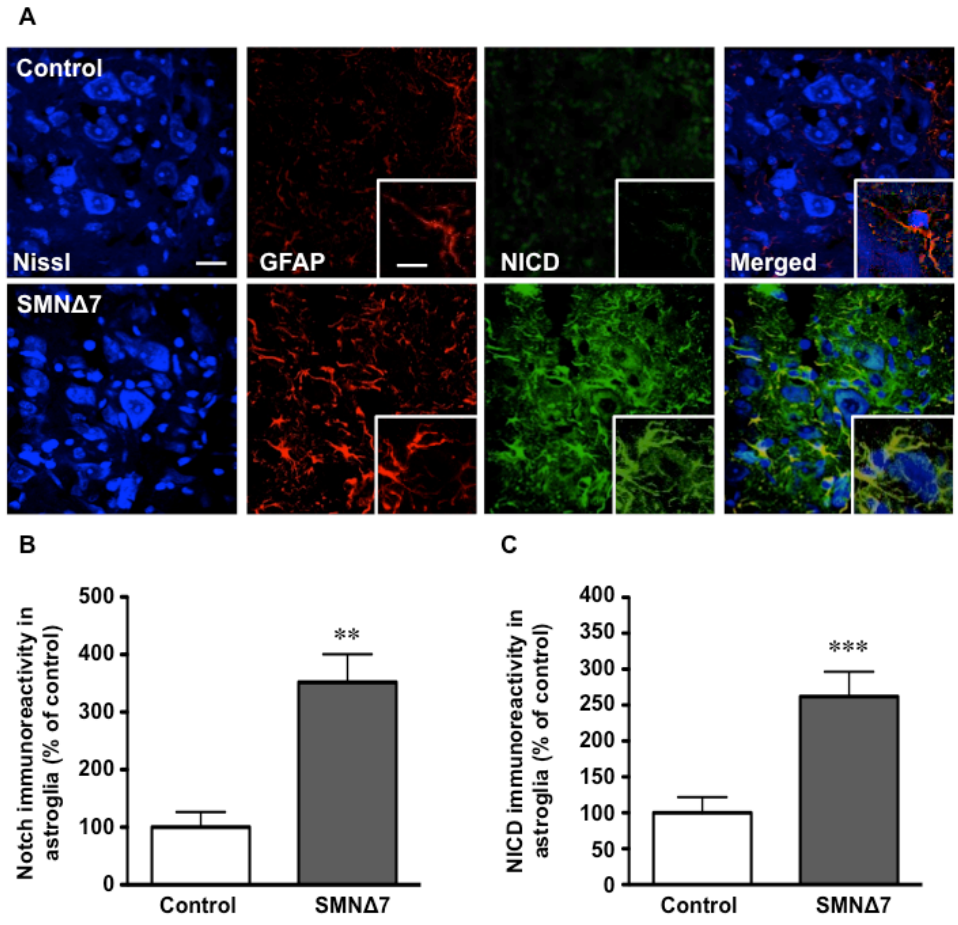

Figure 59: ***Notch is overexpressed and activated in spinal cord astroglia of SMNΔ7 mice.*** (A) Representative images of NICD in astroglia from lumbar spinal cord of P11 SMNΔ7 and wild-type mice. NICD immunoreactivity in astroglia is increased in P11 SMNΔ7 animals. Scale bar = 20 μm; scale bar in insert = 10 μm. (B) Quantification of Notch immunoreactivity in astroglia from lumbar spinal cord. Column bars represent the percentage of increase of Noch immunoreactivity in astroglia ± SEM (error bars) in 8 sections per animal and 4 fields per section of at least 4 mice from each group studied. **p<0.001 as compared to age-matched controls (ANOVA followed by Bonferroni's test). (C) Quantification of NICD immunoreactivity in astroglia from lumbar spinal cord. Column bars represent the percentage of increase of NICD immunoreactivity in astroglia ± SEM (error bars) in 8 sections per animal and 4 fields per section of at least 4 mice from each group studied. ***p<0.0001 as compared to age-matched controls (ANOVA followed by Bonferroni's test).

In figure 59 it is shown the overexpression of Notch and its activation product, NICD, in astrocytes. Notch quantifications (figure 59B) reached about 351 ± 58 % in SMNΔ7 mouse model compared to control. In figure 59C, NICD quantification reached about 261 ± 34 % in SMNΔ7 mouse model compared to control. In figures 58 and 59 we observed that, as we have previously described in figure 48 and 49, the number of astrocytes surrounding motoneurons was increased at P11, moreover they clearly overexpressed Notch pathway ligands, Jagged and Delta, and the activated fragment of the Notch receptor (NICD).

3.3 Notch is overexpressed and activated in SMNΔ7 mice spinal cord motoneurons

Significant increase in the expression of Notch was observed in the motoneurons of the SMNΔ7 mouse model at P11 (215 ± 20 % referred to age-matched controls in figure 60A). Moreover, Notch in motoneurons was cleaved (NICD) in the SMNΔ7 mice, indicating that it was active (308 ± 22 % referred to age-matched controls in figure 60B and C).

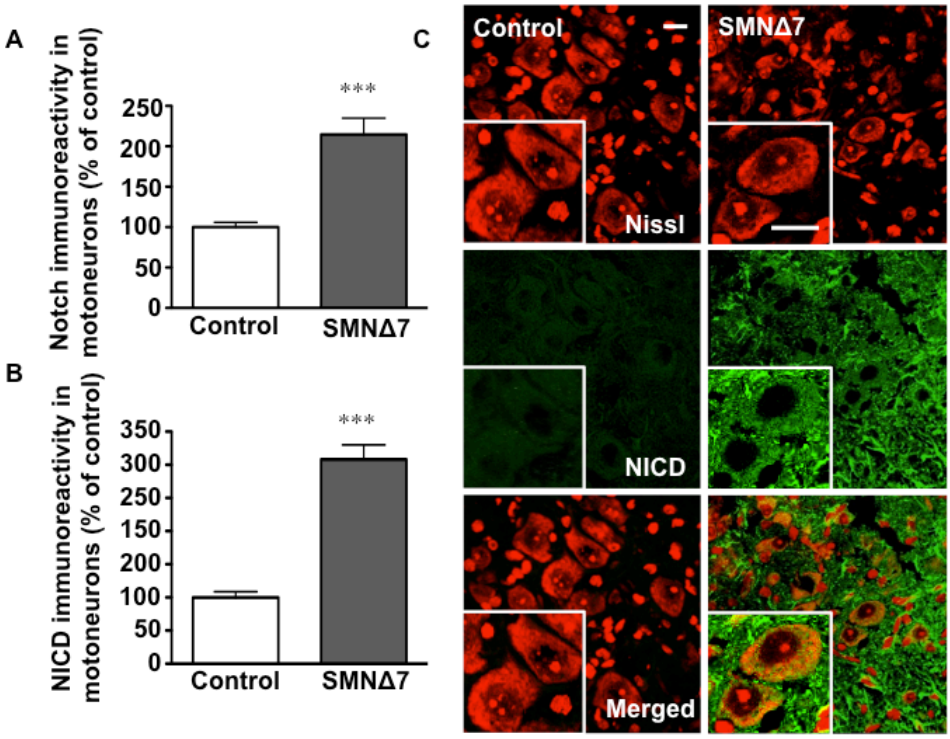

Figure 60: ***Notch overexpression and activation in motoneurons.*** (A) Quantification of Notch immunoreactivity in spinal motoneurons from lumbar spinal cord. Column bars represent the percentage of increase of Notch immunoreactivity in motoneurons ± SEM (error bars) in at least 40 motoneurons per animal of at least 4 mice from P11 studied in SMNΔ7 as compared to control animals. ***p<0.0001 as compared to control animals (ANOVA followed by Bonferroni's test). (B) NICD is more concentrated in motoneurons from the SMA model than in age-matched controls. Quantification of NICD immunoreactivity in motoneurons from lumbar spinal cord. Column bars represent the percentage of increase of fl-Notch immunoreactivity in motoneurons ± SEM (error bars) in at least 40 motoneurons per animal of at least 4 mice from P11 studied in SMNΔ7 as compared to control animals. ***p<0.0001 as compared to control animals (ANOVA followed by Bonferroni's test). (C) Representative images of NICD in motoneurons from lumbar spinal cord of P11 SMNΔ7 and wild-type mice. NICD immunoreactivity in motoneurons is increased in P11 SMNΔ7 animals. Scale bar = 25 μm.

3.4 Neurogenin, regulated by Notch pathway, is reduced in motoneurons of SMNΔ7 mice

Notch signaling inhibits the expression of Neurogenin (Ngn), a proneural gene that is involved in the control of dendrite morphology and synaptic connectivity (Salama-Cohen et al., 2006). In the present work, we observed a decrease in the Neurogenin expression in nuclei, cytoplasm and neurites (figure 61), in motoneurons of SMNΔ7 mice (32 ± 4 % in SMNΔ7 mice as compared to controls). The Neurogenin distribution pattern, shown in figure 61B, where the protein is located in nuclei, cytoplasm and neurite processes has also been described by (Simon-Areces et al., 2010).

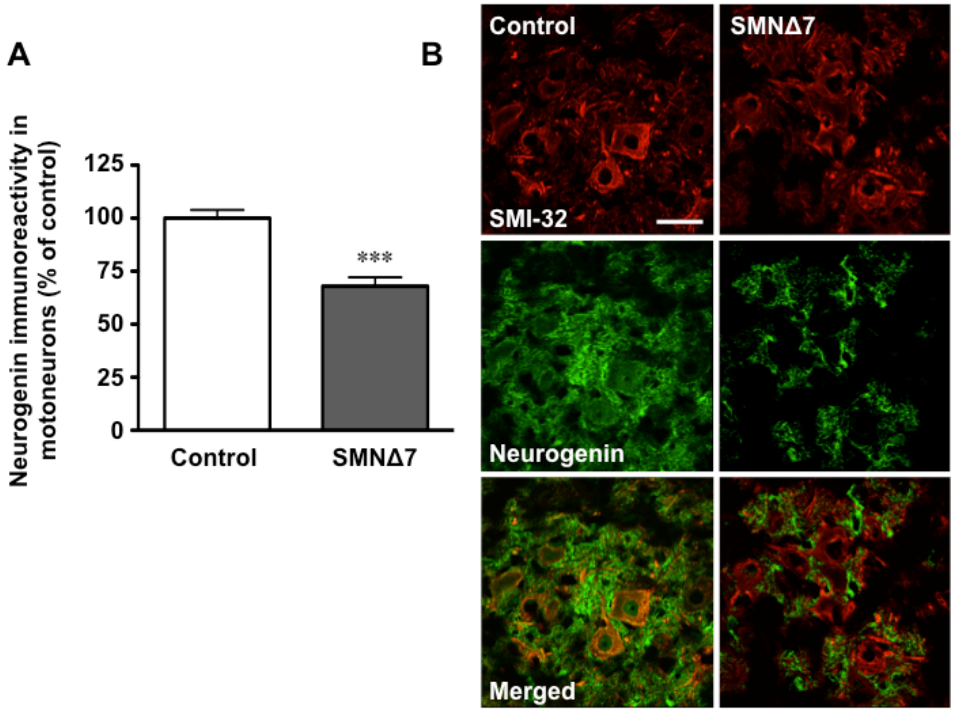

Figure 61: ***Neurogenin reduced expression in spinal cord motoneurons of P11 SMNΔ7 mice.*** (A) Quantification of Neurogenin immunoreactivity in spinal motoneurons from lumbar spinal cord. Column bars represent the percentage of increase of Neurogenin immunoreactivity in motoneurons ± SEM (error bars) in at least 30 motoneurons per animal of at least 4 mice from P11 studied in SMNΔ7 as compared to control animals. ***p<0.0001 as compared to control animals (ANOVA followed by Bonferroni's test). (B) Representative images of Neurogenin in motoneurons from lumbar spinal cord of P11 SMNΔ7 and wild-type mice. The Neurogenin immunoreactivity in motoneurons is decreased in P11 SMNΔ7 animals. Scale bar = 25 μm.

3.5 Active Notch in microglia of SMNΔ7 mice

It has been proved that Notch signalling regulates activation of microglial cells (Grandbarbe et al., 2007). The expression of Notch is upregulated when amoeboid microglial cells are activated (Cao et al., 2008). Moreover, it has been shown that activated murine BV-2 microglial cells and amoeboid microglia primary culture of postnatal rats overexpress Notch (Cao et al., 2010).

In this sense, we studied microglia of the lumbar spinal cord in SMNΔ7 mouse model of SMA at P11. Notch was observed to be active in microglia surrounding motoneurons, in the ventral horn of the lumbar spinal cord in SMNΔ7 mice (261 ± 25 % compared to control in figure 62).

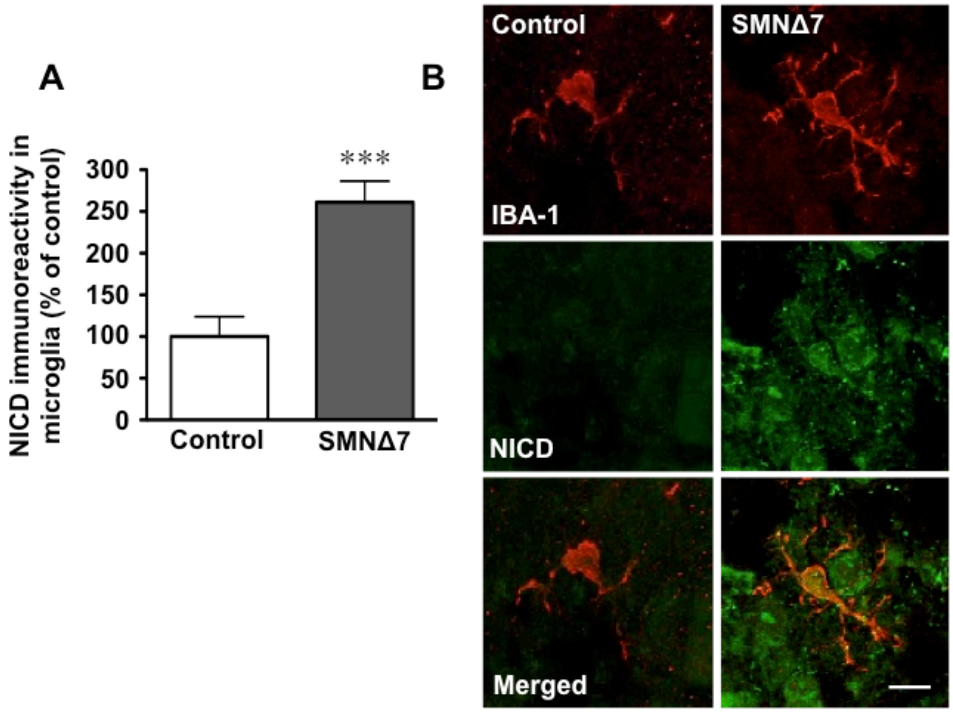

Figure 62: ***Microglia is positive for Notch, NICD, in lumbar spinal cord of P11 SMNΔ7 mice.*** (A) Quantification of NICD immunoreactivity in microglia of lumbar spinal cord. Column bars represent the percentage of increase of NICD immunoreactivity in microglia ± SEM (error bars) in 8 sections per animal and 4 fields per section of at least 4 mice from each group studied. ***$p<0.0001$ as compared to age-matched controls (ANOVA followed by Bonferroni's test). (B) Representative images of NICD in microglia from lumbar spinal cord of P11 SMNΔ7 and wild-type mice. The NICD immunoreactivity in microglia is increased in P11 SMNΔ7 animals. Scale bar = 10 μm.

V. DISCUSSION

V. Discussion

Survival of motor neuron protein deficiency is known to trigger SMA disease, but many of the cellular and molecular mechanisms causing motoneuron loss still remain unknown. There exist at least four different hypotheses explaining possible consequences of low levels of SMN. SMN has been clearly described to develop three housekeeping functions and another one in axons. An inchoate line of research has suggested a SMN role binding profilin. It has been suggested that SMN might play an important role in neuritogenesis and axonal development.

Our main objective in this thesis was to evaluate the effect of SMN deficiency in *in vivo* and *in vitro* models of the disease. We have studied mechanism involved in the SMA pathology, such as cellular migration, neuroinflammation and cytoskeleton alterations; and cellular pathways involved in these effects, such as RhoA/ROCK pathway and Notch pathway.

1 The depletion of SMN via shRNA in motoneurons of rat embryonic explants affects neurofilament distribution

Our initial objective was to develop an *in vitro* model where the depletion of SMN could be studied at molecular level and where cellular pathways affected by SMN depletion could be discerned. First, Dr. Soler's group developed an SMA in vitro model using an RNA interference method to down-regulate Smn protein level in motoneurons. Our first approach was to study the response of rat motoneurons to Smn knock-down using the rat spinal cord embryonic explants developed in our laboratory (Mir et al., 2009). We observed a conspicuous reduction of SMN expression in motoneurons (figure 34A) after transduction with lentiviral vectors, which efficiently induced the expression of GFP in those motoneurons (figure 34A). Although several SMA mice models are available (Hsieh-Li et al., 2000; Monani et al., 2000a), the limited number of mutants present in each litter makes it very difficult to collect enough spinal cord motoneurons to study intracellular molecules by biochemical and molecular approaches. By establishing this model we expected to secure the presence of isolated motoneurons but still in contact with their natural glial environment. Changes in phenotype will be indicative of changes in intracellular proteins and pathways that will help us to understand the physiopathology of SMA disease.

Using a lentiviral transduction of RNA interference, we found an effective method to knock-down Smn protein in rat embryonic explant motoneurons. Smn knock-down caused soma area reduction, and altered pattern of phosphorylated neurofilament in motoneuron neurites (figure 34B and C). Therefore, our data showed that reduction of Smn levels induced a neurodegenerative response in neurites. We did not analyze whether neurite developmental outgrowth or pathfinding is affected in our model, but there are recent evidences supporting that no detectable alterations on neuromuscular connectivity were observed during pre-symptomatic development of SMA (Murray et al., 2010). In contrast, thera are other studies that affirm that reduced SMN impairs maturation of the NMJs in mouse models of SMA (Kariya et al., 2008). In other cellular models of SMA, Acsadi and colleagues (Acsadi et al., 2009) using small interfering RNA, reduced Smn protein level in NSC34 motoneuron-like cell line. They also described cellular changes such as the decrease in mean soma width, the reduction of somas bearing neurites and mitochondrial dysfunction. Although axonal truncation and abnormal neurofilament distribution have been described in SMA models (McGovern et al., 2008) and patients (reviewed by Burghes and Beattie, 2009) their significance

in the pathogenesis of SMA is still unknown. In our model, we describe neurite disruptions, recapitulating what is also observed in SMA models (McWhorter et al., 2003).

Morphological responses of motoneurons to Smn knock-down suggest that neurite degeneration and cell body loss are parallel events, however, further molecular analysis is needed to determine whether neurite degeneration precedes cell body loss or vice versa (Garcera et al., 2011). Rossoll et al. (2003) described the reduction of axon growth without affecting cell survival in cultured motoneurons from a SMA mouse model. However, their conclusion is that disturbances in axon growth and maintenance (defective maturation of growth cone) are the primary cellular defects that ultimately may lead to loss of motoneurons in SMA disease.

In view of our results and others (Hilliard, 2009; King et al., 2011) elucidating the role and the mechanisms involved in axonal degeneration and synaptic loss may be an important step in developing strategies for preventing and treating neurodegenerative diseases.

2 The reduction of SMN in astroglioma cell line reduces the migration capacity via RhoA pathway

After describing cytoskeleton alterations in a model of the SMA disease, where the SMN expression was decreased, we evaluated the impairment of migration capacity after SMN depletion. To investigate the role of SMN in cell migration, U87MG astroglioma cells, a well-established cell line for migration studies, was employed. The SMN protein, proposed to be a ubiquitous protein (Monani, 2005), is also expressed in U87MG cells, with both a nuclear and cytoplasmic distribution (figure 36). The functional implications of SMN in cell migration were studied by interference of RNA, as it is a powerful method to inhibit gene expression at post-transcriptional level (Dykxhoorn et al., 2003). Thus, U87MG cells were transduced with lentiviruses carrying shSMNa and shSMNb constructs, and about 60% reduction in SMN expression was achieved with both (figure 37). This reduction is similar to what has been previously described using the same constructs in motoneurons (Garcera et al., 2011) and in type III SMA patients (Wirth et al., 2006a).

Interestingly, U87MG SMN-depleted cells exhibit reduced cell migration as observed in a wound-healing assay (figure 38). To our knowledge, our results are the first to report decreased cell migration after knocking-down the

expression of SMN, thus suggesting the involvement of SMN in the process of cell migration. Reduced axon growth associated to decreased β-actin staining has been described in SMN-deficient motoneurons and proposed to be the primary cellular cause that ultimately leads to loss of motoneurons in SMA (Rossoll et al., 2003). In this sense, reduction of SMN levels causes axon-specific pathfinding defects in motoneuron development (McWhorter et al., 2003). Since growth cone advance and cell motility share common mechanisms in actin cytoskeleton dynamics (Okabe and Hirokawa, 1991; Lin and Forscher, 1995), the present results could be relevant to understand the molecular mechanisms related to the neurite outgrowth and axonal pathfinding defects described in SMA.

Rho GTPases are crucial regulators of cytoskeletal dynamics in eukaryotic cells, thereby exerting a central role in the control of cell morphology and motility (Takaishi et al., 1993; Nobes and Hall, 1999). According to this, we found that in SMN-depleted U87MG cells RhoA is activated (figure 40). This is in agreement with previous studies in which depletion of SMN in PC12 cells also resulted in an increase in active RhoA (Bowerman et al., 2007). RhoA activates its downstream effector ROCK that, in turn, activates myosin regulatory light chain (MLC) both by direct phosphorylation, and indirectly by the inactivation of myosin phosphatase (MLCP), thus controlling actin–myosin interaction and stress fiber formation (Amano et al., 1996; Pellegrin and Mellor, 2007). An enhancement in the phosphorylation of MLC was observed after depletion of SMN. The observation that the ROCK inhibitor Y-27632 (Uehata et al., 1997) abrogated MLC phosphorylation in SMN-depleted cells (figure 41) suggested that the RhoA/ROCK signaling pathway could be implicated in the migration defects of these cells. This hypothesis was confirmed by demonstrating that Y-27632 restored cell motility to control levels in SMN-depleted cells (figure 42). Together these results can be explained as phosphorylation of MLC by ROCK promotes the interaction of myosin II with actin increasing the speed of myosin II-driven retrograde flow in filopodia and lamellipodia (Luo, 2002), and thus inhibiting cell migration. A similar mechanism has also been proposed to be involved in retraction of axonal growth cones in response to several RhoA-activating stimuli (Benarroch, 2007). Other studies have reported a similar correlation between RhoA activation and the inhibition of cell motility in U87MG cells, for example in response to Ras inhibition with farnesyl-transferase inhibitors (Goldberg and Kloog, 2006).

Both immunocytochemistry and western blot studies in SMN-depleted U87MG cells showed an increase in the immunoreactivity for the actin binding protein profilin I (figure 45). This increased profilin I expression does not seem to be related to RhoA/ROCK activity as the ROCK inhibitor Y-27632 did not modify

levels of profilin I (figure 46). As SMN is known to regulate the assembly of small nuclear ribonucleo-proteins essential for pre-mRNA splicing machinery (Yong et al., 2004), it seems plausible a direct effect of SMN depletion on profilin I expression. Our results are in agreement with previous works describing an increase in profilin IIa in SMN-depleted cells of neuronal origin (Bowerman et al., 2007; 2009). In our study we focused on profilin I because this protein is more ubiquitous, and its expression is well documented in astrocytes, while profilin IIa is neuron-specific (Giesemann et al., 1999). This increased expression of profilin I may also be involved in the reduction of cell motility in U87MG cells. Overexpression of profilin I suppresses the generation of phosphatidylinositol-3,4-biphosphate [PI(3,4)P2] (Das et al., 2009). This phospholipid is a docking molecule for vasodilator stimulated phosphoprotein (VASP), which has a well-established role in promoting membrane protrusion (Rottner et al., 1999). It has been proposed that, through this mechanism, profilin I might reduce cell motility (Bae et al., 2009). Interestingly, in other cellular models, it has been described that overexpression of profilin also reduces the migration of invasive cells (Roy and Jacobson, 2004; Zou et al., 2007).

Profilin is also known to reduce the amount of actin monomers available to polymerize into filamentous actin, both inhibiting actin polymerization and triggering the disassembly of actin filaments (Cao et al., 1992; Schlüter et al., 1997). On the other hand, SMN is known to physically interact with profilin, reducing its actin-sequestering activity (Sharma et al., 2005). Thus, in SMN-depleted cells, there is both an increase in the expression of the actin-scavenger profilin, and a reduction of SMN inhibitory activity on profilin, leading to a reduced F-actin polymerization, i.e. decreased F-/G-actin ratio (figure 43 and 44). By contrast, other authors have shown an increased F-/G-actin ratio in PC12 SMN-depleted cells (van Bergeijk et al., 2007) and also in SMA motoneurons (Nölle et al., 2011). However, Nolle et al. suggest that this increase in the F-/G-actin ratio could be restricted to neuronal cells. Although in general terms activation of RhoA/ROCK has been described to induce an increase in actin stress fibers (Ridley and Hall, 1992), other authors have demonstrated that overexpression of profilin I suppresses Rho-induced stress fiber formation (Suetsugu et al., 1999). This last work further supports our results in U87MG SMN-depleted cells in which increased profilin I expression is associated to decreased stress fibers formation. Thus, the differences between our results in F-/G-actin ratio after SMN depletion and those from other authors could be explained as different cellular models were used. Our hypothesis is exposed in figure 63.

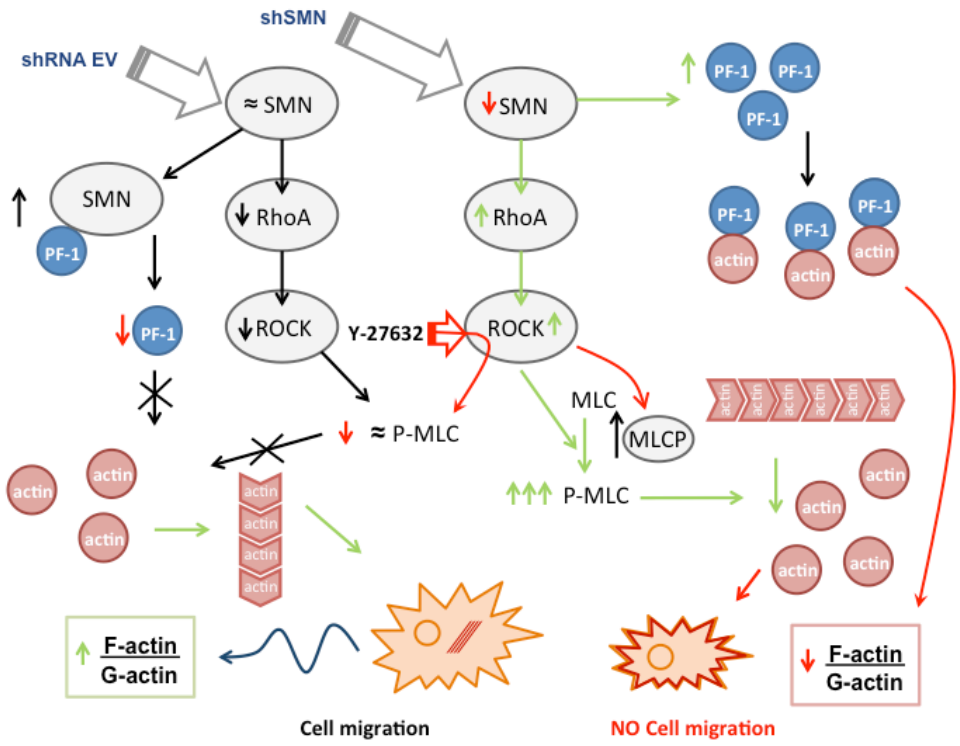

Figure 63: ***Proposed mechanism to explain how SMN deficiency affects RhoA/ROCK pathway and profilin and alters migration capability.*** Depleting cells of SMN via shSMN (right side) activates RhoA, which in turn activates ROCK. ROCK phosphorylates MLC into P-MLC and also inhibits its dephosphorylation inactivating MLCP. High amounts of P-MLC produce F-actin depolymerisation, liberating G-actin. Moreover, SMN depletion causes profilin overexpression. In a low SMN concentration scenario, profilin is free to sequestrate actin monomers, preventing F-actin formation. This extreme low ratio of F-/G-actin avoids creating enough actin filaments to allow cellular migration. In this case, the use of ROCK inhibitor, Y-27632, reduces P-MLC, allowing the normal formation of actin filaments. In a normal situation (left side, shRNA EV), SMN binds to profilin. SMN-profilin cannot sequestrate G-actin, allowing F-actin formation. Moreover, RhoA pathway is not activated, then P-MLC is not producing F-actin depolymerisation. Plain arrows mean regular pathway and bold arrows mean application of an external agent to modify the regular pathway. In palain arrows, green arrows mean activation or increase; red arrows: inhibition or decrease; black arrows: regular pathway. MLC: Myosin Light Chain II or myosin regulatory chain; P-MLC: phosphorylated Myosin Light Chain II; MLCP: Myosin Light Chain Phosphatase; PF: Profilin.

It is still unknown if the absence/deficiency of SMN gene in nervous system cells other than motoneurons can contribute to pathology in SMA. As astrocytes and their processes play a role in guiding migration and axonal growth of neurons during embryonic development (Rakic, 1971; Mason et al., 1988), the abnormal migration of motoneurons observed in SMA (Simic, 2008) could be

linked to abnormal migration of astrocytes during development. In this sense, in cultured astrocytes, the RhoA/ROCK pathway negatively regulates astrocytic process growth and migratory response after injury (Höltje et al., 2005). To our knowledge, the possible involvement of migration defects of glial cells in in vivo models of SMA has not been assessed yet.

We propose that the alterations reported here in migratory activity in SMN-depleted cells, related to abnormal activation of RhoA/ROCK pathway and increased profilin expression, could have a role in developing nervous system by impairing normal neuron and glial cell migration and thus contributing to disease pathogenesis in SMA.

3 Neuroinflammation process is present in SMNΔ7 mouse model of SMA disease

In many neurodegenerative disorders and neuropathological processes, a neuroinflammatory response, characterized by the presence of microglia and astroglia at sites of motoneuron injury, appears to contribute to motoneuron damage in these relentless diseases (Henkel et al., 2004; Boillée et al., 2006; Kassa et al., 2009). To investigate the possible neuroinflammatory or pathogenic process occurring in SMA pathology, we used the SMNΔ7 mouse model, which is largely accepted as a human SMA type II animal model (Le et al., 2005). In these animals maximum lifespan is two weeks. The weight reduction starts at day 2, and neurogenic atrophy of the muscle at day 3 (Sleigh et al., 2011a). A pathological analysis of glial processes and motoneurons in these animals has not been done thoroughly.

Initially, we demonstrated a modest but significant reduction in the number of motoneurons in the lumbar spinal cord of the SMNΔ7 mice in the end-stage, at P14 (figure 47). Only a few works have studied in depth motoneuron loss in the lumbar spinal cord of the SMNΔ7 mouse model. Le and cols. (2005) reported only a modest loss of motoneurons in the lumbar spinal cord starting at P8, whereas Kariya and cols. (2008) showed a significant reduction of axons in the ventral roots and phrenic nerves of SMNΔ7 animals, but the decrease was insignificant in ventral roots at the lumbar level of P14 SMNΔ7 mice (end-stage). Here we show clear pathological hallmarks in the lumbar spinal cord motoneurons from the SMNΔ7 mice such as the presence of phosphorylated neurofilament in motoneurons. Other authors have also shown an increase in phosphorylated neurofilament in motoneurons from a transgenic model of ALS

(Ackerley et al., 2004). Also in agreement with observations in cellular models of SMA, we have reported a reduction in the motoneuron soma area (Acsadi et al., 2009; Garcera et al., 2011).

In addition to our findings, other pathological signs such as ballooned motoneurons (Chou and Fakadej, 1971) and irregular nuclei with indentations (Frugier et al., 2000) have also been described in human and experimental SMA. These pathological marks affecting motoneurons at the final stages of SMNΔ7 mice suggest that motoneuron loss is still an ongoing process at the final stages of the disease.

Only a moderate loss of motoneurons is detected at the end-stage of the disease; thus, some other factor besides motoneuron loss must play a role in the pathogenesis of SMA. In this regard we have observed an increased amount of astroglia surrounding motoneurons in the spinal cord of the SMNΔ7 mouse. In addition, neuroinflammation could also play a role in the pathology of SMA as we have described activated microglia in the SMNΔ7 mice. Traditionally it has been thought that neuroinflammation is a secondary cellular event arising in response to a loss of neurons, aimed at limiting cell damage and promoting cell regeneration; but now, it is proposed that astrocytes and microglia, under certain circumstances, can initiate neurodegeneration (reviewed by Papadimitriou et al., 2010). Our results are in agreement with (Ling et al., 2010) showing an increased association of microglia and motoneurons in the spinal cord of SMNΔ7 mice.

Interestingly, astrogliosis and activated microglia in the ventral horn was detectable in the SMNΔ7 mice before motoneuron death, suggesting that these cells could play a role in the initiation and/or propagation of the disease. Thus, glial activation may not only be a consequence of motoneuron death, but an active player in SMA pathogenesis. Moreover, we have described an initiation of astrogliosis process in the motoneuron region at presymptomatic stage, prior to the extension to the other spinal cord areas (e.g. dorsal horn). This data suggests that astroglia may initiate motoneuron degeneration. Glial bundles in ventral roots have been described previously in human SMA tissue (Chou and Nonaka, 1978; Chou, 1980; Kumagai and Hashizume, 1982; Ghatak, 1983; Kuru et al., 2009); however, to our knowledge, this is the first time that glial activation is reported in the lumbar spinal cord in the SMNΔ7 mouse model of SMA.

We have described a decrease in the number of synaptic boutons on motoneuron cell bodies in the SMNΔ7 mouse (figure 52). In collaboration with Dr. Calderó and Dr. Esquerda group, we have determined that this reduction of synapsis is affecting both glutamatergic and gabaergic inhibitory terminals on

motoneuron soma in the SMNΔ7 mouse (data not shown). This is in agreement with other authors that have also demonstrated a decrease in the glutamatergic synapses on motoneurons of SMA mouse models (Park et al., 2010; Ling et al., 2010). Nevertheless, in contrast to other authors (Ling et al., 2010), we show an important central synapse loss on motoneurons before motoneuron loss is evident, thus discarding the possibility that synapse loss is only due to dying motoneurons.

A loss of central synapses is common in neurodegenerative diseases and precedes motoneuron death in ALS (Ince et al., 1995; Sasaki and Maruyama, 1994; Wishart et al., 2006), and it has also been described in SMA patients (Ikemoto et al., 1996; Yamanouchi et al., 1996). Synapses on the somatodendritic membrane strongly influence excitability of motoneurons. It is well-known that both astrocytes and microglia regulate the activity and functions of neurons (Raivich et al., 1999). Astrocytes are endogenous regulators of basal transmission at central synapses (Panatier et al., 2011), through the ability to modulate intracellular calcium-dependent processes. In addition, they may have a role in network changes of the nervous system, influencing the retraction of boutons as well as providing a proper perisynaptic environment (Emirandetti et al., 2006). However, how reactive astrocytes affect motoneuron function and synaptic connectivity is still under study. Thus, it is plausible that the synapse loss results from the reactive gliosis or microgliosis. In fact, it has been described a synaptic stripping process by microglia in cortical neurons (Trapp et al., 2007) and by microglia and astroglia in motoneurons (Yamada et al., 2008; 2011).

An alternative but not exclusive explanation for the loss of glutamatergic and gabaergic synapses on motoneurons could be the induction of nNOS in motoneurons as it has been described that NO synthesized by nNOS is "necessary" and "sufficient" to induce synaptic detachment from motoneurons (reviewed by Moreno-Lopez et al., 2011). Nitric oxide is a key molecule triggering synapse loss in models of motor pathologies such as physical injury of a motor nerve or in ALS (Moreno-López et al., 2011). In this regard, neuronal NOS (nNOS) seems to be the primary source of NO that is detrimental to the survival of injured motoneurons (reviewed by Moreno-Lopez et al., 2010). Moreover, it has been reported that nNOS up-regulation after nerve injury triggers the loss of excitatory synaptic inputs on injured hypoglossal motoneurons (Sumner, 1975; Sunico et al., 2005). Thus, it is likely that NO production precedes synaptic detachment from motoneurons in the SMNΔ7 mice as we observed an increase in the nNOS positive motoneurons. It has been proposed that the synaptic detachment would be directed by NO produced upon upregulation of nNOS, activation of soluble guanilate cyclase and other mediators that ultimately would lead to activation of the RhoA/ROCK pathway

and thus phosphorylation of myosin light chain (MLC), thereby inducing actomyosin contraction and synaptic bouton retraction (Sunico et al., 2010). It is well-known that ROCK mediates neurite retraction, prevents axon growth initiation (Luo, 2000; 2002). Also, RhoA/ROCK regulates fiber contraction by enhancing MLC phosphorylation, which then induces actomyosin contraction, which, eventually, contributes to bouton retraction (figure 64).

However, it has been demonstrated that nNOS up-regulation is sufficient to induce the detachment of excitatory, but not inhibitory, synapses in adult motoneurons, and both excitatory and inhibitory in neonatal motoneurons (Sunico et al., 2010). NO, via a paracrine action, induces retraction of neighbouring synapses.

On the other hand, expression and activity of the inducible isoform of nitric oxide synthase (iNOS) plays a pivotal role in sustained and elevated NO release. It seems that nNOS generates NO at low concentrations, which acts as a molecular messenger, whereas iNOS produce NO at high concentrations, which results in cytotoxicity (Moreno-López, 2010). The level of iNOS is undetectable in healthy CNS (Wang et al., 2011), but the upregulation of iNOS has been characterized in numerous cell types as a consequence of the inflammatory processes that follow disease (Heneka and Feinstein, 2001). iNOS expression had been initially described in glia but it has been described also in cortical and hippocampal neurons after traumatic brain injury (Petrov et al., 2000). At early times after injury, iNOs is restricted to non-neuronal cells and after appears in neurons. Thus, neurons can respond to proinflammatory stimuli and take part in brain inflammation; in this sense, neuronal iNOS expression may contribute to neuronal damage in traumatic brain injury (Orihara et al., 2001). The inflammatory activation of neurons serves as a source of cytotoxic agents and reactive oxygen species in brain (reviewed by Heneka and Feinstein, 2001). In line with the hypothesis that iNOS may participate in the neuroinflammatory pathological mechanisms involved in some neurodegenerative diseases, it has been found iNOS expression in neurons in Alzheimer's disease (Smith and Bennett, 1997) and ALS (Sasaki et al., 2000). This is in agreement with our finding of iNOS expression in interneurons in the spinal cord of SMNΔ7 mice. Thus, the observed increase in both nNOS and iNOS positive interneurons in the spinal cord of the SMNΔ7 mice suggests that motoneurons are not the only cells producing NO in the the spinal cord of the SMNΔ7 mice.

In ALS, upregulation of both nNOS and iNOS has been evidenced in motoneurons. Interestingly, nNOS immunoreactivity was also observed apposed to anterior horn neurons, suggesting an increased presynaptic source of NO in the pathogenesis of ALS (Sasaki et al., 2000; 2001). In contrast to other

paradigms, we did not observe an increase in iNOS positive astrocytes in the spinal cord of the SMNΔ7 mice (data not shown).

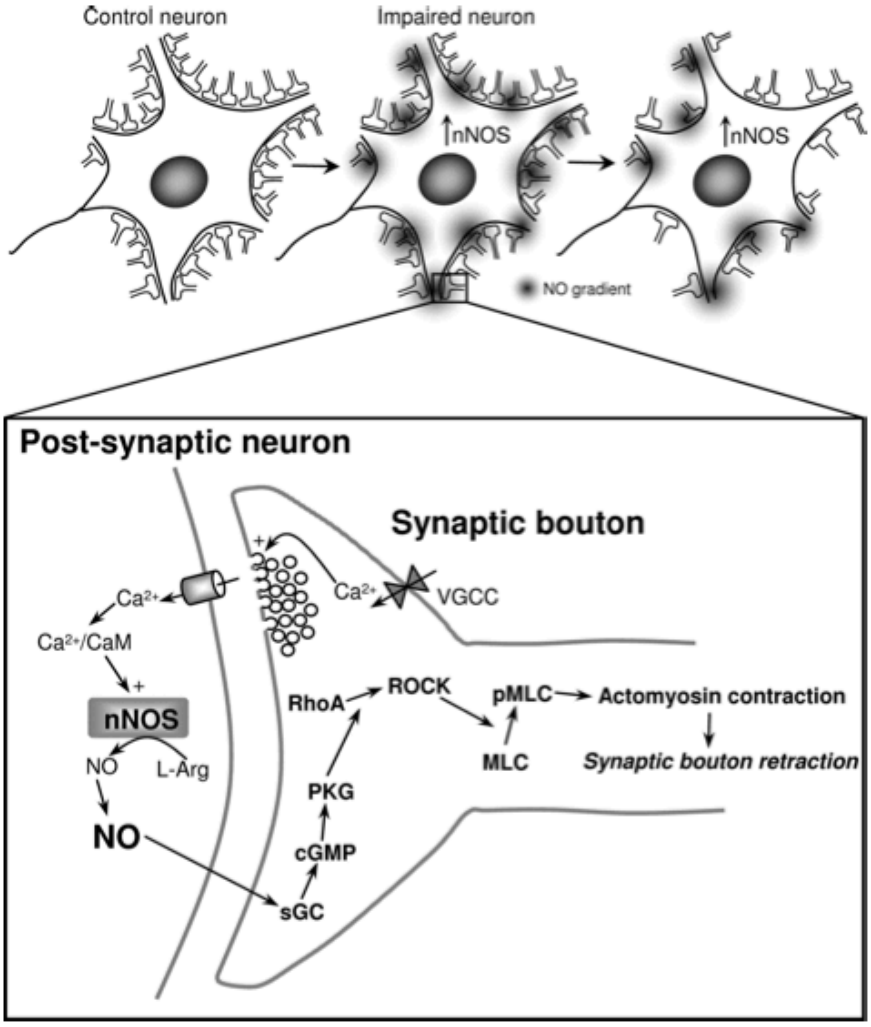

Figure 64: ***Impaired motoneurons produce NO via nNOS that activates RhoA/ROCK pathway in the presynaptic neuron, promoting synaptic bouton retraction.*** nNOS in post-synaptic neurons produces NO, which through a paracrine/retrograde pathway activates sGC in the pre-synaptic neuron. sGC rises cGMP which in turns activates PKG. This kinase activates RhoA/ROCK pathway promoting MLC phosphorylation via direct phosphorylation and MLCP inhibition. The increased presence of P-MLC supposes actomyosin contraction, and therefore synaptic boutons retraction (Sunico et al., 2010).

4 Notch pathway could be a trigger of astrogliosis and inhibition of neuritogenensis in SMA pathology

The Notch pathway is a highly conserved and ubiquitous signalling system that regulates cell fate and many cellular processes, such as astrogliosis and neuritogenesis, during development and throughout adulthood (Nichols et al., 2007; Morga et al., 2009; Ruiz-Palmero et al., 2011). Although Notch signalling plays an important role in the regulation of neuritic growth (Redmond et al., 2000) and there are studies that point to an involvement of Notch in different pathologies of the nervous system (Oh et al., 2005; Arumugam et al., 2006), the possible involvement of Notch in SMA, a disease in which alterations in neuritogenesis have been demonstrated (Bowerman et al., 2007), has not been studied yet.

Initially, we observed increased levels of Notch ligands, Jagged and Delta, in U87MG astroglioma cell line depleted of SMN via shRNA lentiviral vectors. Moreover, Notch full-length protein was also overexpressed. This data suggested that Notch pathway could be activated after SMN depletion. Further data demonstrated an increase in the active form of Notch, NICD, in this astroglioma cell line depleted of SMN.

Classicaly, the Notch-family of receptors and ligands had been described in the context of the development of the nervous system. Nowadays, few studies have already documented the role of the Notch pathway in the control of astrocyte behavior during CNS injuries. More specifically, Morga et al. studied to what degree the Notch-ligand Jagged1 is implicated in reactive astrocytes development and the impact of Notch pathway, via Jagged1-mediated modulation, on the inflammatory phenotype of reactive astrocytes (Morga et al., 2009). Furthermore, Notch signalling contributes to neuroinflammation by stimulating the infiltration of proinflammatory leukocytes and enhancing apoptotic cascades in neurons (Arumugam et al., 2006). In addition, NF-κB and Notch signalling pathways operate in synergy to produce proinflammatory cytokines in activated microglia (Cao et al., 2011)

Our previous *in vitro* results demonstrating Notch pathway activation after SMN depletion in U87MG astroglioma cell line were taken into account and the Notch pathway was studied in a SMNΔ7 mouse model. Some studies have described that Notch and its ligands, Jagged and Delta, are expressed by reactive astrocytes and reactive microglia and regulate glial activation and the inflammatory response of these cells (Grandbarbe et al., 2007; Cao et al., 2008; 2010). We observed astrogliosis and microgliosis processes surrounding

motoneurons in this animal model of SMA (figure 49). Our results demonstrated that astroglia surrounding motoneurons overexpress Notch ligands, Jagged and Delta, at the end-stage of the disease. This overexpression of Notch ligands could led astroglia to activate Notch into NICD in neighbouring astrocytes from SMNΔ7 mouse model.

Notch pathway has been thoroughly demonstrated to cross-talk with NF-κB pathway (Cheng et al., 2001; Vilimas et al., 2007). It is known that NICD is translocated into the nucleus. There, NICD induces p65 overexpression, a member of the NF-κB pathway (Osipo et al., 2007). Moreover, Notch full-length receptor was also overexpressed in astroglia, probably owing to Jagged and Delta activation of Notch, which through NF-κB pathway, leading to increased expression of the Notch receptor (Osipo et al., 2007).

Glia play a neuroprotective role in CNS; astrocytes are involved in metabolic support of neurons (Haydon, 2001; Horner and Palmer, 2003) and microglial cells continuously survey the local microenvironment and work as housekeepers in the brain (Nimmerjahn et al., 2005; Davalos et al., 2005). Nonetheless, in addition to these beneficial functions, glial cells also mediate detrimental effects on neurons under specific pathological conditions. Activated astrocytes may impede neuronal survival and regeneration by forming scar tissue and synthesizing neurotoxic molecules (Marchetti and Abbracchio, 2005). Moreover, activated astroglia have been directly related to synaptic stripping around injured motoneurons (Yamada et al., 2011). Reactive microglial cells kill and phagocytose target neuronal cells following excessive and uncontrolled adverse stimulation (van Rossum and Hanisch, 2004; Cardona et al., 2006). Alltogether, the evidence to date suggests that glial cells may act as a double-edged sword with neuroprotective features predominating in the healthy nervous system and neurodestructive properties in various pathological conditions (Biber et al., 2007). According to these, and taking into account our results, activated astroglia via Notch signalling could initiate motoneuron impairment in SMA pathogenic onset.

The murine model of the SMA, the SMNΔ7, exhibits motoneuron loss only visible at the end-stage of the disease, indicating that it is a late event in this pathology (Le et al., 2005; Kariya et al., 2008). We quantified a motoneuron loss around 24 % at P14 mice compared to control. However, previous to the motoneuron loss, it has been described an important denervation of some muscles (up to 50% in intercostal muscles), together with a functional deficit and arrest of postnatal development of NMJs, showing clusters of unoccupied acetylcholine receptors (Murray et al., 2008; Kariya et al., 2008; McGovern et al., 2008; Kong et al., 2009). Electrophysiological analysis shows that the number of

synaptic vesicles that release neurotransmitter during an action potential is decreased (Kong et al., 2009) as well as severe structural and functional alterations in the organization of the organelles and the cytoskeleton of motor nerve terminals (Torres-Benito et al., 2011; Dachs et al., 2011). In this sense, we described a reduction of more than 60% in the syn-ir puncta around motoneurons, suggesting a loss of synaptic vesicles in motoneurons. Moreover, a reduction in the number and in the section of axons in this mouse model has been described (Kariya et al., 2008).

A relationship between reduced levels of SMN and impaired neuritogenesis was described in PC12 cells: SMN knock-down reduced the length of neurites and increased the incidence of beading and swelling along their length, which is usually indicative of cytoskeletal perturbation and impairment of axonal transport (Bowerman et al., 2007). These data suggest that SMN protein, in addition to being important for the neuromuscular system, is also essential in the development of the nervous system and could be involved in the processes of proliferation, migration and neuritogenesis. In this sense, a link between SMN depletion and neuritogenic defects has not been described yet. Neurogenin is a protein involved in neuritogenesis and the maintenance of correct excitatory/inhibitory synapses ratio (Ruiz-Palmero et al., 2011). In view of a reduction in Neurogenin expression in motoneurons of a mouse model where SMN is depleted and Notch signling is enhanced, we propose that the inhibition of neuritogenesis and axonal maintenance could be due to SMN deficiency through Notch pathway. This hypothesis is in agreement with Venkatesh et al. (2011) where they describe that Notch activation into NICD is activating RhoA/ROCK pathway in endothelial cells. They described that NICD activates RhoA, which in turn activates ROCK (Venkatesh et al., 2011). It is known that ROCK phosphorylates MLC into P-MLC, and also inhibits MLCP, thus controlling actin–myosin interaction and stress fiber formation (Amano et al., 1996; Pellegrin and Mellor, 2007). P-MLC promotes the interaction of myosin II with actin increasing the speed of myosin II-driven retrograde flow in filopodia and lamellipodia (Luo, 2002), and also is involved in retraction of axonal growth cones in response to several RhoA-activating stimuli (Benarroch, 2007). In mouse models it has been demonstrated that axon degeneration leads to soma apoptosis of motoneurons (Ferri et al., 2003).

Microglial activation can be triggered by compounds originating from neurons and astrocytes (Moisse and Strong, 2006). It has been demonstrated that microglial cells expresses enhanced Notch pathway upon activation; and this enhanced Notch expression in activated microglia modulate production of proinflammatory cytokines and nitric oxide (NO), which leads to a neuroinflammation process (Cao et al., 2008). In our study, whereas astroglia

express more Jagged and Delta, microglia only express NICD at end-stage of the mouse model. This Notch enhanced expression may explain microglial activation. Reactive microglial cells kill and phagocytose target neuronal cells following excessive and uncontrolled adverse stimulation (van Rossum and Hanisch, 2004; Cardona et al., 2006). Therefore, this activated microglia can compromise motoneuron survival.

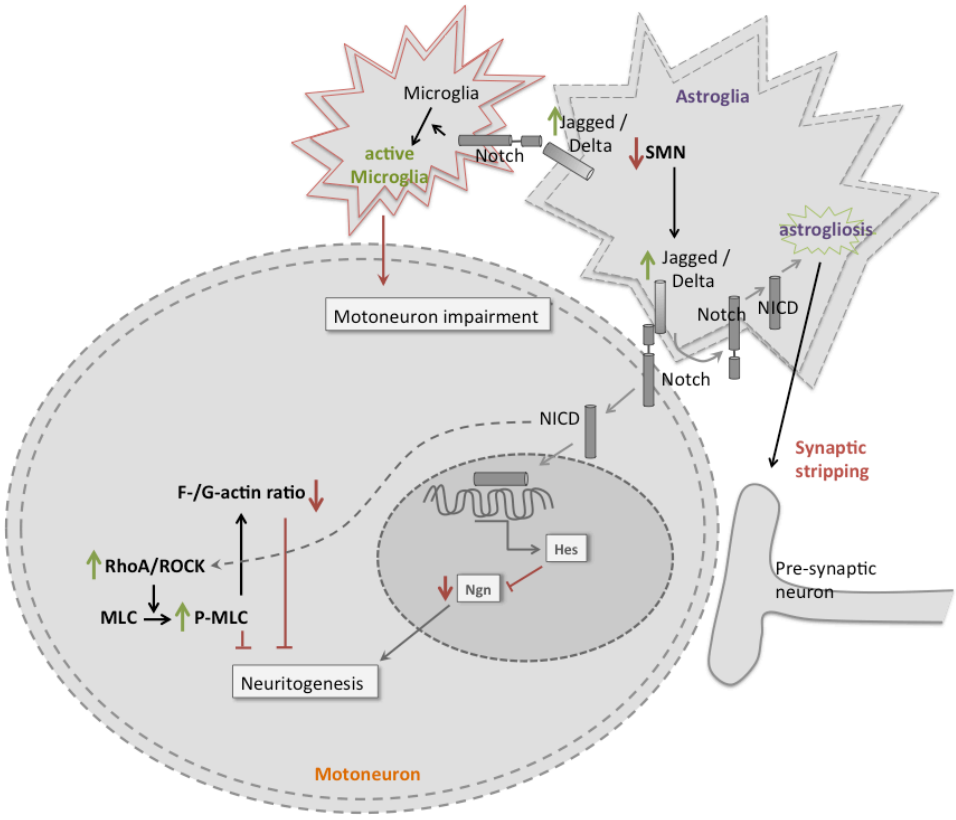

Figure 65: ***Potential mechanisms and consequences of Notch pathway activation in SMNΔ7 mouse motoneurons and glia***. SMN depletion causes Jagged and Delta overexpression in astroglia. These ligands activate Notch in surrounding astroglia, microglia and motoneurons. Activated Notch, NICD, translocates into the nucleus and, via Hes, inhibits Neurogenin expression in motoneurons. Neurogenin is necessary for neuritogenesis and the maintenance of correct excitatory/inhibitory synapses ratio. Therefore, absence of Neurogenin would affect neuritogenesis process and synapses. Moreover, NICD enhancement in motoneurons would affect RhoA/ROCK pathway, increasing P-MLC and affecting neuritogenesis. Gliosis, initiated by Notch enhancement, could compromise motoneuron survival and trigger synaptic stripping.

5 Final discussion

SMA pathology has been clearly described as a disease triggered by a reduction of SMN protein, and a final selective death of spinal motoneurons. Nevertheless, the pathogenic link between the decrease of SMN protein and motoneuron death has not been elucidated yet. The data presented in this thesis suggests that, in addition to motoneurons, glial cells are also involved in the pathology. Taking into account our data and published results from other authors, we propose a potential mechanism where RhoA/ROCK signalling pathway activation, decreased F-/G-actin ratio induced by increased profilin expression, Notch signalling pathway activation, and neuronal nitric oxide synthase overexpression, could be the molecular effectors acting after SMN depletion, thus suggesting their involvement in SMA pathogenesis (figure 66).

As the reduction in the number of motoneurons seems to be modest and late in the mouse models of the disease (Le et al., 2005; Monani et al., 2000b), we hypothesized that, before dying, motoneurons would have hallmarks of pathology. In fact, we have demonstrated soma reduction in 1) motoneurons from the rat spinal cord embryonic explants after SMN-depletion and in 2) spinal cord motoneurons from the SMNΔ7 mouse at end-stage. This reduction, also described by other authors in SMA models (Acsadi et al., 2009), may be a hallmark of SMA pathology indicating alterations in the cytoskeleton of motoneurons. We have also described neurite disruptions in motoneurons from the rat spinal cord embryonic explants after SMN-depletion. This observed neurite disruption may reflect abnormal accumulation of phosphorylated neurofilament in varicosities (Fan and Simard, 2002), that is in agreement with neurite swelling, widely described in motoneurons from SMA mouse models (McGovern et al., 2008).

RhoA/ROCK pathway activation has been clearly related to SMN depletion in several SMA models (Bowerman et al., 2009, 2010). ROCK phosphorylates MLC into P-MLC (Amano et al., 2000; Luo, 2002; Newey et al., 2005), and this phosphorylation leads to axonal retraction and retrograde flow in filopodia (Negishi and Kato, 2002). Moreover, we have observed nNOS overexpression in motoneurons from SMNΔ7 mice. According to Sunico et al. (2010), the nNOS-produced nitric oxide could act as a second messenger, retrogradely activating the RhoA/ROCK pathway in pre-synaptic neurons. The phosphorylation of MLC via ROCK causes actomyosin contraction and synaptic bouton retraction of the pre-synaptic neuron. In this sense, we have observed a reduction in the number of synaptic boutons around motoneuron soma, which exhibit increased phosporylation of MLC, suggesting that activation of RhoA/ROCK, via NO

produced in motoneurons, could be a possible mechanism in the pathogenesis of SMA.

Our data and data published by Bowerman et al. (2007) demonstrate that SMN depletion leads to an overexpression of profilin. In this case, our hypothesis is that in a SMN-depleted scenario, there is not enough SMN to bind to profilin, then profilin is free to sequestrate G-actin. In fact, we have observed a switch from filamentous to globular actin in SMN-depleted U87MG astroglioma cell line. The absence of free G-actin to polymerize into F-actin is impairing cell migration in U87MG astroglioma cell line. Moreover, SMN depletion in U87MG astroglioma cell line is activating RhoA/ROCK pathway. Active ROCK phosphorylates MLC into P-MLC, leading to an interaction of myosin II with actin and increasing the speed of myosin II-driven retrograde flow in filopodia and lamellipodia (Luo, 2002), and thus inhibiting cell migration. This astroglial migration impairment could affect motoneuronal migration and axonal growth in development. In fact, a similar mechanism has also been proposed to be involved in retraction of axonal growth cones in response to several RhoA-activating stimuli (Benarroch, 2007).

We also propose that SMN depletion is not only affecting motoneurons. We have observed enhanced presence of astroglia surrounding motoneurons in ventral region at pre-symptomatic stage in lumbar spinal cord of SMNΔ7 mice, thus suggesting the involvement of astroglia in SMA onset. At symptomatic stage, enhanced microgliosis and astrogliosis were equally distributed in the ventral and dorsal regions of all the lumbar spinal cord, and not only around motoneurons. In this context, Jagged and Delta, ligands of Notch receptor, are overexpressed in astroglia after SMN depletion, both in SMNΔ7 mice and SMN-depleted U87MG human astroglioma cell line. This overexpression of Notch ligands may activate Notch into its active form, NICD, in surrounding astroglia, microglia and motoneurons. In turn, in agreement with our results, the activation of Notch may lead to microgliosis (Cao et al., 2008; Grandbarbe et al., 2007) and astrogliosis (Morga et al., 2009). Gliosis has been described as a potential trigger of neuron death in some neurodegenerative diseases (reviewed by Papadimitriou et al., 2010), and has been linked to synaptic stripping (Raivich et al., 1999; Trapp et at., 2007; Yamada et al., 2011). Thus, the loss of synaptic boutons that we observe on spinal cord motoneurons in the SMNΔ7 mouse model, could be related to 1) the NO produced in motoneurons, and 2) the synaptic stripping induced by glial activation.

In motoneurons, the activation of Notch into NICD may be due, at least in part, to Jagged and Delta overexpression in astroglia, and may be inhibiting Neurogenin expression, via Hes1 (Arevalo et al., 2011). The reduced expression

of this protein, directly involved in neuritogenesis (Simon-Areces et al., 2010; Ruiz-Palmero et al., 2011) could be causing problems in motoneuronal neurite development and maintenance.

Moreover, in endothelial cells, Notch signaling has been linked to RhoA/ROCK activation (Venkatesh et al., 2011). Therefore, we suggest that the depletion of SMN could be activating RhoA/ROCK pathway both via Notch activation (Venkatesh et al., 2011) and nNOS-enhanced expression (Sunico et al., 2010).

In conclusion, astroglia may play an important role initiating Notch signalling activation in SMN-depleted conditions, and exacerbating the neuroinflammatory response. Glial scar (reviewed by Papadimitriou, 2010) and glial bundles produced by astroglial activation in SMA (Chou, 1980) may maintain the motoneuron detriment. Moreover, microglia has been demonstrated to become active after Notch activation (Grandbarbe et al., 2007), and we have observed Notch activation in these cells, probably owing to its exposition to Jagged and Delta from astroglia. The activation of microglia is potentiated as they are exposed to the inflammatory environment around motoneurons, which, in turn, impairs their survival.

Taking all this data into account, we suggest that, in SMA affected motoneurons, neuritogenesis impairment, central synaptic withdrawal, soma reduction and increased presence of phosphorylated neurofilament may be the primary cellular defects that ultimately lead to their loss. In addition, in SMA tissue there is an activation of glia that ultimately could create a detrimental environment leading to motoneuron death. Therefore, we suggest that SMA pathogenesis is not only a single process, but a convergence of pathogenic processes which lead to motoneuron specific impairment and later death.

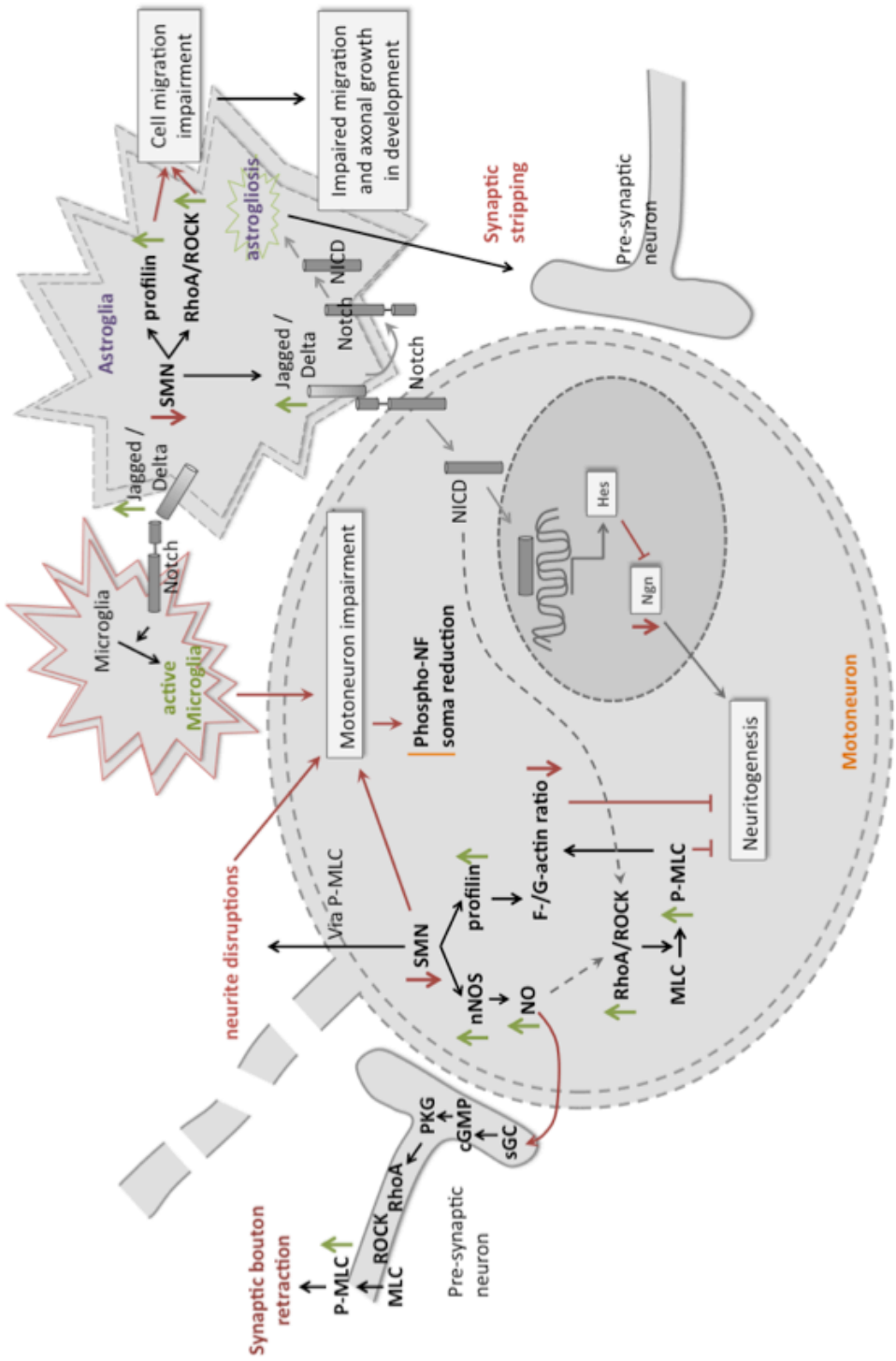

Figure 66: ***Scheme of our hypothesis exposing pathogenic mechanisms involved in SMA.***

VI. CONCLUSIONS

VI. Conclusions

The main conclusions of this thesis are as follows:

1. In the astroglioma cell line, U87MG, SMN depletion results in a reduction of cellular migration capacity. This impairment can be caused by: 1) increased profilin expression, which secuestrates G-actin preventing actin polymerization, and 2) RhoA/ROCK signalling pathway activation, which leads to myosin light chain phosphorylation, which is known to promote interaction of myosin light chain with actin, increasing the speed of retrograde flow in filopodia and lamellipodia.

2. In the SMNΔ7 mouse model of SMA disease and in SMN-depleted motoneurons from rat embryonic spinal cord explants, spinal motoneurons show pathological hallmarks previous to death, such as increased and abnormal neurofilament phosphorylation, neurite disruptions and soma reduction.

3. Astrogliosis is present in the SMNΔ7 mice at pre-symptomatic stage. This astrogliosis starts surrounding motoneurons at pre-symptomatic stage and invades all the lumbar spinal cord at symptomatic stage.

4. There is enhanced microglial presence around motoneuron somas at symptomatic stage, but not at pre-symptomatic, in the lumbar spinal cord of the SMNΔ7 mouse model.

5. At symptomatic stage, the neuronal isoform of nitric oxide synthase is overexpressed in motoneurons and interneurons of the lumbar spinal cord of SMNΔ7 mice, whereas the inducible isoform of this enzyme is overexpressed only in interneurons.

6. At symptomatic stage, reduced number of pre-synaptic boutons is found on motoneuron somata in the lumbar spinal cord of SMNΔ7 mice. In these pre-synaptic boutons there is an increased phosphorylation of myosin light chain.

7. In the U87MG astroglioma cell line, SMN depletion increases the expression of the Notch ligands, Jagged and Delta, and this is associated to an increase in the intracellular fragment of Notch (NICD).

8. In the lumbar spinal cord of SMNΔ7 mice there is an overexpression of the Notch ligands, Jagged and Delta, and this results in an increase in the active intracellular fragment of Notch in motoneurons, astroglia and microglia.

9. The activation of the Notch signalling pathway in motoneurons of the lumbar spinal cord of SMNΔ7 mice, results in decreased expression of Neurogenin, a protein directly involved in neuritogenesis.

10. The depletion of SMN protein in *in vitro* and *in vivo* models is associated to an increased activation of the RhoA/ROCK and Notch signalling pathways resulting in actin cytoskeleton disturbance and decreased Neurogenin expression, thus causing cell migration impairment, loss of synapses onto spinal motoneurons and soma reduction. In addition, the observed gliosis found in the SMNΔ7 mice could contribute to create a detrimental environment in SMA tissue. Therefore, our results suggest that SMA pathogenesis is not only a single process, but a convergence of pathogenic processes in motoneurons and glia which lead to motoneuron specific impairment and later death.

VII. PUBLICATIONS

VII. Publications

Publications related to this thesis:

· **Caraballo-Miralles, V.**, Cardona-Rossinyol, A., Garcera, A., Villalonga, P., Soler, R.M., Olmos, G., Lladó, J. *SMN deficiency attenuates migration of U87MG astroglioma cells through the activation of RhoA*. Mol Cell Neurosci. 2011 Dec 16.

· Garcera, A., Mincheva, S., Gou-Fabregas, M., **Caraballo-Miralles, V.**, Lladó, J., Comella, J.X., Soler, R.M. *A new model to study spinal muscular atrophy: neurite degeneration and cell death is counteracted by BCL-X(L) overexpression in motoneurons.* Neurobiol Dis. 2011 Jun;42(3):415-26.

Publications related to this thesis, in preparation:

· **Caraballo-Miralles, V.**, Cardona-Rossinyol, A., Torres-Benito, L., Tabares, L., Olmos, G., Lladó, J. *Gliosis and motoneuron pathological markers in the SMNΔ7 model of Spinal muscular atrophy*. In preparation.

· **Caraballo-Miralles, V.**, Cardona-Rossinyol, A., Torres-Benito, L., Tabares, L., Olmos, G., Lladó, J. *Notch pathway is activated in the SMNΔ7 model of Spinal muscular atrophy*. In preparation.

Other publications, non-directly related to this thesis:

· **Caraballo-Miralles, V.,** Tolosa, L., Olmos, G., Lladó, J. *TNF-α potentiates glutamate-induced spinal cord motoneuron death via NF-κB.* Mol Cell Neurosci. 2011 Jan;46(1):176-86.

· Ayala, V., Granado-Serrano, A.B., Cacabelos, D., Naudí, A., Ilieva, E.V., Boada, J., **Caraballo-Miralles, V.**, Lladó, J., Ferrer, I., Pamplona, R., Portero-Otin, M. *Cell stress induces TDP-43 pathological changes associated with ERK1/2 dysfunction: implications in ALS.* Acta Neuropathol. 2011 Sep;122(3):259-70.

· Cardona-Rossinyol, A., **Caraballo-Miralles, V.**, Mir, M., Lladó, J., Olmos, G. *Neuroprotective effects of estradiol on motoneurons in a new model of rat spinal cord embryonic explants.* Submitted in Brain Research.

· Peluffo, H., Foster, E., Ahmed, S.G.O., Lago, N., Yip, P., Hutson, T.H., Moon, L., Wanisch, K., **Caraballo-Miralles, V.**, Lladó, J., McMahon, S.B., Yáñez-Muñoz, R.J. *Integration deficient Lentiviral Vectors as efficient tools for in vitro and in vivo transduction of spinal neurons and glia.* Submitted in Gene Therapy.

VIII. REFERENCES

VIII. References

Ackerley S, Grierson AJ, Banner S, Perkinton MS, Brownlees J, Byers HL, Ward M, Thornhill P, Hussain K, Waby JS, Anderton BH, Cooper JD, Dingwall C, Leigh PN, Shaw CE, Miller CCJ (2004) p38alpha stress-activated protein kinase phosphorylates neurofilaments and is associated with neurofilament pathology in amyotrophic lateral sclerosis. Mol. Cell. Neurosci. 26:354-364

Acsadi G, Lee I, Li X, Khaidakov M, Pecinova A, Parker GC, Hüttemann M (2009) Mitochondrial dysfunction in a neural cell model of spinal muscular atrophy. J. Neurosci. Res. 87:2748-2756

Aktan F (2004) iNOS-mediated nitric oxide production and its regulation. Life Sci. 75:639-653

Aldskogius H, Liu L, Svensson M (1999) Glial responses to synaptic damage and plasticity. J. Neurosci. Res. 58:33-41

Amano M, Ito M, Kimura K, Fukata Y, Chihara K, Nakano T, Matsuura Y, Kaibuchi K (1996) Phosphorylation and activation of myosin by Rho-associated kinase (Rho-kinase). J. Biol. Chem. 271:20246-20249

Amano M, Fukata Y, Kaibuchi K (2000) Regulation and functions of Rho-associated kinase. Exp. Cell Res. 261:44-51

Andreassi C, Angelozzi C, Tiziano FD, Vitali T, De Vincenzi E, Boninsegna A, Villanova M, Bertini E, Pini A, Neri G, Brahe C (2004) Phenylbutyrate increases SMN expression in vitro: relevance for treatment of spinal muscular atrophy. Eur. J. Hum. Genet. 12:59-65

Anneser JM, Cookson MR, Ince PG, Shaw PJ, Borasio GD (2001) Glial cells of the spinal cord and subcortical white matter up-regulate neuronal nitric oxide synthase in sporadic amyotrophic lateral sclerosis. Experimental Neurology 171:418-421

Araki S, Hayashi M, Tamagawa K, Saito M, Kato S, Komori T, Sakakihara Y, Mizutani T, Oda M (2003) Neuropathological analysis in spinal muscular atrophy type II. Acta Neuropathol 106:441-448

Arevalo MA, Ruiz-Palmero I, Scerbo MJ, Acaz-Fonseca E, Cambiasso MJ, Garcia-Segura LM (2011) Molecular mechanisms involved in the regulation of neuritogenesis by estradiol: Recent advances. J. Steroid Biochem. Mol. Biol.

Arumugam TV, Chan SL, Jo D, Yilmaz G, Tang S, Cheng A, Gleichmann M, Okun E, Dixit VD, Chigurupati S, Mughal MR, Ouyang X, Miele L, Magnus T, Poosala S, Granger DN, Mattson MP (2006) Gamma secretase-mediated Notch signaling worsens brain damage and functional outcome in ischemic stroke. Nat. Med. 12:621-623

Bae YH, Ding Z, Zou L, Wells A, Gertler F, Roy P (2009) Loss of profilin-1 expression enhances breast cancer cell motility by Ena/VASP proteins. J. Cell. Physiol. 219:354-364

Bash J, Zong WX, Banga S, Rivera A, Ballard DW, Ron Y, Gélinas C (1999) Rel/NF-kappaB can trigger the Notch signaling pathway by inducing the expression of Jagged1, a ligand for Notch receptors. EMBO J. 18:2803-2811

Battaglia G, Princivalle A, Forti F, Lizier C, Zeviani M (1997) Expression of the SMN gene, the spinal muscular atrophy determining gene, in the mammalian central nervous system. Hum. Mol. Genet. 6:1961-1971

Beers DR, Zhao W, Liao B, Kano O, Wang J, Huang A, Appel SH, Henkel JS (2011) Neuroinflammation modulates distinct regional and temporal clinical responses in ALS mice. Brain Behav. Immun. 25:1025-1035

Benarroch EE (2007) Rho GTPases: role in dendrite and axonal growth, mental retardation, and axonal regeneration. Neurology 68:1315-1318

Berezovska O, Xia MQ, Page K, Wasco W, Tanzi RE, Hyman BT (1997) Developmental regulation of presenilin mRNA expression parallels notch expression. J. Neuropathol. Exp. Neurol. 56:40-44

Berezovska O, McLean P, Knowles R, Frosh M, Lu FM, Lux SE, Hyman BT (1999) Notch1 inhibits neurite outgrowth in postmitotic primary neurons. Neuroscience 93:433-439

Bergin A, Kim G, Price DL, Sisodia SS, Lee MK, Rabin BA (1997) Identification and characterization of a mouse homologue of the spinal muscular atrophy-determining gene, survival motor neuron. Gene 204:47-53

Béchade C, Rostaing P, Cisterni C, Kalisch R, La Bella V, Pettmann B, Triller A (1999) Subcellular distribution of survival motor neuron (SMN) protein: possible involvement in nucleocytoplasmic and dendritic transport. Eur. J. Neurosci. 11:293-304

Biber K, Neumann H, Inoue K, Boddeke HWGM (2007) Neuronal 'On' and "Off" signals control microglia. Trends Neurosci. 30:596-602

Blencowe BJ (2000) Exonic splicing enhancers: mechanism of action, diversity and role in human genetic diseases. Trends Biochem. Sci. 25:106-110

Boillée S, Vande Velde C, Cleveland DW (2006) ALS: a disease of motor neurons and their nonneuronal neighbors. Neuron 52:39-59

Boon K, Xiao S, McWhorter ML, Donn T, Wolf-Saxon E, Bohnsack MT, Moens CB, Beattie CE (2009) Zebrafish survival motor neuron mutants exhibit presynaptic neuromuscular junction defects. Hum. Mol. Genet. 18:3615-3625

Bowerman M, Shafey D, Kothary R (2007) Smn depletion alters profilin II expression and leads to upregulation of the RhoA/ROCK pathway and defects in neuronal integrity. J. Mol. Neurosci. 32:120-131

Bowerman M, Anderson CL, Beauvais A, Boyl PP, Witke W, Kothary R (2009) SMN, profilin IIa and plastin 3: a link between the deregulation of actin dynamics and SMA pathogenesis. Mol. Cell. Neurosci. 42:66-74

Bowerman M, Beauvais A, Anderson CL, Kothary R (2010) Rho-kinase inactivation prolongs survival of an intermediate SMA mouse model. Hum. Mol. Genet. 19:1468-1478

Bowerman M, Murray LM, Beauvais A, Pinheiro B, Kothary R (2011) A critical Smn threshold in mice dictates onset of an intermediate spinal muscular atrophy phenotype associated with a distinct neuromuscular junction pathology. Neuromuscul Disord

Brahe C (2000) Copies of the survival motor neuron gene in spinal muscular atrophy: the more, the better. Neuromuscul Disord 10:274-275

Brichta L, Hofmann Y, Hahnen E, Siebzehnrubl FA, Raschke H, Blumcke I, Eyupoglu IY, Wirth B (2003) Valproic acid increases the SMN2 protein level: a well-known drug as a potential therapy for spinal muscular atrophy. Hum. Mol. Genet. 12:2481-2489

Briese M, Esmaeili B, Sattelle DB (2005) Is spinal muscular atrophy the result of defects in motor neuron processes? Bioessays 27:946-957

Briese M, Richter D, Sattelle DB, Ulfig N (2006) SMN, the product of the spinal muscular atrophy-determining gene, is expressed widely but selectively in the developing human forebrain. J. Comp. Neurol. 497:808-816

Briese M, Esmaeili B, Fraboulet S, Burt EC, Christodoulou S, Towers PR, Davies KE, Sattelle DB (2009) Deletion of smn-1, the Caenorhabditis elegans ortholog of the spinal muscular atrophy gene, results in locomotor dysfunction and reduced lifespan. Hum. Mol. Genet. 18:97-104

Burghes AHM, Beattie CE (2009) Spinal muscular atrophy: why do low levels of survival motor neuron protein make motor neurons sick? Nature Publishing Group 10:597-609

Burke RE, Levine DN, Tsairis P, Zajac FE (1973) Physiological types and histochemical profiles in motor units of the cat gastrocnemius. J. Physiol. (Lond.) 234:723-748

Burnett BG, Muñoz E, Tandon A, Kwon DY, Sumner CJ, Fischbeck KH (2009) Regulation of SMN protein stability. Mol. Cell. Biol. 29:1107-1115

Bühler D, Raker V, Lührmann R, Fischer U (1999) Essential role for the tudor domain of SMN in spliceosomal U snRNP assembly: implications for spinal muscular atrophy. Hum. Mol. Genet. 8:2351-2357

Bürglen L, Lefebvre S, Clermont O, Burlet P, Viollet L, Cruaud C, Munnich A, Melki J (1996) Structure and organization of the human survival motor neurone (SMN) gene. Genomics 32:479-482

Byers RK, Banker BQ (1961) Infantile muscular atrophy. Arch. Neurol. 5:140-164

Cao LG, Babcock GG, Rubenstein PA, Wang YL (1992) Effects of profilin and profilactin on actin structure and function in living cells. J. Cell Biol. 117:1023-1029

Cao Q, Lu J, Kaur C, Sivakumar V, Li F, Cheah PS, Dheen ST, Ling EA (2008) Expression of Notch-1 receptor and its ligands Jagged-1 and Delta-1 in amoeboid microglia in postnatal rat brain and murine BV-2 cells. Glia 56:1224-1237

Cao Q, Kaur C, Wu CY, Lu J, Ling EA (2011) Nuclear factor-kappa β regulates Notch signaling in production of proinflammatory cytokines and nitric oxide in murine BV-2 microglial cells. Neuroscience 192:140-154

Cao Q, Li P, Lu J, Dheen ST, Kaur C, Ling EA (2010) Nuclear factor-κB/p65 responds to changes in the Notch signaling pathway in murine BV-2 cells and in amoeboid microglia in postnatal rats treated with the γ-secretase complex blocker DAPT. J. Neurosci. Res.: 88(12):2701-14

Cardona AE, Pioro EP, Sasse ME, Kostenko V, Cardona SM, Dijkstra IM, Huang D, Kidd G, Dombrowski S, Dutta R, Lee J, Cook DN, Jung S, Lira SA, Littman DR, Ransohoff RM (2006) Control of microglial neurotoxicity by the fractalkine receptor. Nat. Neurosci. 9:917-924

Carrel TL, McWhorter ML, Workman E, Zhang H, Wolstencroft EC, Lorson C, Bassell GJ, Burghes AHM, Beattie CE (2006) Survival motor neuron function in motor axons is independent of functions required for small nuclear ribonucleoprotein biogenesis. J. Neurosci. 26:11014-11022

Cartegni L, Hastings ML, Calarco JA, de Stanchina E, Krainer AR (2006) Determinants of exon 7 splicing in the spinal muscular atrophy genes, SMN1 and SMN2. Am. J. Hum. Genet. 78:63-77

Cartegni L, Krainer AR (2002) Disruption of an SF2/ASF-dependent exonic splicing enhancer in SMN2 causes spinal muscular atrophy in the absence of SMN1. Nat. Genet. 30:377-384

Carvalho T, Almeida F, Calapez A, Lafarga M, Berciano MT, Carmo-Fonseca M (1999) The spinal muscular atrophy disease gene product, SMN: A link between snRNP biogenesis and the Cajal (coiled) body. J. Cell Biol. 147:715-728

Catania MV, Aronica E, Yankaya B, Troost D (2001) Increased expression of neuronal nitric oxide synthase spliced variants in reactive astrocytes of amyotrophic lateral sclerosis human spinal cord. J. Neurosci. 21:RC148

Chan YB, Miguel-Aliaga I, Franks C, Thomas N, Trülzsch B, Sattelle DB, Davies KE, van den Heuvel M (2003) Neuromuscular defects in a Drosophila survival motor neuron gene mutant. Hum. Mol. Genet. 12:1367-1376

Chang H, Hung W, Chuang Y, Jong Y (2004) Degradation of survival motor neuron (SMN) protein is mediated via the ubiquitin/proteasome pathway. Neurochem. Int. 45:1107-1112

Chang HC, Dimlich DN, Yokokura T, Mukherjee A, Kankel MW, Sen A, Sridhar V, Fulga TA, Hart AC, Van Vactor D, Artavanis-Tsakonas S (2008) Modeling spinal muscular atrophy in Drosophila. PLoS ONE 3:e3209

Cheng P, Zlobin A, Volgina V, Gottipati S, Osborne B, Simel EJ, Miele L, Gabrilovich DI (2001) Notch-1 regulates NF-kappaB activity in hemopoietic progenitor cells. J. Immunol. 167:4458-4467

Chou SM (1980) Glial bundles of nerve roots in Werdnig-Hoffmann disease. Ann. Neurol. 8:79-82

Chou SM, Fakadej AV (1971) Ultrastructure of chromatolytic motoneurons and anterior spinal roots in a case of Werdnig-Hoffmann disease. J. Neuropathol. Exp. Neurol. 30:368-379

Chou SM, Nonaka I (1978) Werdnig-Hoffmann disease: proposal of a pathogenetic mechanism. Acta Neuropathol 41:45-54

Cifuentes-Diaz C, Frugier T, Tiziano FD, Lacène E, Roblot N, Joshi V, Moreau MH, Melki J (2001) Deletion of murine SMN exon 7 directed to skeletal muscle leads to severe muscular dystrophy. J. Cell Biol. 152:1107-1114

Cifuentes-Diaz C, Nicole S, Velasco ME, Borra-Cebrian C, Panozzo C, Frugier T, Millet G, Roblot N, Joshi V, Melki J (2002) Neurofilament accumulation at the motor endplate and lack of axonal sprouting in a spinal muscular atrophy mouse model. Hum. Mol. Genet. 11:1439-1447

Coovert DD, Le TT, McAndrew PE, Strasswimmer J, Crawford TO, Mendell JR, Coulson SE, Androphy EJ, Prior TW, Burghes AH (1997) The survival motor neuron protein in spinal muscular atrophy. Hum. Mol. Genet. 6:1205-1214

Crawford TO, Pardo CA (1996) The neurobiology of childhood spinal muscular atrophy. Neurobiol. Dis. 3:97-110

Cusin V, Clermont O, Gérard B, Chantereau D, Elion J (2003) Prevalence of SMN1 deletion and duplication in carrier and normal populations: implication for genetic counselling. J. Med. Genet. 40:e39

Da Silva JS, Medina M, Zuliani C, Di Nardo A, Witke W, Dotti CG (2003) RhoA/ROCK regulation of neuritogenesis via profilin IIa-mediated control of actin stability. J. Cell Biol. 162:1267-1279

Dachs E, Hereu M, Piedrafita L, Casanovas A, Calderó J, Esquerda JE (2011) Defective neuromuscular junction organization and postnatal myogenesis in mice with severe spinal muscular atrophy. J. Neuropathol. Exp. Neurol. 70:444-461

Das T, Bae YH, Wells A, Roy P (2009) Profilin-1 overexpression upregulates PTEN and suppresses AKT activation in breast cancer cells. J. Cell. Physiol. 218:436-443

Davalos D, Grutzendler J, Yang G, Kim JV, Zuo Y, Jung S, Littman DR, Dustin ML, Gan W (2005) ATP mediates rapid microglial response to local brain injury in vivo. Nat. Neurosci. 8:752-758

De Hauwer C, Camby I, Darro F, Decaestecker C, Gras T, Salmon I, Kiss R, Van Ham P (1997) Dynamic characterization of glioblastoma cell motility. Biochem. Biophys. Res. Commun. 232:267-272

Deckel AW, Tang V, Nuttal D, Gary K, Elder R (2002) Altered neuronal nitric oxide synthase expression contributes to disease progression in Huntington's disease transgenic mice. Brain Res. 939:76-86

DiDonato CJ, Chen XN, Noya D, Korenberg JR, Nadeau JH, Simard LR (1997) Cloning, characterization, and copy number of the murine survival motor neuron gene: homolog of the spinal muscular atrophy-determining gene. Genome Res. 7:339-352

Didry D, Carlier MF, Pantaloni D (1998) Synergy between actin depolymerizing factor/cofilin and profilin in increasing actin filament turnover. J. Biol. Chem. 273:25602-25611

Dimos JT, Rodolfa KT, Niakan KK, Weisenthal LM, Mitsumoto H, Chung W, Croft GF, Saphier G, Leibel R, Goland R, Wichterle H, Henderson CE, Eggan K (2008) Induced pluripotent stem cells generated from patients with ALS can be differentiated into motor neurons. Science 321:1218-1221

Dominguez E, Marais T, Chatauret N, Benkhelifa-Ziyyat S, Duque S, Ravassard P, Carcenac R, Astord S, de Moura AP, Voit T, Barkats M (2011) Intravenous scAAV9 delivery of a codon-optimized SMN1 sequence rescues SMA mice. Hum. Mol. Genet. 20:681-693

Dubowitz V (1999) Very severe spinal muscular atrophy (SMA type 0): an expanding clinical phenotype. Eur. J. Paediatr. Neurol. 3:49-51

Dykxhoorn DM, Novina CD, Sharp PA (2003) Killing the messenger: short RNAs that silence gene expression. Nat Rev Mol Cell Biol 4:457-467

Eggert C, Chari A, Laggerbauer B, Fischer U (2006) Spinal muscular atrophy: the RNP connection. Trends in Molecular Medicine 12:113-121

Elia LP, Yamamoto M, Zang K, Reichardt LF (2006) p120 catenin regulates dendritic spine and synapse development through Rho-family GTPases and cadherins. Neuron 51:43-56

Emirandetti A, Graciele Zanon R, Sabha M, de Oliveira ALR (2006) Astrocyte reactivity influences the number of presynaptic terminals apposed to spinal motoneurons after axotomy. Brain Res. 1095:35-42

Etienne-Manneville S, Hall A (2002) Rho GTPases in cell biology. Nature 420:629-635

Eve DJ, Nisbet AP, Kingsbury AE, Hewson EL, Daniel SE, Lees AJ, Marsden CD, Foster OJ (1998) Basal ganglia neuronal nitric oxide synthase mRNA expression in Parkinson's disease. Brain Res. Mol. Brain Res. 63:62-71

Fan L, Simard LR (2002) Survival motor neuron (SMN) protein: role in neurite outgrowth and neuromuscular maturation during neuronal differentiation and development. Hum. Mol. Genet. 11:1605-1614

Feldkötter M, Schwarzer V, Wirth R, Wienker TF, Wirth B (2002) Quantitative analyses of SMN1 and SMN2 based on real-time lightCycler PCR: fast and highly reliable carrier testing and prediction of severity of spinal muscular atrophy. Am. J. Hum. Genet. 70:358-368

Feng W, Gubitz AK, Wan L, Battle DJ, Dostie J, Golembe TJ, Dreyfuss G (2005) Gemins modulate the expression and activity of the SMN complex. Hum. Mol. Genet. 14:1605-1611

Fernández-Vizarra P, Fernández AP, Castro-Blanco S, Encinas JM, Serrano J, Bentura ML, Muñoz P, Martínez-Murillo R, Rodrigo J (2004) Expression of nitric oxide system in clinically evaluated cases of Alzheimer's disease. Neurobiol. Dis. 15:287-305

Ferri A, Sanes JR, Coleman MP, Cunningham JM, Kato AC (2003) Inhibiting axon degeneration and synapse loss attenuates apoptosis and disease progression in a mouse model of motoneuron disease. Curr. Biol. 13:669-673

Fields RD, Stevens-Graham B (2002) New insights into neuron-glia communication. Science 298:556-562

Fournier AE, Takizawa BT, Strittmatter SM (2003) Rho kinase inhibition enhances axonal regeneration in the injured CNS. J. Neurosci. 23:1416-1423

Foust KD, Wang X, McGovern VL, Braun L, Bevan AK, Haidet AM, Le TT, Morales PR, Rich MM, Burghes AHM, Kaspar BK (2010) Rescue of the spinal muscular atrophy phenotype in a mouse model by early postnatal delivery of SMN. Nat. Biotechnol. 28:271-274

Francis JW, Sandrock AW, Bhide PG, Vonsattel JP, Brown RH (1998) Heterogeneity of subcellular localization and electrophoretic mobility of survival motor neuron (SMN) protein in mammalian neural cells and tissues. Proc. Natl. Acad. Sci. U.S.A. 95:6492-6497

Frank-Cannon TC, Alto LT, McAlpine FE, Tansey MG (2009) Does neuroinflammation fan the flame in neurodegenerative diseases? Mol Neurodegener 4:47

Franklin JL, Berechid BE, Cutting FB, Presente A, Chambers CB, Foltz DR, Ferreira A, Nye JS (1999) Autonomous and non-autonomous regulation of mammalian neurite development by Notch1 and Delta1. Curr. Biol. 9:1448-1457

Frugier T, Tiziano FD, Cifuentes-Diaz C, Miniou P, Roblot N, Dierich A, Le Meur M, Melki J (2000) Nuclear targeting defect of SMN lacking the C-terminus in a mouse model of spinal muscular atrophy. Hum. Mol. Genet. 9:849-858

Frugier T, Nicole S, Cifuentes-Diaz C, Melki J (2002) The molecular bases of spinal muscular atrophy. Curr. Opin. Genet. Dev. 12:294-298

Fykse EM, Takei K, Walch-Solimena C, Geppert M, Jahn R, De Camilli P, Südhof TC (1993) Relative properties and localizations of synaptic vesicle protein isoforms: the case of the synaptophysins. J. Neurosci. 13:4997-5007

Gabanella F, Butchbach MER, Saieva L, Carissimi C, Burghes AHM, Pellizzoni L (2007) Ribonucleoprotein assembly defects correlate with spinal muscular atrophy severity and preferentially affect a subset of spliceosomal snRNPs. PLoS ONE 2:e921

Garcera A, Mincheva S, Gou-Fabregas M, Caraballo Miralles V, Lladó J, Comella JX, Soler RM (2011) A new model to study spinal muscular atrophy: neurite degeneration and cell death is counteracted by BCL-X(L) Overexpression in motoneurons. Neurobiol. Dis. 42:415-426

García-Cabezas MA, García-Alix A, Martín Y, Gutiérrez M, Hernández C, Rodríguez JI, Morales C (2004) Neonatal spinal muscular atrophy with multiple contractures, bone fractures, respiratory insufficiency and 5q13 deletion. Acta Neuropathol 107:475-478

Garvie JM, Woolf AL (1966) Kugelberg-Welander syndrome (hereditary proximal spinal muscular atrophy). Br Med J 1:1458-1461

Gavrilov DK, Shi X, Das K, Gilliam TC, Wang CH (1998) Differential SMN2 expression associated with SMA severity. Nat. Genet. 20:230-231

Ghatak NR (1983) Glial bundles in spinal nerve roots: a form of isomorphic gliosis at the junction of the central and peripheral nervous system. Neuropathol. Appl. Neurobiol. 9:391-401

Giesemann T, Rathke-Hartlieb S, Rothkegel M, Bartsch JW, Buchmeier S, Jockusch BM, Jockusch H (1999) A role for polyproline motifs in the spinal muscular atrophy protein SMN. Profilins bind to and colocalize with smn in nuclear gems. J. Biol. Chem. 274:37908-37914

Giniger E (1998) A role for Abl in Notch signaling. Neuron 20:667-681

Goldberg L, Kloog Y (2006) A Ras inhibitor tilts the balance between Rac and Rho and blocks phosphatidylinositol 3-kinase-dependent glioblastoma cell migration. Cancer Res. 66:11709-11717

Govek E, Hatten ME, Van Aelst L (2011) The role of Rho GTPase proteins in CNS neuronal migration. Dev Neurobiol 71:528-553

Grandbarbe L, Michelucci A, Heurtaux T, Hemmer K, Morga E, Heuschling P (2007) Notch signaling modulates the activation of microglial cells. Glia 55:1519-1530

Haddad H, Cifuentes-Diaz C, Miroglio A, Roblot N, Joshi V, Melki J (2003) Riluzole attenuates spinal muscular atrophy disease progression in a mouse model. Muscle Nerve 28:432-437

Hannus S, Bühler D, Romano M, Seraphin B, Fischer U (2000) The Schizosaccharomyces pombe protein Yab8p and a novel factor, Yip1p, share structural and functional similarity with the spinal muscular atrophy-associated proteins SMN and SIP1. Hum. Mol. Genet. 9:663-674

Harper JM, Krishnan C, Darman JS, Deshpande DM, Peck S, Shats I, Backovic S, Rothstein JD, Kerr DA (2004) Axonal growth of embryonic stem cell-derived motoneurons in vitro and in motoneuron-injured adult rats. Proc. Natl. Acad. Sci. U.S.A. 101:7123-7128

Haydon PG (2001) GLIA: listening and talking to the synapse. Nat. Rev. Neurosci. 2:185-193

Helmken C, Hofmann Y, Schoenen F, Oprea G, Raschke H, Rudnik-Schöneborn S, Zerres K, Wirth B (2003) Evidence for a modifying pathway in SMA discordant families: reduced SMN level decreases the amount of its interacting partners and Htra2-beta1. Hum. Genet. 114:11-21

Heneka MT, Feinstein DL (2001) Expression and function of inducible nitric oxide synthase in neurons. J. Neuroimmunol. 114:8-18

Henkel JS, Engelhardt JI, Siklós L, Simpson EP, Kim SH, Pan T, Goodman JC, Siddique T, Beers DR, Appel SH (2004) Presence of dendritic cells, MCP-1, and activated microglia/macrophages in amyotrophic lateral sclerosis spinal cord tissue. Ann. Neurol. 55:221-235

Higuchi M, Kiyama H, Hayakawa T, Hamada Y, Tsujimoto Y (1995) Differential expression of Notch1 and Notch2 in developing and adult mouse brain. Brain Res. Mol. Brain Res. 29:263-272

Hilliard MA (2009) Axonal degeneration and regeneration: a mechanistic tug-of-war. J. Neurochem. 108:23-32

Hoffmann, J. (1900) Uber die hereditare progressive spinale muskelatrophie in kindesalter. *Muenchen Med. Wschr*., 47, 1649–1651.

Hofmann Y, Lorson CL, Stamm S, Androphy EJ, Wirth B (2000) Htra2-beta 1 stimulates an exonic splicing enhancer and can restore full-length SMN expression to survival motor neuron 2 (SMN2). Proc. Natl. Acad. Sci. U.S.A. 97:9618-9623

Hofmann Y, Wirth B (2002) hnRNP-G promotes exon 7 inclusion of survival motor neuron (SMN) via direct interaction with Htra2-beta1. Hum. Mol. Genet. 11:2037-2049

Horner PJ, Palmer TD (2003) New roles for astrocytes: the nightlife of an “astrocyte.” La vida loca! Trends Neurosci. 26:597-603

Höltje M, Hoffmann A, Hofmann F, Mucke C, Grosse G, Van Rooijen N, Kettenmann H, Just I, Ahnert-Hilger G (2005) Role of Rho GTPase in astrocyte morphology and migratory response during in vitro wound healing. J. Neurochem. 95:1237-1248

Hsieh-Li HM, Chang JG, Jong YJ, Wu MH, Wang NM, Tsai CH, Li H (2000) A mouse model for spinal muscular atrophy. Nat. Genet. 24:66-70

Hua Y, Vickers TA, Baker BF, Bennett CF, Krainer AR (2007) Enhancement of SMN2 exon 7 inclusion by antisense oligonucleotides targeting the exon. PLoS Biol. 5:e73

Ikemoto A, Hirano A, Matsumoto S, Akiguchi I, Kimura J (1996) Synaptophysin expression in the anterior horn of Werdnig-Hoffmann disease. J. Neurol. Sci. 136:94-100

Ishizaki T, Uehata M, Tamechika I, Keel J, Nonomura K, Maekawa M, Narumiya S (2000) Pharmacological properties of Y-27632, a specific inhibitor of rho-associated kinases. Mol. Pharmacol. 57:976-983

Iso T, Kedes L, Hamamori Y (2003) HES and HERP families: multiple effectors of the Notch signaling pathway. J. Cell. Physiol. 194:237-255

Iwahashi H, Eguchi Y, Yasuhara N, Hanafusa T, Matsuzawa Y, Tsujimoto Y (1997) Synergistic anti-apoptotic activity between Bcl-2 and SMN implicated in spinal muscular atrophy. Nature 390:413-417

Jablonka S, Schrank B, Kralewski M, Rossoll W, Sendtner M (2000) Reduced survival motor neuron (Smn) gene dose in mice leads to motor neuron degeneration: an animal model for spinal muscular atrophy type III. Hum. Mol. Genet. 9:341-346

Jablonka S, Bandilla M, Wiese S, Bühler D, Wirth B, Sendtner M, Fischer U (2001) Co-regulation of survival of motor neuron (SMN) protein and its interactor SIP1 during development and in spinal muscular atrophy. Hum. Mol. Genet. 10:497-505

Jurica MS, Moore MJ (2003) Pre-mRNA splicing: awash in a sea of proteins. Mol. Cell 12:5-14

Kandel ER, Schwartz JH, Jessell TM (2000) Principles of Neural Science. Appleton & Lange. 4th edition.

Kanning KC, Kaplan A, Henderson CE (2010) Motor neuron diversity in development and disease. Annu. Rev. Neurosci. 33:409-440

Kariya S, Park G, Maeno-Hikichi Y, Leykekhman O, Lutz C, Arkovitz MS, Landmesser LT, Monani UR (2008) Reduced SMN protein impairs maturation of the neuromuscular junctions in mouse models of spinal muscular atrophy. Hum. Mol. Genet. 17:2552-2569

Kashima T, Rao N, Manley JL (2007a) An intronic element contributes to splicing repression in spinal muscular atrophy. Proc. Natl. Acad. Sci. U.S.A. 104:3426-3431

Kashima T, Rao N, David CJ, Manley JL (2007b) hnRNP A1 functions with specificity in repression of SMN2 exon 7 splicing. Hum. Mol. Genet. 16:3149-3159

Kashima T, Manley JL (2003) A negative element in SMN2 exon 7 inhibits splicing in spinal muscular atrophy. Nat. Genet. 34:460-463

Kassa RM, Mariotti R, Bonaconsa M, Bertini G, Bentivoglio M (2009) Gene, cell, and axon changes in the familial amyotrophic lateral sclerosis mouse sensorimotor cortex. J. Neuropathol. Exp. Neurol. 68:59-72

Kato S, Hirano A (1990) Ubiquitin and phosphorylated neurofilament epitopes in ballooned neurons of the extraocular muscle nuclei in a case of Werdnig-Hoffmann disease. Acta Neuropathol 80:334-337

Keely PJ, Westwick JK, Whitehead IP, Der CJ, Parise LV (1997) Cdc42 and Rac1 induce integrin-mediated cell motility and invasiveness through PI(3)K. Nature 390:632-636

Keller R (2005) Cell migration during gastrulation. Curr. Opin. Cell Biol. 17:533-541

Kernochan LE, Russo ML, Woodling NS, Huynh TN, Avila AM, Fischbeck KH, Sumner CJ (2005) The role of histone acetylation in SMN gene expression. Hum. Mol. Genet. 14:1171-1182

Kerr DA, Nery JP, Traystman RJ, Chau BN, Hardwick JM (2000) Survival motor neuron protein modulates neuron-specific apoptosis. Proc. Natl. Acad. Sci. U.S.A. 97:13312-13317

King AE, Dickson TC, Blizzard CA, Woodhouse A, Foster SS, Chung RS, Vickers JC (2011) Neuron-glia interactions underlie ALS-like axonal cytoskeletal pathology. Neurobiol. Aging 32:459-469

Kiss T (2004) Biogenesis of small nuclear RNPs. J. Cell. Sci. 117:5949-5951

Kong L, Wang X, Choe DW, Polley M, Burnett BG, Bosch-Marcé M, Griffin JW, Rich MM, Sumner CJ (2009) Impaired synaptic vesicle release and immaturity of neuromuscular junctions in spinal muscular atrophy mice. J. Neurosci. 29:842-851

Környei Z, Czirók A, Vicsek T, Madarász E (2000) Proliferative and migratory responses of astrocytes to in vitro injury. J. Neurosci. Res. 61:421-429

Krstic, R.V. (1997) Human Microscopy Anatomy. Springer-Verlag. Third printing.

Kugelberg E, Welander L (1956) Heredofamilial juvenile muscular atrophy simulating muscular dystrophy. AMA Arch Neurol Psychiatry 75:500-509

Kumagai T, Hashizume Y (1982) Morphological and morphometric studies on the spinal cord lesion in Werdnig-Hoffmann disease. Brain Dev. 4:87-96

Kuru S, Sakai M, Konagaya M, Yoshida M, Hashizume Y, Saito K (2009) An autopsy case of spinal muscular atrophy type III (Kugelberg-Welander disease). Neuropathology 29:63-67

Lai EC (2004) Notch signaling: control of cell communication and cell fate. Development 131:965-973

Le Clainche C, Carlier M (2008) Regulation of actin assembly associated with protrusion and adhesion in cell migration. Physiol. Rev. 88:489-513

Le TT, Pham LT, Butchbach MER, Zhang HL, Monani UR, Coovert DD, Gavrilina TO, Xing L, Bassell GJ, Burghes AHM (2005) SMNDelta7, the major product of the centromeric survival motor neuron (SMN2) gene, extends survival in mice with spinal muscular atrophy and associates with full-length SMN. Hum. Mol. Genet. 14:845-857

Lee J, Ryu H, Ferrante RJ, Morris SM, Ratan RR (2003) Translational control of inducible nitric oxide synthase expression by arginine can explain the arginine paradox. Proc. Natl. Acad. Sci. U.S.A. 100:4843-4848

Lefebvre S, Bürglen L, Reboullet S, Clermont O, Burlet P, Viollet L, Benichou B, Cruaud C, Millasseau P, Zeviani M (1995) Identification and characterization of a spinal muscular atrophy-determining gene. Cell 80:155-165

Lefebvre S, Burlet P, Liu Q, Bertrandy S, Clermont O, Munnich A, Dreyfuss G, Melki J (1997) Correlation between severity and SMN protein level in spinal muscular atrophy. Nat. Genet. 16:265-269

Lesbordes J, Cifuentes-Diaz C, Miroglio A, Joshi V, Bordet T, Kahn A, Melki J (2003) Therapeutic benefits of cardiotrophin-1 gene transfer in a mouse model of spinal muscular atrophy. Hum. Mol. Genet. 12:1233-1239

Levy OA, Lah JJ, Levey AI (2002) Notch signaling inhibits PC12 cell neurite outgrowth via RBP-J-dependent and -independent mechanisms. Dev. Neurosci. 24:79-88

Lim SR, Hertel KJ (2001) Modulation of survival motor neuron pre-mRNA splicing by inhibition of alternative 3' splice site pairing. J. Biol. Chem. 276:45476-45483

Lin CH, Forscher P (1995) Growth cone advance is inversely proportional to retrograde F-actin flow. Neuron 14:763-771

Ling KKY, Lin M, Zingg B, Feng Z, Ko C (2010) Synaptic Defects in the Spinal and Neuromuscular Circuitry in a Mouse Model of Spinal Muscular Atrophy L. Me, ed. PLoS ONE 5:e15457

Linseman DA, Loucks FA (2008) Diverse roles of Rho family GTPases in neuronal development, survival, and death. Front. Biosci. 13:657-676

Liu Q, Dreyfuss G (1996) A novel nuclear structure containing the survival of motor neurons protein. EMBO J. 15:3555-3565

Locascio A, Nieto MA (2001) Cell movements during vertebrate development: integrated tissue behaviour versus individual cell migration. Curr. Opin. Genet. Dev. 11:464-469

Lorson CL, Strasswimmer J, Yao JM, Baleja JD, Hahnen E, Wirth B, Le T, Burghes AH, Androphy EJ (1998) SMN oligomerization defect correlates with spinal muscular atrophy severity. Nat. Genet. 19:63-66

Lorson CL, Hahnen E, Androphy EJ, Wirth B (1999) A single nucleotide in the SMN gene regulates splicing and is responsible for spinal muscular atrophy. Proc. Natl. Acad. Sci. U.S.A. 96:6307-6311

Lorson CL, Rindt H, Shababi M (2010) Spinal muscular atrophy: mechanisms and therapeutic strategies. Hum. Mol. Genet. 19:R111-8

Lorson CL, Androphy EJ (2000) An exonic enhancer is required for inclusion of an essential exon in the SMA-determining gene SMN. Hum. Mol. Genet. 9:259-265

Lunn JS, Sakowski SA, Hur J, Feldman EL (2011) Stem cell technology for neurodegenerative diseases. Ann. Neurol. 70:353-361

Lunn MR, Wang CH (2008) Spinal muscular atrophy. Lancet 371:2120-2133

Luo L (2000) Rho GTPases in neuronal morphogenesis. Nat. Rev. Neurosci. 1:173-180

Luo L (2002) Actin cytoskeleton regulation in neuronal morphogenesis and structural plasticity. Annu. Rev. Cell Dev. Biol. 18:601-635

Luster AD, Alon R, Andrian von UH (2005) Immune cell migration in inflammation: present and future therapeutic targets. Nat. Immunol. 6:1182-1190

Lüth HJ, Holzer M, Gertz HJ, Arendt T (2000) Aberrant expression of nNOS in pyramidal neurons in Alzheimer's disease is highly co-localized with p21ras and p16INK4a. Brain Res. 852:45-55

Ma Q, Sommer L, Cserjesi P, Anderson DJ (1997) Mash1 and neurogenin1 expression patterns define complementary domains of neuroepithelium in the developing CNS and are correlated with regions expressing notch ligands. J. Neurosci. 17:3644-3652

MacLeod MJ, Taylor JE, Lunt PW, Mathew CG, Robb SA (1999) Prenatal onset spinal muscular atrophy. Eur. J. Paediatr. Neurol. 3:65-72

Marchetti B, Abbracchio MP (2005) To be or not to be (inflamed)--is that the question in anti-inflammatory drug therapy of neurodegenerative disorders? Trends Pharmacol. Sci. 26:517-525

Markowitz JA, Tinkle MB, Fischbeck KH (2004) Spinal muscular atrophy in the neonate. J Obstet Gynecol Neonatal Nurs 33:12-20

Markowitz JA, Singh P, Darras BT (2012) Spinal muscular atrophy: a clinical and research update. Pediatr. Neurol. 46:1-12

Mason CA, Edmondson JC, Hatten ME (1988) The extending astroglial process: development of glial cell shape, the growing tip, and interactions with neurons. J. Neurosci. 8:3124-3134

McGovern VL, Gavrilina TO, Beattie CE, Burghes AHM (2008) Embryonic motor axon development in the severe SMA mouse. Hum. Mol. Genet. 17:2900-2909

McWhorter ML, Monani UR, Burghes AHM, Beattie CE (2003) Knockdown of the survival motor neuron (Smn) protein in zebrafish causes defects in motor axon outgrowth and pathfinding. J. Cell Biol. 162:919-931

Mir M, Asensio VJ, Tolosa L, Gou-Fabregas M, Soler RM, Lladó J, Olmos G (2009) Tumor necrosis factor alpha and interferon gamma cooperatively induce oxidative stress and motoneuron death in rat spinal cord embryonic explants. Neuroscience 162:959-971

Miyajima H, Miyaso H, Okumura M, Kurisu J, Imaizumi K (2002) Identification of a cis-acting element for the regulation of SMN exon 7 splicing. J. Biol. Chem. 277:23271-23277

Moisse K, Strong MJ (2006) Innate immunity in amyotrophic lateral sclerosis. Biochim. Biophys. Acta 1762:1083-1093

Monani UR (2005) Spinal muscular atrophy: a deficiency in a ubiquitous protein; a motor neuron-specific disease. Neuron 48:885-896

Monani UR, Lorson CL, Parsons DW, Prior TW, Androphy EJ, Burghes AH, McPherson JD (1999a) A single nucleotide difference that alters splicing patterns distinguishes the SMA gene SMN1 from the copy gene SMN2. Hum. Mol. Genet. 8:1177-1183

Monani UR, McPherson JD, Burghes AH (1999b) Promoter analysis of the human centromeric and telomeric survival motor neuron genes (SMNC and SMNT). Biochim. Biophys. Acta 1445:330-336

Monani UR, Coovert DD, Burghes AH (2000a) Animal models of spinal muscular atrophy. Hum. Mol. Genet. 9:2451-2457

Monani UR, Sendtner M, Coovert DD, Parsons DW, Andreassi C, Le TT, Jablonka S, Schrank B, Rossoll W, Rossol W, Prior TW, Morris GE, Burghes AH (2000b) The human centromeric survival motor neuron gene (SMN2) rescues embryonic lethality in Smn(-/-) mice and results in a mouse with spinal muscular atrophy. Hum. Mol. Genet. 9:333-339

Monani UR, Pastore MT, Gavrilina TO, Jablonka S, Le TT, Andreassi C, DiCocco JM, Lorson C, Androphy EJ, Sendtner M, Podell M, Burghes AHM (2003) A transgene carrying an A2G missense mutation in the SMN gene modulates phenotypic severity in mice with severe (type I) spinal muscular atrophy. J. Cell Biol. 160:41-52

Moreno-López B (2010) Local isoform-specific NOS inhibition: a promising approach to promote motor function recovery after nerve injury. J. Neurosci. Res. 88:1846-1857

Moreno-López B, Sunico CR, González-Forero D (2011) NO orchestrates the loss of synaptic boutons from adult "sick" motoneurons: modeling a molecular mechanism. Mol. Neurobiol. 43:41-66

Moreno-López B, González-Forero D (2006) Nitric oxide and synaptic dynamics in the adult brain: physiopathological aspects. Rev Neurosci 17:309-357

Morga E, Mouad-Amazzal L, Felten P, Heurtaux T, Moro M, Michelucci A, Gabel S, Grandbarbe L, Heuschling P (2009) Jagged1 regulates the activation of astrocytes via modulation of NFkappaB and JAK/STAT/SOCS pathways. Glia 57:1741-1753

Mourelatos Z, Abel L, Yong J, Kataoka N, Dreyfuss G (2001) SMN interacts with a novel family of hnRNP and spliceosomal proteins. EMBO J. 20:5443-5452

Murray LM, Comley LH, Thomson D, Parkinson N, Talbot K, Gillingwater TH (2008) Selective vulnerability of motor neurons and dissociation of pre- and post-synaptic pathology at the neuromuscular junction in mouse models of spinal muscular atrophy. Hum. Mol. Genet. 17:949-962

Murray LM, Lee S, Bäumer D, Parson SH, Talbot K, Gillingwater TH (2010) Pre-symptomatic development of lower motor neuron connectivity in a mouse model of severe spinal muscular atrophy. Hum. Mol. Genet. 19:420-433

Negishi M, Katoh H (2002) Rho family GTPases as key regulators for neuronal network formation. J. Biochem. 132:157-166

Newey SE, Velamoor V, Govek E, Van Aelst L (2005) Rho GTPases, dendritic structure, and mental retardation. J. Neurobiol. 64:58-74

Nichols JT, Miyamoto A, Weinmaster G (2007) Notch signaling--constantly on the move. Traffic 8:959-969

Nimmerjahn A, Kirchhoff F, Helmchen F (2005) Resting microglial cells are highly dynamic surveillants of brain parenchyma in vivo. Science 308:1314-1318

Nobes CD, Hall A (1999) Rho GTPases control polarity, protrusion, and adhesion during cell movement. J. Cell Biol. 144:1235-1244

Novelli G, Calzà L, Amicucci P, Giardino L, Pozza M, Silani V, Pizzuti A, Gennarelli M, Piombo G, Capon F, Dallapiccola B (1997) Expression study of survival motor neuron gene in human fetal tissues. Biochem. Mol. Med. 61:102-106

Nölle A et al. (2011) The spinal muscular atrophy disease protein SMN is linked to the Rho-kinase pathway via profilin. Hum. Mol. Genet. 20:4865-4878

Oh SY, Ellenstein A, Chen C, Hinman JD, Berg EA, Costello CE, Yamin R, Neve RL, Abraham CR (2005) Amyloid precursor protein interacts with notch receptors. J. Neurosci. Res. 82:32-42

Okabe S, Hirokawa N (1991) Actin dynamics in growth cones. J. Neurosci. 11:1918-1929

Orihara Y, Ikematsu K, Tsuda R, Nakasono I (2001) Induction of nitric oxide synthase by traumatic brain injury. Forensic Sci. Int. 123:142-149

Osipo C, Golde TE, Osborne BA, Miele LA (2007) Off the beaten pathway: the complex cross talk between Notch and NF-κB. Lab Invest 88:11-17

Owen N, Doe CL, Mellor J, Davies KE (2000) Characterization of the Schizosaccharomyces pombe orthologue of the human survival motor neuron (SMN) protein. Hum. Mol. Genet. 9:675-684

Pagliardini S, Giavazzi A, Setola V, Lizier C, Di Luca M, DeBiasi S, Battaglia G (2000) Subcellular localization and axonal transport of the survival motor neuron (SMN) protein in the developing rat spinal cord. Hum. Mol. Genet. 9:47-56

Panatier A, Vallée J, Haber M, Murai KK, Lacaille J, Robitaille R (2011) Astrocytes are endogenous regulators of basal transmission at central synapses. Cell 146:785-798

Pantaloni D, Carlier MF (1993) How profilin promotes actin filament assembly in the presence of thymosin beta 4. Cell 75:1007-1014

Papadimitriou D, Le Verche V, Jacquier A, Ikiz B, Przedborski S, Re DB (2010) Inflammation in ALS and SMA: sorting out the good from the evil. Neurobiol. Dis. 37:493-502

Parano E, Pavone L, Falsaperla R, Trifiletti R, Wang C (1996) Molecular basis of phenotypic heterogeneity in siblings with spinal muscular atrophy. Ann. Neurol. 40:247-251

Park G, Maeno-Hikichi Y, Awano T, Landmesser LT, Monani UR (2010) Reduced survival of motor neuron (SMN) protein in motor neuronal progenitors functions cell autonomously to cause spinal muscular atrophy in model mice expressing the human centromeric (SMN2) gene. J. Neurosci. 30:12005-12019

Parsons DW, McAndrew PE, Iannaccone ST, Mendell JR, Burghes AH, Prior TW (1998) Intragenic telSMN mutations: frequency, distribution, evidence of a founder effect, and modification of the spinal muscular atrophy phenotype by cenSMN copy number. Am. J. Hum. Genet. 63:1712-1723

Passini MA, Bu J, Roskelley EM, Richards AM, Sardi SP, O'Riordan CR, Klinger KW, Shihabuddin LS, Cheng SH (2010) CNS-targeted gene therapy improves survival and motor function in a mouse model of spinal muscular atrophy. J. Clin. Invest. 120:1253-1264

Pearn J (1978) Incidence, prevalence, and gene frequency studies of chronic childhood spinal muscular atrophy. J. Med. Genet. 15:409-413

Pearn JH (1973) The gene frequency of acute Werdnig-Hoffmann disease (SMA type 1). A total population survey in North-East England. J. Med. Genet. 10:260-265

Pearn JH, Wilson J (1973) Chronic generalized spinal muscular atrophy of infancy and childhood. Arrested Werdnig-Hoffman disease. Arch. Dis. Child. 48:768-774

Pekny M, Nilsson M (2005) Astrocyte activation and reactive gliosis. Glia 50:427-434

Pellegrin S, Mellor H (2007) Actin stress fibres. J. Cell. Sci. 120:3491-3499

Pellizzoni L, Kataoka N, Charroux B, Dreyfuss G (1998) A novel function for SMN, the spinal muscular atrophy disease gene product, in pre-mRNA splicing. Cell 95:615-624

Pellizzoni L, Charroux B, Dreyfuss G (1999) SMN mutants of spinal muscular atrophy patients are defective in binding to snRNP proteins. Proc. Natl. Acad. Sci. U.S.A. 96:11167-11172

Pellizzoni L, Charroux B, Rappsilber J, Mann M, Dreyfuss G (2001) A functional interaction between the survival motor neuron complex and RNA polymerase II. J. Cell Biol. 152:75-85

Pérez-Severiano F, Escalante B, Vergara P, Ríos C, Segovia J (2002) Age-dependent changes in nitric oxide synthase activity and protein expression in striata of mice transgenic for the Huntington's disease mutation. Brain Res. 951:36-42

Prior TW, Swoboda KJ, Scott HD, Hejmanowski AQ (2004) Homozygous SMN1 deletions in unaffected family members and modification of the phenotype by SMN2. Am. J. Med. Genet. A 130A:307-310

Raivich G, Bohatschek M, Kloss CU, Werner A, Jones LL, Kreutzberg GW (1999) Neuroglial activation repertoire in the injured brain: graded response, molecular mechanisms and cues to physiological function. Brain Res. Brain Res. Rev. 30:77-105

Rajendra TK, Gonsalvez GB, Walker MP, Shpargel KB, Salz HK, Matera AG (2007) A Drosophila melanogaster model of spinal muscular atrophy reveals a function for SMN in striated muscle. J. Cell Biol. 176:831-841

Rakic P (1971) Neuron-glia relationship during granule cell migration in developing cerebellar cortex. A Golgi and electronmicroscopic study in Macacus Rhesus. J. Comp. Neurol. 141:283-312

Redmond L, Oh SR, Hicks C, Weinmaster G, Ghosh A (2000) Nuclear Notch1 signaling and the regulation of dendritic development. Nat. Neurosci. 3:30-40

Redmond L, Ghosh A (2001) The role of Notch and Rho GTPase signaling in the control of dendritic development. Curr. Opin. Neurobiol. 11:111-117

Ren XD, Schwartz MA (2000) Determination of GTP loading on Rho. Meth. Enzymol. 325:264-272

Ridley AJ (2001) Rho GTPases and cell migration. J. Cell. Sci. 114:2713-2722

Ridley AJ, Hall A (1992) The small GTP-binding protein rho regulates the assembly of focal adhesions and actin stress fibers in response to growth factors. Cell 70:389-399

Rossoll W, Kröning A, Ohndorf U, Steegborn C, Jablonka S, Sendtner M (2002) Specific interaction of Smn, the spinal muscular atrophy determining gene product, with hnRNP-R and gry-rbp/hnRNP-Q: a role for Smn in RNA processing in motor axons? Hum. Mol. Genet. 11:93-105

Rossoll W, Jablonka S, Andreassi C, Kröning A, Karle K, Monani UR, Sendtner M (2003) Smn, the spinal muscular atrophy-determining gene product, modulates axon growth and localization of beta-actin mRNA in growth cones of motoneurons. J. Cell Biol. 163:801-812

Rottner K, Behrendt B, Small JV, Wehland J (1999) VASP dynamics during lamellipodia protrusion. Nat. Cell Biol. 1:321-322

Roy P, Jacobson K (2004) Overexpression of profilin reduces the migration of invasive breast cancer cells. Cell Motil. Cytoskeleton 57:84-95

Ruiz R, Casañas JJ, Torres-Benito L, Cano R, Tabares L (2010) Altered intracellular Ca2+ homeostasis in nerve terminals of severe spinal muscular atrophy mice. J. Neurosci. 30:849-857

Ruiz-Palmero I, Simon-Areces J, Garcia-Segura LM, Arevalo M (2011) Notch/neurogenin 3 signalling is involved in the neuritogenic actions of oestradiol in developing hippocampal neurones. J. Neuroendocrinol. 23:355-364

Salama-Cohen P, Arevalo MA, Meier J, Grantyn R, Rodríguez-Tébar A (2005) NGF controls dendrite development in hippocampal neurons by binding to p75NTR and modulating the cellular targets of Notch. Mol. Biol. Cell 16:339-347

Salama-Cohen P, Arevalo MA, Grantyn R, Rodríguez-Tébar A (2006) Notch and NGF/p75NTR control dendrite morphology and the balance of excitatory/inhibitory synaptic input to hippocampal neurones through Neurogenin 3. J. Neurochem. 97:1269-1278

Sasaki S, Shibata N, Komori T, Iwata M (2000) iNOS and nitrotyrosine immunoreactivity in amyotrophic lateral sclerosis. Neurosci. Lett. 291:44-48

Sasaki S, Shibata N, Iwata M (2001) Neuronal nitric oxide synthase immunoreactivity in the spinal cord in amyotrophic lateral sclerosis. Acta Neuropathol 101:351-357

Sasaki S, Maruyama S (1994) Decreased synaptophysin immunoreactivity of the anterior horns in motor neuron disease. Acta Neuropathol 87:125-128

Schlüter K, Jockusch BM, Rothkegel M (1997) Profilins as regulators of actin dynamics. Biochim. Biophys. Acta 1359:97-109

Schrank B, Götz R, Gunnersen JM, Ure JM, Toyka KV, Smith AG, Sendtner M (1997) Inactivation of the survival motor neuron gene, a candidate gene for human spinal muscular atrophy, leads to massive cell death in early mouse embryos. Proc. Natl. Acad. Sci. U.S.A. 94:9920-9925

Schwanbeck R, Martini S, Bernoth K, Just U (2011) The Notch signaling pathway: molecular basis of cell context dependency. Eur. J. Cell Biol. 90:572-581

Sestan N, Artavanis-Tsakonas S, Rakic P (1999) Contact-dependent inhibition of cortical neurite growth mediated by notch signaling. Science 286:741-746

Setola V, Terao M, Locatelli D, Bassanini S, Garattini E, Battaglia G (2007) Axonal-SMN (a-SMN), a protein isoform of the survival motor neuron gene, is specifically involved in axonogenesis. Proc. Natl. Acad. Sci. U.S.A. 104:1959-1964

Sharma A, Lambrechts A, Hao LT, Le TT, Sewry CA, Ampe C, Burghes AHM, Morris GE (2005) A role for complexes of survival of motor neurons (SMN) protein with gemins and profilin in neurite-like cytoplasmic extensions of cultured nerve cells. Exp. Cell Res. 309:185-197

Sherrington, C. S. (1904) The correlation of reflexes and the principle of the common path. *British Association Reports,* 74,728-741.

Shpargel KB, Matera AG (2005) Gemin proteins are required for efficient assembly of Sm-class ribonucleoproteins. Proc. Natl. Acad. Sci. U.S.A. 102:17372-17377

Simic G (2008) Pathogenesis of proximal autosomal recessive spinal muscular atrophy. Acta Neuropathol 116:223-234

Simic G, Seso-Simic D, Lucassen PJ, Islam A, Krsnik Z, Cviko A, Jelasic D, Barisic N, Winblad B, Kostovic I, Kruslin B (2000) Ultrastructural analysis and TUNEL demonstrate motor neuron apoptosis in Werdnig-Hoffmann disease. J. Neuropathol. Exp. Neurol. 59:398-407

Simon CM, Jablonka S, Ruiz R, Tabares L, Sendtner M (2010) Ciliary neurotrophic factor-induced sprouting preserves motor function in a mouse model of mild spinal muscular atrophy. Hum. Mol. Genet. 19:973-986

Simon-Areces J, Membrive G, Garcia-Fernandez C, Garcia-Segura LM, Arevalo MA (2010) Neurogenin 3 cellular and subcellular localization in the developing and adult hippocampus. J. Comp. Neurol. 518:1814-1824

Singh NN, Androphy EJ, Singh RN (2004) An extended inhibitory context causes skipping of exon 7 of SMN2 in spinal muscular atrophy. Biochem. Biophys. Res. Commun. 315:381-388

Sleigh JN, Gillingwater TH, Talbot K (2011a) The contribution of mouse models to understanding the pathogenesis of spinal muscular atrophy. Disease Models & Mechanisms 4:457-467

Sleigh JN, Buckingham SD, Esmaeili B, Viswanathan M, Cuppen E, Westlund BM, Sattelle DB (2011b) A novel Caenorhabditis elegans allele, smn-1(cb131), mimicking a mild form of spinal muscular atrophy, provides a convenient drug screening platform highlighting new and pre-approved compounds. Hum. Mol. Genet. 20:245-260

Smith TS, Bennett JP (1997) Mitochondrial toxins in models of neurodegenerative diseases. I: In vivo brain hydroxyl radical production during systemic MPTP treatment or following microdialysis infusion of methylpyridinium or azide ions. Brain Res. 765:183-188

Soler-Botija C, Ferrer I, Alvarez JL, Baiget M, Tizzano EF (2003) Downregulation of Bcl-2 proteins in type I spinal muscular atrophy motor neurons during fetal development. J. Neuropathol. Exp. Neurol. 62:420-426

Squire L (2003) Fundamental neuroscience. Academic Press. 2nd edition.

Suetsugu S, Miki H, Takenawa T (1999) Distinct roles of profilin in cell morphological changes: microspikes, membrane ruffles, stress fibers, and cytokinesis. FEBS Lett. 457:470-474

Sumner BE (1975) A quantitative analysis of boutons with different types of synapse in normal and injured hypoglossal nuclei. Experimental Neurology 49:406-417

Sumner CJ (2007) Molecular mechanisms of spinal muscular atrophy. J. Child Neurol. 22:979-989

Sumner CJ, Huynh TN, Markowitz JA, Perhac JS, Hill B, Coovert DD, Schussler K, Chen X, Jarecki J, Burghes AHM, Taylor JP, Fischbeck KH (2003) Valproic acid increases SMN levels in spinal muscular atrophy patient cells. Ann. Neurol. 54:647-654

Sun Y, Grimmler M, Schwarzer V, Schoenen F, Fischer U, Wirth B (2005) Molecular and functional analysis of intragenic SMN1 mutations in patients with spinal muscular atrophy. Hum. Mutat. 25:64-71

Sunico CR, Portillo F, González-Forero D, Moreno-López B (2005) Nitric-oxide-directed synaptic remodeling in the adult mammal CNS. J. Neurosci. 25:1448-1458

Sunico CR, González-Forero D, Domínguez G, García-Verdugo JM, Moreno-López B (2010) Nitric oxide induces pathological synapse loss by a protein kinase G-, Rho kinase-dependent mechanism preceded by myosin light chain phosphorylation. J. Neurosci. 30:973-984

Takaishi K, Kikuchi A, Kuroda S, Kotani K, Sasaki T, Takai Y (1993) Involvement of rho p21 and its inhibitory GDP/GTP exchange protein (rho GDI) in cell motility. Mol. Cell. Biol. 13:72-79

Torres-Benito L, Neher MF, Cano R, Ruiz R, Tabares L (2011) SMN requirement for synaptic vesicle, active zone and microtubule postnatal organization in motor nerve terminals. PLoS ONE 6:e26164

Torres-Benito L, Ruiz R, Tabares L (2012) Synaptic defects in spinal muscular atrophy animal models. Dev Neurobiol 72:126-133

Trapp BD, Wujek JR, Criste GA, Jalabi W, Yin X, Kidd GJ, Stohlman S, Ransohoff R (2007) Evidence for synaptic stripping by cortical microglia. Glia 55:360-368

Uehata M, Ishizaki T, Satoh H, Ono T, Kawahara T, Morishita T, Tamakawa H, Yamagami K, Inui J, Maekawa M, Narumiya S (1997) Calcium sensitization of smooth muscle mediated by a Rho-associated protein kinase in hypertension. Nature 389:990-994

Valori CF, Ning K, Wyles M, Mead RJ, Grierson AJ, Shaw PJ, Azzouz M (2010) Systemic delivery of scAAV9 expressing SMN prolongs survival in a model of spinal muscular atrophy. Sci Transl Med 2:35ra42

Valster A, Tran NL, Nakada M, Berens ME, Chan AY, Symons M (2005) Cell migration and invasion assays. Methods 37:208-215

van Bergeijk J, Rydel-Könecke K, Grothe C, Claus P (2007) The spinal muscular atrophy gene product regulates neurite outgrowth: importance of the C terminus. FASEB J. 21:1492-1502

van Rossum D, Hanisch U (2004) Microglia. Metab Brain Dis 19:393-411

Velasco E, Valero C, Valero A, Moreno F, Hernández-Chico C (1996) Molecular analysis of the SMN and NAIP genes in Spanish spinal muscular atrophy (SMA) families and correlation between number of copies of cBCD541 and SMA phenotype. Hum. Mol. Genet. 5:257-263

Venkatesh D, Fredette N, Rostama B, Tang Y, Vary CPH, Liaw L, Urs S (2011) RhoA-mediated signaling in Notch-induced senescence-like growth arrest and endothelial barrier dysfunction. Arterioscler. Thromb. Vasc. Biol. 31:876-882

Vilimas T, Mascarenhas J, Palomero T, Mandal M, Buonamici S, Meng F, Thompson B, Spaulding C, Macaroun S, Alegre M, Kee BL, Ferrando A, Miele L, Aifantis I (2007) Targeting the NF-kappaB signaling pathway in Notch1-induced T-cell leukemia. Nat. Med. 13:70-77

Viollet L, Bertrandy S, Bueno Brunialti AL, Lefebvre S, Burlet P, Clermont O, Cruaud C, Guénet JL, Munnich A, Melki J (1997) cDNA isolation, expression, and chromosomal localization of the mouse survival motor neuron gene (Smn). Genomics 40:185-188

Wan L, Battle DJ, Yong J, Gubitz AK, Kolb SJ, Wang J, Dreyfuss G (2005) The survival of motor neurons protein determines the capacity for snRNP assembly: biochemical deficiency in spinal muscular atrophy. Mol. Cell. Biol. 25:5543-5551

Wang CH, Finkel RS, Bertini ES, Schroth M, Simonds A, Wong B, Aloysius A, Morrison L, Main M, Crawford TO, Trela A, Participants of the International Conference on SMA Standard of Care (2007) Consensus statement for standard of care in spinal muscular atrophy. In Journal of child neurology, p. 1027-1049.

Wang H, Hsieh H, Yang C (2011) Nitric oxide production by endothelin-1 enhances astrocytic migration via the tyrosine nitration of matrix metalloproteinase-9. J. Cell. Physiol. 226:2244-2256

Wanisch K, Yáñez-Muñoz RJ (2009) Integration-deficient lentiviral vectors: a slow coming of age. Mol. Ther. 17:1316-1332

Werdnig, G. (1894) Die fruhinfantile progressive spinale amyotrophie. *Arch. Psychiat.*, 26, 706–744.

Will CL, Lührmann R (2001) Spliceosomal UsnRNP biogenesis, structure and function. Curr. Opin. Cell Biol. 13:290-301

Williams JH, Schray RC, Patterson CA, Ayitey SO, Tallent MK, Lutz GJ (2009) Oligonucleotide-mediated survival of motor neuron protein expression in CNS improves phenotype in a mouse model of spinal muscular atrophy. J. Neurosci. 29:7633-7638

Wirth B, Brichta L, Hahnen E (2006a) Spinal muscular atrophy: from gene to therapy. Semin Pediatr Neurol 13:121-131

Wirth B, Brichta L, Schrank B, Lochmüller H, Blick S, Baasner A, Heller R (2006b) Mildly affected patients with spinal muscular atrophy are partially protected by an increased SMN2 copy number. Hum. Genet. 119:422-428

Wishart TM, Huang JP, Murray LM, Lamont DJ, Mutsaers CA, Ross J, Geldsetzer P, Ansorge O, Talbot K, Parson SH, Gillingwater TH (2010) SMN deficiency disrupts brain development in a mouse model of severe spinal muscular atrophy. Hum. Mol. Genet. 19:4216-4228

Wohlfart G, Fex J, Eliasson S (1955) Hereditary proximal spinal muscular atrophy, a clinical entity simulating progressive muscular dystrophy. Acta Psychiatr Neurol Scand 30:395-406

Wolstencroft EC, Mattis V, Bajer AA, Young PJ, Lorson CL (2005) A non-sequence-specific requirement for SMN protein activity: the role of aminoglycosides in inducing elevated SMN protein levels. Hum. Mol. Genet. 14:1199-1210

Workman E, Saieva L, Carrel TL, Crawford TO, Liu D, Lutz C, Beattie CE, Pellizzoni L, Burghes AHM (2009) A SMN missense mutation complements SMN2 restoring snRNPs and rescuing SMA mice. Hum. Mol. Genet. 18:2215-2229

Wyss-Coray T, Mucke L (2002) Inflammation in neurodegenerative disease--a double-edged sword. Neuron 35:419-432

Yamada J, Hayashi Y, Jinno S, Wu Z, Inoue K, Kohsaka S, Nakanishi H (2008) Reduced synaptic activity precedes synaptic stripping in vagal motoneurons after axotomy. Glia 56:1448-1462

Yamada J, Nakanishi H, Jinno S (2011) Differential involvement of perineuronal astrocytes and microglia in synaptic stripping after hypoglossal axotomy. Neuroscience 182:1-10

Yamanouchi Y, Yamanouchi H, Becker LE (1996) Synaptic alterations of anterior horn cells in Werdnig-Hoffmann disease. Pediatr. Neurol. 15:32-35

Yáñez-Muñoz RJ, Balaggan KS, MacNeil A, Howe SJ, Schmidt M, Smith AJ, Buch P, MacLaren RE, Anderson PN, Barker SE, Duran Y, Bartholomae C, Kalle von C, Heckenlively JR, Kinnon C, Ali RR, Thrasher AJ (2006) Effective gene therapy with nonintegrating lentiviral vectors. Nat. Med. 12:348-353

Yong J, Golembe TJ, Battle DJ, Pellizzoni L, Dreyfuss G (2004) snRNAs contain specific SMN-binding domains that are essential for snRNP assembly. Mol. Cell. Biol. 24:2747-2756

Yoon K, Gaiano N (2005) Notch signaling in the mammalian central nervous system: insights from mouse mutants. Nat. Neurosci. 8:709-715

Young PJ, DiDonato CJ, Hu D, Kothary R, Androphy EJ, Lorson CL (2002) SRp30c-dependent stimulation of survival motor neuron (SMN) exon 7 inclusion is facilitated by a direct interaction with hTra2 beta 1. Hum. Mol. Genet. 11:577-587

Zerres K, Rudnik-Schöneborn S (1995) Natural history in proximal spinal muscular atrophy. Clinical analysis of 445 patients and suggestions for a modification of existing classifications. Arch. Neurol. 52:518-523

Zhang HL, Pan F, Hong D, Shenoy SM, Singer RH, Bassell GJ (2003) Active transport of the survival motor neuron protein and the role of exon-7 in cytoplasmic localization. J. Neurosci. 23:6627-6637

Zou L, Jaramillo M, Whaley D, Wells A, Panchapakesa V, Das T, Roy P (2007) Profilin-1 is a negative regulator of mammary carcinoma aggressiveness. Br. J. Cancer 97:1361-1371